Functional characterization of an acid-regulated sRNA in *Helicobacter pylori*

Funtionelle Charakterisierung einer durch Säure regulierten sRNA in *Helicobacter pylori*

Doctoral thesis for a doctoral degree at the Graduate School of Life Sciences,

Julius-Maximilians-Universität Würzburg,

Section Infection and Immunity

Submitted by

Tan Hock Siew

from Pulau Pinang, Malaysia

Würzburg, 2017

Submitted on: ……..…….

Office stamp

Members of the *Promotionskomitee*:

Chairperson: Prof. Dr. Thomas Dandekar

Primary Supervisor: Prof. Dr. Cynthia Sharma

Supervisor (Second): Prof. Dr. Dagmar Beier

Supervisor (Third): Prof. Dr. Jörg Vogel

Date of Public Defence: ……..……

Date of Receipt of Certificates: …….

Dedicated to my wife, Erin Ju,

who has always been there for me.

Summary

Low pH is the main environmental stress encountered by *Helicobacter pylori* in the human stomach. To ensure its survival under acidic conditions, this bacterium utilizes urease (encoded by the *ureAB* operon), a nickel-activated metalloenzyme, which cleaves urea into ammonia to buffer the periplasmic space. Expression of the *ureAB* operon is tightly regulated at the transcriptional level. Moreover, the urease activity is modulated post-translationally via the activity of nickel-binding proteins such as HP1432 that act as nickel sponges to either sequester or release nickel depending on the pH. However, little is known how the levels of these nickel-binding proteins are regulated at the post-transcriptional level. Interestingly, more than 60 candidate small regulatory RNAs (sRNAs) have been identified in a differential RNA-seq approach in *H. pylori* strain 26695, suggesting an uncharacterized layer of post-transcriptional riboregulation in this pathogen. sRNAs control their *trans*- or *cis*- encoded targets by direct binding. Many of the characterized sRNAs are expressed in response to specific environmental cues and are ideal candidates to confer post-transcriptional regulation under different growth conditions.

This study demonstrates that a small RNA termed ArsZ (Acid Responsive sRNA Z) and its target HP1432 constitute yet another level of urease regulation. *In-vitro* and *in-vivo* experiments show that ArsZ interacts with the ribosome binding site (RBS) of HP1432 mRNA, effectively repressing translation of HP1432. During acid adaptation, the acid-responsive ArsRS two-component system represses expression of ArsZ. ArsRS and ArsZ work in tandem to regulate expression of HP1432 via a coherent feedforward loop (FFL). ArsZ acts as a delay mechanism in this feedforward loop to ensure that HP1432 protein levels do not abruptly change upon transient pH drops encountered by the bacteria. ArsZ "fine-tunes" the dynamics of urease activity after pH shift presumably by altering nickel availability through post-transcriptional control of HP1432 expression. Interestingly, after adaptation to acid stress, ArsZ indirectly activates the transcription of HP1432 and forms an incoherent FFL with ArsRS to regulate HP1432. This study identified a non-standard FFL in which ArsZ can participate directly or indirectly in two different network configurations depending on the state of acid stress adaptation. The importance of ArsZ in the acid response of *H. pylori* is further supported by bioinformatics analysis showing that the evolution of ArsZ is closely related to the emergence of modern *H. pylori* strains that globally infect humans. No homologs of *arsZ* were found in the non-*pylori* species of *Helicobacter*. Moreover, this study also demonstrates that the physiological role of a sRNA can be elucidated without the artificial overexpression of the respective sRNA, a method commonly used to characterize sRNAs. Coupled with time-course experiments, this approach allows the kinetics of ArsZ regulation to be studied under more native conditions. ArsZ is the first example of a *trans*-acting sRNA that regulates a nickel storage protein to modulate apo-urease maturation. These findings may have important implications in understanding the details of urease activation and hence the colonization capability of *H. pylori*, the only bacterial class I carcinogen to date (WHO, 1994).

Zusammenfassung

In der natürlichen Umgebung des menschlichen Magens ist *Helicobacter pylori* insbesondere niedrigen pH-Werten ausgesetzt. Um diese Bedingungen zu überleben, setzt das Bakterium das Enzym Urease ein (kodiert durch das *ureAB* Operon), ein Nickel-aktiviertes Metalloenzym, welches Urea zu Ammonium umsetzt um den pH-Wert des periplasmatischen Raums abzupuffern. Die Expression dieses Operons ist auf transkriptioneller Ebene streng reguliert. Zudem ist die Aktivität des Urease Enzyms auf post-translationaler Ebene moduliert. Dies geschieht durch die Aktivität von Nickel-Bindeproteinen wie HP1432, die in Abhängigkeit vom pH-Wert Nickelionen abfangen oder wieder freigeben. Allerdings ist nur sehr wenig darüber bekannt, wie diese Nickel-Bindeproteine auf post-transkriptioneller Ebene reguliert werden. Interessanterweise wurden mehr als 60 sRNA-Kandidaten (engl. small RNA für dt. kleine RNA) durch eine differentielle RNA-seq Methode im *H. pylori* Stamm 26695 identifiziert. Dies legt eine nicht charakterisierte Ebene post-transkriptioneller Riboregulierung in diesem Pathogen nahe. sRNAs kontrollieren ihre *trans*- oder *cis*-kodierten Zielgene durch direkte Interaktion. Viele der charakterisierten sRNAs werden als Antwort auf spezifische Umweltsignale exprimiert und stellen ideale Kandidaten für post-transkriptionelle Regulatoren unter verschiedenen Wachstumsbedingungen dar.

In dieser Arbeit wird gezeigt, dass die kleine RNA ArsZ (engl. acid responsive sRNA Z für dt. säureabhängige sRNA Z) und ihr Zielgen HP1432 ein zusätzliches Level der Urease-Regulierung darstellen. *In-vitro* und *in-vivo* Experimente zeigen, dass ArsZ mit der Ribosomenbindestelle (RBS) der HP1432 mRNA interagiert, wodurch dessen Translation verhindert wird. Während der Säureanpassung verhindert das säureabhängige ArsRS Zweikomponentensystem die Expression von ArsZ. Zusammen regulieren ArsRS und ArsZ das Zielgen HP1432 in Form eines kohärenten Feed-forward-loops (FFL). ArsZ agiert hier als Verzögerungsmechanismus, um sicherzustellen, dass sich bei einem transienten Abfall des pH-Wertes das Proteinlevel von HP1432 nicht abrupt verändert. Nach pH-Änderungen vermittelt ArsZ eine Feinregulierung der Ureaseaktivität, vermutlich indem es durch die post-transkriptionelle Kontrolle der HP1432 Expression die Verfügbarkeit von Nickel verändert. Interessanterweise aktiviert ArsZ nach der Säureanpassung indirekt die Transkription von HP1432 und schließt dadurch einen inkohärenten FFL mit ArsRS zur Regulierung von HP1432. Diese Studie identifizierte einen Nicht-Standard-FFL, in dem ArsZ abhängig von dem Status der Säureadaptation in zwei verschiedenen Netzwerkkonfigurationen direkt oder indirekt agieren kann. Bioinformatorische Analysen unterstützen die Relevanz von ArsZ in der Säureantwort von *H. pylori* zusätzlich. Hierbei kann gezeigt werden, dass die Evolution von ArsZ mit dem Aufkommen moderner *H. pylori* Stämme einhergeht, die weltweit Menschen infizieren. In nicht-*pylori Helicobacter* Spezies konnten keine Homologe von *arsZ* gefunden werden. Zudem zeigt diese Studie, dass die physiologische Rolle einer sRNA ohne ihre artifizielle Überexpression aufgeklärt werden kann, eine standard-mäßige

Herangehensweise zur Charakterisierung kleiner RNAs. In Kombination mit Zeitverlaufsexperimenten konnte die zeitabhängige Regulierung von Zielgenen durch ArsZ unter natürlicheren Bedingungen untersucht werden. ArsZ ist das erste Beispiel einer *trans*-agierenden sRNA die ein Nickel-Speicherprotein reguliert, um die Reifung der Apo-Urease zu modulieren. Diese Ergebnisse können wichtige Informationen liefern, um die Aktivierung des Urease Enzyms besser zu verstehen und um damit detailliertere Einblicke in die Kolonisierungsfähigkeit von *H. pylori* zu gewinnen, dem bislang einzigen bakteriellen Klasse-I-Karzinogen (WHO, 1994).

List of Figures

Figure 1.1: *Helicobacter pylori* colonization of the gastric mucosa 3

Figure 1.2: Periplasmic buffering and regulation of apo-urease by the ArsRS two-component system in *H. pylori* 5

Figure 1.3: Regulation of urease expression 8

Figure 1.4: Mechanisms of post-transcriptional regulation by *cis*-encoded sRNAs 11

Figure 1.5: Mechanisms of post-transcriptional regulation by *trans*-encoded sRNAs 13

Figure 1.6: Structure of coherent and incoherent FFL motifs 15

Figure 2.1: Conservation of ArsZ in diverse *H. pylori* strains 22

Figure 2.2: ArsZ is constitutively expressed during growth in rich medium at neutral pH 23

Figure 2.3: Bioinformatics-based target prediction for the ArsZ 24

Figure 2.4: ArsZ is regulated by the ArsRS two-component system 27

Figure 2.5: The promoter of ArsZ is de-repressed in the absence of the ArsS sensor kinase 29

Figure 2.6: ArsZ is regulated in response to low pH through the phosphorylated ArsR response regulator 30

Figure 2.7: ArsZ interacts with the 5'UTR of HP1432 mRNA *in vitro* 31

Figure 2.8: In-line and structure probing maps the precise interaction site between ArsZ and HP1432 mRNA *in vitro* 33

Figure 2.9: ArsZ masks the ribosome binding site of HP1432 mRNA to inhibit translation *in vitro* 35

Figure 2.10: ArsZ regulates HP1432 on the protein and mRNA level in *E. coli* Top10 36

Figure 2.11: Effect of ArsZ on HP1432 protein levels under steady-state conditions in *H. pylori* 37

Figure 2.12: Deletion of *arsZ* reduces activity of the HP1432 promoter 38

Figure 2.13: ArsZ represses HP1432 at the post-transcriptional level 40

Figure 2.14: ArsZ affects the half-life of the HP1432 mRNA 41

Figure 2.15: ArsZ is difficult to overexpress by standard approaches 44

Figure 2.16: ArsZ forms a coherent feed-forward loop with ArsRS and HP1432 45

Figure 2.17: ArsZ modulates urease activity via regulation of levels of the nickel-binding factor HP1432 45

Figure 2.18: Levels of urease activity of WT and Δ*arsZ* 47

Figure 2.19: The sRNA ArsZ affects fitness of *H. pylori* following shift to acid pH 48

Figure 2.20: Evolution of the ArsZ sRNA and its target gene HP1432 50

Figure 2.21: Expression of ArsZ and HP1432 in *H. acinonychis* and selected *H. pylori* strains 52

Figure 2.22: Conservation of genome organization in regions flanking *arsZ* 54

Figure 2.23: Loss of the *arsZ* gene in strain B8 56

Figure 3: Overall model for ArsZ regulation of HP1432 and halo-urease levels upon pH shift to 5.5 59

Figure S1: The predicted interaction between ArsZ and its mRNA targets 116

Figure S2: ArsZ is regulated in response to low pH 117

Figure S3: Predicted intermolecular RNA-RNA interaction between ArsZ and 5' UTR of HP1432 118
Figure S4: ArsZ forms a coherent feed-forward loop 119
Figure S5: Acid stress after acid adaptation 119
Figure S6: The role RNase III in ArsZ-HP1432 interaction *in vivo* 120
Figure S7: Global proteomic and transcriptomic analysis of WT and Δ*arsZ* strains for target identification 121

List of Tables

Table 1: The list of predicted target mRNAs in strain 26695 for ArsZ using TargetRNA 25
Table S1: The list of bacterial strains used in this study 122
Table S2: The list of plasmids used in this study 124
Table S3: The list of oligodeoxynucleotides used in this study 126
Table S4: The sequences of T7 transcripts used for *in-vitro* work 131

Abbreviation Index

A	adenine
aa	amino acid
Amp	ampicillin
APS	ammonium persulfate
asRNA	antisense RNA
ATP	adenosine triphosphate
BSA	bovine serum albumin
C	cytosine
cDNA	complementary DNA
CDS	coding sequence
CFU	colony forming units
CHAPS	3-[(3-Cholamidopropyl)dimethylammonio]-1-propanesulfonate
Cm	chloramphenicol
CO_2	carbon dioxide
DMSO	dimethyl sulfoxide
DNA	deoxyribonucleic acid
DNase	deoxyribonuclease
dNTP	deoxyribonucleotide
ds	double-stranded
DTT	dithiothreitol
EDTA	ethylenediamine tetraacetate
EtOH	ethanol
G	guanine
Gen	gentamicin
gDNA	genomic DNA
GFP	green fluorescent protein
H_2O	water (distilled)
H_2O_2	hydrogen peroxide
HCl	hydrochloric acid
HEPES	4-(2-hydroxyethyl)-1-piperazineethanesulfonic acid
IGB	Integrated Genome Browser
IGR	intergenic region
Kan	kanamycin
LPS	lipopolysaccharide
MOPS	3-(N-morpholino)propanesulfonic acid
mRNA	messenger RNA
N_2	nitrogen
NaCl	sodium chloride
NaOH	sodium hydroxide
OD_{600}	optical density at a wavelength of 600 nm
OE	overexpression
ORF	open reading frame
P	promoter
PAA	polyacrylamide
PAGE	polyacrylamide gel electrophoresis
PBS	phosphate buffered saline
PCR	polymerase chain reaction
Phu	Phusion polymerase
RBS	ribosome binding site
RNA	ribonucleic acid
RNase	ribonuclease
RNA-seq	RNA sequencing
RT	room temperature
rRNA	ribosomal RNA
rNTP	ribonucleotide
sRNA	small regulatory RNA
siRNA	short interfering RNA

SD	Shine-Dalgarno
SDS	sodiumdodecylsulfate
SNP	single nucleotide polymorphism
ss	single-stranded
Str	streptomycin
T	thymine
TAE	Tris/Acetate/EDTA
TBE	Tris/Borate/EDTA
TCS	two component system
TEMED	tetramethylethylendiamin
Tm	melting temperature
Tris	tris-(hydroxymethyl)-aminomethan
tRNA	transfer RNA
TSS	transcriptional start site
U	uracil
UTR	untranslated region
UV	ultraviolet
vol	volume
v/v	volume/volume
w/v	weight/volume in g/ml
WT	wild-type

Units

%	percent
° C	degree Celsius
A	ampere
bp	base pair(s)
Ci	Curie
Da	Dalton
g	gram
h/hrs	hour(s)
l	liter
M	molar
min	minute(s)
molar	gram molecule
nt	nucleotide(s)
pH	minus the decimal logarithm of the hydrogen concentration
rpm	rounds per minute
s/sec	second(s)
u	unit
V	Volt
W	Watt

Table of Contents

1. Introduction 1

1.1 The *Helicobacter* genus 1

1.2 Specific colonization and virulence strategies evolved by *Helicobacter pylori* 1

1.3 Acid acclimation by *H. pylori* urease 3

1.4 Regulation of acid-responsive genes by the ArsRS two component system 5

1.5 Bacterial sRNAs 8

1.6 Mechanisms of regulation by sRNAs 9

1.6.1 *cis*-encoded sRNAs 9

1.6.2 *trans*-encoded sRNAs 11

1.7 Regulatory networks involving sRNAs 13

1.7.1 Feedforward loop 13

1.7.2 Other network motifs 15

1.8 Physiological roles of sRNAs 16

1.9 Target identification for sRNAs 17

1.10 sRNAs in *Helicobacter pylori* 19

1.11 Aims of this thesis 20

2 Results 21

2.1 ArsZ is a highly conserved sRNA in *H. pylori* 21

2.2 Bioinformatics-based ArsZ target prediction 23

2.3 The ArsRS TCS regulates expression of ArsZ 26

2.4 *In-vitro* validation of ArsZ-HP1432 mRNA interaction 31

2.5 ArsZ negatively regulates HP1432 protein by masking its ribosomal binding site 34

2.6 ArsZ represses translation of HP1432 mRNA in *H. pylori in vivo* 36

2.7 ArsZ affects HP1432 mRNA stability 41

2.8 Introduction of a stable stem-loop enables strong overexpression of ArsZ 41

2.9 ArsZ forms a coherent feed-forward loop with ArsRS to regulate HP1432 in response to low pH 43

2.10 ArsZ modulates urease activity via repressing HP1432 under acid stress 45

2.11 ArsZ is required for downregulation of urease activity after acid stress 46

2.12 ArsZ confers a growth advantage after acid stress 47

2.13 Evolution of the ArsZ sRNA and its target gene HP1432 49

3 Discussion 58

3.1 Overall model for the regulation of HP1432 and urease activity by ArsZ in response to pH downshift 58

3.2 ArsZ is incorporated into the ArsRS TCS as a delay switch regulating HP1432 59

3.3 ArsZ provides the ArsRS TCS with a regulatory RNA arm to fine-tune urease maturation 62

3.4 Post-transcriptional regulatory mechanism of ArsZ 64
3.5 ArsZ may have been acquired by modern *H. pylori* strains to regulate HP1432 66
3.6 Elucidation of the role of sRNAs in the dense overlapping regulatory networks 67
4 Conclusions and outlook 69
5 Materials and Methods 72
5.1 Materials 72
5.2 Methods 85
6 References 99
7 Appendix 115
8 Curriculum vitae 134
9 Acknowledgement 135
10 Erklärung / Affidavit 136

1. Introduction

1.1 The *Helicobacter* genus

Helicobacter species are Gram-negative bacteria that belong to the epsilon subdivision of *Proteobacteria*. There are more than 20 described species belonging to the *Helicobacter* genus (Fox, 2002), which can be further divided into two major subdivisions, the gastric and non-gastric (enterohepatic) *Helicobacter* species. All members of the *Helicobacter* genus are microaerophilic and are highly adapted to their niche within the host (Kusters *et al.*, 2006). For example, the enterohepatic species such as *H. hepaticus* (Shames *et al.*, 1995), which colonizes the colon and liver of rodents, are unable to colonize the stomach, which is the niche of the gastric species and vice-versa (Solnick & Schauer, 2001). The gastric *Helicobacter* species are specialized in the colonization of their respective host gastric mucosae such as *H. felis*, which colonizes the stomach of cats (Lee *et al.*, 1988), *H. mustelae*, which infects ferrets (Fox *et al.*, 1988), and *H. acinonychis*, which commonly infects large felines such as cheetahs (Eaton *et al.*, 1993). Among the various *Helicobacter* species, *H. pylori* has the most significance to human health and thus, is the most studied and best characterized species.

1.2 Specific colonization and virulence strategies evolved by *Helicobacter pylori*

Despite its long association with humans since ~100,000 years ago (Moodley *et al.*, 2012), *H. pylori* was only discovered in 1984 by endoscopy of the stomach in patients suffering from gastritis (Marshall & Warren, 1984). Contrary to early ideas that the human stomach is sterile and that any bacterium found in the stomach was considered to be a result of contaminated food, the gastric environment is now estimated to support up to 200 different microbial species (Bik *et al.*, 2006). To date, *H. pylori* colonizes the stomachs of about 50 % of the world's population. Infection by *H. pylori* is generally acquired in childhood and colonization is usually asymptomatic until adulthood (Dorer *et al.*, 2009). Gastric colonization by *H. pylori* is often associated with peptic ulcers, chronic gastritis, and gastric cancer (Kusters *et al.*, 2006) (Wroblewski *et al.*, 2010). Thus, *H. pylori* is the only bacterium to be classified as a type I carcinogen by the World Health Organization (Cancer, 1994).

H. pylori uses a wide array of housekeeping genes and virulence factors to withstand the harsh acidic environment of the stomach, to colonize and adhere to gastric epithelial cells, to obtain nutrients, as well as to evade the host's immune response (de Reuse & Bereswill, 2007) (Josenhans *et al.*, 2007). The persistence of *H. pylori* in the human gut is aided by its ability to avoid detection by the host's innate and adaptive immune system. The pathogen-associated molecular patterns (PAMPs) associated with *H. pylori* have evolved to escape detection by pro-inflammatory Toll-like receptors (TLRs) and thus evading the

host's innate immunity. Evasion of adaptive immunity is achieved by modulation of the host's effector T-cells by the vacuolating cytotoxin protein (VacA) (Salama *et al.*, 2013) (Figure 1.1).

With a pH of 1-2, the stomach lumen is highly acidic and thus, a harsh environment for microbial survival and growth. As a neutralophile, *H. pylori* uses a unique acid acclimation strategy that is distinct from other neutralophiles or acidophiles (Krulwich *et al.*, 2011) to survive these drastic acidic conditions. During the initial stages of colonization, *H. pylori* needs to escape from the acidic lumen to the less acidic gastric mucus layer (pH 3-6), since *H. pylori* can survive only for a few minutes in the stomach lumen (Schreiber *et al.*, 2005). This is accomplished by rapid movement towards neutral pH along the pH gradient between the lumen and the gastric mucus layer. In turn, *H. pylori* loses its spatial orientation when the pH gradient in the stomach is disturbed (Schreiber *et al.*, 2004). Hence, in addition to flagella and its helical corkscrew morphology (Sycuro *et al.*, 2010), pH chemotaxis is important for successful colonization of the host (Terry *et al.*, 2005) (Rolig *et al.*, 2012). Moreover, *H. pylori* employs the urease enzyme, which converts urea to ammonium ions to increase the local pH around the cell (described in more detail below, Figure 1.3). At high pH, the gel-like gastric mucus undergoes transition into a less viscous solution-like layer (Celli *et al.*, 2007). This allows *H. pylori* to swim across the gastric mucos to reach the apical side of the underlying epithelium by reducing the viscoelasticity of the mucus (Celli *et al.*, 2009). In order to adhere to gastric epithelial cells, *H. pylori* uses several of its outer membrane proteins including BabA (Boren *et al.*, 1993) and SabA (Mahdavi *et al.*, 2002) as adhesins (Alm *et al.*, 2000).

H. pylori secretes two toxin proteins to manipulate host tissues and promote its own persistence. One is the 140 kDa VacA protein, which is present in all identified *H. pylori* strains. In addition to its pore-forming and apoptotic activity, VacA can affect mucosal barrier function by increasing the permeability of polarized cells (Palframan *et al.*, 2012) (Willhite *et al.*, 2003). Moreover, VacA can transverse via the paracellular route through disrupted tight junctions to inhibit T cell proliferation (Sundrud *et al.*, 2004). The second effector protein is the cytotoxin-associated gene A (CagA), which plays a major role in the gastric biology of *H. pylori* (Backert & Blaser, 2016). The 128 kDa protein is translocated into the host cell via the needle-like pilus type-IV secretion system (T4SS) (Kwok *et al.*, 2007) (Murata-Kamiya, 2011). After translocation into host cells, the EPIYA motif of CagA can be phosphorylated by SRC and ABL family kinases (Hayashi *et al.*, 2013). Both phosphorylated and unphosphorylated CagA bind to a variety of host proteins (Murata-Kamiya, 2011), resulting in host phenotypes that confer nutritional benefits for the bacteria (Tan *et al.*, 2011).

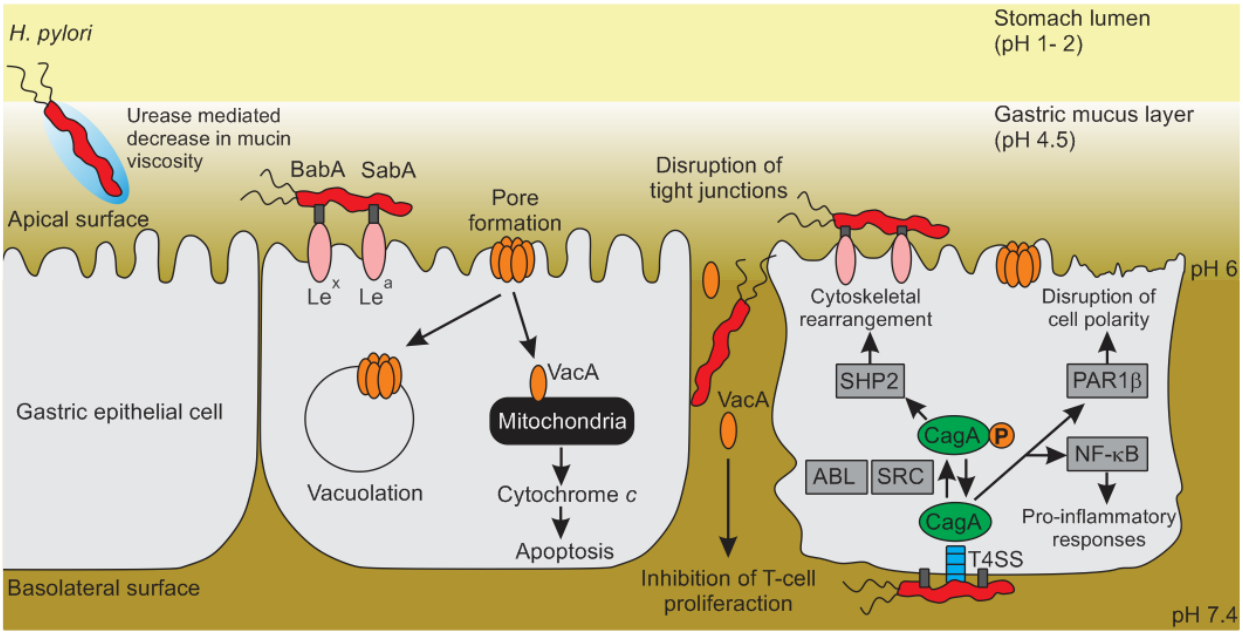

Figure 1.1: *Helicobacter pylori* colonization of the gastric mucosa. *H. pylori* escapes from the very acidic stomach lumen into the less acidic gastric mucus layer. The urease enzyme converts urea to ammonium ions to increase the local pH around the cell and to reduce viscosity of the mucus. This helps *H. pylori* to swim to the apical surface of epithelial cells and adhere to the cells using BabA and SabA adhesins. Oligomerization of secreted VacA promotes pore formation and vacuolization of the host cell. VacA interacts with mitochondria to trigger apoptosis. CagA is translocated into the host cell via the type-IV secretion system. Phosphorylated and unphosphorylated CagA interacts with host proteins to disrupt cell polarity and trigger cytoskeletal rearrangements.

1.3 Acid acclimation by *H. pylori* urease

pH homeostasis is important for physiology and survival of bacteria. Due to the limited range of pH within which their proteins can function, bacteria have evolved both active and passive strategies to maintain optimal pH when challenged with acid. One of the main strategy for active pH homeostasis is to use transporters such as primary proton pumps and secondary cation-proton antiporters to catalyze active proton transport (Krulwich *et al*., 2011). The proton motive force (PMF) generated via respiration in respiratory bacteria (*e.g*. *E. coli*) can be used to drive the proton transporters as well as to limit proton intake by reducing expression of ATPase, which brings protons into the cell (Slonczewski *et al.*, 2009). In non-respiratory bacteria (*e.g*. *Streptococcus mutants*), the F_1F_0 ATPase promotes the expulsion of protons (Kobayashi *et al.*, 1986). A second strategy involves upregulation of enzymatic reactions that consume cytoplasmic protons such as specific hydrogenases and decarboxylases (Slonczewski *et al*., 2009) (Maurer *et al.*, 2005) (Stancik *et al.*, 2002). Glutamate and arginine decarboxylases are crucial in the acid resistance response in

E. coli. Glutamate decarboxylase β (GadB) works together with an antiporter (GadC) to convert glutamate to γ-aminobutyric acid (GABA) (Foster, 2004) (Gut *et al.*, 2006). Moreover, passive pH homeostasis strategies that involve adaptation of surface proteins with residues containing high isoelectric points could be found in many bacteria including *H. pylori* (Tomb *et al.*, 1997). The positively charged surface proteins act as proton repellents. The composition of porins and membrane lipids could also be used to reduce inward proton leakage (Broadbent *et al.*, 2010) (Hayes *et al.*, 2006) (Kim *et al.*, 2005) (Shabala & Ross, 2008).

However, *H. pylori* uses a different active strategy to overcome extreme pH fluctuations that could be triggered during the transition between gastric starvation (pH 1) and digestive phase (pH 5) (Sachs *et al.*, 2003). This strategy known as periplasmic pH homeostasis utilizes the urease metalloenzyme, consisting of two polypeptide subunits, UreA and UreB, to cleave urea into ammonia (NH_3) and carbon dioxide (CO_2). The inactive apo-urease, a heterodimer encoded by the *ureAB* operon (Labigne *et al.*, 1991), requires four chaperones encoded by the *ureEFGH* transcript for insertion of 24 nickel ions (Ni^{2+}) to produce the final mature, active urease enzyme (Mobley *et al.*, 1995) (Figure 1.2 A).

Although *H. pylori* can produce urea endogenously using its arginase activity (McGee *et al.*, 2004), urea uptake from the host can be further promoted by the acid-activated urea channel UreI, which is required for colonization of the gastric mucosa (Mollenhauer-Rektorschek *et al.*, 2002) (Weeks *et al.*, 2000). The crystal structure of UreI, which was recently solved (Strugatsky *et al.*, 2013), has provided detailed insights into the mechanism of urea uptake by this protein. The UreI channel starts to open at pH 6.2, and is fully open when the pH is equal to or lower than 5.0 (Bury-Mone *et al.*, 2001), allowing urea uptake only at an acidic pH. The NH_3 and carbonic acid (H_2CO_3) that is produced by urease in the cytoplasm moves to the periplasm via UreI and buffers the periplasm ($H^+ + NH_3 \rightarrow NH_4^+$) while the H_2CO_3 is converted to CO_2 by the cytoplasmic β-carbonic anhydrase (Bury-Mone *et al.*, 2008). The CO_2 diffuses into the periplasmic space and is further converted into bicarbonate (HCO_3^-) by the periplasmic α-carbonic anhydrase (Marcus *et al.*, 2005). Together, the CO_2/HCO_3^- and NH_3/NH_4^+ acid-base pairs provide efficient buffering of the periplasmic space at pH 6 (Krulwich *et al*., 2011). To avoid excessive accumulation of ammonia and thus over-alkalinization of the cytoplasm, CO_2 and ammonia are transported out of the cytoplasm into the periplasmic space (Scott *et al.*, 2010).

In line with the importance of urease in acid acclimation, apo-urease is constitutively expressed in *H. pylori* (Akada *et al.*, 2000) at high levels, with concentrations reaching about 10 % of the total cellular protein content (Bauerfeind *et al.*, 1997). Moreover, urease has been shown to be essential for *H. pylori* colonization of the gastric mucosa and survival at acidic pH (Eaton & Krakowka, 1994) and is present in all known gastric *Helicobacter* species (Solnick & Schauer, 2001).

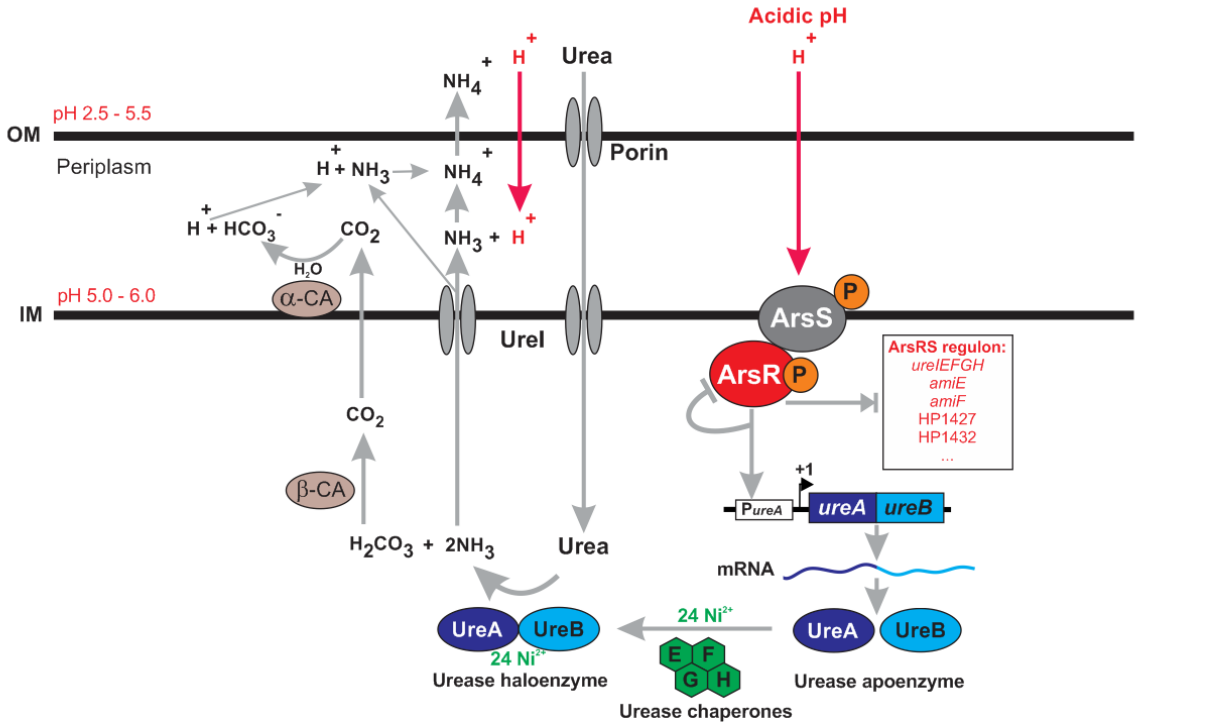

Figure 1.2: Periplasmic buffering and regulation of apo-urease by the ArsRS two-component system in *H. pylori*. The signal of acidic pH is transduced by the ArsRS two-component system (TCS), which regulates ~ 109 genes including the *ureAB* genes, which encode the subunits of the urease apo-enzyme (ArsRS regulon). The urease halo-enzyme converts urea into ammonia and carbonic acid. UreI release ammonia into the periplasmic space to buffer the acidic pH with the help of bicarbonate produced from α- and β-carbonic anhydrase enzymes.

1.4 Regulation of acid-responsive genes by the ArsRS two component system

The small *H. pylori* genome (1.67 Mb) encodes relatively few transcriptional regulators, including only three complete regulatory two-component systems (TCS) (Tomb *et al.*, 1997) (Scarlato *et al.*, 2001). In general, the function of these systems in bacteria is to sense a particular signal in the environment and trigger an appropriate adaptive response. TCS usually consist of a sensor kinase protein and a response regulator protein. A conserved histidine residue at the C-terminal domain of the sensor kinase is usually autophosphorylated in the presence of a certain stimulus. The cognate response regulator is often a transcriptional regulator with an N-terminal receiver domain and a C-terminal DNA-binding domain. The aspartic acid residue at the N-terminal receiver domain of the response regulator is modulated by the

phosphorylation state of the kinase. This in turn affects the DNA-binding activity of the response regulator and elicits the appropriate gene expression changes for the environmental signal.

One of the TCS in *H. pylori* responsible for sensing the environmental pH is the ArsRS (Acid responsive signalling) TCS (Beier & Frank, 2000) (Figure 1.2 B). The ArsRS TCS is important for acid adaptation in the gut, since a mutant without the ArsS sensor kinase is unable to colonize a mouse infection model (Panthel *et al.*, 2003). This TCS is also negatively autoregulated, since, an ArsR binding site was found downstream of the promoter and transcription start site of *arsR* (Dietz *et al.*, 2002) and transcription of the response regulator gene *arsR* is downregulated at a pH lower than 5 (Pflock *et al.*, 2006). Interestingly, while the sensor kinase gene *arsS* can be deleted without affecting *in-vitro* growth of *H. pylori*, the response regulator ArsR is essential (Beier & Frank, 2000). The *arsR* gene cannot be deleted, but can be rendered catalytically inactive by substituting the phosphate-accepting aspartic acid residue at position 52 with asparagine (D52N) (Schar *et al.*, 2005). This suggests that there are two distinct sets of genes belonging to the ArsRS regulon: one that is regulated by the non-phosphorylated ArsR, which is essential for growth, and a second that is regulated by the phosphorylated ArsR (ArsR~P) in response to acid. This idea was experimentally supported by a recent study using the ArsRD52N mutant under acidic and neutral conditions (Marcus *et al.*, 2016).

A total of 109 members of the ArsRS regulon were identified by transcriptional profiling of a wild-type and an *arsS* mutant strain (Pflock *et al*., 2006). 75 genes seemed to be activated by ArsRS, while 34 genes were negatively regulated by ArsR~P. In line with earlier observations that the promoter region of *ureAB* and *ureIEFGH* are regulated by ArsR~P (Pflock *et al.*, 2004) (Pflock *et al.*, 2005), all the genes encoded within the urease operons were found to be positively regulated by ArsR~P. Besides the urease operons, *amiE*, *amiF*, as well as genes encoding the two nickel-binding proteins HP1427 (Gilbert *et al.*, 1995) and HP1432 (Zeng *et al.*, 2008) showed the highest positive regulation by ArsRS under acidic conditions (Pflock *et al*., 2006). The *amiE* and *amiF* genes, which encode two aliphatic amidases (Skouloubris *et al.*, 2001), are part of the endogenous ammonia production pathway and are found in *Helicobacter* species that are able to colonize the stomach (Bury-Mone *et al.*, 2003).

Under acidic conditions, the solubility of metal ions such as nickel increases. Hence, the nickel-dependent regulator NikR was reported to affect a subset of acid responsive genes (Contreras *et al.*, 2003) and may play a role in acid adaptation (Bury-Mone *et al.*, 2004). The induced transcription of *nikR* under acidic conditions (van Vliet *et al.*, 2004b) is thought to be induced by increased bioavailability of nickel ions under acidic conditions (van Vliet *et al.*, 2004a). In addition, NikR is also negatively autoregulated (Contreras *et al*., 2003). The *ureAB* (van Vliet *et al.*, 2001) (van Vliet *et al.*, 2002) and HP1432

(Muller *et al.*, 2011) genes were shown to be also regulated by NikR in the presence of nickel. Moreover, *in vitro* studies showed that NikR binds directly to the promoter of *ureA* (Delany *et al.*, 2005) and HP1432 (Muller *et al.*, 2011). Interestingly, the ArsRS TCS was recently reported to be regulated by the iron-responsive ferric uptake regulator (Fur) via a metal-responsive DNA condensation mechanism (Roncarati *et al.*, 2016). Furthermore, NikR was reported to compete with Fur for binding upstream of the promoter region of *arsR* (Roncarati *et al*., 2016).

The levels of urease are regulated at multiple levels (Figure 1.3). First, the expression of the *ureAB* operon mRNA is controlled by transcription factors such as ArsR and NikR in response to acid and nickel (Contreras *et al*., 2003) (van Vliet *et al*., 2002). Additionally, the nickel-binding protein Mua represses the expression of *ureAB*, presumably to prevent overproduction of ammonia, which is detrimental to cells (Benoit & Maier, 2011). Next, *ureB* mRNA is post-transcriptionally downregulated by the *cis*-encoded small RNA (sRNA, see Figure 1.7 below) 5'*ureB*-sRNA at neutral pH. This *cis*-encoded sRNA induces degradation of *ureB* mRNA by base-pairing, resulting in reduced levels of UreB (Wen *et al.*, 2011). Finally, urease activity is also controlled on the post-translational level via regulated loading of its essential cofactor Ni^{2+} (Cussac *et al.*, 1992). In particular, the two histidine-rich proteins HP1427 (Hpn) and HP1432 (Hpn2), which are unique to the gastric *Helicobacter* species, are known to affect urease activity. Due to the presence of poly-Histidine residues, these proteins can bind to nickel and could serve as nickel storage proteins (Gilbert *et al*., 1995). Both HP1427 and HP1432 are regulated by NikR (Muller *et al*., 2011). HP1427 represent about 2 % of total proteins in *H. pylori* (Gilbert *et al*., 1995) and consists of 28 Histidine (His) residues. HP1432 consists of 16 His residues with glutamine (Gln) residues enriched at the C-terminal region. Both proteins can bind nickel with high affinity and other metal ions (zinc, cobalt, copper and bismuth) at lower affinity (Rowinska-Zyrek *et al.*, 2011) (Witkowska *et al.*, 2011) (Witkowska *et al.*, 2012) (Chiera *et al.*, 2013) (Zeng *et al.*, 2011).HP1427 and HP1432 exist as a 20-mer and 22-mer protein respectively. While each monomer of HP1427 binds 5 Ni^{2+} with a K_d of 7.1 µM (Ge *et al.*, 2006b) a single monomer of HP432 binds only 2 Ni^{2+} with K_d of 3.8 µM (Zeng *et al*., 2008). Although *in-vitro* purified HP1427 could form amyloid-like fibers and is cytotoxic to gastric epithelial cell cultures (Ge *et al.*, 2011) (Zhou *et al.*, 2014), the existence of such fibers has yet to be shown *in vivo*. The metal binding capacity of both proteins has been determined *in vivo* in *E. coli* by FRET and showed that Gln-rich domain do not affect the metal binding activity (Chang *et al.*, 2015). Expression of both proteins conferred protection against nickel toxicity in *E. coli* (Zeng *et al*., 2008) (Ge *et al.*, 2006a). *In-vivo* studies suggest that both proteins protect *H. pylori* against nickel toxicity (Mobley *et al.*, 1999) and play important roles in colonization of animal infection models (Benoit *et al.*, 2013) (Vinella *et al.*, 2015). The multitude of

regulatory factors modulating the levels of urease underscores the importance of precise control of this enzyme's activity in response to nickel availability and pH levels.

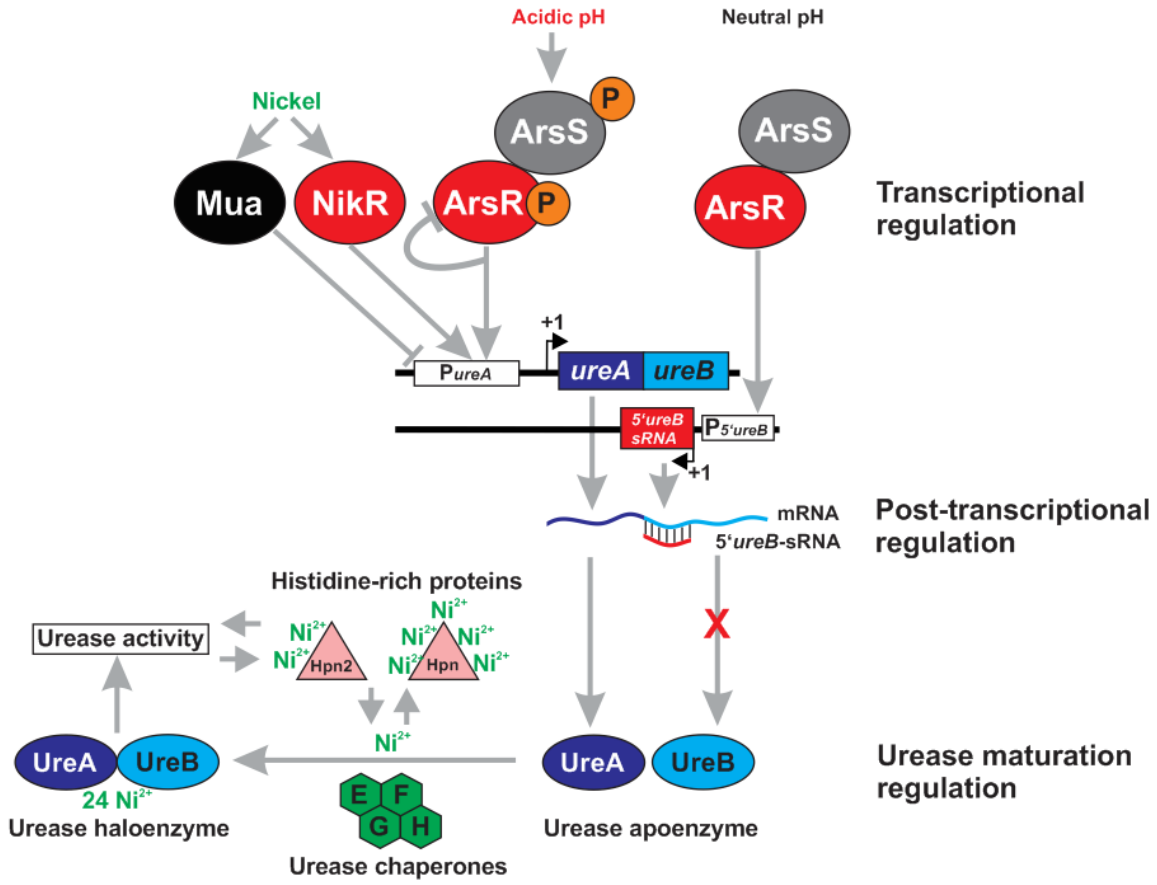

Figure 1.3: Regulation of urease expression at the transcriptional and post-transcriptional level as well as urease maturation regulation in *H. pylori*.

1.5 Bacterial sRNAs

The first bacterial regulatory RNAs were identified in the 1980s (Stougaard *et al.*, 1981) (Mizuno *et al.*, 1984) but the importance of this class of RNAs in various cell processes and adaptive responses has only been recognized rather recently (Papenfort & Vogel, 2010) (Storz *et al.*, 2011). In many cases, these RNAs have been found to be the missing links in bacterial regulatory pathways involved in fine-tuning of cell metabolism (Oglesby-Sherrouse & Murphy, 2013), quorum sensing, virulence (Roberts & Scott, 2007), and envelope stress (Chao & Vogel, 2016). Many of them have been discovered in various pathogenic and non-

pathogenic bacteria, resulting in numerous review articles detailing their regulatory mechanisms and functions (Storz *et al*., 2011) (Waters & Storz, 2009) (Caldelari *et al.*, 2013) (Svensson & Sharma, 2016). In general, sRNAs can be categorized into four classes based on their regulatory mechanism (described in more detail below, Figure 1.8): sRNAs that directly modulate protein activity, CRISPR RNAs (clustered regulatory interspaced short palindromic repeats), *cis*-encoded base-pairing sRNAs, and *trans*-encoded base-pairing sRNAs [104]. In addition, there are unique non-coding small RNAs that perform housekeeping functions such as tmRNA, which acts as both a tRNA and an mRNA to rescue stalled ribosomes (Moore & Sauer, 2007), 4.5S RNA, which is part of the signal recognition peptide (Herskovits *et al.*, 2000), as well as RNase P, which is involved in the processing of tRNAs and other RNAs (Kazantsev & Pace, 2006).

Bacterial sRNAs are typically 50-200 nt in length. They usually do not code for proteins (non-coding RNA), with a few exceptions such as RNAIII, SgrS, Psm-mec RNA, SR1 and Pel RNA that also encode for small peptides (Balaban & Novick, 1995) (Wadler & Vanderpool, 2007) (Kaito *et al.*, 2011) (Gimpel *et al.*, 2010) (Mangold *et al.*, 2004). Most of the characterized sRNAs interact with their target mRNAs by base-pairing to either activate or repress gene expression (Storz *et al*., 2011). A single sRNA can regulate multiple target genes (Papenfort & Vogel, 2009). There are also sRNAs that are encoded within the pathogenicity islands or virulence plasmids of various pathogenic bacteria (Pichon & Felden, 2005) (Padalon-Brauch *et al.*, 2008) and some of these sRNAs can also regulate genes from the core genome (Pfeiffer *et al.*, 2007).

1.6 Mechanisms of regulation by sRNAs

1.6.1 *cis*-encoded sRNAs

The *cis*-encoded sRNAs (asRNAs) are encoded on the opposite DNA strand of their target RNA and thus often share an extensive region of complementarity (75 nucleotides or more) to their targets (Wagner *et al.*, 2002). Both the sRNA and its target are transcribed independently of each other from opposite directions. The first identified asRNAs were found to control the copy number of mobile genetic elements by inhibiting primer formation and/or transposase translation (Brantl, 2007). Subsequent studies revealed asRNAs that are part of specific toxin-antitoxin (TA) systems (TA type I) (Brantl & Jahn, 2015). In this case, the asRNA functions as the antitoxin, which base-pairs with the toxin mRNA in order to inhibit its translation and additionally promote degradation of the transcript (Jahn & Brantl, 2013).

In general, asRNAs can exert either negative or positive regulatory effects on their target (Georg & Hess, 2011) (Thomason & Storz, 2010). An asRNA can be encoded complementary to the 5'UTR of its target gene to repress translation initiation (Figure 1.4 A). For example, the constitutively expressed

SymR asRNA in *E. coli* overlaps with the 5'UTR of *symE* mRNA and prevents translation of SymE, an SOS-response protein (Kawano *et al.*, 2007). It is not clear whether the mRNA degradation that ensues is triggered directly by base-pairing with SymR or if it is a secondary effect due to the lack of protection from actively translating ribosomes. Some asRNAs have been reported to trigger premature transcription termination of their target mRNA upon binding to its 5'UTR (Figure 1.4 B). In *Shigella flexneri*, the *icsA* mRNA, which encodes for a virulence protein, is regulated by the asRNA RnaG (Giangrossi *et al.*, 2010). The 5'UTR of *icsA* forms an anti-terminator hairpin structure that allows the mRNA to be transcribed in the absence of RnaG. Binding of RnaG to *icsA* mRNA promotes formation of a terminator hairpin structure, leading to transcription termination and formation of a truncated mRNA that does not encode the entire *icsA* open reading frame (ORF). Moreover, there are also asRNAs that are expressed antisense to coding regions of mRNAs (Figure 1.4 C). The IsiA protein is part of the iron stress response regulon of *Synechocystis* PCC6803, and is regulated by the asRNA IsrR (Duhring *et al.*, 2006). The asRNA is transcribed constitutively on the opposite strand of *isiA* in the middle of the ORF. Both RNAs exist as mutually-exclusive species. However, when *isiA* mRNA and IsrR are present simultaneously, they are rapidly co-degraded via an unknown mechanism.

Although negative regulation is a common mode of regulation for sRNAs, RNA duplex formation can also lead to mRNA stabilization (Figure 1.4 D). In *E. coli* the GadY asRNA is encoded on the opposite strand of its target's 3'UTR (*gadX*) (Opdyke *et al.*, 2004). The downstream gene of *gadX* is *gadW*. The bicistronic *gadXW* mRNA is unstable, and binding of GadY to *gadX* forms a duplex, which is cleaved by RNase III and promotes separation of *gadXW* into individual transcripts. The processed *gadX* and *gadW* mRNAs are more stable compared to *gadXW* (Tramonti *et al.*, 2008). The GadY asRNA is an interesting sRNA within the context of this thesis due to its role in acid adaptation. Further details regarding the physiological role of this asRNA is covered in the "Physiological roles of sRNAs" section.

Despite the large number of asRNAs that have been observed consistently in various bacterial transcriptome studies, it is still unclear whether all of these asRNAs are just pervasively transcribed due to transcriptional noise, or play actual regulatory roles (Wade & Grainger, 2014).

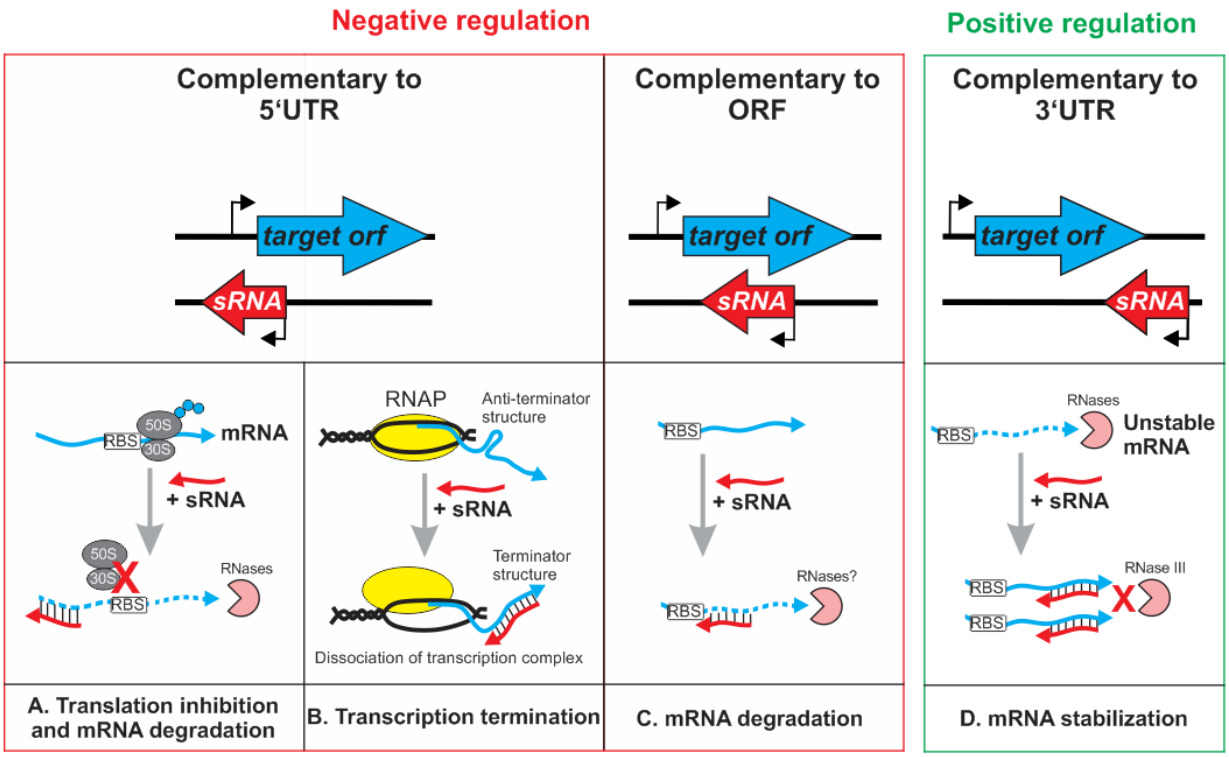

Figure 1.4: Mechanisms of post-transcriptional regulation by *cis*-encoded sRNAs. (Left red panel) An asRNA can negatively regulate its target by binding antisense to the 5'UTR or ORF of its target mRNA and induce translation inhibition, transcription termination or mRNA degradation. (Right panel) An asRNA can positively regulate target mRNAs by binding antisense to the 3'UTR of its target mRNA to stabilize the transcript.

1.6.2 *trans*-encoded sRNAs

In contrast to asRNAs, *trans*-encoded sRNAs (also commonly referred to as just "sRNAs") are encoded in a chromosomal locus that is distant from their targets (Figure 1.5). They share only limited complementarity with their target RNAs. Comparative analysis of many sRNAs in enterobacteria that require the RNA chaperone Hfq for proper function showed that these sRNAs have a modular structure. Most of these sRNAs have a short 6-7 nt single-stranded region termed the "seed region", which is required for interaction with target mRNAs (Papenfort *et al.*, 2010), followed by an AU-rich Hfq binding site and finally a transcription terminator loop [101]. In some cases, this base-pairing can be imperfect, with intervening non-complementary bases, allowing sRNAs to act as global regulators by interacting with multiple mRNAs (Valentin-Hansen *et al.*, 2007) (Bejerano-Sagie & Xavier, 2007) (Masse *et al.*, 2007), a role that was once thought to be performed solely by transcription factors. Moreover, a single mRNA can be targeted by multiple sRNAs, increasing the robustness of the regulatory network (Valentin-Hansen *et al.*, 2007).

In general, *trans*-encoded sRNAs can either repress or activate their target mRNAs. Most of these sRNAs repress protein levels post-transcriptionally by base-pairing at the 5'UTR region, which contains ribosome binding site (RBS) and start codon of their respective targets. This interferes with translation initiation and/or elongation of the target protein (Gottesman, 2005) (Figure 1.5 A). Small RNAs can also target regions that are further upstream or downstream from the canonical RBS region. For example, the GcvB sRNA can inhibit translation of its target *gltI* mRNA by binding at a C/A-rich translation enhancer element at -57 to -45 upstream of the start codon (Sharma *et al.*, 2007). On the other end of the spectrum, the MicC sRNA can target up to the 26th codon in the coding region of its target mRNA to promote mRNA degradation by RNase E (Pfeiffer *et al.*, 2009). This promotion of degradation is an indirect since non-translating mRNAs are not protected by ribosomes (Deana & Belasco, 2005) (Figure 1.5 B). Additionally, sRNAs such as SgrS and RyhB can promote degradation of target mRNAs by exposing the otherwise hidden RNase E cleavage sites (Morita *et al.*, 2005) (Bandyra *et al.*, 2012).

A subset of sRNAs can activate target mRNAs by increasing their translation or stability (Papenfort *et al.*, 2015). One of the earliest discovered of these mechanisms is termed anti-antisense control (Figure 1.5 C). In this situation, the long 5'UTR of the mRNA forms a structure that inhibits translation, typically by sequestering the RBS in stable secondary structures. Binding of a sRNA at an upstream region of the UTR increases the translation rate by disrupting such inhibitory secondary structures. The binding of a sRNA at sites upstream of the RBS promotes structural rearrangements, which increase the access of ribosomes to the RBS (Frohlich & Vogel, 2009). One such example is the DsrA sRNA that is induced by an increase in temperature. This sRNA binds to the 5'UTR of the *rpoS* mRNA, which encodes the alternative sigma factor σ-S, and promotes its translation (Lybecker & Samuels, 2007). Small RNAs can also stabilize their target mRNAs by blocking the access of their 5'UTR to ribonucleases (Figure 1.5 D). For example, the FasX sRNA of *Streptococcus* base-pairs with the 5'UTR of the *ska* mRNA and prevents its degradation by RNases (Ramirez-Pena *et al.*, 2010). This further promotes the translation of the *ska* mRNA, which encodes a secreted virulence factor streptokinase. In *Salmonella* enterica, the RydC sRNA protects its target *cfa* mRNA encoding the cyclopropane fatty acid synthase, from RNase E degradation by blocking the cleavage sites at the 5'UTR region.

Importantly, most of the known sRNAs can either be co-degraded with their targets (Masse *et al.*, 2003) or recycled to repress other mRNAs (Overgaard *et al.*, 2009). Moreover, there are also sRNAs that can function as both an activator and a repressor. In fact, the same sRNA can use up to four distinct mechanisms (catalytic degradation, coupled degradation, RBS sequestration without degradation, and activation by revealing the RBS) to regulate different target mRNAs (Feng *et al.*, 2015).

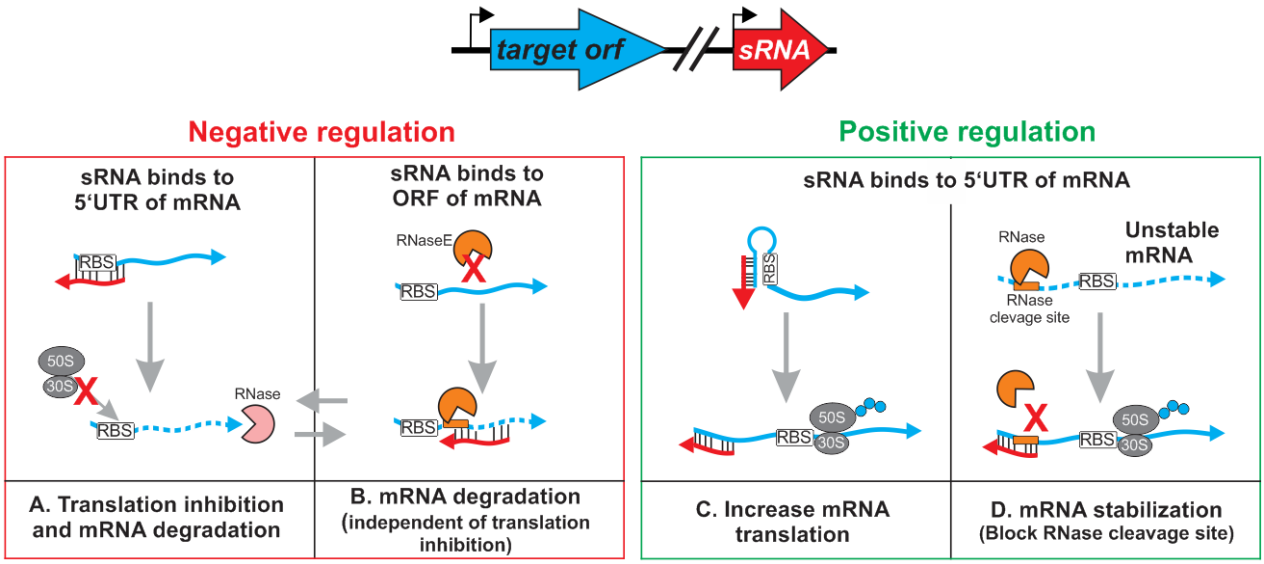

Figure 1.5: Mechanisms of post-transcriptional regulation by *trans*-encoded sRNAs. *trans*-encoded sRNAs are encoded in a chromosomal locus that is distant from their targets. These sRNAs negatively regulate their targets by binding to the 5'UTR or the ORF of their targets to promote translation inhibition and/or mRNA degradation. (Right green panel) Positive regulation by sRNAs is achieved by binding to the 5'UTR of mRNAs to increase their translation or stability.

1.7 Regulatory networks involving sRNAs

1.7.1 Feedforward loop

Bacteria often encounter environmental fluctuations in their respective habitats and have evolved recurring regulatory network motifs to respond to these stimuli (Shen-Orr *et al.*, 2002) (Alon, 2007). One of the most common network motifs found in nature is the so-called feed-forward loop (FFL) (Mangan & Alon, 2003). Such loops typically consist of two transcription factors (X and Y) that act in a hierarchical manner to regulate the expression of a third downstream gene (Z) (Milo *et al.*, 2002). There are eight possible configurations of FFLs (Figure 1.6 A). These loops can be divided evenly into coherent (C1, C2, C3, C4) and incoherent (I1, I2, I3, I4) FFLs (Mangan & Alon, 2003). Coherent FFLs feature both X and Y to synergistically regulate Z while incoherent FFLs consist of X and Y acting antagonistically to regulate Z (Mangan & Alon, 2003). Coherent FFLs have been proposed to act as persistence detectors by delaying response times while incoherent FFLs have been shown to act as pulse expressors by accelerating response times in transcription networks (Mangan & Alon, 2003). Interestingly, eukaryotic microRNAs (Gurtan & Sharp, 2013) and bacterial sRNAs (Beisel & Storz, 2010) (Papenfort *et al.*, 2015) have been

reported to replace the role of transcription factors (X or Y) in these networks. A post-transcriptional regulation is inserted into the FFL when X or Y is replaced by sRNAs and therefore are known as mixed FFLs (Mangan & Alon, 2003) (Mank *et al.*, 2013). These confer tight controlled inhibition or activation of target genes (Shimoni *et al.*, 2007). Moreover, mixed FFLs also reduce response time compared to protein-based regulators due to the absence of a translational step (Shimoni *et al*., 2007).

In *E. coli*, the expression of *ompF* and *ompC* encoding outer membrane proteins are regulated directly by the transcriptional regulator OmpR (Egger *et al.*, 1997) (Chen *et al.*, 2004). Additionally, OmpR directly activates expression of MicF and inhibits MicC, both of which post-transcriptionally repress *ompF* and *ompC* respectively. *ompF* is repressed by OmpR and MicF leading to increased inhibition of *ompF* while *ompC* is activated by OmpR and by de-repression of MicC (Aiba *et al.*, 1987) (Chen *et al*., 2004). In both cases, OmpR and the sRNAs act on the target mRNAs synergistically in the form of coherent FFLs. In *S. aureus*, the RNAIII sRNA directly activates *hla* mRNA encoding for hemolysin α and represses the Rot transcription factor. Inhibition of Rot by RNAIII increases transcription of *hla* since Rot represses *hla* (Morfeldt *et al.*, 1995) (Boisset *et al.*, 2007). Although the hierarchy of transcription factor and sRNA has been exchanged in this example, they nevertheless act as coherent FFL. A similar coherent FFL was recently found in *Salmonella* in the form of RprA/σ^S system, which regulates the *ricI* mRNA (Papenfort *et al*., 2015). Examples of sRNAs involved in incoherent FFLs include the RpoE/RybB (Gogol *et al.*, 2011) and PrrA/PcrZ systems in *E. coli* and *Rhodobacter* respectively (Mank *et al.*, 2012). The PrrA/PcrZ system contributes to the regulation of photosynthetic genes where PcrZ counteracts the expression of the photosynthetic genes at post-transcriptional level (Mank *et al*., 2012).

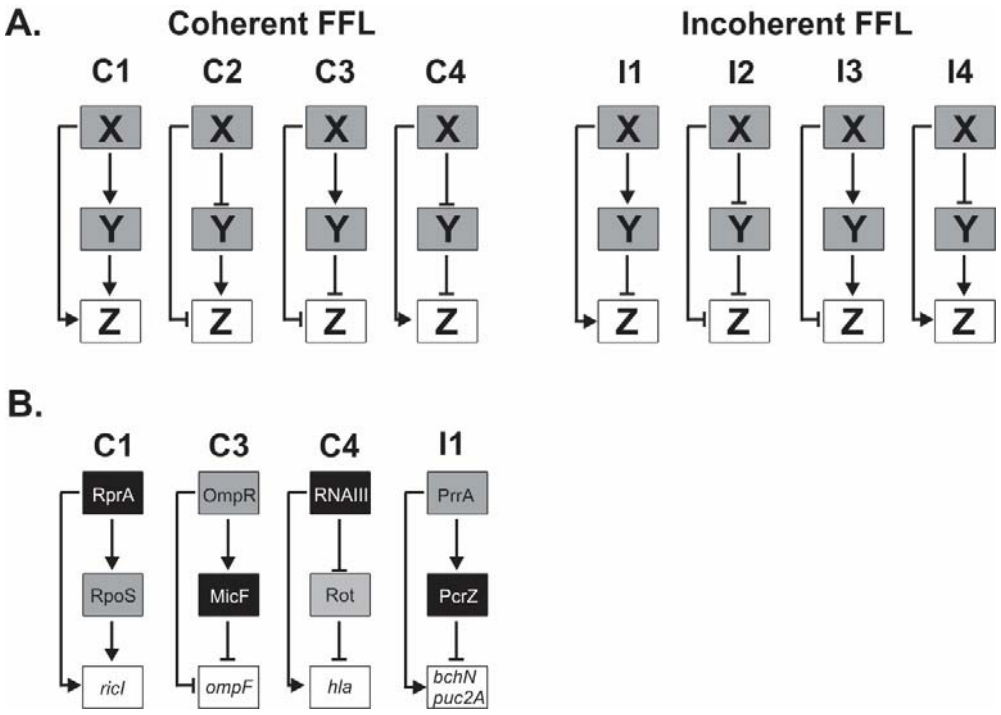

Figure 1.6: Structure of coherent and incoherent FFL motifs. (A) Eight different possible combinations of FFLs as described by Alon and co-workers (Mangan & Alon, 2003). X and Y represent upstream genes that control a third downstream gene, Z. (B) Examples of mixed FFLs in bacteria. The grey boxes refer to transcription factors while black boxes represent sRNAs.

1.7.2 Other network motifs

Besides the feedforward loop circuit, sRNAs have been found in other network motifs such as the single-input module (SIM), the dense overlapping regulon (DOR), and the feedback loop (Beisel & Storz, 2010). In a SIM regulatory circuit, a single regulator coordinates the expression of multiple genes. For example, the RyhB sRNA, which is regulated by the iron-responsive transcriptional regulator Fur, represses the expression of at least 18 operons involved in iron-utilization pathways (Masse *et al.*, 2005). Alternatively, a sRNA can regulate multiple genes indirectly by regulating a master regulator as in the case of the OxyS sRNA, which inhibits expression of *fhlA*, a transcriptional activator in order to downregulate operons involved in formate metabolism (Altuvia *et al.*, 1998). The DOR motif combines multiple SIMs that respond to different environmental stimuli. In *E. coli*, the alternative sigma factor σ^S is regulated by four different sRNAs: ArcZ, RprA, DsrA and OxyS (Altuvia *et al.*, 1997) (Majdalani *et al.*, 1998) (Majdalani *et al.*, 2002) (Papenfort & Vogel, 2009). These sRNAs are expressed under different conditions, suggesting that sRNAs help to integrate different stress signals to a common stress regulator, σ^S. Finally, sRNAs can

be incorporated into feedback loops to negatively regulate the expression of their own regulator. For example, OmrA and OmrB sRNAs inhibit expression of their regulator, OmpR to autoregulate their amount in each cell (Guillier & Gottesman, 2008).

1.8 Physiological roles of sRNAs

sRNAs play important biological roles in various cell processes such as metabolism, pathogenesis, and adaptation to stress (Michaux *et al.*, 2014). Under the cellular metabolism category, sRNAs have been shown to participate in carbon, amino acid, and iron regulation. In *E. coli*, the Spot42 sRNA controls sugar metabolism by preventing translation of the *galK* mRNA to mediate discoordinate expression of the *galETKM* operon, which encodes for enzymes that convert galactose to glucose-1-phosphate (Beisel & Storz, 2011). Moreover, the amino acid metabolism can be controlled by sRNAs as well. In *Salmonella* for example, high concentration of glycine induces expression of GcvB, a sRNA that targets various mRNAs encoding for amino acid transporters (Pulvermacher *et al.*, 2009) (Urbanowski *et al.*, 2000). Interestingly, GcvB enhances the ability of *E. coli* to survive acidic conditions by upregulating the translation of alternative sigma factor RpoS (Jin *et al.*, 2009). In *E. coli*, RyhB is important for adaptation to iron-limiting conditions (Richards & Vanderpool, 2011). This particular sRNA inhibits translation of new iron-utilizing proteins, redirecting cellular iron usage and making iron available for essential proteins (Masse & Gottesman, 2002) (Masse *et al*., 2003) (Masse *et al*., 2007). Moreover, sRNAs are capable of regulating quorum sensing and biofilm formation. In *Vibrio cholerae*, at low cell density, the response regulator LuxO induces expression of five sRNAs (Qrr1-5) (Bardill *et al.*, 2011). These sRNAs act redundantly to inhibit translation of three target genes involved in global regulation of *V. cholerae* pathogenicity (Lenz *et al.*, 2004) (Rutherford *et al.*, 2011) (Hammer & Bassler, 2007). Recently, it was reported that the Qrr sRNA uses up to four different mechanisms to regulate target mRNAs, each with distinct regulatory strength and dynamics (Feng *et al*., 2015). Since sRNAs participate in a wide range of cellular processes, they can influence the ability of pathogenic bacteria to persist during infection. There are also sRNAs that regulate expression of virulence factors. For example, the FasX sRNA in *S. pyogenes* directly controls the expression of adhesins and secreted virulence factors (Ramirez-Pena *et al*., 2010) while LhrA sRNA in *Listeria monocytogenes* regulates a chitinase gene, which contributes to pathogenesis in a mouse model (Mraheil *et al.*, 2010) (Mraheil *et al.*, 2011).

Importantly, many sRNAs are usually expressed in response to different environmental stresses (Hoe *et al.*, 2013). Transcription of the OxyS sRNA is induced by hydrogen peroxide via the OxyR regulator (Altuvia *et al*., 1997). OxyS in turn regulates the expression of *flhA* (Altuvia *et al*., 1998) and in the absence

of OxyS, the cells have been shown to be more susceptible to hydrogen peroxide and show attenuated colonization in a mouse model (Johnson *et al.*, 2006). Under osmotic stress, many sRNAs in *E. coli* including MicC, MicF, OmrA, OmrB and RybB are differentially expressed (Chen *et al*., 2004) (Ramani *et al.*, 1994) (Guillier & Gottesman, 2008) (Papenfort *et al.*, 2006). For instance, deletion of RybB results in increased resistance to envelope stress (Hobbs *et al.*, 2010).

There are currently only two known *cis*-encoded sRNAs, which are related to the acid stress response: 5'*ureB*-sRNA in *H. pylori* and GadY in *E. coli*. The glutamate-dependent (*gad*) system is the most effective acid resistance system in *E. coli* (De Biase *et al.*, 1999). GadA and GadB are two glutamate decarboxylase isoforms essential for conversion of glutamate to GABA (Castanie-Cornet *et al.*, 1999) (De Biase *et al*., 1999). The *gadA* gene is encoded within a 15 kb acid fitness island (Hommais *et al.*, 2004) that also includes the GadY sRNA as well as the acid-responsive transcriptional regulators GadX and GadW. GadY is highly expressed during stationary phase and at pH 5.5 (Tramonti *et al*., 2008). GadY base-pairs at the 3'end of *gadX* mRNA and confer increased stability. This leads to accumulation of *gadX* which upregulate expression of downstream acid resistance genes (Opdyke *et al*., 2004).

1.9 Target identification for sRNAs

Many experimental and computational approaches have been utilized to identify potential targets for sRNAs (Vogel & Wagner, 2007). Computational predictions are the least labour-intensive approach, utilizing various mathematical models and algorithms to identify potential base-pairings between sRNAs and target mRNAs (Pichon & Felden, 2008). However, these *in silico* approaches often predict false positives, depending on the software and parameters used for the prediction (Pain *et al.*, 2015). To reduce the high false positive rate, a new computational approach that combines phylogenetic information and target RNA predictions was recently introduced (Wright *et al.*, 2013). This method called CopraRNA (Comparative Prediction Algorithm for sRNA Targets), was shown to match microarray-based sRNA target prediction and represents a significant improvement over previous *in silico* methods.

Early discovery of sRNA targets via experimental methods have often relied on constitutive overexpression of sRNAs from strong promoters (Vogel & Wagner, 2007). Although this approach successfully identified targets for many sRNAs (Sharma & Vogel, 2009), overexpression of sRNAs may also be lethal for the cell in some cases such as overexpression of GcvB in *Salmonella* (Sharma *et al*., 2007). Comparison of the proteome profiles between sRNA deletion and wild-type strains, resolved by either 1D or 2D gel electrophoresis, has led to the identification of many targets. However, approaches that employ

constitutive overexpression or deletion of a sRNA are unable to distinguish direct targets from secondary targets. For example, constitutive overexpression of a sRNA may alter the whole protein profile indirectly leading to pleiotropic effects, especially if the target mRNA encodes a transcriptional regulator such as RpoS in *E. coli* (Lease *et al.*, 2004). To overcome this limitation, sRNAs have been pulse-expressed (10 to 15 minutes) in many bacteria such as *E. coli* or *Salmonella* to identify direct mRNA targets (Masse *et al*., 2005) (Papenfort *et al*., 2006). This system capitalizes on the strong, but tightly regulated, arabinose-inducible promoter to overexpress the sRNA just long enough to induce degradation of the direct target mRNA but stop short at triggering changes in protein levels that may lead to secondary effects. This pulse-expression system however is still lacking in many bacteria including *H. pylori*.

The *in-vivo* experimental methods described above are still limited to target identification for a single sRNA at a time. Interestingly, a few recent studies have now utilized a global approach to obtain global RNA inventories in various bacteria (Saliba *et al.*, 2017). RIP-seq (native RNA immunoprecipitation followed by RNA-seq) provides an overview on major RNA regulons. This method applies RNA-seq on transcripts pulled-down via co-immunoprecipitation (coIP) with an RNA binding protein (RBP) (Chao *et al.*, 2012). To further define the exact binding sites of the RBP, *in-vivo* UV treatment was introduced to covalently cross-link RNAs to proteins prior to coIP. This approach known as CLIP-seq (cross-linking immunoprecipitation high-throughput sequencing) allows stringent purification steps and reduces false-positive targets (Holmqvist *et al.*, 2016).

To map global sRNA-target interactions, two methods were recently developed (Melamed *et al.*, 2016) (Waters *et al.*, 2016). These approaches were inspired by an earlier study on the miRNA interactome in eukaryotes (Helwak *et al.*, 2013) and capitalize on the ability to pull-down sRNA-target pairs by using a tagged variant of either Hfq (Melamed *et al*., 2016) or RNase E (Waters *et al*., 2016). An RNA-RNA ligation step (ligating the Hfq-bound sRNA to its mRNA target) immediately after the pull-down, followed by stringent washing steps, ensures that direct interaction partners can be recovered with minimal bias. These global approaches do not require any prior knowledge of the RNA sequences and provide specific sRNA-target networks for each condition tested (Melamed *et al*., 2016). However, this approach requires a known global RNA-binding protein, and will also not identify sRNA-mRNA interactions that are chaperone or RNase-independent. Alternatively, to overcome the limitation of requiring a known RBP, MAP-seq (MS2-affinity purification coupled with RNA-seq) was used to purify RNA binding partners that co-purify with an MS2-affinity-tagged sRNA of interest (Lalaouna *et al.*, 2015). GRIL-seq (global small non-coding RNA target identification by ligation and sequencing) takes this approach a step further by expressing RNA ligase *in vivo* to ligate a sRNA to its target(s) prior to capturing of the RNA pairs with a sRNA-specific oligonucleotide (Han *et al.*, 2016).

Understandably, a major drawback of these transcriptome-based target identifications is the inability to directly discover effects on the translational level. To address this matter, ribosome profiling (Ribo-seq), which can simultaneously provide information on total RNA and translation levels *in vivo* has been used in bacteria to identify targets for sRNAs (Guo *et al.*, 2014) (Wang *et al.*, 2015). Actively translating ribosomes protects about 30 nucleotides of an mRNA from nucleases (Wolin & Walter, 1988). The Ribo-seq technique is based on deep-sequencing of ribosome-protected mRNA fragments termed ribosome footprints to estimate the rate of protein synthesis (Ingolia *et al.*, 2009) (Brar & Weissman, 2015). Although improvements in high-throughput techniques return many high-confidence targets, these sRNA-target pairs nevertheless still require further validation to determine their regulatory mechanism and physiological role in the cell.

1.10 sRNAs in *Helicobacter pylori*

In *H. pylori*, little is known about post-transcriptional regulation. Similar to 50 % of all sequenced bacteria, *H. pylori* does not encode a homolog of the RNA chaperone Hfq, a key player in sRNA-mediated regulation in enterobacteria (Chao & Vogel, 2010) (Vogel & Luisi, 2011) and was therefore thought to lack riboregulation alltogether. Moreover, a very limited number of regulatory RNAs were reported in *H. pylori* prior to 2010 (Xiao *et al.*, 2009a) (Xiao *et al.*, 2009b). However, a genome-wide differential RNA-seq study in *H. pylori* strain 26695 identified more than 60 candidate sRNAs (Sharma *et al.*, 2010), suggesting that an uncharacterized layer of post-transcriptional riboregulation is present in this pathogen (Pernitzsch & Sharma, 2012).

To date, only two *trans*-encoded sRNAs (RepG and CncR1) and two *cis*-encoded sRNAs (5'*ureB*-sRNA and IsoA1) have been characterized in *H. pylori*. RepG (HPnc5490) controls levels of the TlpB chemotaxis receptor by a novel mechanism involving interaction with a variable homopolymeric G-rich targeting sequence in the leader of the *tlpB* mRNA (Pernitzsch *et al.*, 2014). This particular sRNA can mediate both repression and activation of *tlpB* depending on the length of the G-repeat. The other sRNA CncR1 (HPnc2630) is encoded within the *cag* pathogenicity island and binds directly to *fliK* mRNA encoding a flagellar checkpoint protein. Although CncR1 negatively regulates motility of *H. pylori*, this effect is likely indirect through regulation of σ-54-dependent genes (Vannini *et al.*, 2016). While the first *cis*-encoded sRNA 5'*ureB*-sRNA regulates urease expression, the recently characterized IsoA1 acts as an RNA antitoxin in a Type I TA. The expression of the AapA1 toxin is inhibited via blocking of translation and subsequent degradation of the *aapA1* mRNA promoted by binding of IsoA1 (Arnion *et al.*, 2017).

However, the function of the remaining sRNAs identified in the transcriptome analysis (Sharma *et al*., 2010), including some sRNAs that were induced under acid, remain so far unknown.

1.11 Aims of this thesis

The importance of regulatory sRNAs in cellular processes and adaptive responses in bacteria are now widely recognized. Most of the knowledge about bacterial sRNAs has been revealed by work in model enteric organisms such as *E. coli* and *Salmonella* of the *Gammaproteobacteria* family. However, the sRNA repertoire between different microorganisms is not conserved, even among closely related bacteria (Updegrove *et al.*, 2015). The *Epsilonproteobacteria* family includes important human pathogens such as *C. jejuni* and *H. pylori*. Although many sRNAs have been discovered in these two members of this family (Dugar *et al.*, 2013) (Sharma *et al*., 2010), to date only a few of these sRNAs have been characterized.

ArsZ (HPnc2420) was originally identified in a transcriptome wide screen for regulatory RNAs in *H. pylori* (Sharma *et al*., 2010). This sRNA candidate is particularly interesting due to its abundance and high conservation in many *H. pylori* strains. Moreover, the presence of an anti-Shine-Dalgarno sequence within the single-stranded region of this sRNA indicates its potential to base-pair with target mRNA(s) and is thus unlikely to be a *cis*-encoded sRNA. These features suggest that ArsZ may play important role(s) in this highly specialized bacterium. However, the role of ArsZ in the biology of this pathogen was not yet known. The focus of this work is to understand the physiological role of ArsZ and its underlying regulatory mechanisms during acid adaptation in *H. pylori* by addressing its mRNA targets, and the phenotypes it controls in the cell.

2 Results

2.1 ArsZ is a highly conserved sRNA in *H. pylori*

ArsZ is a highly conserved, 105 nt-long sRNA that has been previously identified in *H. pylori* strain 26695 by differential RNA-seq (Sharma *et al*., 2010). The RNA secondary structure prediction tool mFold (Zuker, 2003) indicates that ArsZ consists of a single-stranded region (SSR) flanked by a 5' hairpin (SL1) and a 3' terminator stem-loop (SL2) in *H. pylori* 26695 (Figure 2.1 A). The SSR of ArsZ contains a potential anti-Shine-Dalgarno (SD) sequence "CTCCT" (indicated by blue letters in Figure 2.1 A), which could potentially bind to the ribosomal binding site (RBS) of target mRNAs. This suggests that ArsZ might act as a negative regulator of gene expression and competes with ribosome binding at target mRNA(s) at the post-transcriptional level. Synteny analysis of *arsZ* flanking genes showed that the genomic location of *arsZ* is highly conserved among diverse *H. pylori* strains. The *arsZ* gene is always encoded between the glutamine synthetase (*glnA*) and dihydropicolinate reductase (*dapB*) (Figure 2.1 B). Moreover, a putative urease-enhancing factor (blue arrows in Figure 2.1 B), HP0511, was identified downstream of *arsZ* in some strains. A multiple sequence alignment of *arsZ* homologues including its promoter region showed that the ArsZ nucleotide sequence is also highly conserved among different *H. pylori* species (Figure 2. 1 C). Expression of ArsZ is driven by a housekeeping, sigma-80 promoter, which contains an extended -10 motif (TGnTATAAT). Taken together, ArsZ fulfills many characteristics of a functional sRNA and the highly conserved anti-SD sequence could potentially regulate target mRNA(s) in *H. pylori.*

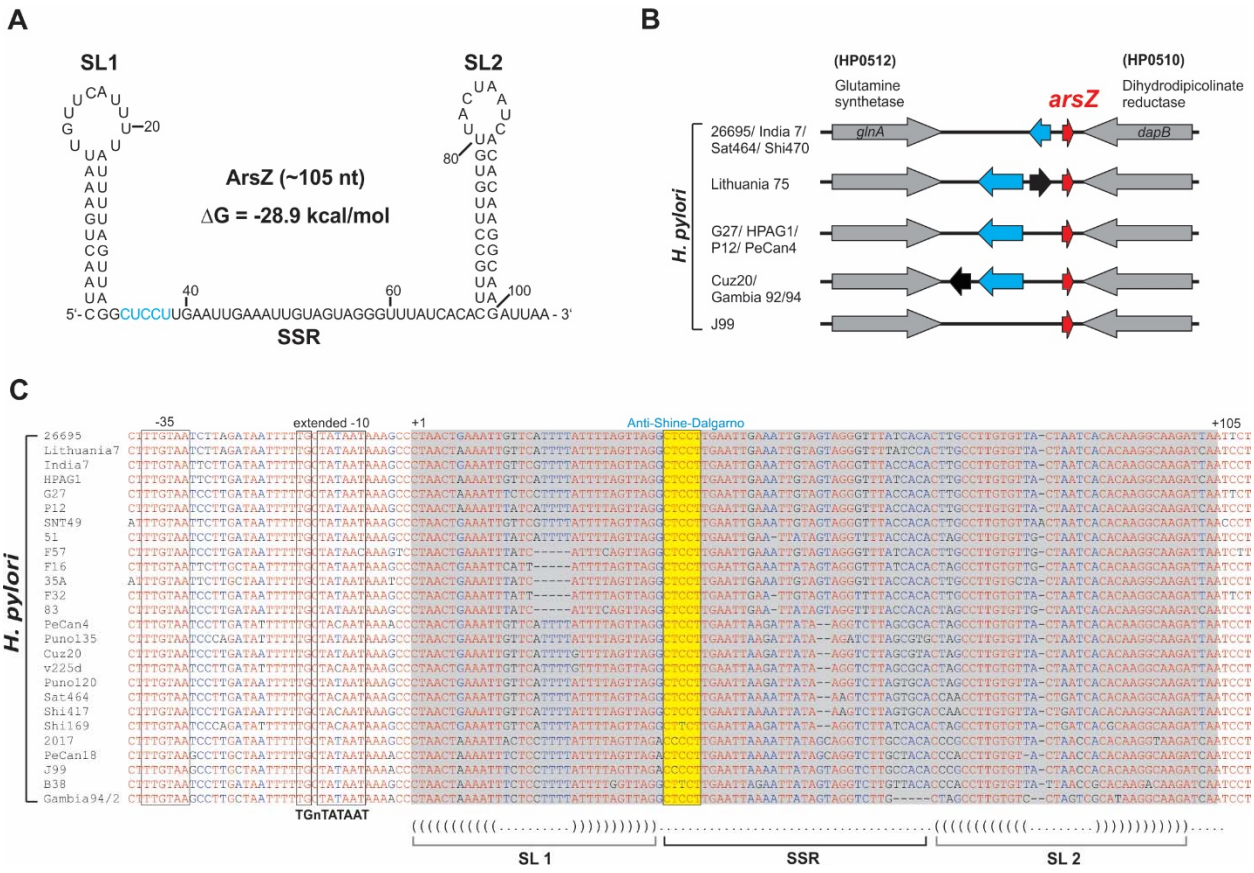

Figure 2.1: Conservation of ArsZ in diverse *H. pylori* strains. (A) The predicted secondary structure of ArsZ from *H. pylori* strain 26695 using Mfold (Zuker, 2003). (B) Genomic location of *arsZ*. In all the investigated *H. pylori* strains, *arsZ* gene (red) is flanked by a glutamine synthetase gene (HP0512) and an ORF encoding a dihydropicolinate reductase (HP0510). Gene names in brackets refer to those in strain 26695. A urease-enhancing factor (blue) or a hypothetical protein (black) are annotated upstream of *arsZ* in some *H. pylori* strains. (C) Multiple sequence alignment of genes encoding non-redundant *arsZ* sRNA homologues from different *H. pylori* strains. The -35 and extended -10 regions of the promoter are boxed. The 105 nt-long ArsZ sRNA (grey) contains a potential anti-Shine-Dalgarno sequence (yellow box) in a single-stranded region (SSR) flanked by a 5' stem-loop (SL1) and a terminator loop (SL2). The structure of ArsZ, as determined by in-line probing (Figure 2.1.10) and *in silico* predictions using Mfold (Zuker, 2003) for the *H. pylori* 26695 homologue, is indicated below the alignment with brackets (base-paired regions) and dots (single-stranded regions).

In this study, *H. pylori* strain 26695 preferentially served as the model strain. However, all experiments requiring a *gfp* reporter gene were conducted in strain G27 because GFP expression is toxic for strain 26695, according to previous observations (Pernitzsch *et al*., 2014). We first measured the levels of the ArsZ sRNA in the two model strains over growth. In nutrient rich BHI-medium and under neutral

pH conditions, northern blot analysis revealed that ArsZ is constitutively expressed from early log phase (OD_{600} of 0.2) to early stationary phase (OD_{600} of 2.0) in both *H. pylori* strains 26695 and G27 (Figure 2.2 A). Using a standard curve generated by predetermined amounts of *in-vitro* transcribed ArsZ, an average of 126 copies of ArsZ were estimated to be present in each *H. pylori* 26695 cell during mid-log growth phase (Figure 2.2 B). The copy number of ArsZ is comparable to sRNAs in enteric bacteria which is in the range of 10 to 300 copies per cell (Frohlich *et al.*, 2013) (Pfeiffer *et al.*, 2007) (Frohlich *et al.*, 2012), suggesting that ArsZ is a relatively abundant sRNA.

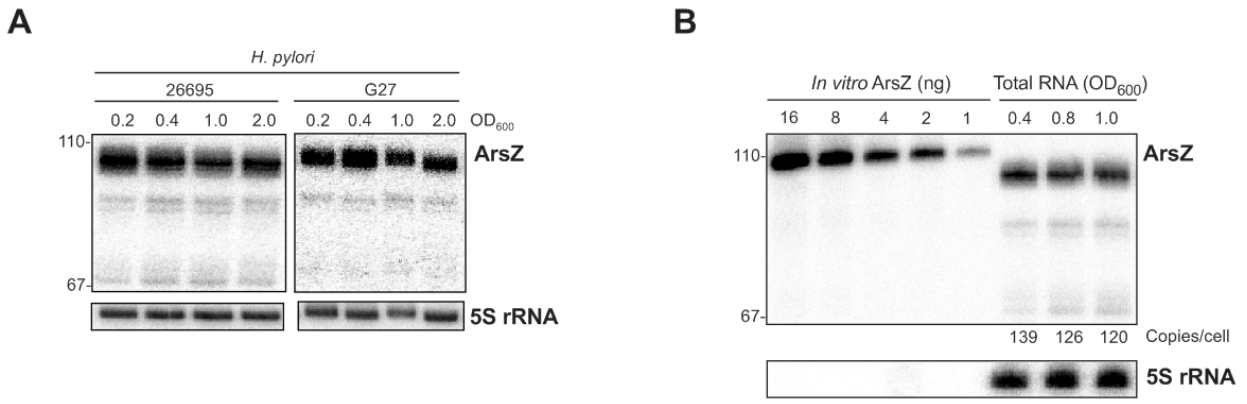

Figure 2.2: ArsZ is constitutively expressed during growth in rich medium at neutral pH. (A) Expression of ArsZ in *H. pylori* strains 26695 and G27 at different growth phases [OD_{600} of 0.2 (early log), 0.4 (mid-log), 1.0 (stationary), and stationary (2.0)] in standard BHI media (pH 7) was determined by Northern blot analysis. (B) Determination of ArsZ copy number in *H. pylori* 26695 over growth. Using Northern blot analysis, ArsZ levels at chosen growth phases (OD_{600} of 0.4, 0.8, and 1.0) were compared to predefined amounts of *in-vitro* transcribed ArsZ. The blot was probed for ArsZ, and the signal for the *in-vitro* transcribed ArsZ was used to create a standard curve. 5S rRNA served as a loading control.

2.2 Bioinformatics-based ArsZ target prediction

The bioinformatics tool TargetRNA (Tjaden, 2008) was applied to predict potential mRNA targets for ArsZ in *H. pylori* strain 26695. To reduce the number of false positive target mRNA candidates, the single stranded region of ArsZ containing the anti-Shine Dalgarno sequence as well as 50 nt upstream and 20 nt downstream of all mRNA translation start sites were used for prediction. Only target candidates with a p-value threshold of < 0.01 were considered for further analysis A total of 21 mRNAs were predicted to be targeted by the ArsZ sRNA. Among them, 14 genes have been reported to be regulated in response to acid

(Sharma *et al.*, 2010), five of which belong to the ArsRS regulon (Pflock *et al*., 2006). In line with the settings chosen for the prediction parameters, ArsZ was predicted to bind 17 out of 21 predicted targets within the Shine-Dalgarno region (Table 1). Overall, this *in-silico* target prediction indicated that ArsZ might base-pair and thus, regulate several mRNAs belonging to the regulon of the acid-responsive ArsRS TCS (Pflock *et al.*, 2006) (Figure 2.3 and Table 1). This includes the best-scoring target, HP1432 mRNA, which encodes a histidine- and glutamine-rich nickel-binding protein (also known as Hpn2). The low free energy of hybridization (-27.2 kcal mol^{-1}) predicted for this interaction suggests that ArsZ has the potential to form a stable 19-nt-long duplex with HP1432 mRNA in strain 26695. Due to the high sequence conservation of the interaction sites, a similar interaction between ArsZ and HP1432 mRNA could be also predicted for various other *H. pylori* strains (Figure 2.3 B).

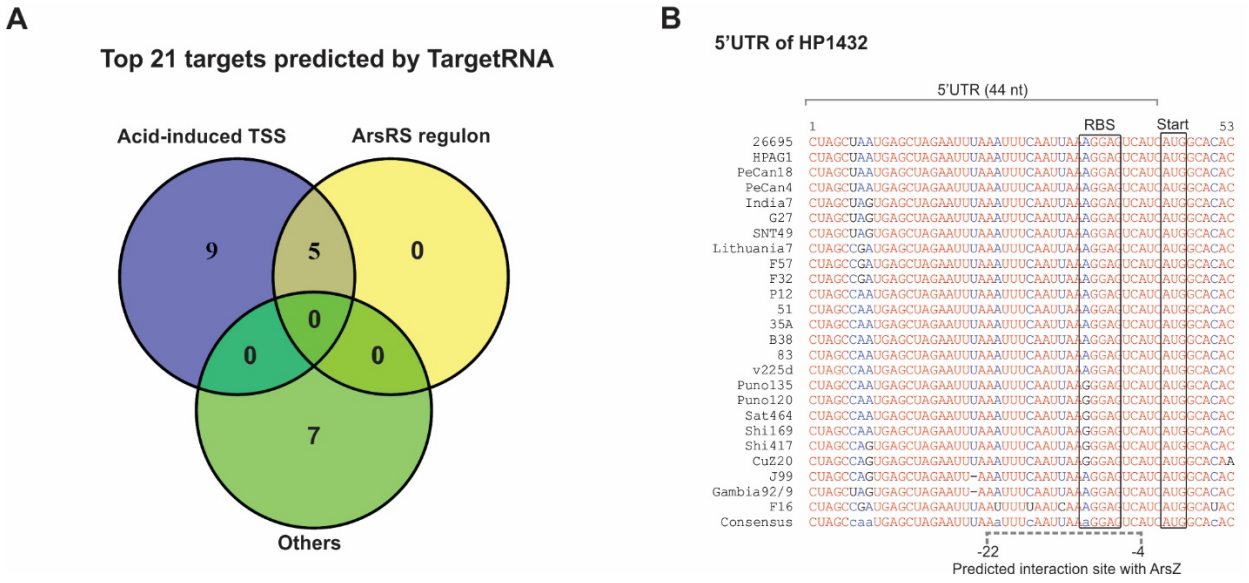

Figure 2.3: Bioinformatics-based target prediction for the ArsZ. (A) The top 21 mRNA targets of ArsZ as predicted by TargetRNA using the single-stranded region of ArsZ in *H. pylori* strain 26695. (B) Sequence alignment of the 5'UTR of HP1432 in various *H. pylori* strains. Only the 5'UTR and first three codons of HP1432 are shown. The dashed lines indicate the predicted interaction site of HP1432 and ArsZ.

Table 1: List of predicted ArsZ target mRNAs using TargetRNA (Tjaden, 2008). Targets in bold are also regulated by the ArsRS TCS (Pflock *et al.*, 2006) (Loh *et al.*, 2010). TSS is the abbreviation for transcription start site.

Rank	Target	Gene name	Functional class	p-value	Anti-SD	Acid-induced TSS (Sharma *et al.*, 2010)	Regulated by ArsRS
1	**HP1432**	*hpn2*	Transport and binding protein	0.00005	YES	YES	(Pflock *et al.*, 2006) Activated
2	HP1091	*kgtP*	Transport and binding protein	0.00025	YES	NO	NO
3	**HP0891**	-	Fatty acid and phospholipid metabolism	0.00069	YES	YES	(Pflock *et al.*, 2006) Activated
4	HP1193	-	Energy metabolism	0.00069	YES	NO	NO
5	HP0139	-	Hypothetical	0.00084	YES	YES	NO
6	HP0896	*babA*	Cell envelope	0.00084	YES	YES	NO
7	HP1268	*nuoI*	Energy metabolism	0.00152	YES	NO	NO
8	HP1413	-	Hypothetical	0.00152	YES	YES	NO
9	HP1086	*tlyA*	Virulence	0.00186	NO	NO	NO
10	HP0052	-	Hypothetical	0.00227	YES	YES	NO
11	**HP0695**	*hyuA*	Amino acid biosynthesis	0.00278	YES	YES	(Loh *et al*., 2010)
12	**HP0953**	-	Hypothetical	0.00278	YES	YES	In operon with HP0954 (Pflock *et al.*, 2006) Activated
13	**HP0243**	*napA*	Transport and binding protein	0.00338	YES	YES	(Pflock *et al.*, 2006) Activated
14	HP0920	-	Hypothetical	0.00338	YES	YES	NO
15	HP0926	-	Hypothetical	0.00338	YES	NO	NO
16	HP0993	-	Hypothetical	0.00338	YES	YES	NO
17	HP0838	-	Hypothetical	0.00412	NO	NO	NO
18	HP0263	*hpaim*	DNA metabolism	0.00614	NO	NO	NO
19	HP0217	*cgtA*	Cell envelope	0.00749	YES	YES	NO
20	HP0371	*aacB*	Fatty acid and phospholipid metabolism	0.00914	NO	YES	NO
21	HP0546	*cagC*	Virulence	0.00914	YES	YES	NO

2.3 The ArsRS TCS regulates expression of ArsZ

Since several members of the ArsRS regulon were predicted to be targeted by the ArsZ sRNA, we reasoned that the expression of the sRNA itself might also be controlled by the ArsRS TCS. The ArsS sensor kinase is activated under low pH conditions and phosphorylates its cognate response regulator ArsR (Pflock *et al*., 2004, Wen *et al.*, 2006). As an initial screen, levels of ArsZ in individual mutants of *arsS* and also *flgS* were checked on a Northern blot (Figure 2.4 A). FlgS is a cytoplasmic sensor kinase that is responsible for sensing extremely low pH (pH 2.5) (Wen *et al.,* 2009). Already under neutral pH conditions, a significant increase in ArsZ levels was only observed in the Δ*arsS* mutant background, suggesting that ArsZ is specifically regulated by the ArsRS TCS.

To determine whether the phosphorylated form of the response regulator ArsR (ArsR~P) plays a role in affecting expression of ArsZ, sRNA levels were monitored in a *H. pylori* 26695 strain, in which the response regulator cannot be phosphorylated (ArsR D52N) (Schar *et al*., 2005) as well as in the Δ*arsS* mutant. ArsZ sRNA levels were almost three-fold elevated in the Δ*arsS* strain compared to WT at pH 5.5 (Figure 2.4 B, lanes 1-2, and Figure 2.4 C), suggesting that ArsZ is negatively regulated by ArsRS. A weaker, but significant 1.5-fold up-regulation of the ArsZ sRNA was also observed in the ArsR D52N mutant (Figure 2.4 B, lanes 1 and 3, and Figure 2.4 C), suggesting that phosphorylated ArsR represses ArsZ expression *in vivo*. At neutral pH 7, a smaller regulation of ArsZ levels (1.6-fold and 1.3-fold) was observed in the Δ*arsS* deletion strain and ArsR D52N, respectively.

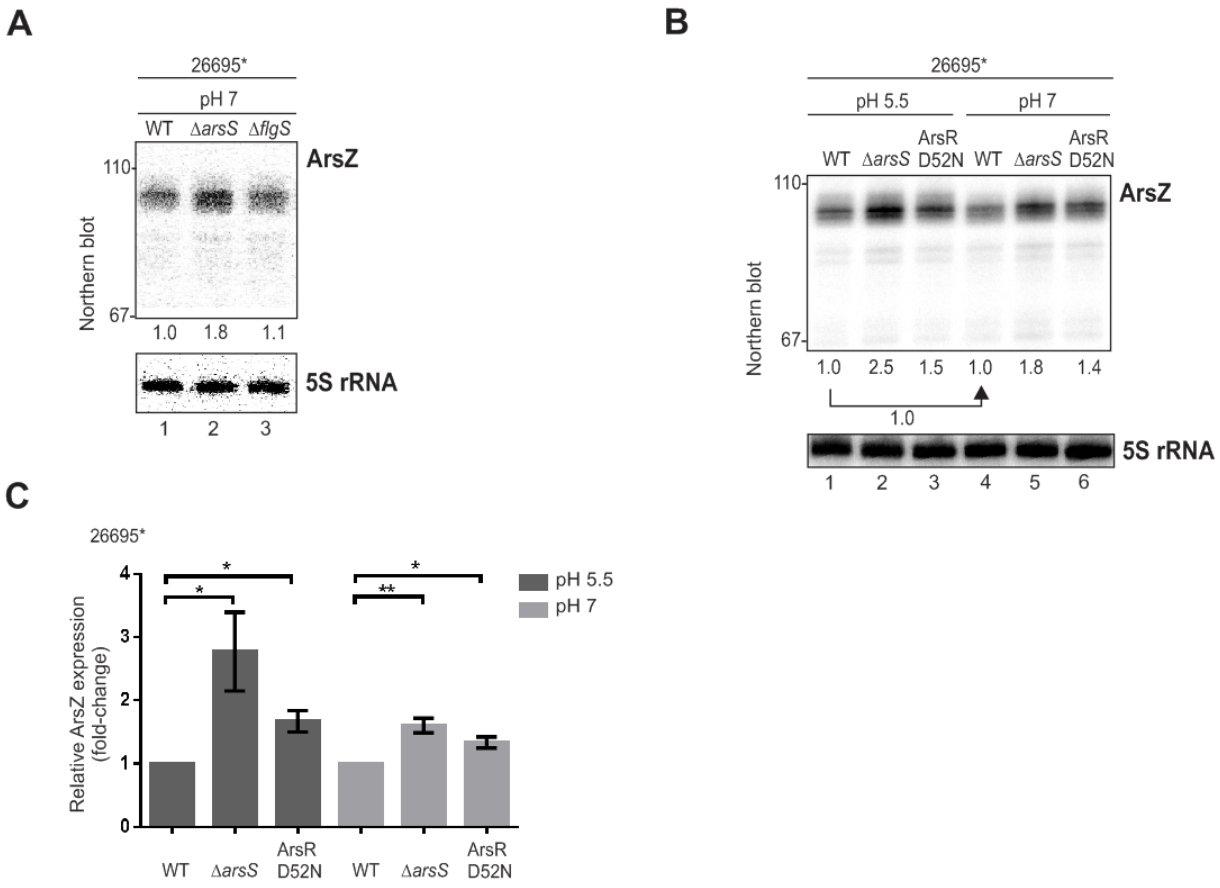

Figure 2.4: ArsZ is regulated by the ArsRS two-component system. (A) ArsZ expression in *arsS* and *flgS* deletion mutant backgrounds was compared to the wild-type (WT) of *H. pylori* strain 26695 at pH 7. The asterisk next to the strain number indicates that a 26695 strain background from the Dagmar Beier lab was used (see materials and methods section for details). (B) ArsZ expression analyzed in an *arsS* deletion mutant and an ArsR D52N mutant (unable to be phosphorylated), and compared to the wild-type strain (WT) at pH 5.5 and pH 7. All strains were grown to an OD_{600} of 0.8. Total RNA was analyzed by Northern blot using a specific oligonucleotide for ArsZ. The expression in each mutant strain was quantified and represented as fold-change relative to WT. 5S rRNA levels served as a loading control. (C) Quantification of ArsZ expression in WT, *arsS* deletion mutant and an ArsR D52N mutant (shown in B). Data are the average of three independent experiments, with error bars representing standard errors. The Student's *t*-test was used for statistical analysis. A single asterisk indicates a *p*-value of less than or equal 0.05; double asterisks indicate a *p*-value of less than or equal 0.01; ns: not significant (*p*-value > 0.05).

Due to technical issues in our *in-vitro* DNaseI footprinting assays, we were not able to show that the *arsZ* promoter is a direct target of the ArsR response regulator. Therefore, transcriptional *gfp* reporter fusions were chosen to investigate whether the activity of the *arsZ* promoter is affected by the ArsRS TCS *in vivo*. In these, 144 nt upstream of the *arsZ* TSS (originated from *H. pylori* strain 26695) were fused to a

gfp transcriptional reporter construct and introduced in the unrelated *rdxA* locus of both the WT strain and the Δ*arsS* mutant of *H. pylori* strain G27 (Figure 2.5 A). As a negative control, the promoter region of the *tlpB* gene, which is not regulated by the ArsRS TCS (Delany *et al.,* 2002, Pflock *et al.,* 2006), was fused to the same *gfp* transcriptional reporter and also introduced into the WT and Δ*arsS* mutant strains. The promoter region of the *ureA* gene, which is activated by the ArsRS TCS (Pflock *et al*., 2005), was included as positive control. Western blot analysis revealed three-fold increased GFP protein levels in the Δ*arsS* mutant when compared to the WT strain at pH 5.5 (Figure 2.5 B, lane 2-3) and pH 7 (Figure 2.5 B, lane 9-10), confirming that the *arsZ* promoter is de-repressed in the absence of ArsS. In contrast, no significant change in GFP protein levels was observed between the Δ*arsS* mutant and WT when *gfp* expression was driven from the *tlpB* promoter (Figure 2.5 B, lanes 4-5 and 11-12). The strength of the *ureA* promoter was about seven-fold downregulated in Δ*arsS* when compared to the WT strain (Figure 2.5 B, lanes 6-7) at pH 5.5, but not at pH 7 (Figure 2.5 B, lanes 13-14). Northern blot analyses confirmed that ArsZ is upregulated in all G27 Δ*arsS* background strains (Figure 2.5 B, lanes 3, 5, 7, 10, 12 and 14), similar to what is observed in strain 26695 (Figure 2.4 B). Overall, these *in-vivo* results indicate that the expression of ArsZ sRNA is repressed by the ArsRS TCS at low and neutral pH conditions. Referring to the conserved ArsRS binding motif identified in the *arsZ* promoter region, this might be likely due to direct binding of the response regulator.

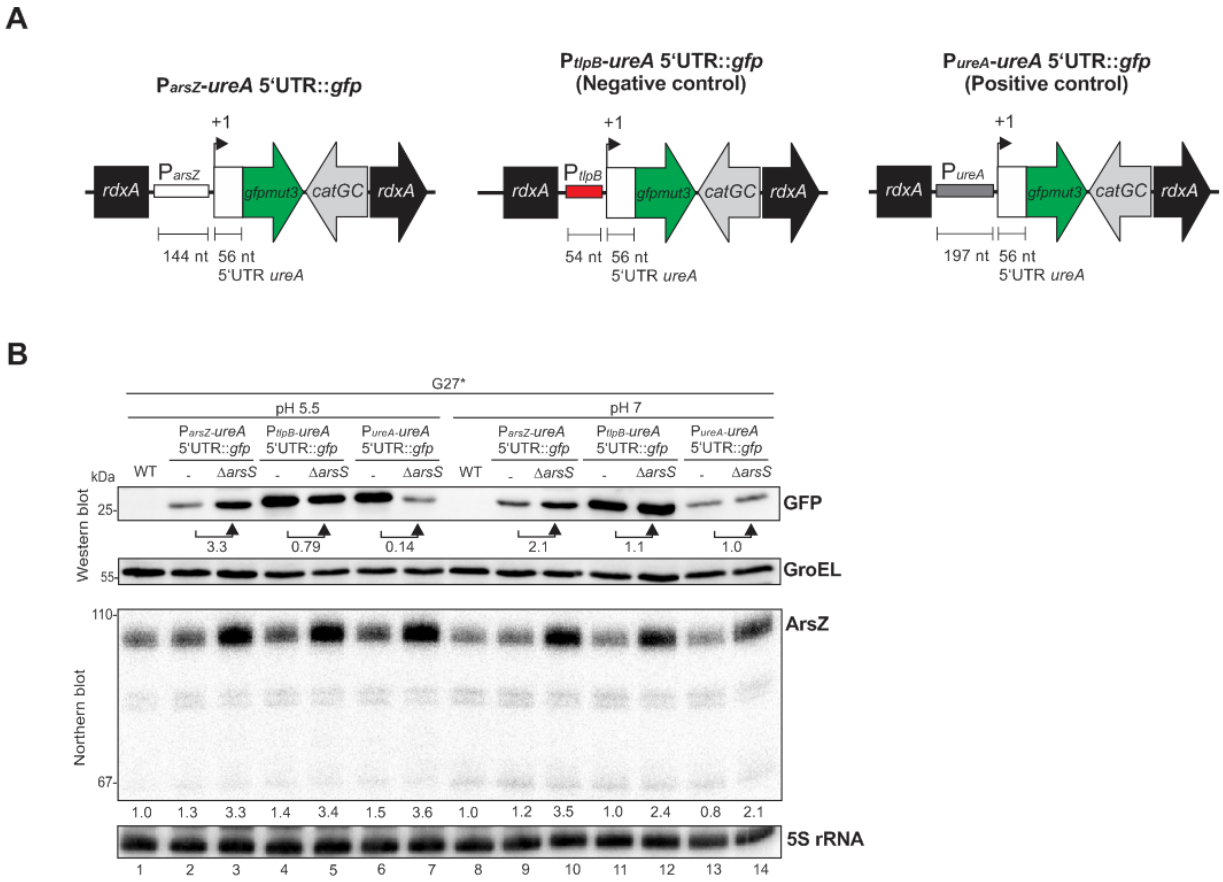

Figure 2.5: The promoter of ArsZ is de-repressed in the absence of the ArsS sensor kinase. (A) The promoter region of *arsZ* from strain 26695 was transcriptionally fused to a *gfp* reporter gene and integrated into the *H. pylori* G27 genome at the unrelated *rdxA* locus. As negative control, the promoter of *tlpB* was transcriptionally fused to *gfp*. The promoter of *ureA,* which is known to be activated by the ArsRS TCS, was included as positive control. (B) Levels of the GFP protein and ArsZ sRNA in the absence or presence of ArsS were analyzed by Western and Northern blotting, respectively. Total protein and RNA samples were harvested from indicated wild-type and mutant strains grown o log phase at pH 5.5 and pH 7. An anti-GFP antibody was used to monitor GFP protein levels, while GroEL served as a loading control. The expression of ArsZ was quantified by Northern blot. 5S rRNA served as a loading control.

Although ArsR is phosphorylated under low pH (Pflock *et al.,* 2005, Wen *et al.,* 2006) and we observed a de-repression of the *arsZ* promoter in the absence of the ArsS sensor kinase (Figure 2.6), no decrease in ArsZ sRNA levels was observed over growth in the *H. pylori* 26695 WT strain at pH 5.5 when compared to pH 7 (Figure 2.4 B lanes 1 and 4). Despite *H. pylori* grows slightly slower at pH 5.5, all samples were harvested at a similar OD_{600}. Since the strains were grown at low pH during the whole experiment, one possible explanation is that the acid-responsive system may have already achieved a

steady-state level, thus masking any regulatory effect on ArsZ sRNA expression. To further illustrate the dynamics of ArsZ regulation by low pH, presumably via the ArsRS TCS, expression of ArsZ sRNA was monitored over a time-course of eight hours upon shift of the *H. pylori* 26695 wild-type and ArsR D52N mutant strain from neutral pH to pH 5 (Figure 2.6). In WT, the levels of ArsZ were decreased by about four-fold after two hours of acid exposure when compared to ArsZ levels before the shift of the bacteria to low pH (time 0) and remained low for the following two hours. ArsZ levels then returned to initial levels after eight hours of acid exposure. This is consistent with the absence of lowered ArsZ levels at pH 5.5 observed under steady-state conditions (Figure 2.4 B, lanes 1 and 4). Importantly, and in contrast to the WT, only a slight decrease in ArsZ expression was observed in the ArsR D52N mutant (grey dotted line) over time, suggesting that ArsZ is specifically repressed by phosphorylated ArsR in response to acid exposure. In control experiments where the pH was kept constant at pH 7, ArsZ levels increased only slightly over time in both WT and ArsR D52N (solid black and grey lines). Together, these results strongly suggest that ArsZ is an acid-responsive sRNA regulated by the ArsRS TCS.

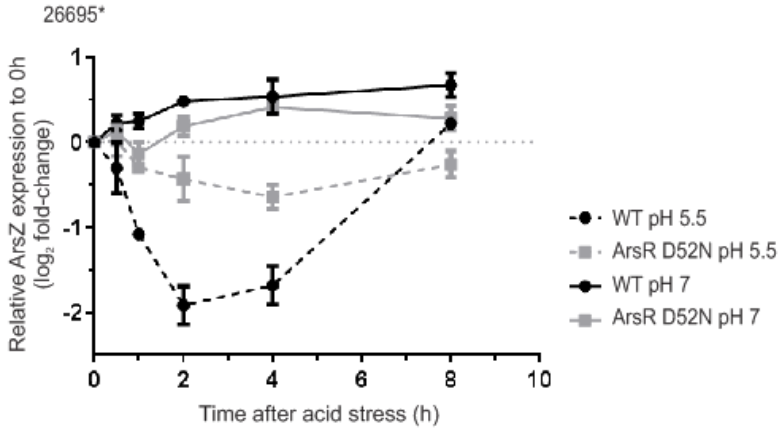

Figure 2.6 ArsZ is regulated in response to low pH through the phosphorylated ArsR response regulator. All strains were grown to an OD_{600} of 0.4 at pH 7. The medium was then either adjusted to pH 5.5 (dotted lines) or maintained at pH 7 as a control (solid lines). ArsZ levels from various time points throughout the acid time-course were quantified by Northern blot analysis (see also Figure S2). The fold-change is shown as the $\log_2$ ratio of a specific time point relative to the time point where medium pH was changed (0 hours). The data shown are the average of two independent experiments, with error bars representing standard errors.

2.4 *In-vitro* validation of ArsZ-HP1432 mRNA interaction

After clarifying ArsZ sRNA regulation, we further investigated the regulation of its predicted mRNA targets. Inspection of the HP1432 mRNA leader, the best-scoring ArsZ target predicted by TargetRNA, revealed a potential for extensive base-pairing between the sRNA and the ribosomal binding site (RBS) of the mRNA (Figure 2.7 A). In particular, the potential anti-Shine-Dalgarno (SD) sequence of ArsZ forms eight consecutive base-pair interactions with the RBS of the HP1432 mRNA, followed by a small bulge and a second stretch of ten consecutive base-pair interactions covering up to 22 nt upstream of the HP1432 start codon. Electrophoretic gel mobility shift assays (EMSAs) with radiolabeled *in-vitro* transcribed ArsZ and the unlabelled HP1432 5'UTR confirmed that both RNAs could bind each other (Figure 2.7 B, top left panel). *Vice versa*, radiolabeled, *in-vitro* transcribed HP1432 5'UTR showed a similar shift with increasing concentrations of the ArsZ sRNA (Figure 2.7 B, top middle panel). In contrast, HP1432 5'UTR did not shift with the *H. pylori* RepG sRNA, which is not predicted to interact with HP1432, *in vitro* (Figure 2.7 B, top right panel). Importantly, introduction of three consecutive point mutations (M3) into the predicted ArsZ-HP1432 interaction site upstream of the RBS abolished sRNA-mRNA interaction (Figure 2.7 B, bottom left panel). Moreover, compensatory base-pair exchanges in ArsZ M3 and 5'UTR of HP1432 restored the shift (bottom right panel), confirming the specific interaction between the two RNA species.

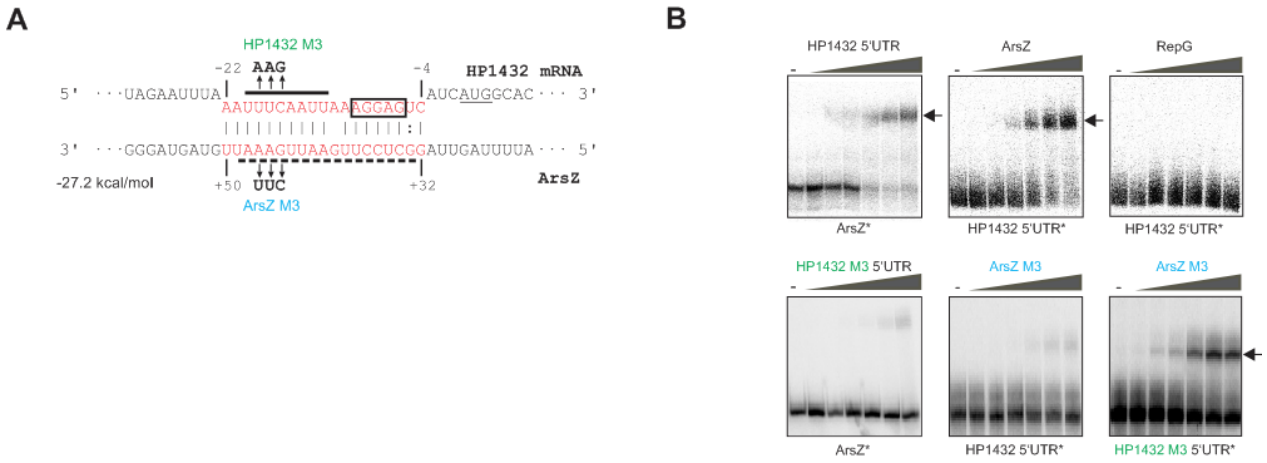

Figure 2.7 ArsZ interacts with the 5'UTR of HP1432 mRNA *in vitro*. (A) Predicted interaction between ArsZ and the HP1432 mRNA using the TargetRNA program (Tjaden, 2008). The horizontal lines indicate the validated interaction region from in-line probing assays (Figure 2.8). The Shine-Dalgarno sequence of HP1432 is boxed, and the start codon (AUG) is underlined. The arrows indicate nucleotides used for compensatory base-pair exchanges ("M3"). (B) EMSAs showing binding between ArsZ and the 5'UTR of HP1432 mRNA *in vitro*. T7-transcribed full-length ArsZ and the 5'UTR of HP1432 mRNA plus its first ten codons were used. RNA* (~ 4 nM) was 5'-^{32}P-radiolabeled. Corresponding point mutations (ArsZ M3 and HP1432 5'UTR M3, shown in (A) in blue and green letters, respectively) were used to show specificity of the binding. Increasing concentrations of non-labeled RNA

(8 nM, 16 nM, 125 nM, 250 nM, 500 nM, and 1000 nM) were incubated with the labeled RNA*. Unlabeled RepG served as negative control. Arrowheads indicate shifted bands.

To map the precise position of the sRNA-mRNA interaction *in vitro*, in-line probing assays were performed with radioactively-labeled ArsZ and the 5'UTR of HP1432 mRNA. In this assay, double-stranded RNA regions are protected from spontaneous cleavage following extended incubation, while single-stranded regions are susceptible to cleavage (Regulski & Breaker, 2008). The protected region (Figure 2.8 A, lane 6, position 33 to 49) is indicative of RNA duplex formation and overlaps with the predicted seed (region of at least seven consecutive base-pairs) and anti-SD region predicted to interact with the HP1432 mRNA (Figure 2.7 A). This region of protection was lost when point mutations were introduced into the 5'UTR of HP1432 (Figure 2.8 A, lanes 7 and 8) or ArsZ (Figure 2.8 A, lanes 13 and 14). Protection was successfully restored by introduction of compensatory base-pair exchanges (Figure 2.8 A, lanes 15 and 16), demonstrating the specificity of the interaction between ArsZ and HP1432. Overall, in-line probing analysis showed that ArsZ interacts with the SD region of HP1432 mRNA. This specific interaction was further confirmed by *vice versa* experiments with the radiolabeled 5'UTR of HP1432 mRNA and unlabeled ArsZ (Figure 2.8 D), confirming ArsZ-dependent protection sites consistent with the above mentioned prediction (Figure 2.7 A).

To complement the in-line probing method, *in-vitro* structure probing was performed using commercially available RNase III on radiolabeled ArsZ with unlabeled 5'UTR of HP1432. RNase T1, which only cleaves G residues at single stranded regions, and lead (II), which cleaves single stranded RNA non-specifically, were included as additional controls. In the absence of HP1432, RNase III cleaves all the predicted double-stranded regions of ArsZ (Figure 2.8 B, lane 10). Addition of HP1432 produced an additional RNA duplex region, which was also cleaved by RNase III (Figure 2.8 B, lanes 11 and 12). The absence of cleavage by lead at these regions further confirms that these regions are indeed double-stranded. *Vice versa* experiments using the radiolabeled 5'UTR of HP1432 mRNA with unlabeled ArsZ showed similar RNase III cleavage patterns (Figure 2.8 E). The *in-vitro* structure probing data fits the RNA-RNA interaction predicted by the RNAstructure tool (Reuter & Mathews, 2010) (Figure S3). Thus, the *in-vitro* experiments further confirmed that the interaction between ArsZ and HP1432 occurred at the single-stranded region of ArsZ (Figure 2.8 C) and HP1432 (Figure 2.8 F).

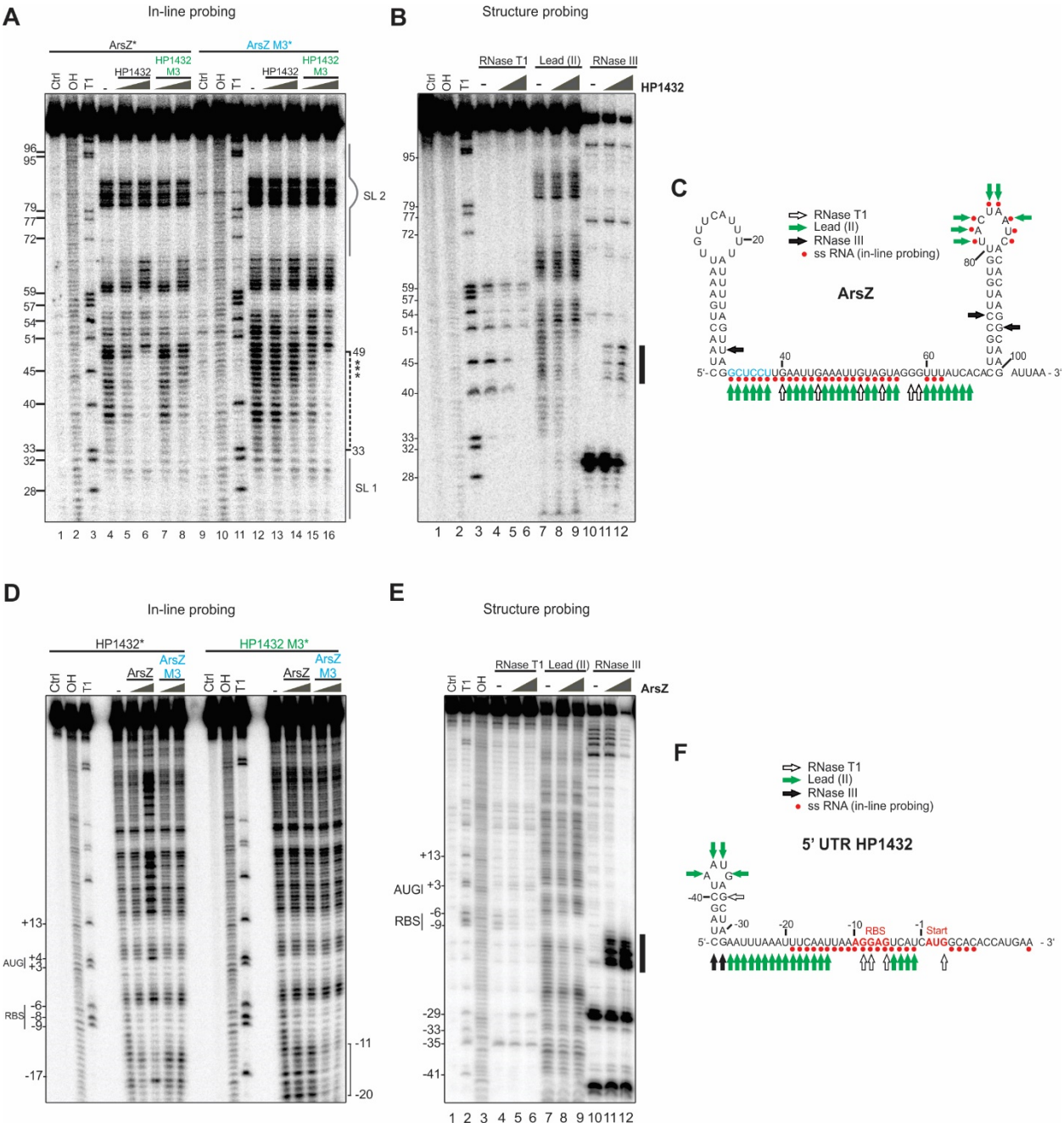

Figure 2.8 In-line and structure probing maps the precise interaction site between ArsZ and HP1432 mRNA *in vitro*. (A) In-line probing assay of radiolabeled ArsZ with HP1432 or HP1432 M3. Radiolabeled ArsZ (~ 4 nM) was mixed with increasing concentration of either HP1432 or HP1432 M3 and incubated for 40 hours under mild alkaline conditions to allow spontaneous RNA cleavage. Cleavage products were separated on a 10% polyacrylamide-urea sequencing gel and visualized by phosphorimaging. The numbers on the left indicate the position of guanine residues of ArsZ that are cleaved by RNase T1. The dotted vertical line (33 to 49) indicates the interaction site between ArsZ and HP1432. (D) *Vice versa* experiment was performed with radiolabeled HP1432 5'UTR and unlabeled ArsZ. End-labeled HP1432 or HP1432 M3 RNA was incubated with increasing concentrations of unlabeled ArsZ in in-line buffer.

(B) Structure probing assay of radiolabeled ArsZ (~ 4 nM) with HP1432 and the *vice versa* experiment (E) with radiolabeled HP1432 5'UTR. Samples were treated with either RNase T1 (cleaves after single-stranded guanines), lead (II) acetate (cleaves single-stranded regions), or RNase III (specific for double-stranded regions). The vertical lines next the blots indicate region is cleaved by RNase III in the presence of both ArsZ and HP1432 5'UTR. Minus (-): labelled RNA without addition of cold RNA; Ctrl: untreated control; T1: RNase T1; OH: alkaline ladder. Secondary structures of ArsZ (C) and the 5'UTR of HP1432 (F) validated by in-line probing and *in-vitro* structure probing. White arrows indicate RNase T1 cleavage sites, green arrows indicate lead (II) cleavage sites, black arrows mark RNase III cleavage sites, and red circles mark RNA cleavage sites from the in-line probing assay.

2.5 ArsZ negatively regulates HP1432 protein by masking its ribosomal binding site

Base-pairing sRNAs that interact with the RBS of target mRNAs often repress target mRNA translation. An *in-vitro* translation system using purified *E. coli* ribosomes was used to test whether ArsZ represses translation of HP1432 mRNA Incubation of *in -vitro*-transcribed mRNA representing the 5'UTR of HP1432 from strain 26695 fused to GFP with this cell-free translation system resulted in the appearance of an HP1432::GFP fusion protein, which was detected by Western blotting (Figure 2.9, lane 1). The addition of increasing amounts of *in vitro*-transcribed ArsZ to the reactions resulted in decreased 1432::GFP protein levels (Figure 2.9, lanes 2 to 5), indicating that ArsZ blocks the translation of the 1432 mRNA *in vitro*. Furthermore, addition of three consecutive point mutants (M3) ArsZ or the unrelated RepG sRNA in excess did not markedly reduce translation of the reporter protein when compared to wild-type ArsZ (Figure 2.9, lanes 1,6 and 7), confirming the specificity of 1432 regulation by ArsZ. Translation inhibition by ArsZ was also not seen when point mutations (M3) were introduced into the HP1432::*gfp* fusion mRNA (Figure 2.9, lane 11). Finally, the loss of ArsZ regulation upon introduction of point mutations into one of the RNA species was restored by compensatory base-pair exchanges (Figure 2.9, lane 10). RepG-mediated regulation of *tlpB*::*gfp* fusion mRNA (Pernitzsch *et al.,* 2014) were used as positive control and likewise showed repression (Figure 2.11, lanes 7, 11, 12 to 14).

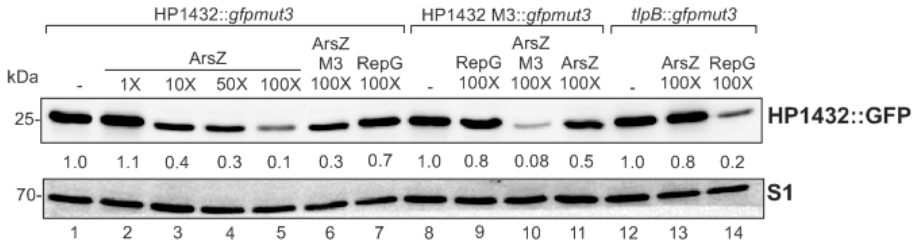

Figure 2.9 ArsZ masks the ribosome binding site of HP1432 mRNA to inhibit translation *in vitro*. An *in-vitro* translation assay with purified *E. coli* ribosomes (PURExpress) was used to reconstitute post-transcriptional regulation by ArsZ on HP1432 mRNA. The RepG sRNA and its target, the chemotaxis receptor *tlpB* mRNA, were included as a positive control. The 5'UTR of either HP1432, HP1432 M3, or *tlpB* were translationally fused to a GFP reporter gene and *in-vitro* transcribed. The indicated molar ratio/excess of ArsZ, ArsZ M3, or RepG over mRNA-*gfp* are indicated. An anti-GFP antibody was used to monitor GFP levels. An anti-S1 ribosomal protein served as a loading control.

In order to validate the direct interaction between ArsZ and HP1432 *in vivo*, we made use of an *E. coli* two-plasmid reporter system previously developed to validate sRNA-mRNA interactions in enterobacteria (Urban & Vogel, 2007) (Corcoran *et al.*, 2012). ArsZ was cloned under an arabinose-inducible promoter (p_{BAD}-ArsZ) in a plasmid (pPT106-1) and co-transformed with a compatible plasmid carrying HP1432 under control of the constitutive P_{LtetO} promoter (pHP1432, pPT42-1) in *E. coli* strain Top10 (Figure 2.10 A). The HP1432 protein contains a stretch of six consecutive histidine residues. Therefore, an anti-6xHis antibody was used to specifically detect this protein in the following Western blot analyses (Zeng *et al*., 2008). Because no homologs of the ArsZ sRNA or HP1432 protein have been identified in enterobacteria, *E. coli* Top10 provides a clean bacterial host background to investigate ArsZ-mediated regulation. In the absence of arabinose, no ArsZ was expressed (Figure 2.10 B, lane 5). Introduction of the p_{BAD}-ArsZ plasmid slightly reduced HP1432 mRNA levels in the absence of arabinose (Figure 2.10 B, lane 5ane 5). Albeit not detected by Northern blot analysis, slightly reduced HP1432 mRNA levels could be due to leaky expression of ArsZ. Nevertheless, the emphasis of this experiment is on the post-transcriptional regulation of ArsZ on HP1432. After 1 hour of pulse-expression of ArsZ by addition of arabinose, two-fold and four-fold reduced HP1432 mRNA and protein levels were detected, respectively (Figure 2.10 B, lane 6). All together, these experiments further support that ArsZ masks the RBS of HP1432 mRNA, leading to its translational repression. Moreover, the decreased in mRNA levels (Figure 2.10 B, lane 6) suggest that high levels of ArsZ might indirectly destabilize transcript of HP1432 since less translated HP1432 mRNA is not protected by translating ribosomes.

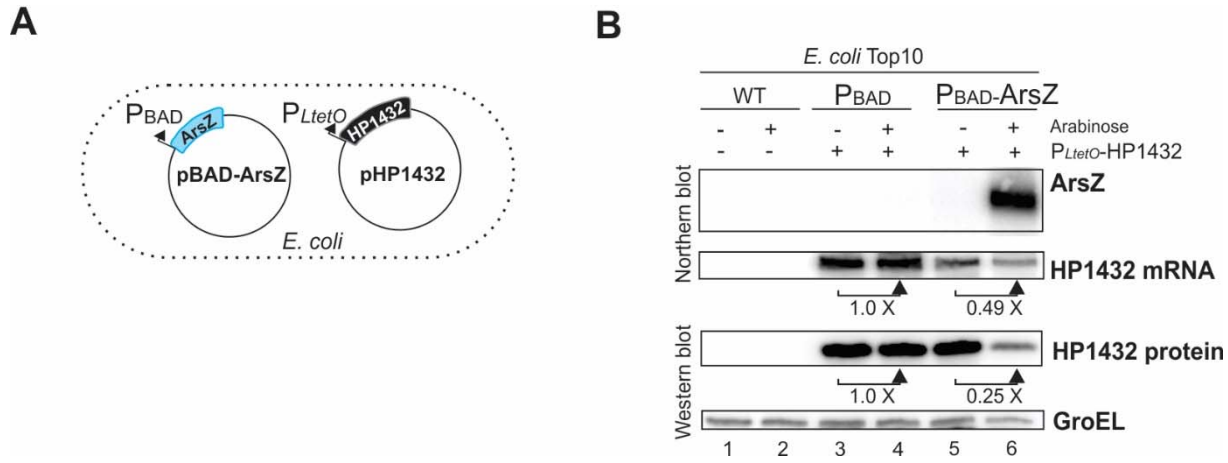

Figure 2.10: ArsZ regulates HP1432 on the protein and mRNA level in *E. coli* Top10. (A) Schematic representation of the two plasmids used to co-express ArsZ and HP1432 in the *E. coli* Top10. (B) *E. coli* cells containing either only HP1432 under the control of P*LtetO* promoter (pHP1432), or in combination with ArsZ under the p_{BAD} promoter (P_{BAD}ArsZ), were grown to an OD_{600} of 1.0. Expression of ArsZ was induced with 0.02% arabinose for 1 hour prior to sample (RNA and protein) collection. The expression of ArsZ and HP1432 mRNA was quantified by Northern blot analysis. 5S rRNA served as a loading control. Anti-6xHis antibody was used to monitor HP1432 protein levels, while GroEL served as a loading control.

2.6 ArsZ represses translation of HP1432 mRNA in *H. pylori in vivo*

The *in-vitro* experiments as well as reconstitution of the two-plasmid system in *E. coli* provided evidence that ArsZ potentially represses HP1432 at the protein and/or mRNA level in *H. pylori*. To further characterize the influence of ArsZ on HP1432 mRNA expression *in vivo, arsZ* deletion (Δ*arsZ*), its complementation (C_{ArsZ}), and ArsZ overexpression (OE-ArsZ) mutants were constructed in *H. pylori* strain 26695 and tested for their potential to affect HP1432 protein levels. Under steady-state conditions at pH 5.5 HP1432 protein levels decreased two-fold upon ArsZ over-expression. However, ArsZ overexpression did not affect HP1432 mRNA levels (Figure 2.11, lanes 1 and 4). This suggests that ArsZ might post-transcriptionally repress HP1432 translation initiation *in vivo*, rather than affecting mRNA turnover. Surprisingly, HP1432 mRNA levels were downregulated in the Δ*arsZ* mutant (Figure 2.11, lane 2). Nevertheless, HP1432 mRNA levels could be restored to wild-type levels upon providing a wild-type copy of *arsZ* under the control of its native promoter at the unrelated *rdxA* locus (Figure 2.11, lane 3). HP1432 protein levels were not affected by the deletion of *arsZ* (Figure 2.11, lane 2).

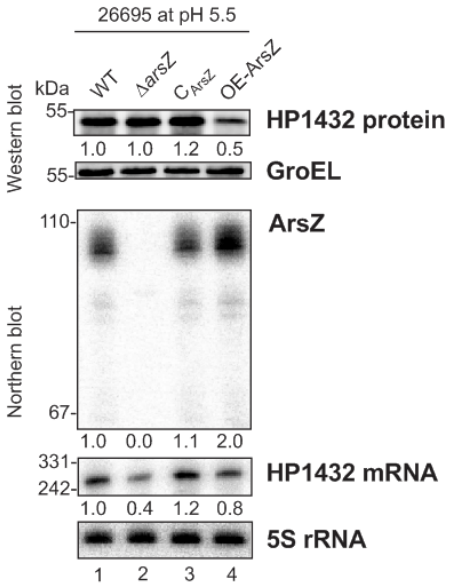

Figure 2.11: Effect of ArsZ on HP1432 protein levels under steady-state conditions in *H. pylori*. *H. pylori* 26695 wild-type (WT), deletion of *arsZ* (Δ*arsZ*), complementation of Δ*arsZ* (C_{ArsZ}), and ArsZ overexpression (extra copy in *rdxA* locus, OE-ArsZ) mutants were grown to an OD_{600} of 0.4 at pH 5.5. The expression of ArsZ and HP1432 mRNA was quantified on a Northern blot. 5S rRNA served as a loading control. Anti-6xHis antibody was used to monitor HP1432 protein levels, while GroEL served as a loading control.

Similar levels of the HP1432 protein in the Δ*arsZ* mutant relative to wild-type (Figure 2.11, lane 2) suggested that deletion of the *arsZ* sRNA might indirectly impact on HP1432 transcription, which in turn, masks its effect on HP1432 mRNA translational regulation. This hypothesis was further investigated in *H. pylori* strain G27 carrying a GFP transcriptional reporter for the HP1432 promoter (Figure 2.12 A). In the GFP transcriptional strain background, absence of ArsZ (Δ*arsZ*) is expected to decrease the GFP levels while the strains with GFP translational fusion act as controls since the effect of losing ArsZ was not observed at protein level of HP1432 (Figure 2.11, lane 2). GFP reporter protein levels of *H. pylori* G27 carrying the transcriptional P_{1432}-*ureA*-5'UTR::*gfp* fusion were significantly decreased (two-fold) upon deletion of *arsZ* (Figure 2.12 B and Figure 2.12 C, dark grey bars), indicating that the promoter activity of HP1432 is indeed affected by the deletion of *arsZ*. In contrast, no significant change in the GFP protein levels was observed in the translational 1432::GFP reporter fusion (P_{1432}-1432-5'UTR::*gfp*) between the wild-type and Δ*arsZ* mutant (Figure 2.12 C, light grey bars). This confirms that, despite lower level of HP1432::*gfpmut3* mRNA were observed in the absence of ArsZ, more translation occurred upon sRNA deletion, thereby maintaining similar levels of GFP relative to wild-type (Figure 2.11, lanes 1 and 2).

Together, these observations support that ArsZ represses translation of the mRNA encoding HP1432 in *H. pylori in vivo*.

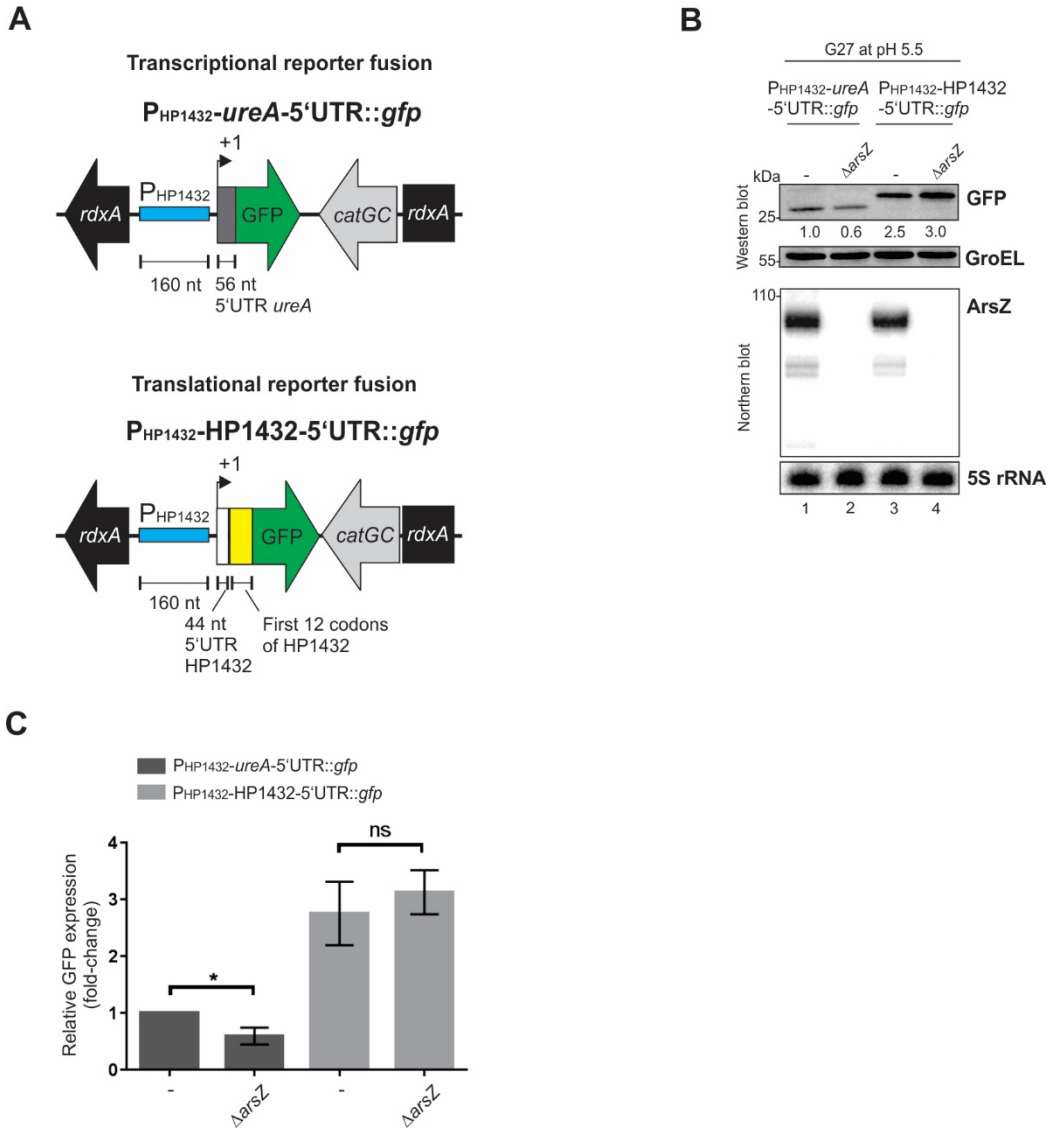

Figure 2.12: Deletion of *arsZ* reduces activity of the HP1432 promoter. (A) The native promoter region of HP1432 (of strain 26695) was fused either transcriptionally or translationally to a *gfp* reporter gene and reporter fusion constructs were introduced into the *rdxA* locus of *H. pylori* strain G27 wild-type or Δ*arsZ* background. The Scheme illustrates characteristics of used reporter fusions. (B) Cultures were grown at pH 5.5 and an anti-GFP antibody was used to monitor GFP reporter protein levels on a Western blot. GroEL served as a loading control. ArsZ levels in the corresponding total RNA was analyzed on a Northern blot and levels of 5S rRNA served as a loading control. (C) Relative GFP levels on Western blots from three independent experiments were quantified with error bars representing standard errors. The Student's *t*-test was used for statistical analysis. Asterisks indicate a *p*-value of less than or equal 0.05; ns: not significant ($p > 0.05$).

The downregulation of the HP1432 promoter activity in the Δ*arsZ* mutant (Figure 2.12) showed the complexity of HP1432 regulation. In addition to effect caused by *arsZ* deletion, HP1432 expression has been described to be regulated by various transcription factors, including ArsR (Pflock *et al*., 2006), NikR (Contreras *et al*., 2003) and Fur (Gancz *et al.*, 2006) (Figure 2.13 A). To provide evidence that ArsZ regulates HP1432 at the post-transcriptional level, rather than through indirect transcriptional effects, promoter exchange experiments were performed to uncouple HP1432 translational and transcriptional control from each other. The 5'UTR of HP1432 mRNA was translationally fused to GFP and placed under the control of the promoter of the unrelated chemotaxis receptor TlpB (Delany *et al*., 2002) in its endogenous gene locus (Figure 2.13 B). The *tlpB* promoter is not affected by acid stress. This GFP reporter fusion was investigated in the wild-type, Δ*arsZ* deletion and ArsZ M3 complementation mutant background of *H. pylori* strain G27. An about two-fold increase in GFP protein levels was observed in the absence of ArsZ (Figure 2.13 C, lanes 3-4). This indicates that the 5'UTR of HP1432 is sufficient to mediate regulation by ArsZ, even when the mRNA is expressed from a heterologous promoter. Similarly, disruption of base-pairing between ArsZ and the HP1432 mRNA via point mutations introduced into ArsZ (ArsZ M3) resulted in a similar, two-fold increase in GFP reporter levels (Figure 2.13 C, lane 5). Likewise, introduction of point mutations in the 5'UTR of HP1432 mRNA (HP1432 M3) also increased levels of the GFP reporter two-fold (Figure 2.13 C, lane 6), which was not further increased upon deletion of *arsZ* (Figure 2.13 C, lane 7). Importantly, the compensatory base-pair exchange (ArsZ M3 and HP1432 M3; Figure 2.13 C, lane 8) successfully restored GFP reporter levels to that of the "WT" (P_{tlpB}HP1432) strain. Taken together, these observations strongly support that HP1432 is regulated by the ArsZ sRNA at the post-transcriptional level.

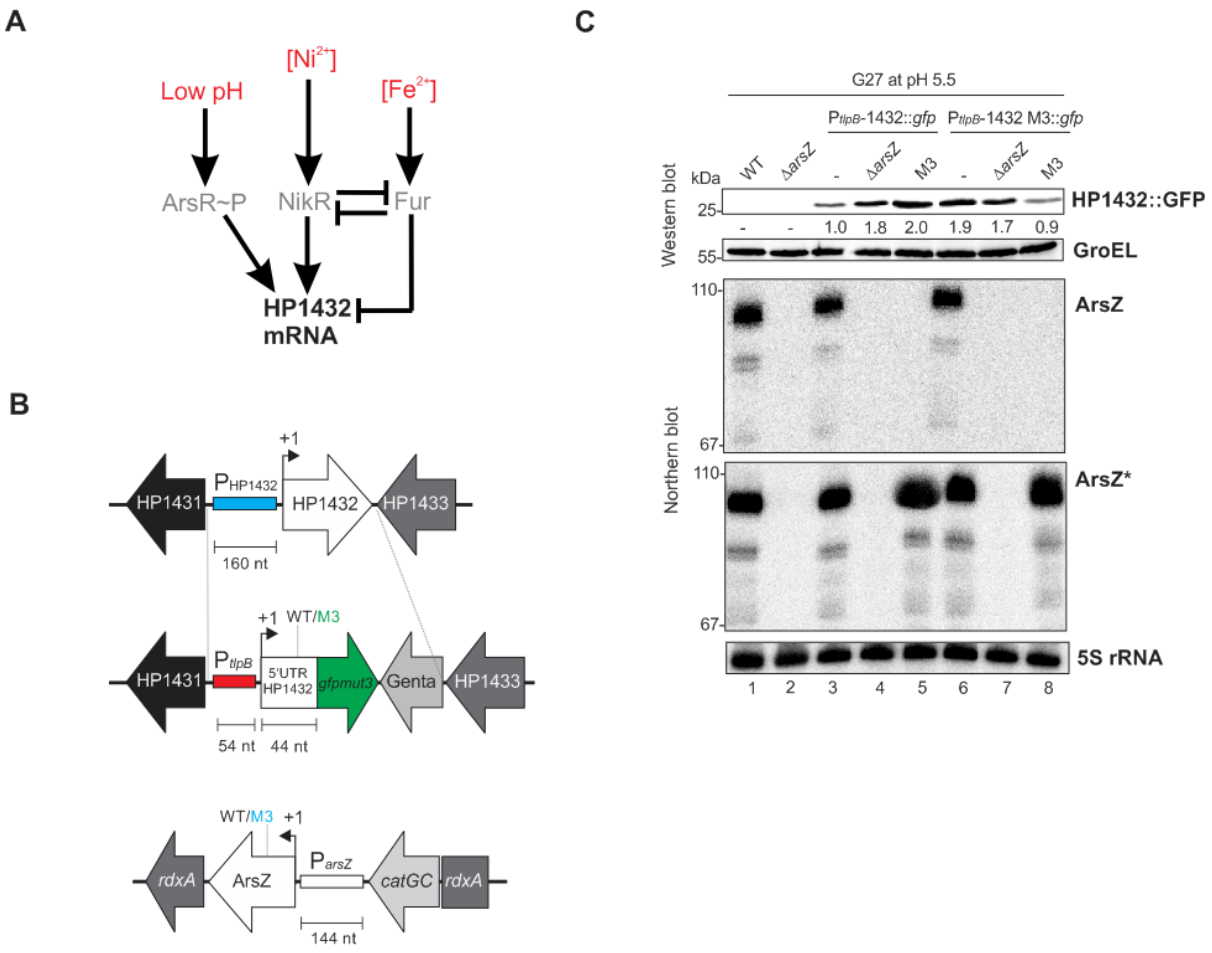

Figure 2.13: ArsZ represses HP1432 at the post-transcriptional level. (A) The promoter region of HP1432 is regulated by three transcription factors in response to three different signals (Pflock *et al.*, 2006) (Contreras *et al.*, 2003) (Gancz *et al*., 2006) (Delany *et al*., 2005). (B) The HP1432 promoter was exchanged to the unrelated *tlpB* promoter, which is not affected by acid. Under the control of the *tlpB* promoter, the 5'UTR of HP1432 or HP1432 M3 was fused to *gfp* and introduced at the native HP1432 locus (top panel). The point mutant version of ArsZ (ArsZ M3) was introduced at the *rdxA* locus of a Δ*arsZ* background strain (middle panel). (C) *H. pylori* strain G27 carrying indicated GFP reporter fusions and sRNA mutants (*arsZ* deletion or ArsZ M3) were grown to exponential growth phase and RNA as well as protein samples were collected. The expression of ArsZ was inspected on a Northern blot by using an ArsZ-specific probe (ArsZ) and another probe which binds to ArsZ at a region upstream of the base-pair exchange (M3) region (ArsZ*). 5S rRNA served as a loading control. An anti-GFP antibody was used to monitor GFP reporter levels, while GroEL served as a loading control.

2.7 ArsZ affects HP1432 mRNA stability

While steady-state levels of HP1432 mRNA in *H. pylori* 26695 were slightly affected (1.2-fold downregulated) by *arsZ* over-expression (Figure 2.11, lane 4), rifampicin stability assays showed that ArsZ over-expression in fact destabilizes HP1432 mRNA levels by at least 1.6-fold, reducing its half-life from more than 32 minutes (Figure 2.14 A, solid line) to 20 minutes (Figure 2.14 A, dotted line). The rifampicin assay also showed that HP1432 mRNA is slightly more stable in Δ*arsZ* when compared to WT. These results are consistent with translational repression of HP1432 by ArsZ. Non-translating mRNAs are less protected by ribosomes and therefore, are more sensitive to endo- or exonucleolytic attacks, resulting in shorter mRNA half-life. A similar destabilization effect on HP1432 mRNA was observed in *H. pylori* strain G27 (Figure 2.14 B). Taken together, these results support the conclusion that ArsZ post-transcriptionally represses HP1432 mRNA by direct base-pairing interactions with its single-stranded targeting region to the RBS of the HP1432 mRNA.

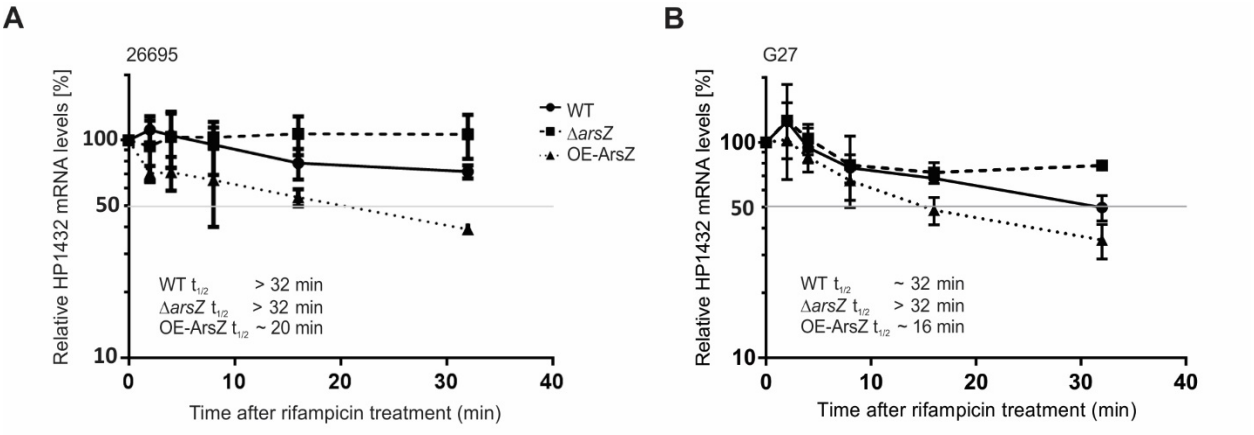

Figure 2.14: ArsZ affects the half-life of the HP1432 mRNA. The half-life ($t_{1/2}$) of HP1432 mRNA was determined after inhibition of transcription by rifampicin treatment in *H. pylori* strains 26695 (A) and G27 (B) in WT, Δ*arsZ*, and ArsZ overexpression (OE-ArsZ) mutants at pH 5.5. Strains were grown to an OD_{600} of 0.4 and RNA samples were taken before and at indicated time points after rifampicin treatment. Analysis of HP1432 mRNA levels was done by Northern blot quantification. The half-life of HP1432 mRNA was determined to be the time point at which 50 % of its "starting" mRNA levels remained.

2.8 Introduction of a stable stem-loop enables strong overexpression of ArsZ

Unlike many sRNAs which can be easily overexpressed using strong promoters, initial attempts to overexpress ArsZ from strong *H. pylori* promoters, such as the *repG* and *ureA* promoters, were not

successful (Figure 2.15 A). It might be possible that ArsZ adopts unstable RNA conformations upon high expression. Manual inspection of the first stem-loop of ArsZ (ArsZ-SL1) revealed this stem-loop could be unstable due to its low GC content (Figure 2.15 B). Thus the stability of ArsZ might be increased by exchanging SL1 with another stem-loop of similar length (27 nt), but higher stability. One stem-loop that meets both criteria is the stem-loop 1 of RepG (RepG-SL1) (Figure 2.15 B). It was reported that RepG-SL1 is not involved in target regulation, however significantly affects sRNA stability (Pernitzsch *et al*., 2014). The ArsZ-SL1 was replaced by the RepG-SL1, resulting in the slightly shorter hybrid construct RepG-SL1-ArsZ. This hybrid sRNA was placed under the control of RepG promoter in the *rdxA* locus of *H. pylori* strain 26695 and Northern blot analysis revealed that we could successfully overexpress ArsZ by five-fold relative to WT (Figure 2.15 C). HP1432 mRNA levels were about two-fold decreased upon this strong overexpression of ArsZ, which nicely recapitulates previous experiments (Figure 2.14) and further demonstrate that ArsZ also destabilizes the HP1432 mRNA. HP1432 protein levels decreased by four-fold in line with earlier results that ArsZ post-transcriptionally repress translation of HP1432 mRNA.

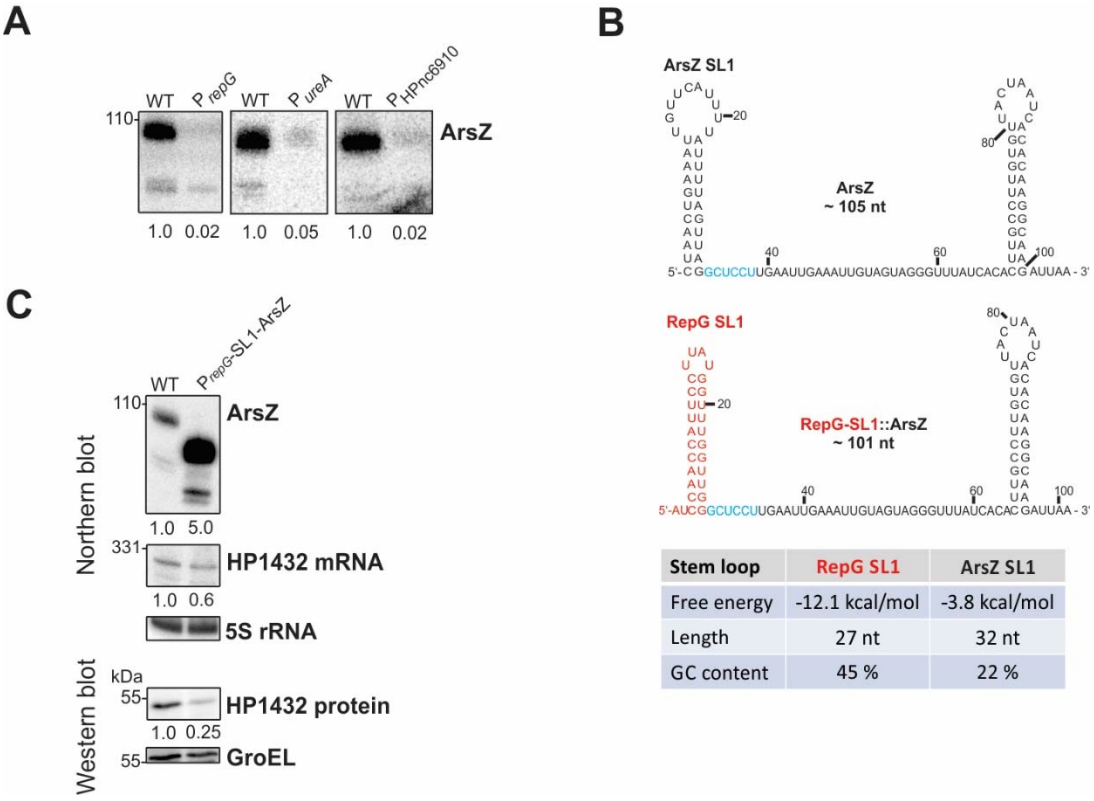

Stem loop	RepG SL1	ArsZ SL1
Free energy	-12.1 kcal/mol	-3.8 kcal/mol
Length	27 nt	32 nt
GC content	45 %	22 %

Figure 2.15: ArsZ is difficult to overexpress by standard approaches. (A) The expression of ArsZ from two strong *H. pylori* promoters, P*repG* and P*ureA*, was quantified on a Northern blot. (B) Secondary structure for ArsZ and the chimeric RepG-SL1-ArsZ. Lower table indicates the free energy, length and GC content of the first stem loop of each sRNA. (C) The expression of chimeric RepG-SL1-ArsZ under RepG promoter was quantified by Northern blotting.

5S rRNA served as a loading control. Anti-6xHis antibody was used to monitor HP1432 protein levels, while GroEL served as a loading control.

2.9 ArsZ forms a coherent feed-forward loop with ArsRS to regulate HP1432 in response to low pH

Both the *in-vitro* and *in-vivo* data indicate that the *H. pylori* sRNA ArsZ represses HP1432 at the post-transcriptional level. Moreover, expression of ArsZ itself appears to be repressed in response to low pH by the ArsRS TCS (Figure 2.6). Also, previous studies reported that the HP1432 promoter is also positively regulated by ArsRS at low pH (Pflock *et al*., 2004). These observations suggest that ArsZ, together with the ArsRS TCS, might form a coherent feed-forward loop (C-FFL) to regulate HP1432 expression in *H. pylori*. Coherent FFLs involve two regulators that act synergistically on the same downstream target gene (Mangan & Alon, 2003). Specifically, in the type- 4 FFL (C4-FFL), a regulator both directly activates a target gene, and represses a repressor of the same target gene (Figure 2.16 A). In this model, for the *H. pylori* target gene HP1432 at pH 5.5, phosphorylated ArsR would simultaneously directly activate the transcription of HP1432 mRNA as well as repress the transcription of its translational repressor, ArsZ. Since ArsZ is repressed transiently after low pH shift by ArsR-P (Figure 2.6), the dynamics of ArsZ regulation of HP1432 upon exposure to acid were explored. Specifically, levels of ArsZ, HP1432 mRNA, and HP1432 protein were quantified following downshift to pH 5.5. In WT, ArsZ was mildly downregulated (Figure 2.16 B, black line) in the first hour after shift to acidic conditions, while HP1432 mRNA levels were upregulated, independent of ArsZ (Figure 2.16 B, grey lines). This is consistent with repression of the sRNA and activation of the mRNA by the ArsRS TCS upon acidification of the pH.

Although no significant change in HP1432 mRNA levels was observed in the Δ*arsZ* mutant compared to the WT (Figure 2.16 B), a more rapid increase in HP1432 protein levels was detected in Δ*arsZ* mutant following acid exposure (Figure 2.16 C). This suggests that the levels of the HP1432 protein increase upon exposure of *H. pylori* to low pH conditions, and the ArsZ sRNA might serve as a delay switch in the regulation of HP1432 by the ArsRS TCS under acid shock, thereby affecting the dynamics of HP1432 induction. Interestingly, the indirect activation of HP1432 promoter by ArsZ (Figure 2.16 A, dotted line with arrow and Figure 2.12) was only observed after adaptation to low pH stress has occurred (overnight growth, steady-state in pH 5.5). This network did not form during the process of rapid pH adaptation, since the levels of HP1432 mRNA were not lower in Δ*arsZ* compared to WT (Figure 2.16 B, Figure S4). Hence, ArsZ can additionally participate in an incoherent FFL after adaptation to low pH, giving rise to a non-

standard FFL in which ArsZ can participate directly or indirectly in two different network configurations depending on the state of acid stress adaptation.

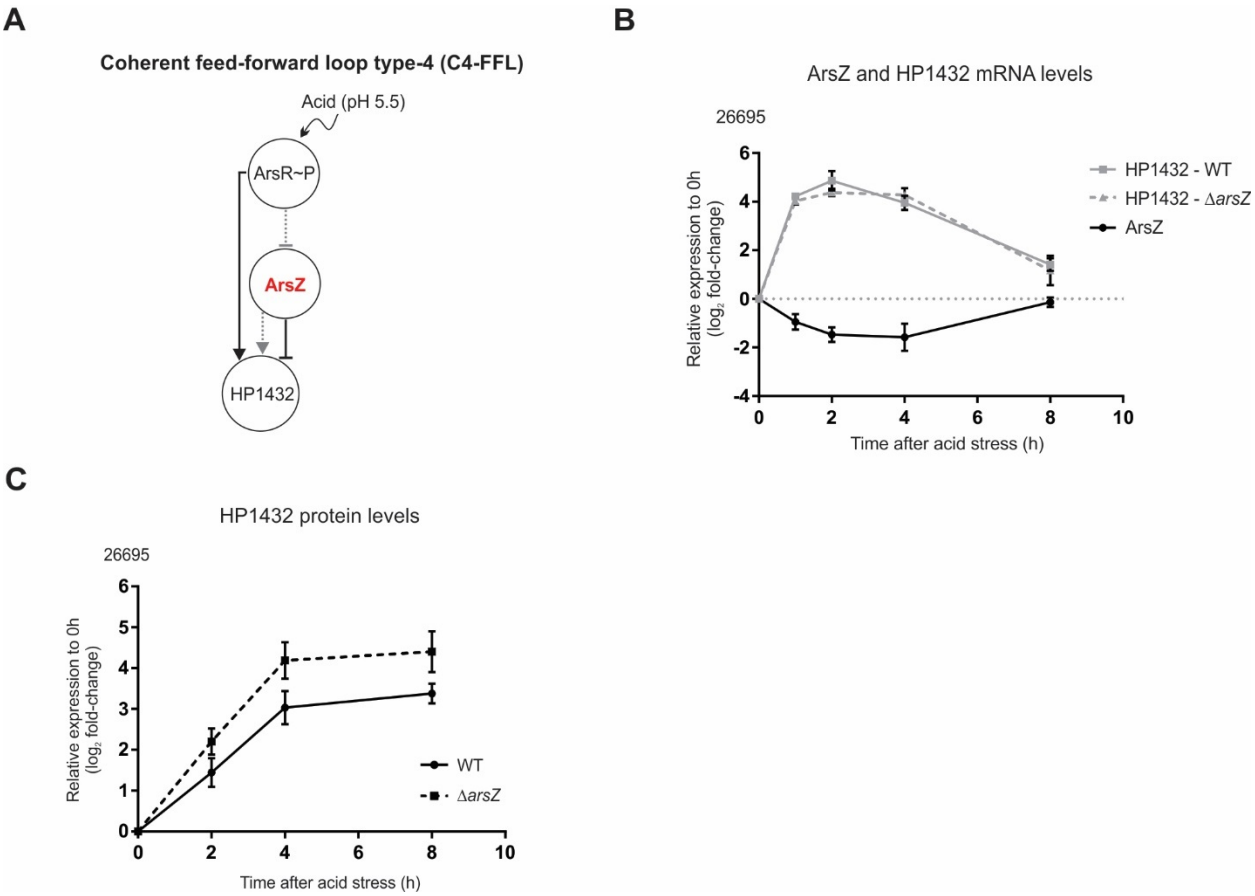

Figure 2.16: ArsZ forms a coherent feed-forward loop with ArsRS and HP1432. (A) A schematic diagram of the proposed type-4 coherent feed-forward loop formed by ArsRS, ArsZ, and HP1432. The solid arrows indicate direct interactions, while dotted arrows indicate indirect regulation. (B) Acid stress increases HP1432 mRNA levels in both WT and Δ*arsZ*. Levels of HP1432 and ArsZ in WT, as well as HP1432 in Δ*arsZ*, were measured in total RNA following shift of log-phase bacteria to acidic medium by Northern blotting. All strains were grown to an OD_{600} of 0.4 at pH 7. The medium was then adjusted to pH 5.5, and HP1432 mRNA and ArsZ levels from various time points following the shift were quantified on a Northern blot. The fold-change was quantified as $\log_2$ ratio of a specific time point relative to the 0 hour time-point. The data are average of three independent experiments, with error bars representing standard errors. (C) HP1432 protein levels increase more rapidly in Δ*arsZ* compared to WT. Corresponding protein samples from (B) were analyzed by Western blotting for levels of the HP1432 protein with an anti-6xHis antibody.

2.10 ArsZ modulates urease activity via repressing HP1432 under acid stress

H. pylori must tightly regulate urease activity in order to ensure rapid induction at low pH, but conversely to limit its activity when the pH is neutral. The histidine-rich HP1432 protein is assumed to lower urease activity at neutral pH by decreasing the levels of free Ni^{2+} cofactor available for urease activation (Seshadri *et al.*, 2007). In contrast, at low pH or under nickel-deficient conditions, the HP1432 protein releases nickel and thus, contributes to a rapid increase in mature urease levels (Zeng *et al*., 2008) (Seshadri *et al*., 2007, Ge *et al*., 2006a). These observations have given rise to the hypothesis that ArsZ might affect urease maturation via regulation of nickel availability through its regulation of HP1432 protein levels.

To test this hypothesis, urease activity from various mutants after four hours of exposure to pH 5.5 or pH 7 were quantified by urease activity assay (Figure 2.17). Compared to the WT, elevated urease activity was observed in Δ*arsZ* mutant at pH 5.5 and could be restored back to wild-type levels by complementation of ArsZ in *trans*, while over-expression of ArsZ further decreased urease activity about three-fold at low pH (Figure 2.17, dark grey bars). Moreover, lower urease activity in the ΔHP1432 deletion mutant and no increase in urease activity in of the ΔHP1432 Δ*arsZ* double deletion mutant indicated that the increase of urease activity in Δ*arsZ* is dependent on HP1432. Importantly, the ArsZ-dependent increase of urease activity only observed under low pH, as only minor variations in urease activities were measured among the different strains at neutral pH (Figure 2.17, light grey bars). These results suggest that ArsZ influences halo-urease maturation in an HP1432-dependent manner upon shift to low pH.

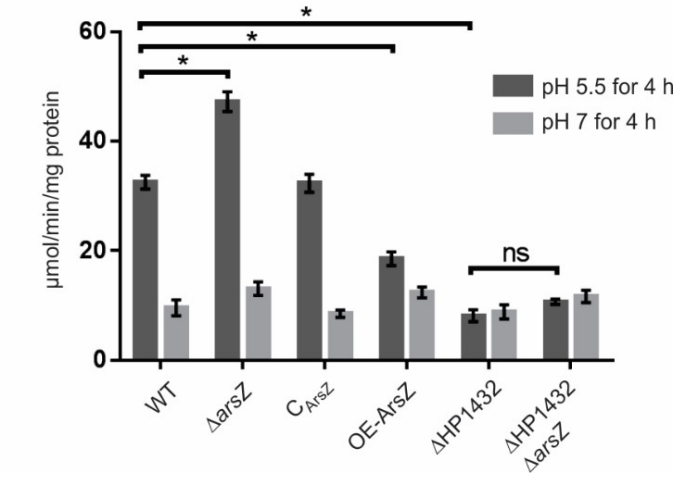

Figure 2.17: ArsZ modulates urease activity via regulation of levels of the nickel-binding factor HP1432. Indicated *H. pylori* 26695 wild-type and mutant strains were grown to an OD_{600} of 0.4 at pH 7. The medium was then adjusted to pH 5.5. Protein samples were collected from indicated strains after either 4 hours of exposure to pH 5 or

to neutral pH. The urease activity for these samples was quantified using method previously described (van Vliet *et al*., 2001). The Student's *t*-test was used for statistical analysis. A single asterisk indicates a *p*-value ≤ 0.05; ns: not significant (P > 0.05).

2.11 ArsZ is required for downregulation of urease activity after acid stress

H. pylori induces urease activity in order to cope with acid stress, as the urease enzyme neutralizes intracellular acid (Scott *et al.*, 2002). Presumably, once an acid challenge has been neutralized, the urease system returns to steady-state levels/activity in order to prevent over-alkalization, which could in principle, also negatively affect bacterial fitness.

To determine the kinetics of urease regulation, the urease activity of WT, Δ*arsZ*, ΔHP1432, and a ΔHP1432 Δ*arsZ* double mutant were measured at various time points under acidic stress conditions (Figure 2.18 A). In agreement with previous reports (Scott *et al*., 2002), urease activity gradually increased upon exposure to acid in *H. pylori* 26695 wildytpe (Figure 2.18 A, solid black line). In contrast, the Δ*arsZ* mutant (Figure, 2.18 A, dotted black line) showed a more rapid increase in urease activity relative to wild-type after exposure to acid. To determine whether this increase in urease activity after exposure to acid was due to increased expression of the urease protein, levels of UreA, a subunit of the urease complex were quantified by Western blotting (Figure 2.18 B). No alterations in the UreA protein levels was observed, neither upon deletion of *arsZ* nor following acid exposure. This suggests that the observed increase in urease activity is specifically due to an increase in the fraction of active enzyme, presumably due to nickel cofactor levels. Although the *ureAB* operon has been reported to be induced under acid (Pflock *et al*., 2005), it has also been reported that the UreA protein levels remained similar to those under pH 7 – even after thirty minutes of exposure to acid (Marcus *et al*., 2016). This is in line with the here described observations. Relative urease activity of WT and Δ*arsZ* increased over time, reaching a maximum at four hours after acid shift (Figure 2.18 C). After eight hours, however, the urease activity returned to pre-acid exposure levels in WT. Interestingly, the levels of urease activity in Δ*arsZ* at the same time points were still at least two-fold higher than in the WT, suggesting that the loss of ArsZ affected both the induction of urease activity following acid exposure and the re-adaptation of urease activity to neutral conditions following neutralization of the environment.

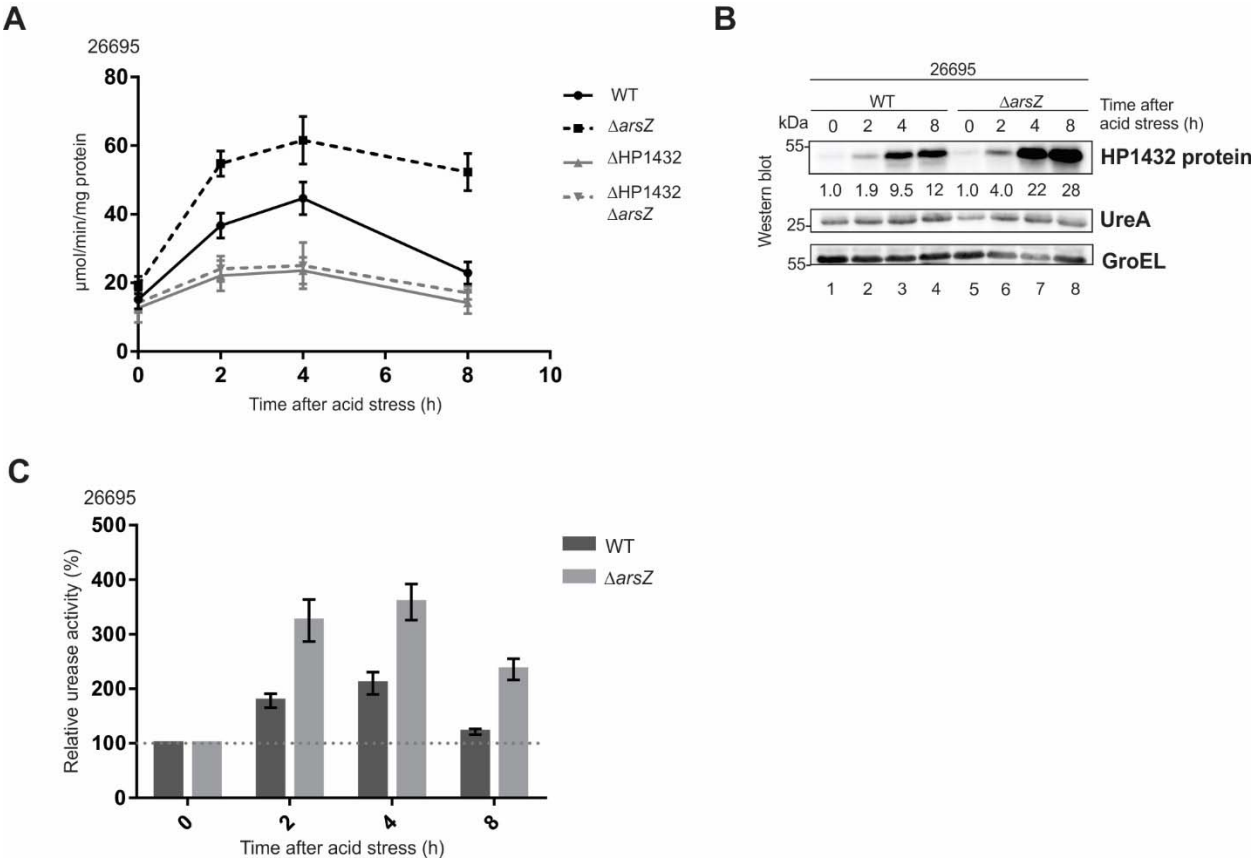

Figure 2.18: Levels of urease activity of WT and Δ*arsZ* following shift from neutral to acidic medium at extended time points. *H. pylori* 26695 WT and Δ*arsZ* were grown overnight to an OD_{600} of 0.4 at pH 7. The medium was then adjusted to pH 5.5, and at indicated time points, bacteria were harvested for total RNA and protein extraction. (A) The urease activity for each strain at different time points was quantified using a method previously described (van Vliet *et al.*, 2001). (B) UreA protein levels remain unchanged, while HP1432 protein levels increase, following exposure to acid. Samples were analyzed by Western blotting for the levels of UreA with an anti-UreA antibody. GroEL served as a loading control. (C) Relative urease activity of WT and Δ*arsZ* following shift *H. pylori* 26695 cells from neutral to acidic medium. The urease activity for each strain at different time points was quantified.

2.12 ArsZ confers a growth advantage after acid stress

Since high urease activity might lead to the production of ammonia levels high enough to be detrimental to *H. pylori* cells, the fitness of WT, Δ*arsZ* and C_{ArsZ} was inspected after eight hours of exposure to either pH 5.5 or pH 7. A significant, about three-fold decrease in cell fitness at pH 5.5 was observed in Δ*arsZ* deletion mutant compared to WT after eight hours of acid exposure (Figure 2.19 A). The growth defect could be rescued by complementing ArsZ expression in *trans*. In contrast, the Δ*arsZ* mutant showed no difference

from WT under neutral pH conditions, suggesting that the survival phenotype was related to acid adaptation, rather than a general survival defect.

The observed fitness defect of *H. pylori* 26695 Δ*arsZ* indicated that wild-type cells could outcompete cells that do not express ArsZ. To test this hypothesis, growth competition experiments with WT and Δ*arsZ* under pH 4 supplemented with 10 mM urea or neutral pH were performed. WT and Δ*arsZ* contained streptomycin and erythromycin selectable antibiotics markers, respectively, to allow specific recovery and quantification of each strain. Competition experiments revealed that the Δ*arsZ* mutant can outcompete WT in the first two hours after pH stress, but loses this benefit after 8 hours (Figure 2.19 B). The growth advantage at two hours after acid stress in Δ*arsZ* is in line with the higher urease activity observed previously (Figure 2.18 A, C). Moreover, the increased urease activity in Δ*arsZ,* but not in WT, after 8 hours of acid exposure possibly explains the growth advantage of WT cells over Δ*arsZ* mutant bacteria at this later time point. Taken together, these data suggest that the ArsZ sRNA might play an important role in modulating the levels of active urease by ensuring that the active enzyme is not over-activated, as well as a timely return to pre-exposure levels once the environment of the bacterium has been neutralized again.

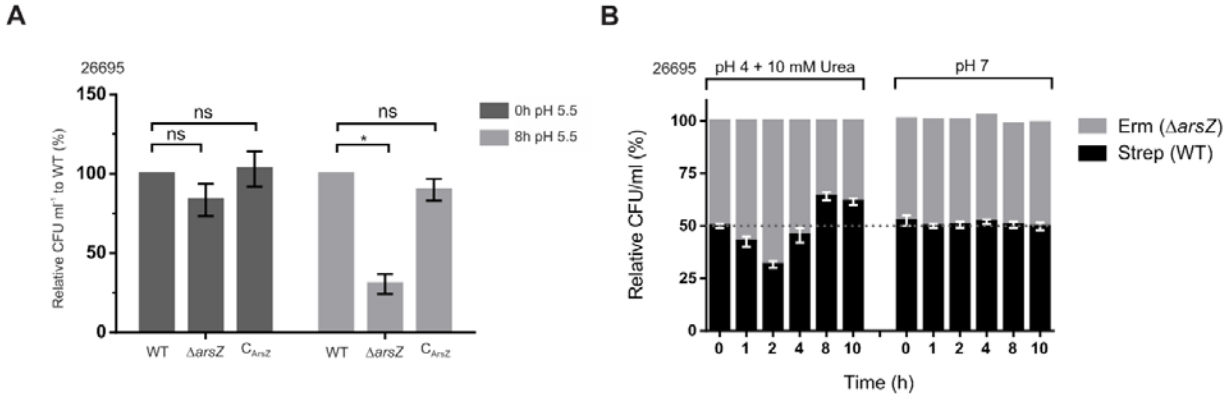

Figure 2.19: The sRNA ArsZ affects fitness of *H. pylori* following shift to acid pH. (A) Viability of WT, Δ*arsZ* and C_{ArsZ} following shift to acidic medium. Cells were harvested immediately after exposure to pH 5.5 (0h), and after eight hours of acid exposure (8h). At each time point, the cells were serially diluted, spread on plates, and incubated microaerobically for 3 to 5 days. Data are average of three independent experiments, with error bars representing standard errors. The Student's *t*-test was used for statistical analysis. Double asterisks indicate a *p*-value of less than or equal 0.01; ns: not significant ($p > 0.05$). (B) Equal number of cells from WT and Δ*arsZ* were mixed and incubated in BHI, pH 4 and supplemented with 10 mM urea or BHI, pH 7. At each time point, were serially diluted, spread on selective antibiotic plates, and incubated microaerobically for 3 to 5 days. The ratio between WT and Δ*arsZ* were

calculated as relative CFU/ml. Data shown are the average of three independent experiments, with error bars representing standard errors.

2.13 Evolution of the ArsZ sRNA and its target gene HP1432

The pH-dependent cell fitness advantage conferred by ArsZ is supported by the fact that there has been a selective pressure to maintain *arsZ* in the genome of *H. pylori* strains after its initial acquisition. Since this bacterium has been associated with humans for more than 100,000 years ago (Moodley *et al*., 2012), the evolution of the ArsZ sRNA was further investigated. A phylogenetic tree of selected *Helicobacter* species was extracted from the PATRIC database (Wattam *et al.,* 2014), which contains only completed genomes of *H. pylori* and representative gastric species. Major evolutionary events are indicated on this unrooted tree (Figure 2.20 A). About 100,000 years ago, *H. pylori* diverged into two major super-lineages, one which includes two branches that are associated with hunter-gatherers in southern Africa (hpAfrica2, Figure 2.20 A, blue lines and pink circle) (Henn *et al.,* 2011) and another branch which is associated all other *H. pylori* strains including hpAfrica1 (Figure 2.20 A, black lines and grey circles) (Pot *et al.,* 2001). *H. acinonychis*, the closest known relative of *H. pylori,* emerged within the hpAfrica2 branch after a host jump from early humans to big cats (Eppinger *et al.,* 2006). About 60,000 years ago, *H. pylori* strains of the second branch accompanied anatomically-modern humans during the out-of-Africa human migration event. This event split this second branch into hpAfrica1 (Figure 2.20 A, dark grey circle) and all other non-African strains, which includes hpEurope, hpAsia2, hspEAsia, hpSahul, and hspAmerind (Figure 2.20 A, light grey circle) (Linz *et al.,* 2007).

We next included the conservation of the ArsZ sRNA and HP1432 on a phylogenetic tree of *Helicobacter* species, rooted to *H. mustelae* (a gastric pathogen of ferrets). The homologs of ArsZ and HP1432 were determined from BLAST analysis with a cut-off E-value of 1 E-05 and minimum sequence identity of 80 %. ArsZ seems to have emerged exclusively in the hpAfrica1 and non-African *H. pylori* branch, as no orthologs of ArsZ were found in the hpAfrica2 branch or the non-*pylori* species (Figure 2.20 B, origin of ArsZ). Interestingly, ArsZ is found only in *H. pylori* species. In contrast, other *H. pylori* sRNAs such as RepG (Pernitzsch *et al*., 2014) and HPnc4160 are not only limited to *H. pylori* species, which infects human almost exclusively (Kusters *et al*., 2006). The target of ArsZ, HP1432, which arose from a gene duplication event of another histidine-rich protein, HP1427, in the lineage leading to *H. pylori* and *H. acinonychis* (Vinella *et al*., 2015) is present in both branches (Figure 2.20 B, origin of HP1432). The *ureAB* operon encoding urease, which is required for successful colonization of the stomach, as well as the housekeeping gene, 6S RNA, are present in all the gastric *Helicobacter* species.

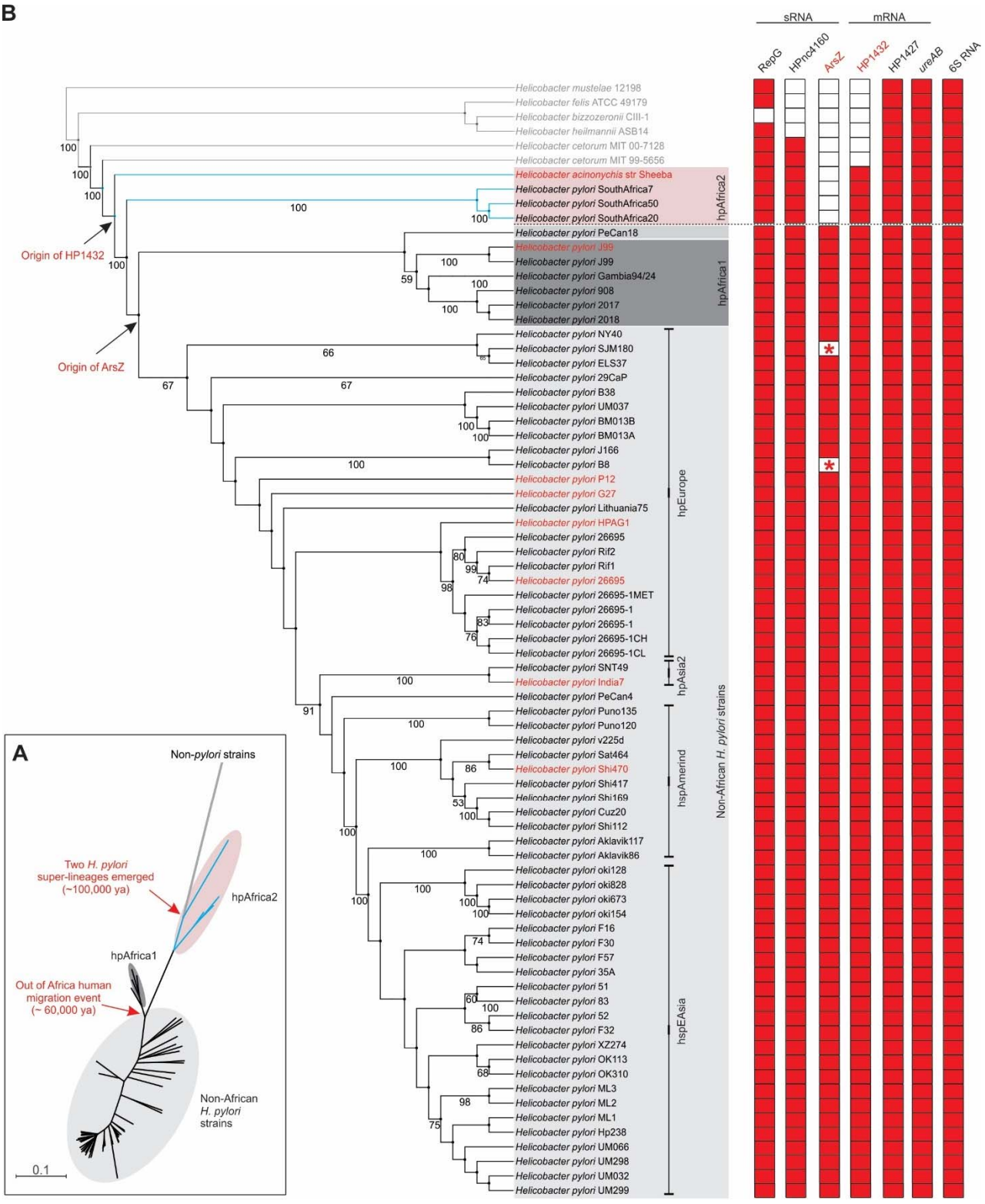

Figure 2.20: Evolution of the ArsZ sRNA and its target gene HP1432. (A) The unrooted phylogenetic tree of *H. acinonychis* and *H. pylori* was extracted from the PATRIC database. The tree was manually curated in the iTOL webserver (Letunic & Bork, 2007, Letunic & Bork, 2016) to retain only strains that have complete genome in the

NCBI database (as of November 2015). The two super lineages are indicated as colored ovals (pink and dark/light grey). The hpAfrica1 clade is a sub-branch of the second super lineage that evolved after the out-of-Africa human migration event. (B) The phylogenetic tree in (A) was rooted to *H. mustelae*. All non-*pylori* gastric *Helicobacter* species analyzed in this figure are indicated in grey text. Within the non-African strains, the phylogeography for each strain is indicated. The right panel indicates the presence (red) or absence (white) of the indicated genes based on BLAST analysis using a cut-off E-value of 1 E-05 and sequence similarity of at least 80 %. The asterisk indicates a truncation in the *arsZ* gene. The grey and pink boxes corresponds to the circles in (A).

Next, the expression ArsZ and HP1432 was validated in a small subset of representative *H. pylori* strains as well as *H. acinonychis* (Figure 2.20 B, strains in red). While Northern blot and Western blot analysis confirmed that HP1432 is expressed in all the investigated strains, ArsZ is expressed exclusively in the *H. pylori* strains (Figure 2.21 A). Strain-specific variations in expression levels of the ArsZ sRNA and HP1432 mRNA could be due to differences in the binding affinity of the used probes for both RNAs in the Northern blot. The presence of a conserved stretch of six consecutive histidine residues in all the strains tested (sequence conservation see Figure 2.21 B) suggests that the anti-6xHis antibody has been successfully used to detect HP1432.

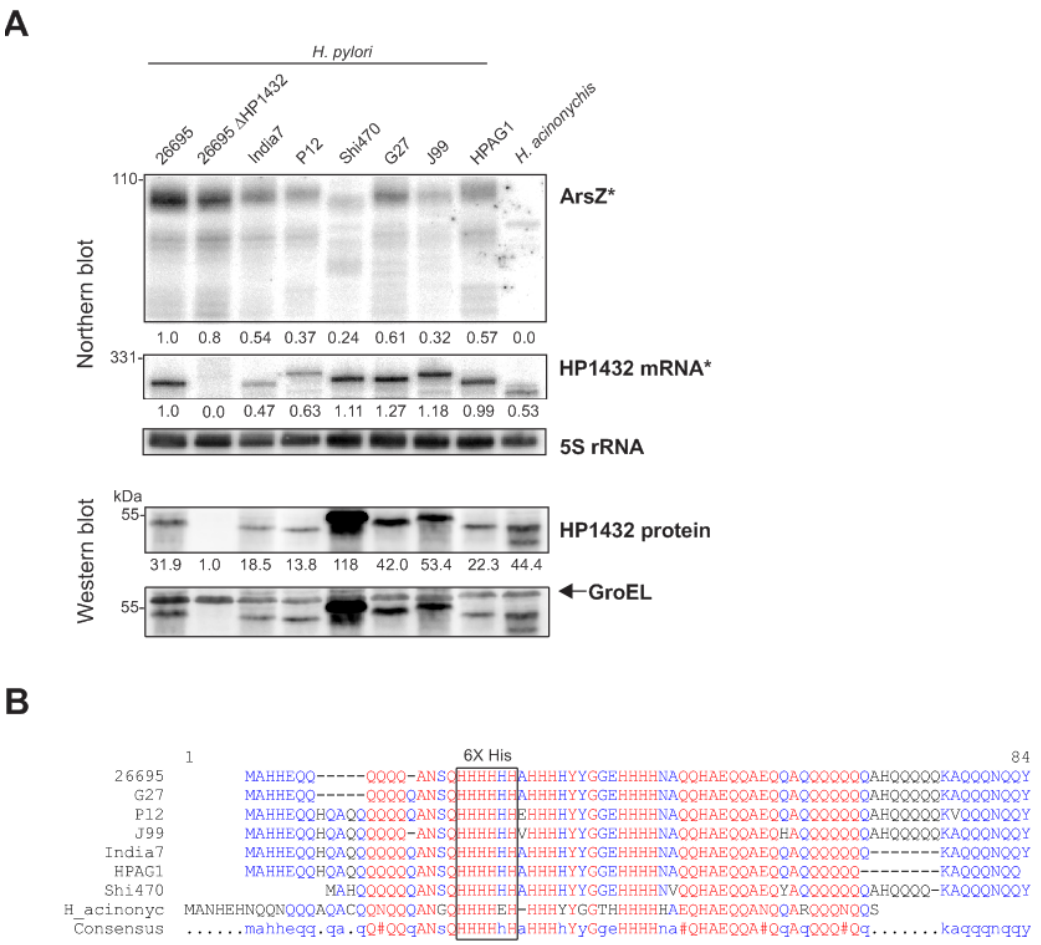

Figure 2.21: Expression of ArsZ and HP1432 in *H. acinonychis* and selected *H. pylori* strains. The expression of ArsZ and HP1432 in various *H. pylori* strains grown to an OD_{600} of ~ 0.4 was quantified by Northern blot and Western blot. 5S rRNA served as a loading control. Anti-6xHis antibody was used to monitor HP1432 protein levels. GroEL served as a loading control. The additional bands below the GroEL are leftover signals from the anti-6xHis antibody. (B) Multiple sequence alignment for HP1432 protein in different *H. pylori* strains investigated in (A). The conserved stretch of six consecutive histidine residues, which is recognized by the anti-6xHis antibody, is indicated in a box.

Since ArsZ appears to have been acquired exclusively in the second branch of the *Helicobacter* super-lineage (Figure 2.20 B), the genome organization of genes flanking *arsZ* in these strains was compared to the corresponding genes of the first branch (hpAfrica2), which could represent the state prior to acquisition of the *arsZ* gene. *H. acinonychis* and *H. pylori* SouthAfrica7 were chosen as representative members of the hpAfrica2 branch, while *H. pylori* strains G27 and 26695 were selected as members of the second branch. *H. pylori* J99 was included as a representative of the sub-branch hpAfrica1 (Figure 2.22 A). Clusters of homologous genes upstream (magenta arrows) and downstream (orange arrows) of *arsZ* from

these selected strains were aligned with the multiple genome alignment tool MAUVE (Darling *et al.,* 2004) and visualized with EasyFig (Sullivan *et al.,* 2011). Within the hpAfrica2 branch, which does not contain ArsZ, the homologous genes were inverted in *H. acinonychis* when compared to *H. pylori* SouthAfrica2. The fragmented gene in *H. acinonychis* is a common feature of genomes of host jump strains (Eppinger *et al.,* 2006). Some genome rearrangement events appear to have occurred in *H. pylori* J99, including loss of genes that are present in *H. pylori* SouthAfrica7 (pink, white, and black arrows) and inversion of a gene cluster (magenta arrows). The *arsZ* gene (green arrow) is absent in *H. pylori* SouthAfrica7 and only emerged in the intergenic region of this cluster of genes in *H. pylori* J99 (Figure 2.22 B). In line with a previous report, genome rearrangement events can either form or erode sRNA genes (Raghavan *et al.,* 2015). After the split between into two super-lineages, *arsZ* may have been acquired by *H. pylori* in the second lineage due to a genome rearrangement event involving a group of genes or in combination with a horizontal gene transfer event. Although with some minor differences in exact genome organization, members of the second super lineage have maintained similar genome organization and have kept the *arsZ* gene.

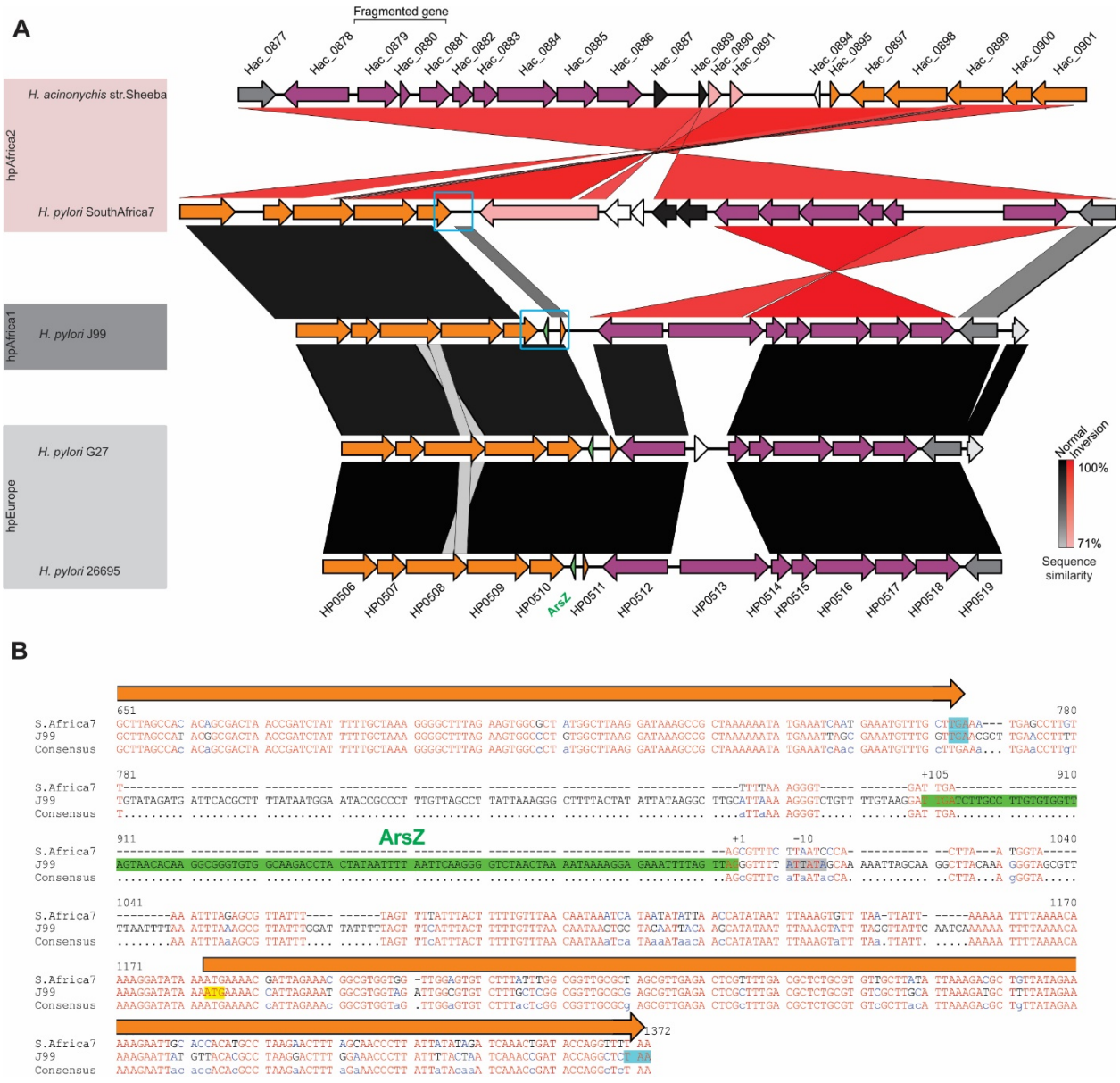

Figure 2.22: Conservation of genome organization in regions flanking *arsZ* in hpEurope and hpAfrica1 compared to similar regions in hpAfrica2 isolates. (A) All colored genes indicate homologous genes based on BLAST cut-off E-value 1 E-05 and minimum sequence similarity of 70 %. White arrows indicate non-conserved genes. Clusters of homologous genes downstream and upstream of *arsZ* were colored orange and magenta, respectively. The black connecting lines indicate conserved genomic organization, while red lines indicate gene inversions. Blue box indicate region used for multiple sequence alignment in B. The synteny and conservation of the flanking genes were derived from multiple genome alignments using the MAUVE tool (Darling *et al.,* 2004). All the figures were visualized and constructed using EasyFig (Sullivan *et al.,* 2011). (B) Multiple sequence alignment of DNA from the flanking region of *arsZ* in *H. pylori* SouthAfrica7 and J99.

Interestingly, in two *H. pylori* strains (B8 and SJM180), the *arsZ* gene has been truncated by an inversion of the *cag* PAI cluster (Figure 2.23 A, blue arrows). This suggests that after the acquisition of *arsZ*, a second genome rearrangement event might have occurred during the acquisition of the *cag* PAI cluster, which in turn, had led to the disruption of the gene encoding the sRNA. Northern blot analysis confirmed that the truncated *arsZ* in strain B8 is not expressed (Figure 2.23 B). Since the ArsZ binding site remains intact in the 5'UTR of the HP1432 ortholog in B8 (Figure 2.23 C, upper panel) and the amino acids sequence is highly similar to 26695, it might be possible to artificially regulate levels of HP1432 and urease activity by introducing a copy of *arsZ* from *H. pylori* 26695. In agreement with this hypothesis, an about two-fold reduction in HP1432 protein levels (Figure 2.23 B, lane 3 and 4) and a 1.5-fold reduction in urease activity (Figure 2.23 D) was observed upon introduction of *arsZ* from 26695 into B8. The levels of HP1432 protein positively correlated with the levels of urease activity, in line with the model that HP1432 modulates urease activity under acid stress conditions. Although the B8 strain is a Gerbil-adapted laboratory strain (Farnbacher *et al.,* 2010), a similar truncation pattern of *arsZ* was found in the draft genome of the parental strain, B128 (McClain *et al.,* 2009). The SJM180 strain was isolated from an Amerindian patient with gastritis and hence, there is no clear link between the two strains. It remains to be answered as to why these strains have lost ArsZ.

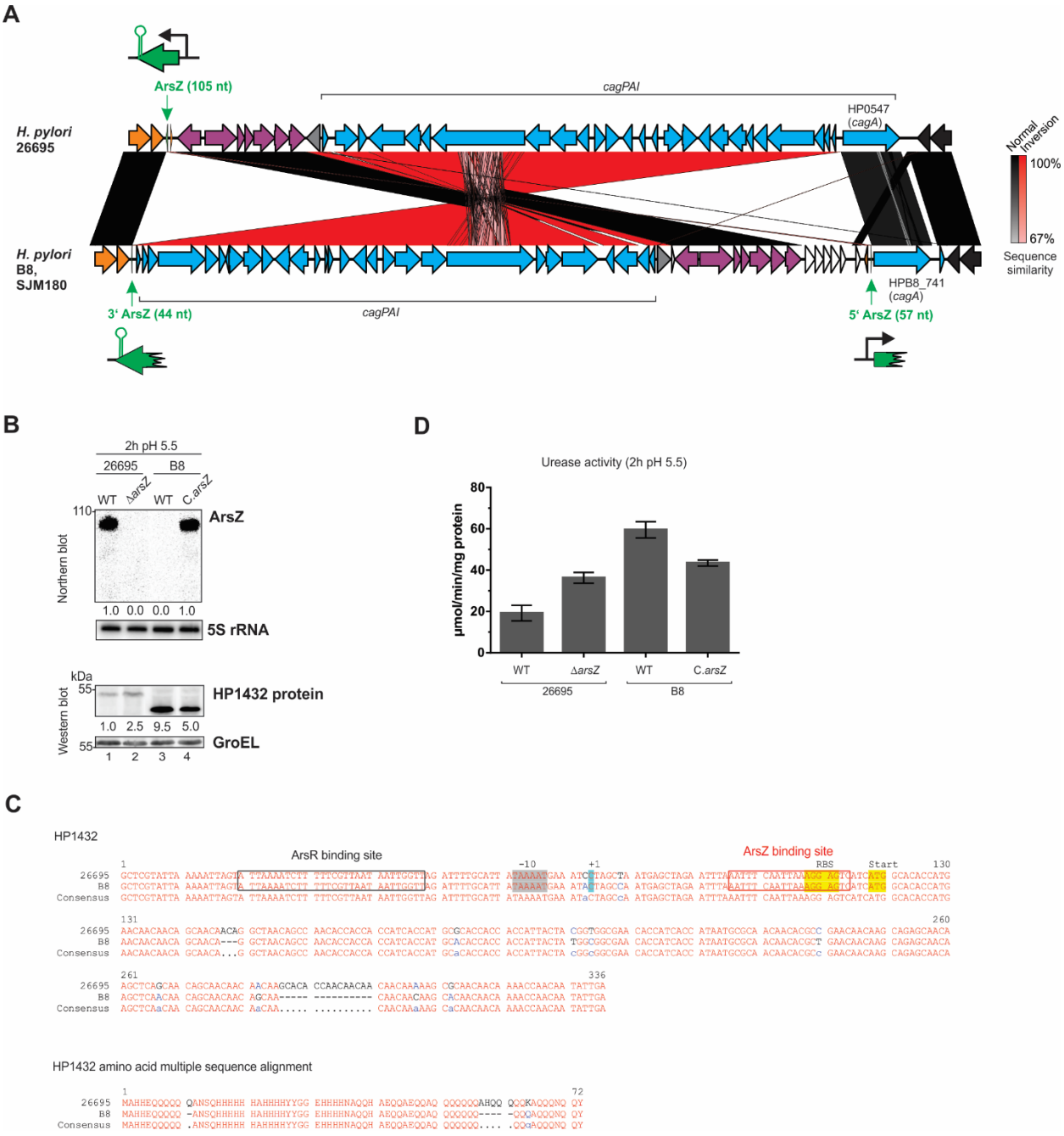

Figure 2.23: Loss of the *arsZ* gene in strain B8. (A) All colored genes indicate homologous open reading frames. White arrows indicate non-conserved genes. Clusters of homologous genes downstream and upstream of *arsZ* were colored orange and magenta, respectively. The black connecting lines indicate conserved genomic organization while red lines indicate gene inversions. The synteny and conservation of the flanking genes were derived from multiple genome alignment using the MAUVE tool (Darling *et al.*, 2004). All the figures were constructed using EasyFig (Sullivan *et al.*, 2011). The *cag* pathogenicity island (*cagPAI*) genes are colored blue. For better visualization, the truncated *arsZ* gene is shown as cartoon arrows. (B) The expression of ArsZ in *H. pylori* strain 26695 and B8 after 2 hours at pH 5.5 were quantified on a Northern blot. 5S rRNA served as a loading control. An anti-6xHis antibody was

used to monitor HP1432 protein levels. GroEL served as a loading control. (C) Multiple sequence alignment of DNA (upper panel) and amino acid (lower panel) sequences of HP1432 in *H. pylori* strains 26695 and B8. (D) Protein samples were collected from the indicated strains after either 2 hours of exposure to pH 5. The urease activity for these samples was quantified as described previously (Figure 2.17).

3 Discussion

3.1 Overall model for the regulation of HP1432 and urease activity by ArsZ in response to pH downshift

Exposure to low pH is one of the main environmental stresses encountered by *H. pylori* during colonization of the human stomach. The level of active urease plays a central role in ensuring its survival under acidic conditions and continued colonization of the host (Eaton & Krakowka, 1994). Activity of the urease enzyme does not only depend on the levels of apo-urease (*i.e.*, the protein subunits), but also on the loading of the protein with its essential nickel cofactor.

In the absence of a low pH signal, the TCS ArsRS is inactive and the ArsZ sRNA is not repressed and thus abundantly expressed. High levels of ArsZ post-transcriptionally repress translation of the HP1432 mRNA. As the TCS is not active in this condition, via the sRNA the levels of the HP1432 mRNA are also lower. Under acidic conditions, the UreI urea channel opens up allowing uptake of urea. The sensor kinase ArsS undergoes autophosphorylation and activates ArsR. The phosphorylated response regulator ArsR then simultaneously activates the transcription of the HP1432 mRNA while repressing expression of the sRNA ArsZ. Both actions allow HP1432 protein levels to increase. In turn, higher expression of HP1432 under low pH promotes activity of the urease enzyme. This could be achieved by to conceivable mechanisms. Either by releasing nickel into the cell or by facilitating loading of nickel into the apo-form of urease. The presence of nickel then increases the fraction of halo-urease, which cleaves urea into ammonia in order to buffer and/or raise the cellular pH.

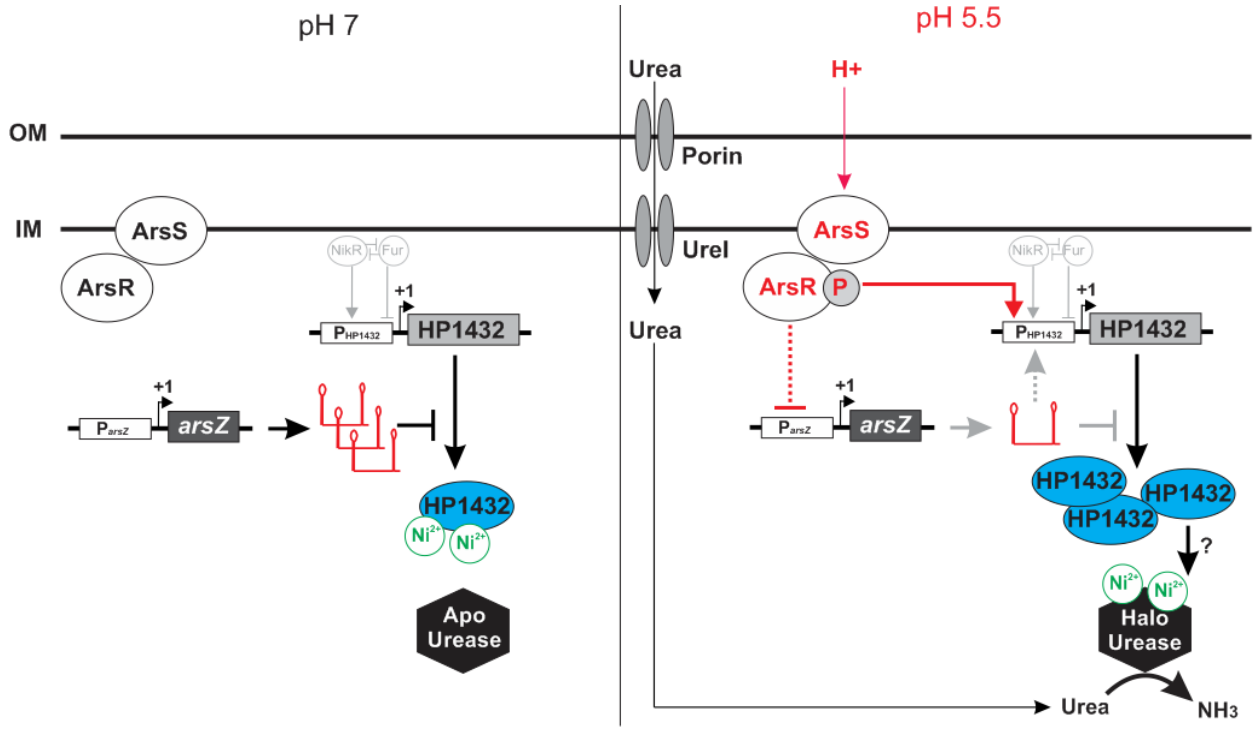

Figure 3: Overall model for ArsZ regulation of HP1432 and halo-urease levels upon pH shift to 5.5. (Left panel): At neutral pH, ArsRS is not active leading to de-repression of ArsZ and low expression levels of HP1432. Constitutively expressed ArsZ represses translation of HP1432 mRNA. (Right panel): Low pH signal (H^+) activates ArsRS, which simultaneously activates transcription of HP1432 while repressing expression of ArsZ. This switches on the coherent feedforward loop that works synergistically to increase HP1432 protein levels. It should be noted that ArsZ also affects expression of the HP1432 mRNA directly or indirectly by a so far unknown mechanism (grey dotted line). At low pH, urea is imported into the cytoplasm via porins and UreI channels. Higher urease activity is promoted by increased expression of HP1432 via a yet-to-be-established mechanism or by facilitating loading of nickel into apo-urease. The active halo-urease cleaves urea into ammonia, which diffuses into the periplasmic space to buffer and/or raise the cellular pH.

3.2 ArsZ is incorporated into the ArsRS TCS as a delay switch regulating HP1432

ArsZ forms a coherent feed-forward loop with ArsRS to regulate HP1432 in response to pH (Figure 2.16). Upon pH downshift, the ArsRS TCS is activated and the phosphorylated ArsR regulator represses ArsZ and also simultaneously activates transcription of the HP1432 mRNA. Both actions act coherently to increase the transcription and translation of HP1432, rapidly increasing the pool of HP1432 protein. Although such a loop typically consists of two transcription factors that act in a hierarchical manner to regulate the expression of a third downstream gene (Milo *et al*., 2002), it has been established that genes

are not only regulated at the DNA/transcriptional level but also regulated post-transcriptionally at the RNA level by bacterial small RNAs (sRNAs) in the form of mixed FFLs (Beisel & Storz, 2010) (Papenfort *et al*., 2015).

The coupling of sRNAs and TCSs in mixed coherent FFLs is a common theme in many enteric bacteria (Gopel & Gorke, 2012). Coherent FFLs have been proposed to function as persistent detectors of environmental stimuli by incorporating a delay component into the regulatory pathway (Mangan & Alon, 2003). The architecture of coherent FFLs allows the sRNA component to act as a deferral mechanism in the regulatory circuit. In *E. coli*, the MicF and MicC sRNAs form a type-4 (C4) and type-3 (C3) coherent FFL, respectively with the EnvZ/OmpR TCS to regulate various outer membrane proteins in response to osmolarity and cell envelope stress (Aiba *et al*., 1987) (Mizuno *et al*., 1984, Coornaert *et al.*, 2010, Chen *et al*., 2004, Guillier & Gottesman, 2008). Another sRNA, Spot42, which regulates multiple metabolic genes in response to high glucose, is part of a multi-output type-4 coherent FFL that has been proposed to reduce leaky expression of target genes (Beisel & Storz, 2011). Spot42 maintains repression of target genes under changing nutrient conditions. The here presented study revealed that ArsZ participates in a type-4 coherent FFL that allows the specialized bacterium *H. pylori* to respond and adapt to its niche-specific challenge (low pH). A constant signal of low pH for at least 2 hours is required to initiate repression of ArsZ expression (Figure 2.6). Consistent with the role of coherent FFLs as a delay mechanism, translation of the HP1432 mRNA increased more rapidly in a Δ*arsZ* mutant compared to the wildtype (Figure 2.16 C). This presumably ensures that HP1432 protein levels do not abruptly change upon transient pH changes encountered by the bacteria, and thus delays the increase in HP1432 levels until a sustained reduction in pH is achieved. This way, the incorporation of the sRNA into the FFL "fine-tunes" the response of the regulatory module to suit the needs of the bacterium *in vivo*. Same as MicF, MicC, and Spot42, ArsZ participates as the "Y" component in the coherent FFL and is thus regulated by a transcription factor (Figure 1.6). In contrast, there are sRNAs that act as the "X" component, giving rise to an sRNA-controlled FFL instead of the usual transcription-factor-controlled FFL. Apart from the RNAIII sRNA in *S. aureus*, which regulates the expression of the transcription factor Rot (Figure 1.6 B), the RprA sRNA in *Salmonella* also acts upstream of a transcription factor, the alternative sigma factor S (σ^S). RprA participates in a type-1 coherent FFL (C1) with AND-gate logic to directly and indirectly (via regulation of σ^S) modulate levels of the RicI conjugation inhibitor protein (Papenfort *et al*., 2015). Although the sRNA can act as a top-tier transcription regulator, this configuration might not allow the sRNA to "sense" environmental signals afforded by coupling of the sRNA to a TCS. In this aspect, expression of ArsZ is timely regulated by the ArsRS TCS when required (*i.e.* only during acid adaptation).

Besides the coherent FFL, very few examples where sRNAs participate in mixed incoherent FFLs exist. Incoherent FFLs have been proposed to speed up target gene activation. All three of the experimentally validated mixed incoherent FFLs (PrrA/PcrZ sRNA, RpoE/RybB sRNA and PhoP/AmgR sRNA systems) so far only involve type-1 incoherent FFL (I1) (Figure 1.6 B) (Mank *et al*., 2012) (Gogol *et al*., 2011) (Lee & Groisman, 2010). Interestingly, after adaptation to low pH (overnight growth in pH 5.5-adjusted media), ArsZ directly or indirectly activates the promoter of HP1432 (Figure 2.11, 2.12). This gives rise to a mixed type-4 incoherent FFL (I4), a phenomenon that has never been described to include a sRNA before. Although an I1 can be commonly found in transcriptional networks, the occurrence of an I4 is very rare in *E. coli* (Mangan & Alon, 2003). The unique role of ArsZ to additionally participate in the transcriptional regulation of its target, puts this particular sRNA into a non-standard FFL. During the initial acid adaptation process (the first 8 hours of acid exposure), ArsZ functions exclusively as a delay mechanism in a C4-FFL (Figure 2.16). However, after acid adaptation, the sRNA additionally participates in an I4-FFL (Figure 2.12 and Figure S5). Further acid exposure after the initial acid adaptation phase, ArsZ participates in both the I4-FFL and the C4-FFL(Figure S5). A potential role of ArsZ in the I4-FFL could be to accelerate the production of HP1432 mRNA once the bacteria have adapted to the acidic environment.

Apart from feedforward loops, an interesting feature of transcriptional networks in *H. pylori* is the use of negative interactions to constantly monitor the bacterium's environment and provide a rapid response upon transduction of regulatory stimuli (Danielli *et al.*, 2010). It seems plausible that the ArsZ-HP1432 regulation adopts a similar strategy in the absence of low pH signals. At neutral pH the ArsRS TCS is not active and thus the coherent feedforward loop is switched off. In this mode, ArsZ which is constantly expressed at high levels is not repressed by ArsR~P. A ratio of ArsZ to HP1432 in favor of the sRNA allows ArsZ to "silence" the expression of HP1432 and may play an important role in preventing overexpression of HP1432 in the absence of acidic conditions. This is in line with the role of sRNAs as fine-tuners of gene expression (Storz *et al*., 2011).

In summary, ArsZ is the first example of a single sRNA that can regulate the same target as part of two different FFL configurations at transcriptional and post-transcriptional levels. C4-FFL is the major regulatory circuit while I4-FFL comes into play once adaptation to acidic conditions has been achieved. This study also characterized the first mixed FFL in the major human pathogen *H. pylori* contributing to the understanding of how this bacterium can survive and colonize the harsh environment of the human stomach.

3.3 ArsZ provides the ArsRS TCS with a regulatory RNA arm to fine-tune urease maturation

HP1432 is one of the three atypical histidine-rich proteins (the others being HspA and HP1427) encoded by *H. pylori* strains. The numerous conserved histidine residues of these proteins are thought to be involved in binding nickel cations (Kansau *et al.*, 1996, Ge *et al*., 2006a, Zeng *et al*., 2008, Zeng *et al*., 2011, Gilbert *et al*., 1995). While the HspA protein, a homologue of GroES, is a dedicated chaperone for [NiFe]-hydrogenase maturation (Schauer *et al.*, 2010), the paralogous HP1427 and HP1432 have been proposed to comprise an intracellular nickel sink (Seshadri *et al*., 2007), releasing the ion at low pH for urease activation, but sequestering Ni^{2+} at neutral pH (Ge *et al*., 2006a, Seshadri *et al*., 2007).

The urease enzyme is essential for *H. pylori* gastric colonization (Eaton & Krakowka, 1994), and nickel-binding proteins such as HP1432 have been proposed to affect activation of urease at low pH. Two important studies have provided *in-vivo* (Seshadri *et al*., 2007) and *in-vitro* (Zeng *et al*., 2008) evidence that HP1432 releases nickel at pH 5. Moreover, a stomach colonization defect in a mouse model was observed in the absence of either HP1432 alone (Vinella *et al*., 2015) or in a double deletion mutant of HP1432 and HP1427 (Benoit *et al*., 2013, Vinella *et al*., 2015). The regulation of HP1432 by multiple transcription factors (ArsR and NikR) underscores the importance of maintaining precise levels, or having specific induction dynamics, of the HP1432 protein.

Although an asRNA (5'*ureB*-sRNA) was reported to regulate expression of the urease operon in *H. pylori* by promoting premature transcription termination of the *ureAB* mRNA under acidic conditions (Wen *et al.*, 2013), the implications of such a regulation is unclear. For example, the 5'*ureB*-sRNA is activated by the non-phosphorylated TCS regulator ArsR rather than its phosphorylated form, which is the predominant form under acidic conditions (Wen *et al*., 2011). Moreover, the presence of this asRNA seems to be strain specific (strain 43504) since 5'*ureB*-sRNA was not detected in the global transcriptome analysis of the major *H. pylori* strain 26695 (Sharma *et al*., 2010).

The discovery that ArsZ post-transcriptionally represses HP1432 suggests that ArsZ provides an additional layer of regulation to ensure that HP1432 is precisely regulated. Although the mechanism by which HP1432 affects urease maturation is currently unknown, an increase in nickel content has been positively correlated with an increase in urease activity (van Vliet *et al*., 2001). It is therefore conceivable that ArsZ regulates HP1432 as a way to maintain precise levels of halo-urease by affecting nickel levels. Importantly, the increase of urease activity in the absence of ArsZ is dependent on HP1432, suggesting that nickel released from this protein is sufficient to modulate urease activity at pH 5.5. The delay mechanism conferred by ArsZ may prevent a transient drop in pH from accidentally activating the urease maturation

pathway. This may be important to prevent alkalization of the cytoplasm due to high ammonia production under neutral conditions by urease (Clyne *et al.*, 1995). While the exact mechanism of nickel release and transfer from HP1432 to urease is still unclear and warrants further investigation, a possible route of nickel transfer could be via protein-protein interaction between HP1432, the related nickel-binding protein HP1427, and UreA. This hypothesis is supported by recent bacterial two-hybrid experiments that showed direct interaction between these factors (Vinella *et al*., 2015).

Even though the urease protein is expressed at high levels (approximately 10 % of total cellular protein), only 7 to 25 % of urease is present in the active form (Stingl & De Reuse, 2005). This suggests that *H. pylori* might control urease activity via levels of halo-urease, in addition to transcriptional control by numerous transcription factors, including ArsRS. It is possible that ArsZ provides ArsRS with an additional regulatory arm to modulate the final step of the apo-urease activation pathway by controlling the availability of nickel via HP1432.

The regulation of HP1432 by ArsZ in response to low pH seems to be conceptually similar to the regulation of iron binding proteins by RyhB in response to iron availability by Fur in *E. coli*. Although expression of both RyhB and ArsZ is regulated in response to environmental signals, these two sRNAs in fact use very different mechanisms to maintain homeostasis in the cell. At low iron conditions, RyhB is derepressed by Fur leading to high expression of this sRNA (Masse & Gottesman, 2002). RyhB activates the expression of genes that are important in the siderophore production pathway (Prevost *et al.*, 2007) (Salvail *et al.*, 2010). Siderophores are low molecular weight iron-binding proteins, which are secreted into the environment to scavenge for iron. The siderophore-iron complexes are transported back into the cell to increase cellular iron concentration. The intracellular iron levels serve as a negative feedback to inhibit Fur expression once iron homeostasis has been achieved (Prevost *et al*., 2007). In contrast, ArsZ is not a metal responsive sRNA that is involved in metal homeostasis. ArsZ post-transcriptionally regulates the expression of the nickel-binding protein, HP1432 to control the final maturation step of the metaloenzyme urease. The conversion of urea to ammonia by the active urease enzyme to increase the pH is dependent on the availability of nickel in the cell. Thus, it might be metabolically advantageous to utilize a sRNA to rapidly fine-tune a nickel sponge protein for optimal levels of active urease.

ArsZ is the first example of a *trans*-acting sRNA that regulates a nickel storage protein to modulate apo-urease maturation. This study adds a new concept of sRNA regulation by demonstrating that a sRNA can indirectly regulate a metalloenzyme at the post-translational level. These findings may have important implications in understanding the details of urease activation and hence the colonization capability of *H. pylori*.

3.4 Post-transcriptional regulatory mechanism of ArsZ

The two previously characterized *trans*-acting sRNAs (RepG and CncR1) in *H. pylori* negatively regulate their targets. Similarly, this study reports the third *trans*-acting sRNA, ArsZ and shows that its target HP1432 is negatively regulated by this sRNA. However, all of the three sRNAs have very different post-transcriptional regulation on their targets. RepG uses its C/U-rich loop to target the variable homopolymeric G-repeat in the mRNA leader of TlpB, an acid-sensing chemotaxis receptor. Depending on the length of this G-repeat, the translation of *tlpB* is post-transcriptionally regulated and can mediate both activation and repression of *tlpB* (Pernitzsch *et al*., 2014). Contrary to that, CncR1 binds at multiple sites within the *fliK* mRNA, encoding for a flagellar checkpoint protein. Although the exact mechanism of regulation of *fliK* by CncR1 remains unclear, the authors could show that CncR1 post-transcriptionally represses translation of the *fliK* mRNA (Vannini *et al*., 2016). In contrast, ArsZ binds exclusively at the RBS region of the HP1432 mRNA to post-transcriptionally repress its translation (Figure 2.9, 2.11). Thus, the regulatory mechanism employed by ArsZ to regulate HP1432 is thematically similar to those reported in enteric bacteria (Gottesman, 2005) whereby the translation of the target mRNA is repressed by a sRNA which titrates the RBS away from ribosomes (Figure 1.5 A). This study shows that the direct mechanism to repress mRNA translation by a sRNA exists in *H. pylori* as well.

It is important to note that unlike most sRNAs in many enteric bacteria that require Hfq for productive interaction with their targets, *H. pylori* lacks the homolog of this important RNA chaperone. None of the characterized sRNAs in *H. pylori* has so far reported the requirement of an RNA binding protein (RBP) for their regulation. It is possible that an unknown RBP may substitute the role of Hfq in *H. pylori*. Alternatively, the role of Hfq might be altogether dispensable in *H. pylori* such as in the case of Gram positive bacteria. It was proposed that the requirement for an RNA chaperone such as Hfq in terms of proper sRNA function can be proportionately correlated with a smaller genome size, a lower GC genome content, and a higher free energy of sRNA-mRNA base-pairing (Jousselin *et al.*, 2009). The genome size of *H. pylori* is at least 25 % smaller (1.6 Mb) compared to most gammaproteobacteria (~ 4-6 Mb). In addition, its GC genome content is only 39 % compared to 50 – 67 % in the gammaproteobacteria clade (Sittka *et al.*, 2008) (Viegas *et al.*, 2007) (Sonnleitner *et al.*, 2008). In fact, genome size and GC content of *H. pylori* is very similar to *S. pyogenes* (genome size of 1.8 Mb and GC content of 38 %) (Kreikemeyer *et al.*, 2001) and the cyanobacterium *Prochlrococcus marinus* (genome size of 1.6 Mb and GC content of 31 %) (Axmann *et al.*, 2005). While Hfq is absent in *S. pyogenes*, the genome of *P. marinus* encodes for an Hfq homolog but it is completely dispensable for sRNA function in this bacterium. Moreover, the free energy of ArsZ-HP1432 mRNA pair is -27.9 kcal/mol. This is comparable to the RNAIII-*spa* mRNA pair (-22.5 kcal/mol) in *S. aureus*, which does not require Hfq (Huntzinger *et al.*, 2005).

Both pairs of sRNA-mRNA have extended base-pairing with 19 bp and 44 bp, respectively. These sRNA-mRNA duplexes are much more stable compared to the ones form *E. coli*. For example, RyhB-*sodB* mRNA interaction only involves 9 bp with a free energy of -5.5 kcal/mol and requires Hfq to enhance the rate of duplex formation (Geissmann & Touati, 2004). Thus, it might be possible that Hfq or any other RNA chaperone is dispensable in the duplex formation of ArsZ and HP1432 mRNA in *H. pylori*.

Interestingly, ArsZ is highly resistant to overexpression. Under native conditions (*i.e.* using WT ArsZ), the maximum threshold for overexpression of ArsZ seems to be two-fold because ArsZ could not be expressed under stronger promoters (Figure 2.15 A). It is possible that the levels of ArsZ need to be strictly regulated, forcing the cell to immediately downregulate any attempts to overexpress ArsZ. One possible mechanism of regulation could involve rapid degradation of ArsZ by ribonucleases when extremely high levels of ArsZ are present. Indeed, substituting the original unstable stem-loop (SL1) of ArsZ with the more stable stem-loop from the RepG sRNA successfully allows the chimeric ArsZ to be overexpressed (Figure 2.15 B, C). This suggests that the native ArsZ has a built-in mechanism to prevent its own overexpression. Other sRNAs that have been shown to exhibit only week phenotypes *in vitro* and are reluctant to overexpression, may likewise be central players in fine control of gene expression in bacteria such as *H. pylori*.

Many sRNAs often use RNA decay as a post-transcriptional control of gene expression (Laalami *et al.*, 2014). sRNA can regulate mRNA stability either by directly recruiting ribonucleases (RNases) to their targets or indirectly via blocking translation, promoting degradation of ribosome-free mRNAs by RNases. For example, the MicC sRNA binds to the coding sequence of *ompD* and promotes its direct degradation by recruiting RNase E to the interaction site to initiate the mRNA decay (Pfeiffer *et al*., 2009). Moreover, it was proposed that a 5' monophosphate group on MicC stimulates *ompD* cleavage by RNase E (Bandyra *et al*., 2012). In bacteria that lack a homolog of RNase E, RNase III could directly participate in mRNA degradation pathways mediated by sRNAs. RNase III in particular has been shown to be involved in sRNA-mediated regulation in diverse bacteria (Arraiano *et al.,* 2010). This enzyme is involved in the decay of various sRNA/mRNA duplexes (Vogel *et al.,* 2004), resembling the RNA interference (RNAi) mechanism of eukaryotic cells (Agrawal *et al.,* 2003). Under *in-vitro* conditions, RNase III can cleave RNA duplexes as short as 11 bp (Gan *et al.,* 2006).

According to in-line probing data (Figure 2.8 A, D), ArsZ can form a 19 base-pair duplex with HP1432, suggesting that this interaction could potentially be cleaved by RNase III. The *in-vitro* structure probing data (Figure 2.8 B, E) falls in line with the RNA-RNA interaction predicted by the RNAstructure tool (Reuter & Mathews, 2010) (Figure S3). This suggests that RNase III may play a role in the interaction

between ArsZ and HP1432. *In vivo*, in the absence of RNase III, expression of both ArsZ and HP1432 mRNA increases about two-fold (Figure S6). Not all sRNAs were affected by the absence of RNase III. For example, no increase in RepG levels was observed in a Δ*rnc* mutant compared to WT. Interestingly, the protein levels of HP1432 decreased by three-fold in the Δ*rnc* background and were restored to WT levels upon deletion of *arsZ* in the same background (Δ*rnc* Δ*arsZ*). One possible explanation for this observation is that in Δ*rnc*, higher levels of ArsZ might be able to form duplex structures with the HP1432 mRNA, leading to decreased translation of HP1432 mRNA. Upon relieve of repression by ArsZ (Δ*rnc* Δ*arsZ*), HP1432 mRNA can be translated. Although an RNA degradosome organized by RNase E is the major ribonuclease that promotes degradation of many transcripts in enteric bacteria, RNase III has emerged as an important endoribonuclease that controls RNA stability (Jaskiewicz & Filipowicz, 2008). It has been proposed that RNase III can replace RNase E (Lalaouna *et al.*, 2013). Since *H. pylori* lacks a homolog of RNase E, RNase III might be a major player in sRNA-mediated regulation in this bacterium. Although a minimal degradosome consisting of RNase J was identified in *H. pylori* (Redko *et al.*, 2013), a recent study has shown that this ribonuclease is not likely to be involved in sRNA-mediated regulation of gene expression (Redko *et al.*, 2016). Nevertheless, this study does not rule out the role of other RNases in the regulation of ArsZ-HP1432.

3.5 ArsZ may have been acquired by modern *H. pylori* strains to regulate HP1432

The phylogeographic patterns of *H. pylori* have been associated with migration events throughout the human evolution (Falush *et al.*, 2003) (Moodley & Linz, 2009). Given the importance of precise urease levels for successful host colonization, it can be postulated that there is a selective pressure for this bacterium to preserve ArsZ. The slight growth defect observed in a Δ*arsZ* mutant after prolonged acid exposure (Figure 2.1.21B) may provide a selective advantage for cells to retain ArsZ. This seemingly limited phenotype associated with the absence of ArsZ is in fact in line with the regulatory, but not essential roles of sRNA in bacteria (Updegrove *et al*., 2015).

It was proposed that sRNAs, which have only a single target and share extensive complementarity with their target mRNAs, such as MicL in *E. coli* (Guo *et al*., 2014), might be young sRNAs from the evolutionary point of view (Updegrove *et al*., 2015). The ArsZ and HP1432 pair is similar to the MicL-*lpp* pair in this respect, where HP1432 is (so far) the only known target of ArsZ and shows extensive base-pairing. This might suggest that ArsZ is a fairly young sRNA. Moreover, compared to RepG, which seems to have emerged earlier in the phylogenetic tree of *Helicobacter*, ArsZ only appeared much later in the evolution of *H. pylori* (Figure 2.20 B). This suggests that the evolution of ArsZ is closely tied to the emergence of *H. pylori* strains in the non hpAfrica2 branch. HP1432 as the target of ArsZ emerged at the

split of *H. pylori* into two super lineages (Figure 2.20 B) via a gene duplication event. This was proposed to provide an additional gastric colonization advantage (Vinella *et al*., 2015). The gene encoding ArsZ may have been acquired after the split to regulate urease levels via HP1432 in the *H. pylori* strains of the second branch. The strains from hpAfrica2 infect members of geographically-isolated ancient African tribes, while strains from the second branch spread and infects humans globally. Although the difference in diet and lifestyle between these groups could explain the reasons as to why only members of the second branch require precise urease regulation. However, further investigations are required to support this hypothesis. Nevertheless, the requirement for a precise control of urease activity in the second branch was accomplished by incorporating a sRNA, ArsZ to post-transcriptionally modulate levels of a histidine-rich protein, HP1432.

3.6 Elucidation of the role of sRNAs in the dense overlapping regulatory networks

Like many bacteria, *H. pylori* encounters environmental fluctuations in its habitats and has evolved various strategies to efficiently respond to these conditions. The genome of *H. pylori* is about four times smaller than *E. coli* and contains only 17 transcription factors (Scarlato *et al*., 2001) compared to 210 transcription factors in *E. coli* (RegulonDB April 2017, (Salgado *et al.*, 2006). Contrary to the common belief that bacteria with small genomes have simple regulatory networks, *H. pylori* has dense, overlapping transcriptional regulatory networks (TRN) (Danielli *et al*., 2010). The four so far well-characterized regulatory modules (termed as origons) in *H. pylori* are the heat shock stress response module, the flagellar biosynthesis module, the acid acclimatization module, and the metal homeostasis module, which includes iron and nickel homeostasis networks (Danielli *et al*., 2010). Moreover, the long sequential regulatory cascades that are common in many bacteria to regulate processes such as biofilm formation (Martinez-Antonio *et al.*, 2008) are absent in *H. pylori*. Hence, shallow but dense overlapping regulatory networks at the transcriptional level between metal-responsive regulation, acid regulation, and two other networks in *H. pylori* have been suggested (Danielli *et al*., 2010). Shallow network architecture reduces the number of cascade steps required to transmit a signal and enables bacteria to response more rapidly (Alon, 2007).

This unique network structure could complicate efforts to identify potential targets for fine-tuning molecules such as sRNAs. A global proteomic approach was initially performed to identify potential targets of ArsZ. Two-dimensional polyacrylamide gel electrophoresis (2D-PAGE) was used to compare the proteome of wild-type and an *arsZ* deletion mutant (Δ*arsZ*) grown at either pH 5.5 or pH 7 (Figure S7 A). This method failed to identify differentially expressed proteins between WT and Δ*arsZ*. Due to the technical limitations of 2D-PAGE, which can only resolve abundant and soluble proteins (Petrak *et al.,* 2008), it is be possible that the targets of ArsZ are either weakly expressed or part of the insoluble fraction. A second

approach using RNA-seq based transcriptome analysis offers higher sensitivity (Figure S7 B). This approach successfully identified HP1432 as a potential target (~5 fold downregulated in Δ*arsZ*). Besides the RNA-seq method, computational approaches could be advantageous as a first-line screen for potential targets. Although *in-silico* methods may produce high rates of false positive targets, these predictions can be carefully curated and a small subset of these top targets can be simultaneously investigated *in vitro* for potential base-pairing with the sRNA. Moreover, computational methods combining phylogenetic information and target RNA predictions such as CopraRNA significantly reduce the number of false positive targets (Wright *et al*., 2013). The identification of HP1432 as the top predicted target compliments the RNA-seq results. This suggests that bioinformatics approaches can provide a high confidence target, which could be further characterized exhaustively *in vivo*.

Moreover, it is useful to study the sRNA-mRNA interaction under dynamic conditions for targets that are extensively regulated by various transcription factors. HP1432 is regulated at the transcriptional level by three different transcription factors belonging to three different origons. Hence, the effect of losing ArsZ may not be easily identified when studied under steady-state conditions, since a perturbed origon can be effectively compensated for by other origons. This study shows that the physiological role of a sRNA can be elucidated without artificially overexpressing the sRNA. Coupled with time-course experiments under specific environmental signals, this approach allows the kinetics of a sRNA regulation to be studied under more native conditions.

4 Conclusions and outlook

This thesis showed that the small RNA ArsZ and its target mRNA HP1432 constitute yet another level of urease regulation that contributes to adaptation to acidic pH by *H. pylori,* which is central to colonization of the gastric environment. At otherwise neutral conditions, ArsZ represses HP1432 translation. The acid-responsive ArsRS two-component system represses ArsZ transcription, allowing de-repression of HP1432 translation at low pH. ArsZ fine-tunes urease activity following a shift to low pH presumably by altering nickel availability through control of expression of the nickel-binding protein HP1432. This precise temporal control of HP1432 expression occurs via a coherent FFL, whereby ArsZ works in tandem with the response regulator ArsR of the ArsRS acid-response TCS to allow appropriate activation of urease activity. *In-vitro* and *in-vivo* experiments showed that ArsZ interacts with the ribosomal binding site of HP1432 mRNA, repressing translation of HP1432. Following acid adaptation, ArsZ additionally participates in a second incoherent FFL to activate the promoter of HP1432 via an unknown mechanism.

This thesis also provided new insights into the role of sRNAs in FFLs in bacteria. First, ArsZ is part of a non-standard FFL in which this single sRNA can participate in two different FFLs depending on the state of adaptation towards a specific stress. Second, this work also revealed that a FFL can be employed upstream of a metalloenzyme, possibly to filter environmental noise from the real signal. Third, this study demonstrated that an sRNA can expand the repertoire of a TCS from typical transcriptional control to additional post-transcriptional and post-translational control. It remains to be seen whether additional sRNAs in *H. pylori* or other bacteria also mediate this "extended" post-translational TCS regulation. Moreover, this study provided an interesting example of how a conserved sRNA has co-evolved with its target to regulate an important physiological aspect of a human pathogen. In a broader sense, many other bacterial pathogens might employ similar strategies to manage fluctuating environmental signals during transmission and colonization. Importantly, this study revealed that the characterization of a sRNA under dynamic native conditions can help to elucidate the kinetics of regulation kinetics, which may be missed under steady-state conditions.

The characterization of ArsZ has opened up interesting questions for future work. Although it was demonstrated in this study that the promoter of HP1432 is either directly or indirectly affected by ArsZ, the exact mechanism surrounding this mode of regulation is still unclear. Since the promoter of HP1432 is regulated by three transcription factors (ArsR, NikR and Fur), one approach could be to inspect the regulation of HP1432 in single, double, and triple deletion mutants of these regulators. Alternatively, a transposon screen in a HP1432 promoter reporter strain could be performed to identify additional potential regulators of HP1432 that might be responsible for the downregulation of its promoter upon deletion of the

sRNA Combination of a mutation in this potential regulator could be then be combined with a Δ*arsZ* mutation to show that this regulator is responsible for the downregulation. Moreover, a biochemical "fishing" experiment could be performed using the promoter of HP1432 as a bait to pull-down its interacting protein partners *in vitro* using the lysate of WT and/or a Δ*arsZ* mutant. Another interesting and speculative possibility for the mechanism of the effect of ArsZ on the HP1432 promoter could involve direct binding of ArsZ to the promoter region of HP1432 to form a RNA-DNA-DNA triplex. Recently, microRNAs were reported to form triplexes with double-stranded DNA to regulate gene expression at sequence-specific sites in eukaryotes (Paugh *et al.*, 2016). Although relatively unknown in bacteria, this idea is well established in the gene regulation of eukaryotic organisms (Bacolla *et al.*, 2015) (Li *et al.*, 2016).

Another aspect that requires further work is the question whether promoter of ArsZ is directly or indirectly regulated by phosphorylated ArsR. Since *in-vitro* phosphorylation of ArsR was highly inefficient, it may instead be possible to construct a mutant form of ArsR that behaves as if it is constitutively phosphorylated, and use the recombinant protein for *in-vitro* DNase I footprinting experiments.

Although HP1432 is the only target of ArsZ so far, it might be possible that this sRNA regulates additional targets which were not apparent by proteome or transcriptome analyses. There are two global approaches that may be used to identify potential targets of HP1432 and could even complement one another. The first method is the classical approach of pulse-overexpressing the sRNA, followed by transcriptome-wide analyses, as has been used to identify sRNA targets in many enteric bacteria. However, such a system has yet to be established for overexpression of sRNAs in *H. pylori*. The arabinose-inducible system that is widely used in *E. coli* and many other bacteria may not work in *H. pylori* because this bacterium only utilizes glucose as the sole sugar carbon source and lacks the cyclic AMP-based catabolic repression system (Marais *et al.*, 1999). Other inducible systems, such as the iron-responsive *pfr* promoter (Delany *et al*., 2002), the plasmid-based IPTG-inducible *lacI*^{q}-p*Tac* system (Boneca *et al.*, 2008), and *tet* inducible promoters (McClain *et al.*, 2013) (Debowski *et al.*, 2013) (Debowski *et al.*, 2015) have been reported in *H. pylori*. However, these inducible systems were mainly developed for the purpose of generating conditional mutants and thus, the rate of induction was determined to be in the range of hours (Boneca *et al*., 2008, Tjaden, 2008, Cancer, 1994), which is not ideal for rapid pulse-expression. A *tet*-inducible promoter system that is suitable for rapid expression of sRNAs and mRNAs is currently being developed by the author of this thesis (Tan HS & C. Sharma, unpublished data).

The second method is to use a GRIL-seq (global small non-coding RNA target identification by ligation and sequencing) approach to ligate all interacting RNA partners of ArsZ *in vivo* by overexpression of an RNA ligase, followed by deep sequencing to identify these targets (Han *et al.*, 2016). This method is

particularly appealing in bacteria such as *H. pylori*, which lack known global sRNA-binding proteins such as Hfq, since all other methods such as RIL-seq (RNA interaction by ligation and sequencing) or RNase E-CLASH (cross-linking, ligation, and sequencing of hybrids) requires an RNA-binding protein as a bait to pull down the sRNA-mRNA duplexes. The authors of the GRIL-seq method have combined the pulse-expression of the sRNA of interest shortly after inducing the expression of T4 RNA ligase and used an sRNA-specific oligonucleotide to recover sRNA-mRNA pairs. This system could be easily adapted for *H. pylori* with the help of the aforementioned *tet*-inducible system to pulse-express ArsZ. An additional inducible promoter such as the IPTG-inducible *lacI*^{q}-p*Tac* system (Boneca *et al*., 2008) could be adapted to conditionally drive the expression of the T4 RNA ligase *in vivo*.

In conclusion, this work demonstrated that ArsZ is an important sRNA that play a role in acid adaptation of *H. pylori*. ArsZ is the first example of a *trans*-acting sRNA that regulates a nickel storage protein to modulate apo-urease maturation post-translationally.

5 Materials and Methods

5.1 Materials

5.1.1 Equipment

Equipment and instruments	Manufacturer
analytical balances TE64, TE601	Sartorius
Bio-Link BLX 254 UV-Crosslinker	Peqlab
cell culture hood, HERASafe	Thermo Scientific
Celltron Shaker	Infors HT
centrifuge Eppendorf 5415R	Eppendorf
centrifuge Eppendorf 5424	Eppendorf
centrifuge Eppendorf 5810R	Eppendorf
eraser for imaging plates FLA	GE Healthcare
gel documentation system Gel iX Imager	Intas
gel dryer Bio-Rad Model 583	Bio-Rad
heating block Eppendorf comfort	Eppendorf
horizontal electrophoresis systems PerfectBlue Mini S, M, L	Peqlab
hybridization oven UVP HB-1000	Thermo Fisher Scientific
imaging plate cassettes BAS 2325, 2340	Fujifilm
imaging System Image Quant LAS 4000	GE Healthcare
incubator for *E. coli*, HERAcell (Kendro)	Thermo Scientific
incubator for *H. pylori* liquid cultures, HERAcell 150i	Thermo Scientific
incubator for *H. pylori* plates, Galaxy 170R	Eppendorf
Orbital Shaker NB-101S RC	N-BIOTEK
PCR machine, T3 thermocycler	Biometra
phosphorimager Typhoon FLA 7000	GE Healthcare
photometer Ultrospec 3100 pro Cell Density Meter	GE Healthcare
Pipetman P10, P20, P200, P1000, P5000	Gilson
power supplies peqPOWER E250, E300	Peqlab
Retsch MM400 ball mill	Retsch
Rotamax 120	Heidolph
rotator – SB2 STUART	STUART
scanner for protein gels, HP Scanjet 7400c	HP
semi-dry electroblotter PerfectBlue SEDEC M	Peqlab
shaker 37 °C room, SM-30	Bühler
SORVALL centrifuge RC5B	Thieme Labortechnik
spectrophotometer NanoDrop 2000	Peqlab
tank electroblotter PerfectBlue WebS, M	Peqlab
thermal cycler MJ Mini	Bio-Rad
Thermo Mixing Block MB-102	BIOER
vacuum pump	KnF LAB

vertical electrophoresis systems PerfectBlue Twin S, ExW S, L	Peqlab
vertical sequencing gel system CBS SG-400-20	C.B.S. Scientific
Victor3 1420 multilabel counter	Perkin-Elmer
Vortex-Genie 2	Scientific Industries
waterbath, GFL	Hartenstein

5.1.2 Consumables

Items	**Manufacturer**
boxes (plastic), 20.5 x 20.5 cm or 9.5 x 20.5 cm	Hartenstein
boxes (metal), 10 x 21 cm	Hartenstein
cell culture flasks 25 cm^3	PAA, Corning
cell culture flasks 75 cm^3	PAA, Corning
Cellstar serological pipets (plastic) 5 ml, 10 ml, 25 ml, 50 ml	Greiner bio-one
chromatography columns	Biorad
cotton swaps	DELTALAB, Stein
cover slips	Hartenstein
dewar canister	Hartenstein
Erlenmeyer glass flasks 250 ml, 1l	DURAN, SIMAX
G-25, G-50 MicroSpin columns	GE Healthcare
Gilson pipets 10 µl, 20 µl, 200 µl, 1000 µl	Gilson
glass beads (2.85 – 3.35 mm) for plating of CFU/ml	Roth
glass bottles	Schott
glass test tubes and lids	Roth
hard-shell PCR plates 96-well	Biorad
Hybond-XL membrane for nucleic acid transfer	GE Healthcare
imaging plate cassettes BAS 2325, 2340	Fujifilm
L-shape bacteriology loops	VWR
object slides	Hartenstein
PCR tubes 8 x 0.5 ml	Thermo Scientific
petri dishes	Corning
Phase Lock Gel (PLG)-tubes, 2 ml	5 Prime
Pipetboy accu-jet pro	BRAND
pipet tips	Sarstedt
PolyScreen PVDF Transfer Membrane	PerkinElmer
racks for PCR tubes / reaction tubes	Hartenstein
reaction tubes 1.5 ml, 2.0 ml	Sarstedt
reagent and centrifuge tubes 15 ml, 50 ml	Sarstedt
safe-lock tubes 1.5 ml, 2.0 ml	Eppendorf
spectrophotometer cuvettes	BRAND
sterile filters (0.20 µm pore size)	Sarstedt
tube holder 15 ml, 50 ml	Hartenstein

Whatman paper	ALBET LabScience

5.1.3 Reagent and chemicals

2 x gel loading buffer II (RNA)	Ambion
10 x RNA structure buffer	Ambion
1 x alkaline hydrolysis buffer	Ambion
20 x SSC (saline sodium citrate buffer)	Sigma
acetic acid (100 %)	Roth
acetone	Roth
agarose	Roth
albumin Fraktion V (BSA)	Roth
ampicillin sodium salt	Roth
chloramphenicol	Roth
DEPC-water	Roth
Difco-agar	BD
dimethyl sulfoxide (DMSO)	Roth
dithiothreitol (DTT)	Roth
ethanol	Roth
ethanol (absolute for analysis)	Merck
ethylenediaminetetraacetic acid disodium salt dehydrate (EDTA)	Merck
formamide (99.5 %)	Roth
formaldehyde (37 %)	Roth
gentamicin sulfate	Roth
glycerol (99 %)	Sigma
GlycoBlue™	Ambion
hydrochloric acid (HCl, 32 %)	Roth
isopropanol	Roth
kanamycin sulfate	Roth
lead (II)-acetate	Roth, Fluka
magnesium chloride	Roth
Midori Green	Nippon Genetics GmbH
milk powder (blotting grade)	Roth
Mueller-Hinton media	Becton, Dickinson and
PAGE Blue staining solution	Thermo Scientific
PBS	Gibco
phenol	Roth
rifampicin	Fluka
Roti-Aqua-P/C/I	Roth
Roti-Hybri-Quick	Roth
Rotiphorese gel 40 (19:1)	Roth
Rotiphorese gel 40 (37.5:1)	Roth

sodium carbonate (Na_2CO_3)	Roth
sodium dodecyl sulfate (SDS)	Roth
sodium hydroxide (NaOH)	Roth
Triton-X100	Sigma
TRIzol Reagent	Invitrogen
Tween^{20}	Roth
vancomycin sulfate	Roth
yeast tRNA	Ambion
γ-^{32}P-ATP (^{32}P; 222TBq (6000Ci)/mmol 370MBq (10mCi)/ml)	Hartmann Analytic

5.1.5 Enzymes and size markers

Antarctic Phosphatase	New England Biolabs
Calf Intestinal Phosphatase (CIP, 10 u/µl)	New England Biolabs
Deoxyribonuclease (DNase I, 1 u/µl)	Thermo Scientific
DpnI (20 u /µl)	New England Biolabs
Maxima Reverse Transcriptase	Thermo Scientific
Phusion High-Fidelity DNA polymerase (2 u/µl)	Thermo Scientific
Protease Inhibitor Cocktail (EDTA-free)	Roche
Ribonuclease III (RNase III, 1.3 u/µl)	New England Biolabs
Ribonuclease A (RNase A)	Qiagen
Ribonuclease T1 (RNase T1, 1 u/µl)	Ambion
Shrimp Alkaline Phosphatase (SAP, 1 u/µl)	Thermo Scientific
SUPERaseIN RNase Inhibitor	Ambion
T4 DNA Ligase (5 u/µl)	Thermo Scientific
T4 Polynucleotide Kinase (PNK, 10 u/µl)	Thermo Scientific
Taq DNA polymerase (5 u/µl)	New England Biolabs
lysozyme	Roth
restriction enzymes	New England Biolabs
Gene Ruler 1 kb plus DNA ladder	Thermo Scientific
Gene Ruler 100 bp DNA ladder	Thermo Scientific
PageRulerTM Plus Prestained Protein Ladder	Thermo Scientific
pUC Marker Mix, 8	Thermo Scientific

5.1.6 Commercial kits

Kits	**Manufacturer**
MEGAscript T7 *in vitro* Transcription	Ambion
NucleoSpin Plasmid	Macherey-Nagel
NucleoSpin Gel and PCR Clean-up	Macherey-Nagel
Power SYBR GREEN RNA-to-CT^{TM} 1-Step	Life Technologies

PureExpress	New England Biolabs
SequiTherm EXCEL™ II DNA Sequencing	Epicentre

5.1.7 Antibodies

Antibody	Origin	Dilution	Manufacturer
polyclonal anti-GroEL	rabbit	1:10,000	Sigma-Aldrich, # G6532-5ML
monoclonal anti-FLAG M2	mouse	1:1000	Sigma-Aldrich # F3165
monoclonal anti-GFP antibody	mouse	1:1000	Roche, #11814460001
Monoclonal anti-poly-Histidine	mouse	1:2000	Sigma-Aldrich, # H1029
ECL anti-mouse IgG, HRP-	goat	1:10,000	GE-Healthcare, #RPN4201
ECL anti-rabbit IgG, HRP-	donkey	1:10,000	GE-Healthcare, #RPN4301

5.1.8 Strains, oligonucleotides and plasmids

The list of *Helicobacter pylori* and *Escherichia coli* strains used in this study are compiled in Table S1. Plasmids are listed in Table S2. Oligodeoxynucleotides (Sigma) used for cloning, Northern blot probing, and T7 transcription template generation are listed in Table S3.

5.1.9 Media and supplements

Lennox Broth (LB) medium:

10 g tryptone or peptone
5 g yeast extract
5 g NaCl
ad 1 l H_2O

LB-agar plates:

LB medium (see above)
1.5 % (w/v) Difco-agar

BHI medium:

36 g Brain Heart Infusion medium
ad H_2O 900 ml
add after autoclaving:
10 % (w/v) heat-inactivated fetal bovine serum
5 µl/ml trimethoprim

1 µg/ml	nystatin
10 µg/ml	vancomycin

GC Agar:

36 g	GC-agar

ad H_2O 900 ml

add after autoclaving:

10 % (w/v)	donor horse serum
5 µl/ml	trimethoprim
1 µg/ml	nystatin
10 µg/ml	vancomycin
1 % (v/v)	vitamin mix

SOC medium:

1 l SOB medium

add 5 ml magnesium chloride

add 20 ml 1 M glucose

5.1.10 Buffers

30:1 ethanol/sodium acetate (pH 6.5):

30 parts of 100 % ethanol

1 part of 3 M sodium acetate (pH 6.5)

10 x DNA loading dye:

1.66 ml	1 M Tris-HCl (pH 7.5)
12 ml	0.5 M EDTA (pH 8.0)
0.05 g	bromophenol blue
0.05g	xylene cyanol
60 ml	glycerol

ad 100 ml H_2O

2 x gel loading buffer II (RNA, GL II):

0.13 % (w/v)	SDS
18 µM	EDTA (pH 8.0)

95 %	formamide
0.025 % (w/v)	bromophenol blue
0.025 % (w/v)	xylene cyanol

5 x native sample buffer:

50 %	glycerol
0.02 %	bromophenol blue
0.5 x	TBE buffer

5 x protein loading dye:

10 g	SDS pellets
31.3 ml	1 M Tris-HCl (pH 6.8)
50 ml	glycerol

add 2.5 ml of 2 % (w/v) bromophenol blue

ad 100 ml H_2O

1 x protein loading dye:

40 ml	5 x protein loading dye
10 ml	2 M DTT

ad 200 ml H_2O

2D PAGE – lysis buffer:

20 mM	Tris-HCl pH 8.8
1 mM	EDTA
40 U/mL	DNase I
25 µg/mL	RNase A

Protease Inhibitor

1 mM	PMSF

2D PAGE – solubilization buffer:

7M	Urea
2M	Thiourea
4 %	CHAPS

2D PAGE – equilibration buffer:

2.5 ml	1M Tris-HCL pH 8.8
6M	Urea
15 ml	Glycerol
5 ml	20 % SDS

ad 50 ml H_2O

2D PAGE – running buffer:

25 mM	Tris-HCL pH 8.8
192 mM	Glycine
0.1 %	SDS

2D PAGE – staining solution:

0.4 g	Coomassie Briliant Blue G-250
100 g	aluminium sulfate-(14-18)-hydrate
200 ml	ethanol (96 %)
47 ml	orthophosphoric acid (85 %)

ad 2000 ml H_2O

2D PAGE – destaining solution:

200 ml	ethanol (96 %)
47 ml	orthophosphoric acid (85 %)

ad 2000 ml H_2O

agarose gel electrophoresis solution:

X % (w/v)	agarose in 1 x TAE/TBE buffer

Chemiluminescence solution A:

0.1 M	Tris-HCl (pH 8.6)
0.025 % (w/v)	luminol

Chemiluminescence solution B:

0.11 % (w/v)	*p*-coumaric acid (in DMSO)

In-line probing colorless loading buffer:

10 M	urea
1.5 mM	EDTA

In-line probing buffer (2 x):

100 mM	Tris-HCl (pH 8.3)
40 mM	$MgCl_2$
200 mM	KCl

PAA gel electrophoresis solution for western blots:

PAA gel for separation gel (10 ml)	**12 %**	**15 %**
1 M Tris "lower" buffer (pH 8.8)	3.75 ml	3.75 ml
40 % PAA solution (37.5:1 acrylamide/bisacrylamide)	3 ml	3.75 ml
H_2O	3.25 ml	2.5 ml
10 % (w/v) SDS	100 µl	100 µl
10 % (w/v) APS	75 µl	75 µl
TEMED	7.5 µl	7.5 µl

PAA gel for stacking gel (10 ml)	**4 %**
1 M Tris "upper" buffer (pH 6.8)	1.25 ml
40 % PAA solution (37.5:1 acrylamide/bisacrylamide)	1 ml
H_2O	7.5 ml
10 % (w/v) SDS	100 µl
10 % (w/v) APS	150 µl
TEMED	15 µl

PAA gel electrophoresis solution for northern blots and sequencing gels:

PAA gel (500 ml, stock solution, 7 M urea)	**4 %**	**6 %**
40 % PAA solution (19:1 acrylamide/bisacrylamide)	50 ml	75 ml
urea	210 g	210 g
10 x TBE buffer	50 ml	50 ml

1 gel (70 ml):

70 ml	stock solution
700 µl	10 % (w/v) APS
70 µl	TEMED

PAA gel electrophoresis solution for gel-shift assays (native PAGE):

1 gel (70 ml, 6 % PAA):

10.5 ml	40 % PAA sol. (19:1)
3.5 ml	10 x TBE
56 ml	H_2O
700 µl	10 % (w/v) APS
70 µl	TEMED

Phosphorylation buffer (5 x):

250 mM	Tris-HCl (pH 7.4)
25 mM	$MgCl_2$
250 mM	KCl
5 mM	DTT

Phosphate Buffered Saline (10 x):

80 g	sodium chloride
2 g	potassium chloride
17.7 g	disodiumhydrogen phosphate
2.72 g	monopotassium phosphate

ad 800 ml H_2O

adjust to pH 7.4

ad 1 l H_2O

RNA elution buffer:

0.1 M	sodium acetate
0.1 %	SDS
10 mM	EDTA (pH 8.0)

RNA structure buffer (10 x):

100 mM	Tris-HCl (pH 7.0)
1 M	potassium chloride
100 mM	magnesium chloride

SDS running buffer (10 x stock):

30.275 g	Tris base
144 g	glycin
10 g	SDS

ad 1 l H_2O

SSC (saline-sodium citrate) buffer (20 x stock):

173.5 g	sodium chloride
88.2 g	sodium citrate

ad 800 ml H_2O

adjust to pH 7.0 (using HCl)

ad 1 l H_2O

Stains-All:

30 ml	Stains-All stock
90 ml	formamide

ad 200 ml H_2O

Stains-All stock:

0.03 g dissolved in 30 ml formamide

Stop mix:

95 % (v/v)	ethanol (absolute)
5 % (v/v)	phenol

TAE buffer (50 x stock):

242 g	Tris base
51.7 ml	acetic acid
100 ml	0.5 M EDTA (pH 8.0)

ad 1 l H_2O

TBE buffer (10 x stock):

108 g	Tris base
55 g	boric acid
40 ml	0.5 M EDTA (pH 8.0)

ad 1 l H_2O

Tbf I buffer:

1.47 g	potassium acetate
4.975 g	manganese(II)-chloride
3.73 g	potassium chloride

ad 400 ml H_2O

Tbf I buffer:

adjust pH to 5.8 (using CH_3COOH)

add 75 ml glycerin

ad 500 ml H_2O

Tbf II buffer:

2 ml	1 M MOPS
150 ml	0.1 M calcium chloride
8 ml	250 mM potassium chloride
30 ml	glycerin

ad 200 ml H_2O

TBS buffer (10 x stock):

24.11 g	Tris base
87.66 g	NaCl

adjust to pH 7.4 (using HCl)

ad 1 l H_2O

TBS-T buffer (1 x):

100 ml	10 x stock solution
1 ml	Tween^{20}

ad 1 l H_2O

TE buffer (1 x):

100 mM	Tris-HCl (pH 8.0)
10 mM	EDTA (pH 8.0)

Transfer buffer (10 x stock):

30 g	Tris base
144 g	glycin
ad 1 l H_2O	

Transfer buffer (1 x):

100 ml	10 x stock solution
200 ml	methanol
ad 1 l H_2O	

Tris "lower buffer" solution:

1.5 M	Tris-HCl (pH 8.8)
0.4% (w/v)	SDS

Tris "upper buffer" solution:

0.5 M	Tris-HCl (pH 6.8)
0.4% (w/v)	SDS

Urease buffer:

50 mM	HEPES (pH 7.5)
50 mM	urea

Urease assay solution A:

3% (w/v)	phenol
0.015% (w/v)	sodium nitroprusside

Urease assay solution B (100 ml):

2 % (w/v)	NaOH,
5 ml	NaOCl

Western development solution:

2 mL	chemiluminescence solution A
200 µl	chemiluminescence solution B
6 µL	3% (v/v) H_2O_2

5.1.11 Sterilization

All media and solutions used in this study were sterilized by autoclaving for 20 min at 120 °C and 1 bar prior to use. For heat-labile compounds, solutions were sterile filtered. Glassware was sterilized by heating to 180 °C for a minimum of three hours.

5.2 Methods

5.2.1 Bacterial growth conditions

Helicobacter strains were grown on GC-agar (Oxoid) plates supplemented with 10 % (v/v) donor horse serum (Biochrom AG), 1 % (v/v) vitamin mix, 10 µg ml^{-1} vancoymcin, 5 µg ml^{-1} trimethoprim, and 1 µg ml^{-1} nystatin. For liquid cultures, 15 or 50 ml Brain Heart Infusion medium (BHI, Becton, Dickinson and Company) supplemented with 10 % (v/v) FBS (Biochrom AG) and 10 µg ml^{-1} vancoymcin, 5 µg ml^{-1} trimethoprim, and 1 µg ml^{-1} nystatin were inoculated with *Helicobacter* from plate to a final OD_{600} of 0.02 – 0.05 and grown under agitation at 140 rpm in 25 cm^3 or 75 cm^3 cell culture flasks (PAA). Bacteria were grown at 37 °C in a HERAcell 150i incubator (Thermo Scientific) in a microaerobic environment (10 % CO_2, 5 % O_2, and 85 % N_2). *E. coli* strains were grown in Luria-Bertani (LB) medium supplemented with 100 µg ml^{-1} ampicillin and/or 20 µg ml^{-1} chloramphenicol whenever applicable.

5.2.2 General *H. pylori* genetic manipulation techniques

All *H. pylori* mutant strains listed in Table S1 were generated by homologous recombination into the chromosome of PCR-amplified constructs, introduced by natural transformation as previously described (Bury-Mone *et al*., 2001, Pernitzsch *et al*., 2014). In general, constructs containing ~ 500 bp of the up- and downstream regions of the target region of the chromosome, flanking an antibiotic resistance cassette [either the *catGC* chloramphenicol (Boneca *et al*., 2008), the *aphA-3* kanamycin (Skouloubris *et al*., 1998), the *erm* erythromycin (Dailidiene *et al.*, 2006), or the *aac(3)-IV* gentamicin resistance cassette (Bury-Mone *et al*., 2003)] were used (as described in detail below for each mutant construction). Either overlap PCR or PCR products amplified from plasmids (Table S2) were used as donor DNA. Oligonucleotides used for

cloning are listed in Table S3. Prior to natural transformation, recipient *H. pylori* strains were grown from -80 °C frozen stocks for two passages, and then streaked into small circles on fresh non-selective plates. After 6 hours of incubation at 37 °C under microaerobic conditions, 500 to 1000 ng of purified PCR product was added to the cells, and they were additionaly incubated for 15 to 18 hours at 37 °C. Transformed cells were then passed onto plates with the appropriate antibiotics for selection of the transformed DNA. Genomic DNA (gDNA) from potential clones was purified using the NucleoSpin Plasmid kit (Macherey & Nagel) and used for validation by PCR and Sanger sequencing (Macrogen).

5.2.3 Deletion of *arsZ* in *H. pylori* background strains 26695 and G27.

The *arsZ* gene was deleted in *H. pylori* strains 26695 and G27 (CSS-0065 and CSS-0066 for WT) by replacement of the entire *arsZ* sequence with the *erm* erythromycin resistance cassette via overlap PCR. Briefly, purified PCR products corresponding to ~ 500 bp upstream of *arsZ* (amplified with JVO-5198 / CSO-0161 on CSS-0065 gDNA for 26695; CSO-0343 / CSO-0161 on CSS-0066 for G27) and ~ 500 bp downstream of *arsZ* (JVO-5183 / CSO-0163 on CSS-0065; CSO-0344 / CSO-0162 on CSS-0066), as well as the *erm* cassette (obtained by PCR with CSO-0160 / CSO-0101 on *H. pylori* 26695 carrying a chromosomal *erm* cassette [CSS-0163]) were mixed in an equimolar ratio and subjected to overlap extension PCR using JVO-5198 / JVO-5183. PCR conditions for overlap PCR were as follows: 1 cycle of [98°C, 3 min; 62°C, 1 min; 72 °C, 10 min; 98 °C, 1 min], 35 cycles of [98 °C, 15 s; 58 °C, 30 s; 72 °C, 2 min], followed by 72 °C for 10 min. Primers were used at a final concentration of 0.06 µM ($1/10^{th}$ dilution of the primer concentration used in standard PCR). Overlap PCR products were checked for size by agarose gel electrophoresis, purified (Macherey & Nagel), and naturally transformed into the appropriate 26695 or G27 recipient strain. Erythromycin-resistant clones were checked for deletion of *arsZ* by PCR on gDNA using primers CSO-0309 / CSO-0094. Resulting positive clones, for transformation into WT backgrounds of 26695 and G27 were labeled CSS-0107 and CSS-0292, respectively.

5.2.4 Complementation of the Δ*arsZ* mutation and construction of an ArsZ over-expression strain

ArsZ expression in Δ*arsZ* was complemented in *trans* at the *rdxA* locus, which is commonly used for genetic complementation of *H. pylori* (Goodwin *et al.*, 1998, Pernitzsch *et al*., 2014). The previously-described pSP39-3 plasmid (Pernitzsch *et al*., 2014) was used as a backbone to introduce *arsZ* into the *rdxA* locus, along with a *catGC* resistance cassette for selection. The plasmid backbone was PCR-amplified from pSP39-3 using primers CSO-0146 / CSO-0147. The *arsZ* gene, including its own promoter, was amplified from *H. pylori* 26695 (CSO-0479 / CSO-0687 on CSS-0065) or G27 (CSO-0478 / CSO-0687 on CSS-0066) gDNA. PCR products were then *Cla*I- and *Nhe*I-digested, ligated using T4 DNA ligase (NEB), and transformed into *E. coli* TOP10. Colony PCR was performed with primers pZE-A / CSO-0205 on putative

clones, and plasmids from positive clones were harvested with NucleoSpin Plasmid kit (Macherey & Nagel). The resulting plasmids were termed pPT20-1 (C_{ArsZ} from 26695) and pPT32-1 (C_{ArsZ} from G27). For transformation into *H. pylori*, the *rdxA-catGC-arsZ* constructs were amplified from the respective plasmids with CSO-0017 / CSO-0018 and introduced into strains CSS-0107 (26695 Δ*arsZ*), CSS-0292 (G27 Δ*arsZ*) and CSS-0213 (B8 WT) via natural transformation. Chloramphenicol-resistant clones were checked for insertion of *arsZ* at the *rdxA* locus by PCR on gDNA using CSO-0207 / CSO-0205. Positive clones from 26695, G27 and B8 were labeled CSS-2168, CSS-0816 and CSS-4446 respectively.

For over-expression of ArsZ in strain 26695 and G27, the ArsZ complementation construct described above was introduced into the wild-type strain, CSS-0065 (26695) and CSS-0066 (G27), providing an additional copy of *arsZ* resulting in strain CSS-2169 and CSS-0818, respectively.

5.2.5 Expression of ArsZ and RepG-SL1-ArsZ chimera under strong promoters

The pSP39-3 plasmid was used as a backbone to place *arsZ* and *repG-SL1-arsZ* chimera under the control of the strong *repG* promoter (Pernitzsch *et al*., 2014). The plasmid backbones for the 2 different inserts were PCR-amplified using primers CSO-0146 / CSO-0232 and CSO-0146 / CSO-0060, respectively. The *arsZ* gene was amplified with CSO-0476 / CSO-0480 or CSO-3320 / CSO-0687 on CSS-0065 gDNA (26695 WT). PCR products were then *Cla*I-digested, ligated together with T4 DNA ligase (NEB), and transformed into *E. coli* TOP10. Colony PCR was performed with primers pZE-A / CSO-0480 or pZE-A / CSO-3320 on putative clones, and plasmids from positive clones were harvested with NucleoSpin Plasmid kit (Macherey & Nagel). The resulting plasmids were termed pPT7-1 and pPT156-1, respectively. For transformation into *H. pylori*, the construct was amplified from both plasmids with CSO-0017 / CSO-0018 and introduced into strain CSS-0107 (26695 Δ*arsZ*) via natural transformation. Chloramphenicol-resistant clones were checked for insertion of *arsZ* at the *rdxA* locus by PCR on gDNA using CSO-0207 / CSO-0205. Positive clones were labeled as CSS-0453 and CSS-4039, respectively.

For the expression of *arsZ* under the control of the *ureA* promoter, the backbone plasmids were amplified from pPT3-1 using primers CSO-1781 / CSO-1266. The *arsZ* gene was amplified with CSO-0477 / CSO-0687 on CSS-0066 gDNA (G27 WT). PCR products were then *Cla*I-digested, ligated, and transformed into *E. coli* TOP10. Colony PCR was performed with primers pZE-A / CSO-0687 and plasmids from positive clones were harvested. The resulting plasmid was termed pPT66-1. The construct was amplified from this plasmid with CSO-0017 / CSO-0018 and introduced into strain CSS-0292 (G27 Δ*arsZ*)

via natural transformation. Chloramphenicol-resistant clones were checked for insertion of *arsZ* at the *rdxA* locus by PCR on gDNA using CSO-0207 / CSO-0205. The positive clone was labeled CSS-2273.

5.2.6 Generation of single ΔHP1432 and double ΔHP1432 Δ*arsZ* mutants

The HP1432 gene was deleted in strain CSS-0065 (*H. pylori* 26695 WT) by replacement of the coding sequence with the *aphA-3* cassette, which confers kanamycin resistance, by overlap PCR. Purified PCR products corresponding to ~ 500 bp upstream (CSO-0675 / CSO-0676 on CSS-0065) and ~ 500 bp downstream of HP1432 (CSO-0677 / CSO-0470 on CSS-0065), as well as the *aphA-3* cassette (HPK1 / HPK2 on *H. pylori* carrying a chromosomal *aphA-3* cassette [CSS-0169]), were mixed at an equimolar ratio and subjected to overlap extension PCR as described above using primers CSO-0675 / CSO-0470. The resulting PCR products were purified and used for natural transformation of CSS-0065. Kanamycin resistant clones were checked by PCR on extracted gDNA using CSO-0734 / CSO-0023, and a resulting positive clone was labeled CSS-0691. To create the double deletion mutant of ΔHP1432 Δ*arsZ*, the Δ*arsZ* deletion construct was amplified from CSS-0107 by PCR using primers JVO-5198 / JVO-5183, transformed into CSS-0691, and verified by PCR using CSO-0309 / CSO-0094. The resulting positive clone was termed CSS-3333.

5.2.7 Construction of a transcriptional fusion of the *ureA* promoter to *gfpmut3*

The promoter region of *ureA* was transcriptionally fused to *gfpmut3* and the 5'UTR of *ureA*. The linker region upstream of the *gfpmut3* gene, which was originally present in pPT3-1 (Pernitzsch *et al.*, 2014, Carpenter *et al.*, 2007), was removed by inverse PCR using the primer pair CSO-0594 / CSO-0683. The resulting plasmid carries the promoter region of *ureA*, 5'UTR of *ureA* and *gfpmut3*. The PCR product was digested with *Nhe*I, ligated, and transformed into *E. coli* TOP10. Colony PCR was performed with CSO-0411 / CSO-0789 and the plasmid of a positive clone was saved as pPT65-1. The P*ureA*::*gfpmut3* construct was then amplified from pPT65-1 with CSO-0017 / CSO-0018 and transformed into G27* (CSS-0050). Chloramphenicol-resistant clones were checked by PCR using primers CSO-0207 / CSO-0205, and a positive clone was labeled as CSS-4001.

For the construction of *ureA* transcriptional fusion to *gfpmut3* in the Δ*arsS* background, the P*ureA::gfpmut3* transcriptional fusion escribed above was amplified with CSO-0017 / CSO-0018 from

pPT65-1 and transformed into CSS-0051 (Δ*arsS*). A resulting positive clone, verified by PCR with CSO-0207 / CSO-0205, was termed CSS-4003.

5.2.8 Construction of a transcriptional fusion of the *arsZ* promoter to *gfpmut3*

The promoter region of *arsZ* was transcriptionally fused to *gfpmut3* and the 5'UTR of *ureA*. The 144 bp promoter region of *arsZ* was amplified from strain CSS-0050 (WT / G27*) gDNA using primers CSO-0411 / CSO-3317. The plasmid backbone was amplified from pPT65-1, which contains the 5'UTR of *ureA* fused to *gfpmut3,* using the primer pair CSO-3316 / CSO-0146. Both PCR products were digested with *Cla*I, ligated, and transformed into *E. coli* TOP10. Colony PCR was performed with CSO-0411 / CSO-0789 and the plasmid of a positive clone was saved as pPT150-1. The P*arsZ*::*gfpmut3* construct was then amplified from pPT150-1 with CSO-0017 / CSO-0018 and transformed into CSS-0050 (WT / G27*). Chloramphenicol-resistant clones were checked by PCR using primers CSO-0207 / CSO-0205, and a positive clone was labeled CSS-4009.

For the construction of *arsZ* transcriptional fusion to *gfpmut3* in the Δ*arsS* background, the P*arsZ::gfpmut3* transcriptional fusion described above was amplified with CSO-0017 / CSO-0018 from pPT150-1 and transformed into CSS-0051 (Δ*arsS*). A resulting positive clone, verified by PCR with CSO-0207 / CSO-0205, was termed CSS-4011.

5.2.9 Construction of a transcriptional fusion of the *tlpB* promoter to *gfpmut3*

The 5'UTR of *ureA* fused to *gfpmut3* was amplified from pPT65 using primers CSO-3316 / CSO-0441. The plasmid backbone was amplified from pPT150-1, which contains the promoter of *tlpB,* using the primer pair CSO-1772 / CSO-0443. Both PCR products were digested with *Not*I, ligated together, and transformed into *E. coli* TOP10. Colony PCR was performed with pZE-A / CSO-0789 and the plasmid of a positive clone was saved as pPT152-1. The P*tlpB*::*gfpmut3* construct was then amplified from pPT152-1 with CSO-0017 / CSO-0018 and transformed into CSS-0050 (WT / G27*). Chloramphenicol-resistant clones were checked by PCR using primers CSO-0207 / CSO-0205, and a positive clone was labeled as CSS-4013.

For the construction of *tlpB* transcriptional fusion to *gfpmut3* in the Δ*arsS* background, the P*tlpB::gfpmut3* transcriptional fusion described above was amplified with CSO-0017 / CSO-0018 from pPT152-1and transformed into CSS-0051 (Δ*arsS*). A resulting positive clone, verified by PCR with CSO-0207 / CSO-0205, was termed CSS-4015.

5.2.10 Construction of translational and transcriptional fusions of the HP1432 promoter to *gfpmut3*

For the construction of the HP1432 translational fusion to *gfpmut3*, the 160 bp promoter region of HP1432, including the RBS and first ten codons, was amplified (CSO-0736 / CSO-0737) from gDNA of 26695 WT (CSS-0065) and fused to the second codon of *gfpmut3*. The plasmid backbone, containing *gfpmut3*, was amplified with primers CSO-0146 / CSO-0683 from pPT3-1. Both PCR products were *Cla*I- and *Nhe*I-digested and ligated together, resulting in the plasmid pPT22-1. The HP1432::*gfpmut3* translational fusion was then amplified from this plasmid with primers CSO-0017 / CSO-0018 and transformed into CSS-0066 (*H. pylori* G27 WT). The resulting clones were checked by PCR as described above for the HP1432 transcriptional fusion to *gfpmut3,* and a positive clone was saved as CSS-0713.

For the construction of the HP1432 transcriptional fusion to *gfpmut3,* the plasmid backbone including the promoter of HP1432 was amplified from pPT22-1 using CSO-0110 / CSO-0443. The 5'UTR of *ureA* fused to *gfpmut3* was amplified from pPT65 using primers CSO-3316 / CSO-0441. Both PCR products were digested with *Not*I, ligated, and transformed into *E. coli* TOP10. Colony PCR was performed with pZE-A / CSO-0205 on putative clones and the plasmid of a positive clone was termed pPT151-1. The HP1432::*gfpmut3* transcriptional fusion construct was then amplified with CSO-0017 / CSO-0018 and transformed into CSS-0066 via natural transformation. Chloramphenicol-resistant clones were checked for insertion of the reporter by PCR on gDNA using CSO-0207 / CSO-0205, and a positive clone was labeled CSS-4005.

For the introduction of Δ*arsZ* into HP1432 transcriptional- or translational- *gfpmut3* fusion backgrounds, the *arsZ* deletion construct was amplified from CSS-0292 by PCR with CSO-0343 / CSO-0344 and transformed into CSS-4005 (transcriptional *gfpmut3* fusion background) and CSS-0713 (translational *gfpmut3* fusion background), respectively. Putative clones were checked by PCR with CSO-0309 / CSO-0094, and the resulting positive clones were labeled CSS-4007 and CSS-0723, respectively.

5.2.11 Exchange of the HP1432 promoter for the *tlpB* promoter in the HP1432::*gfpmut3* translational fusion

A construct containing the translational fusion of the 5'UTR of HP1432 to the *gfpmut3* gene was amplified (CSO-1255 / CSO-1257) from pPT22-1. The plasmid backbone was amplified (CSO-1772 / CSO-0443) from pSP109-6 containing the *tlpB* promoter. Both PCR products were digested with *Not*I, ligated together, and transformed into *E. coli* TOP10. The primer pair pZE-A / CSO-0789 was used to check putative clones

by colony PCR and the plasmid of a positive clone was termed pPT86-1. Next, the *catGC* chloramphenicol resistance cassette was exchanged with the gentamicin resistance cassette by introducing the HP1432::*gfpmut3* fusion from the *tlpB* promoter construct (amplified with CSO-0581 / CSO-1255 on pPT86-1) into a plasmid backbone that carries the gentamicin resistance cassette (amplified with CSO-0146 / CSO-0443 on pBA4-2). Both PCR products were digested with *Cla*I and *Not*I, ligated together, and transformed into *E. coli* TOP10. Colony PCR was performed with primers pZE-A / CSO-0789 to identify a positive clone (termed pPT105-1). Finally, the construct containing the translational fusion of HP1432 to *gfpmut3* under control of the *tlpB* promoter including the newly-integrated gentamicin cassette was amplified with CSO-0581 / CSO-0313 on pPT105-1. This construct was fused to the PCR-amplified (CSO-2901 / CSO-0792) plasmid backbone (from pPT28-1) carrying the flanking region of HP1432 locus. The *Cla*I- and *Bam*HI-digested PCR products were ligated and transformed into *E. coli* TOP10. Colony PCR was performed with pZE-A / CSO-0789 and the plasmid of a positive clone was labeled pPT142-1. The construct was amplified with CSO-0790 / CSO-0793 and transformed into CSS-0066 (*H. pylori* 26695 WT) via natural transformation. The cells were passed onto chloramphenicol plates, putative clones were checked by PCR on gDNA using CSO-0734 / CSO-0789, and a positive clone was labeled CSS-3335.

For the introduction of Δ*arsZ* into the HP1432 promoter exchange background, the *arsZ* deletion construct was amplified from CSS-0292 with the primer pair CSO-0343 / CSO-0344 and transformed into CSS-3335. Putative clones were checked by PCR with primers CSO-0309 / CSO-0094, and a resulting positive clone was termed CSS-3337.

5.2.12 Compensatory base-pair exchanges in the 5'UTR of HP1432 and ArsZ

Three consecutive base-pair exchanges were introduced into the 5'UTR of HP1432 in plasmid pPT142-1 by inverse PCR with the mutagenic primers CSO-2878 / CSO-2879. Following *Dpn*I-digestion of the amplicon and transformation into *E. coli* TOP10, putative clones were checked by sequencing (CSO-0206) and the plasmid from a positive clone was termed pPT147-1. The mutagenized HP1432 construct was amplified from this plasmid with CSO-0790 / CSO-0793 and transformed into CSS-0066. Chloramphenicol-resistant clones were checked by PCR on gDNA using CSO-0734 / CSO-0789. A positive clone was labeled CSS-3341.

For introduction of Δ*arsZ* into this CSS-3341 background, the *arsZ* deletion construct was amplified from CSS-0292 by PCR using primers CSO-0343 / CSO-0344 and transformed into CSS-3341.

Erythromycin-resistant clones were checked by PCR with primers CSO-0309 / CSO-0094, and the resulting positive clone was labeled as CSS-3343.

The compensatory base-pair exchange in ArsZ was performed by inverse PCR on pPT32-1 with the mutagenic primers CSO-2880 / CSO-2881, *Dpn*I digestion of the template plasmid, and transformation into *E. coli* TOP10. The mutagenized ArsZ construct was amplified from the resulting plasmid (pPT108-1) with CSO-0017 / CSO-0018 and transformed into either CSS-3337 or CSS-3343 to generate strains CSS-3339 and CSS-3345, respectively. Both strains were check by PCR (CSO-0205 / CSO-0207) and sequencing (CSO-0206).

5.2.13 Construction of point mutant versions of ArsZ and 5'UTR of HP1432 in *H. pylori* strain 26695 as templates for *in-vitro* transcription

Three consecutive base-pair exchanges were introduced into ArsZ via inverse PCR on pPT20-1 with the mutagenic primers CSO-3217 / CSO-2881, *Dpn*I digestion of the template plasmid, and transformation into *E. coli* TOP10. Putative clones were checked by sequencing (CSO-0206) and the plasmid from a positive clone was termed pPT138-1.

The HP1432 gene including 160 bp upstream of the transcription start site and 100 bp downstream of the stop codon was amplified with primers CSO-0736 / CSO-0110. The backbone plasmid was amplified with primers CSO-0146 / CSO-0147 from pSP39-3. Both PCR products were digested with *ClaI* and *NdeI*, ligated, and transformed into *E. coli* TOP10. Colony PCR was performed with pZE-A / CSO-0110 on putative clones and the plasmid of a positive clone was termed pPT34-1. Three consecutive base-pair exchanges were introduced into the 5'UTR of HP1432 in plasmid pPT34-1 by inverse PCR with the mutagenic primers CSO-2878 / CSO-3216. Following *Dpn*I-digestion of the amplicon and transformation into *E. coli* TOP10, putative clones were checked by sequencing (CSO-0206) and the plasmid from a positive clone was termed pPT153-1.

5.2.14 Construction of two plasmids system for validation of interaction of ArsZ and HP1432 in *E. coli*

The HP1432 gene was amplified from gDNA of CSS-0065 (26695 WT) with primers CSO-1257 / CSO-1299. The backbone plasmid was amplified from pXG-10-sfGFP (Corcoran *et al*., 2012) using primers pZE-STOP-XbaI / pZE-tetO. Both PCR products were digested with *Xba*I, ligated, and transformed into *E.*

coli TOP10. Colony PCR was performed with pZE-A / CSO-1299 on putative clones and the plasmid of a positive clone (CSS-2189) was termed pPT42-1.

The *arsZ* gene was amplified with CSO-0477 / CSO-1298 on CSS-0065 gDNA (26695 WT). The backbone plasmid was amplified from pPT33-1 with JVO-0900 / JVO-0901. Both PCR products were *Xba*I-digested, ligated, and transformed into *E. coli* TOP10. Colony PCR was performed with primers pBADfw / CSO-1298 on putative clones, and plasmids from positive clones were harvested and termed pPT106. This plasmid was transformed into CSS-2198 and verified by colony PCR using primers pBADfw / CSO-1298. One positive clone was termed CSS-4448.

5.2.15 Determination of ArsZ *in-vivo* copy number

The copy number of ArsZ was estimated *in vitro* by comparing total RNA corresponding to 0.5 OD_{600} of wild-type *H. pylori* strain 26695 to serial dilutions of *in-vitro* transcribed ArsZ on Northern blots hybridized with ArsZ probe. Calculation for RNA per cell were based on number of viable cells per OD_{600} as described in (Sittka *et al.*, 2007).

5.2.16 Total RNA preparation

H. pylori cells were grown in liquid culture to mid-exponential growth phase (OD_{600} 0.4 – 0.6) and culture volumes corresponding to a total of ~ 4 OD_{600}, were mixed with 0.2 volumes of stop-mix (95 % ethanol and 5 % buffer-saturated phenol, v/v), snap frozen in liquid N_2 and stored at −80 °C until RNA extraction. Frozen cell pellets were thawed on ice and re-suspended in lysis solution containing 600 µl of 0.5 mg/ml lysozyme in TE (Tris-EDTA) buffer (pH 8.0) and 60 µl 10 % SDS. Bacterial cells were lysed by incubating the samples for 1–2 minutes at 64 °C. Afterwards, total RNA was extracted using the hot-phenol method described previously (Sharma *et al*., 2010).

5.2.17 Northern blot analysis

For Northern blotting, 5–10 µg of total RNA was separated on 6 % (v/v) polyacrylamide (PAA) gels containing 7 M urea and electro-blotted onto Hybond-XL nylon membranes (GE-Healthcare). Following transfer, RNA was UV cross-linked to the membrane prior to hybridization at 42 °C with ^{32}P' end-labeled

DNA oligonucleotides in Roti-Hybri-Quick hybridization buffer as described previously (Urban & Vogel, 2007). The blots were quantified using Aida software (Raytest).

5.2.18 2D gel electrophoresis

Cells were grown in liquid culture at pH 5.5 or pH 7 to mid-exponential growth phase (OD_{600} 0.4 – 0.6) and 25 OD_{600} of cells were pelleted. The cells were lysed with 4 ml lysis buffer, followed by sonication and centrifuged at 13,000 x g, 4 °C for 20 min. Supernatant were subjected to ultracentrifugation at 100,000 x g, 4 °C for 1 hour. The resulting supernatant was precipitated with TCA (trichloroacetic acid) and re-suspended in 150 µl solubilization buffer. Approximately 150 µg of total protein were separated on a 24cm IEF strip (pH 3.0 – pH 10.0 NL). Upon completion of the first dimension run, the IEF strips were equilibrated with equilibration buffer. Subsequently, the IEF strip was loaded onto a 12.5 % PAA gel and sealed with a sealing buffer. The gel electrophoresis lasted for 5-7 hours at 17 Watt per gel. The gel was visualized with colloidal Coomassie staining (Dyballa & Metzger, 2009).

5.2.19 RNA stability assay

Cells were grown in liquid culture to mid-exponential growth phase (OD_{600} 0.4 – 0.6) and treated with rifampicin (final concentration of 500 µg ml^{-1}). At the indicated time points (0, 2, 4, 8, 16, and 32 min) 5 ml of culture was mixed with 0.2 volumes of stop-mix (95 % EtOH and 5 % phenol, v/v), frozen in liquid N_2, and stored at −80 °C until RNA extraction. Total RNA was subjected to Northern blotting, and the RNA half-life was determined from the RNA decay rate analyzed by hybridizing the Northern blot with a HP1432-specific DNA probe.

5.2.20 Western blot analysis

H. pylori cells was grown in liquid culture to mid-exponential growth phase (OD_{600} 0.4 – 0.6) and cells corresponding to 0.8 OD_{600} units were centrifuged at 16,000 x g at 4 °C for 1 min. Cell pellets were resuspended in 80 µl of 1× protein loading buffer [62.5 mM Tris·HCl pH 6.8, 100 mM DTT, 10 % (v/v) glycerol, 2 % (w/v) SDS, 0.01 % bromophenol blue]. Samples were boiled at 95 °C for 8 min and samples corresponding to 0.1 OD_{600} were separated on a 12 % (v/v) SDS-PAA gels. For total protein analysis, the gels were stained with PAGE-Blue (Thermo Scientific) according to the manufacturer's instructions. For

Western blot analysis, protein samples were transferred to a nitrocelluloase membrane (GE Healthcare) by semidry blotting. A suspension of 10 % (w/v) milk powder in TBS-T were used to block the membranes for 1 h. Primary monoclonal antibody (anti-Histidine [Sigma], anti-GFP [Roche] or anti-GroEL [Sigma]) was incubated with the membrane overnight at 4 °C. Membranes were washed with TBS-T, followed by incubation with a secondary antibody (anti-mouse IgG [GE Healthcare] or anti-rabbit [GE Healthcare]) linked to horseradish peroxidase for 1 hour. Specific bands were detected by chemiluminescence using the ECL-reagent and analyzed with a biomolecular imager (ImageQuant LAS 4000, GE Healthcare).

5.2.21 *In-vitro* transcribed RNA

The T7 promoter sequence was introduced into DNA templates by PCR using oligonucleotides and DNA templates listed in Table S4. The MEGAscript® T7 kit (Ambion) was used to perform T7 transcription and the resulting sequences of the T7 transcripts are listed in Table S5. The quality of *in-vitro* transcribed RNAs was inspected by gel electrophoresis and subjected to 5' end labeling (^{32}P) as previously described (Papenfort *et al*., 2006, Sittka *et al*., 2007).

5.2.22 Electrophoretic mobility shift assays (EMSA)

Gel-shift assays were performed as previously described (Pernitzsch *et al*., 2014). Increasing amounts of unlabeled RNA (8 nM, 16 nM, 125 nM, 250 nM, 500 nM, and 1000 nM) were added to ~ 0.04 pmol 5'-end labeled RNA (4 nM final concentration) in 10 µl reactions. Labeled RNAs and unlabeled RNAs were denatured at 95 °C for 1 min and cooled on ice for 5 min. Following this, 10x RNA structure buffer (Ambion) and 1 µg yeast RNA was added to the mixture incubated at 37 °C for 15 min. To stop the reaction, 3 µl of 5x native loading dye [0.5x TBE, 50 % (v/v) glycerol, 0.2 % (w/v) xylene cyanol and 0.2 % (w/v) bromophenol blue] was added to each sample before loading immediately to a pre-cooled 6 % (v/v) native PAA gel and electrophoresed in 0.5x TBE buffer. The gels were dried at 80 °C for 1 hour, exposed to a phosphorimager screen, and analyzed using a PhosphorImager (FLA-3000 Series, Fuji) and AIDA software (Raytest).

5.2.23 *In vitro* structure probing

In vitro structure probing assays were performed as described previously (Sharma *et al*., 2007, Pernitzsch *et al*., 2014). Briefly, ~ 0.2 pmol of 5' end labeled RNA and unlabeled RNA (at a 10- or 100-fold excess) were denatured at 95 °C for 1 min and cooled on ice for 5 min. Next, 10x RNA structure buffer and 1 µg yeast tRNA were added to the labeled RNA followed by the unlabeled RNA and incubated at 37 °C for 10 min. Following binding, 2 µl of 0.01 U μl^{-1} RNase T1 (Ambion) or 2 µl freshly prepared 25 mM lead(II)-acetate solution (Fluka) was added and reactions were incubated at 37 °C for 3 min or 90 sec, respectively. For RNase III assays, 1.3 U μl^{-1} of enzyme (NEB) was added to the reactions in 1x structure buffer containing 1 mM DTT and incubated at 37 °C for 6 min. RNase T1 ladders were generated by denaturing ~ 0.2 pmol labeled RNA in 1x structure buffer for 1 min at 95 °C and further incubated with 0.1 U μl^{-1} RNase T1 for 5 min. OH ladders were generated by the incubating ~ 0.2 pmol of labeled RNA in 1x alkaline hydrolysis buffer (Ambion) at 95 °C for 5 min. The reactions were stopped by the addition of 12 µl RNA loading buffer (95 % (v/v) formamide, 18 mM EDTA, and 0.025 % (w/v) SDS, xylene cyanol, and bromophenol blue) and kept on ice. The ladders and samples were denatured at 95 °C for 3 min prior to loading on 6 % (v/v) PAA/7 M urea sequencing gels in 1x TBE buffer. Following electrophoresis, the gels were dried at 80 °C for 1 hour, exposed to a phosphorimager screen, and analyzed using a PhosphoImager (FLA-3000 Series, Fuji) and AIDA software (Raytest).

5.2.24 In-line probing

In-line probing assays were performed as previously described (Regulski & Breaker, 2008, Pernitzsch *et al*., 2014). Briefly 20 nM (0.2 pmol) labeled RNA was incubated in absence or presence of 20 nM or 200 nM unlabeled sRNA or 5'UTR of mRNA for 40 hours at room temperature in 1x in-line probing buffer (50 mM Tris-HCl, pH 8.3 at 20 °C, 20 mM $MgCl_2$, and 100 mM KCl). RNase T1 and alkaline (OH) ladders were generated as described above. Following incubation, 10 µl of colorless gel-loading solution (10 M urea, 1.5 mM EDTA, pH 8.0 at 23 °C) was added to stop all the reactions, which were then kept on ice prior to analysis. RNA cleavage patterns were resolved on 6 % (v/v) PAA gels under denaturing conditions and visualized as described above.

5.2.25 *In-vitro* translation assay

In-vitro translation reactions were performed using the PURExpress kit (NEB) according to the manufacture's protocol. Briefly, 1 pmol of *in-vitro*-transcribed mRNAs (HP1432::*gfp* or *tlpB*::*gfp*) were denatured in the absence or presence of 1, 10, 50, and 100 pmol of ArsZ, or 100 pmol ArsZ M3 mutant RepG (refer to figure legend for details) for 1 min at 95 °C and chilled on ice for 5 min. Prior to addition of PURExpress mix, the mRNA and sRNA were pre-incubated for 10 min at 37 °C. The translation reaction was carried out at 37 °C for 30 min, and then 60 µl acetone was immediately added to the mixture to stop the reaction followed by incubation on ice for 15 min prior to centrifugation at 10,000 x g at 4 °C for 10 min. Western blot analysis was used to quantify translation using anti-GFP and anti-mouse IgG (GE-Healthcare) antibodies.

5.2.26 Urease activity assay

The Berthelot reaction (Cussac *et al*., 1992) was used to determine the urease activity of *H. pylori* cell lysates as previously described with some modifications (van Vliet *et al*., 2001). Briefly, 0.5 to 1 OD_{600} of cells either grown at pH 5.5, pH 7, or after acid stress at specific time points were harvested by centrifugation and washed twice with 50 mM HEPES buffer, pH 7.5. The cell pellets were immediately snap frozen in liquid nitrogen and kept at -80 °C until analysis. The pellets were thawed for 5 min on ice and immediately resuspended in 250 µl of 50 mM HEPES buffer pH 7.5. The cells were lysed by sonication and lysates were clarified by centrifugation at 14,000 x g for 10 min at 4 °C. The protein concentration of each sample was quantified with Bradford reagent (Carl-Roth) according to manufacturer's protocol. Total protein (1 µg) was mixed with 500 µl urease buffer (50 mM HEPES, pH 7.5, 50 mM urea) and incubated for 10 min at 37 °C. Subsequently, 90 µl aliquots were mixed with 150 µl of solution A containing 3 % (w/v) phenol, 0.015 % (w/v) sodium nitroprusside (Carl Roth), 150 µl of solution B containing 2 % (w/v) NaOH, 0.2 % NaOCl, pH 13.5 and 750 µl of distilled water. The mixtures were incubated for 30 min at 37 °C for color development. The OD_{625} of samples was then measured. A standard curve using known concentrations of NH_4Cl was used to infer the amount of ammonia present in each bacterial sample and expressed as micromoles of urea hydrolyzed per minute per milligram of protein.

5.2.27 Growth competition assay under acid stress

Cells were grown at pH 7 until OD_{600} ~ 0.5. Cells corresponding to 3 OD_{600} were centrifuged at 500 x g at room temperature for 3 min. Cell pellets were resuspended in either 6 ml BHI pH 4 supplemented with 3 mM urea or 6 ml BHI pH 7. 100 µl of this culture were serially diluted and plated on streptomycin and erythromycin plates. Equal volume of WT and Δ*arsZ* from each culture condition were mixed and incubated while shaking under microaerobic conditions. At the indicated time points (0, 1, 2, 4, 8, and 10 hour) 100 µl of culture was serially diluted and plated on streptomycin and erythromycin plates. Plates were incubated microaerobically for 3 to 5 days. The ratio between WT and Δ*arsZ* was calculated as relative CFU/ml.

5.2.28 Bioinformatics analysis

The mfold program (Zuker, 2003) was used to predict the secondary structure of ArsZ in strains 26695 and G27. The full-length sequence of ArsZ (105 nt) was used for this prediction, using default parameters. TargetRNA program (Tjaden, 2008) was used to predict potential targets for ArsZ in strain 26695. The single-stranded region of ArsZ inferred from the mfold prediction was employed, using default parameters. A list of the top 21 targets is summarized in Table 1.

The phylogenetic tree of *H. acinonychis* and *H. pylori* was extracted from the PATRIC database (Wattam *et al*., 2014). The tree was constructed based on core protein families within the Helicobacter clade (under Taxanomy id 209 in PATRIC database). The tree was manually curated in the iTOL webserver (Letunic & Bork, 2007, Letunic & Bork, 2016) to retain only strains that have a complete genome sequence in the NCBI database (as of November 2015).

The synteny and conservation of the flanking genes of *arsZ* was derived from multiple genome alignments using the MAUVE tool (Darling *et al*., 2004). All the figures were visualized and constructed using EasyFig (Sullivan *et al*., 2011). All colored genes indicate homologous genes based on BLAST cut-off E-value 1E-05 and minimum sequence similarity of 70 % to reference genes in *H. pylori* strain 26695. White arrows indicate non-conserved genes.

6 References

Agrawal, N., P. V. Dasaradhi, A. Mohmmed, P. Malhotra, R. K. Bhatnagar & S. K. Mukherjee, (2003) RNA interference: biology, mechanism, and applications. *Microbiol. Mol. Biol. Rev.* **67**: 657-685.

Aiba, H., S. Matsuyama, T. Mizuno & S. Mizushima, (1987) Function of micF as an antisense RNA in osmoregulatory expression of the ompF gene in Escherichia coli. *J. Bacteriol.* **169**: 3007-3012.

Akada, J. K., M. Shirai, H. Takeuchi, M. Tsuda & T. Nakazawa, (2000) Identification of the urease operon in Helicobacter pylori and its control by mRNA decay in response to pH. *Mol. Microbiol.* **36**: 1071-1084.

Alm, R. A., J. Bina, B. M. Andrews, P. Doig, R. E. Hancock & T. J. Trust, (2000) Comparative genomics of Helicobacter pylori: analysis of the outer membrane protein families. *Infect. Immun.* **68**: 4155-4168.

Alon, U., (2007) Network motifs: theory and experimental approaches. *Nat Rev Genet* **8**: 450-461.

Altuvia, S., D. Weinstein-Fischer, A. Zhang, L. Postow & G. Storz, (1997) A small, stable RNA induced by oxidative stress: role as a pleiotropic regulator and antimutator. *Cell* **90**: 43-53.

Altuvia, S., A. Zhang, L. Argaman, A. Tiwari & G. Storz, (1998) The Escherichia coli OxyS regulatory RNA represses fhlA translation by blocking ribosome binding. *EMBO J.* **17**: 6069-6075.

Arnion, H., D. N. Korkut, S. Masachis Gelo, S. Chabas, J. Reignier, I. Iost & F. Darfeuille, (2017) Mechanistic insights into type I toxin antitoxin systems in Helicobacter pylori: the importance of mRNA folding in controlling toxin expression. *Nucleic Acids Res.*

Arraiano, C. M., J. M. Andrade, S. Domingues, I. B. Guinote, M. Malecki, R. G. Matos, R. N. Moreira, V. Pobre, F. P. Reis, M. Saramago, I. J. Silva & S. C. Viegas, (2010) The critical role of RNA processing and degradation in the control of gene expression. *FEMS Microbiol. Rev.* **34**: 883-923.

Axmann, I. M., P. Kensche, J. Vogel, S. Kohl, H. Herzel & W. R. Hess, (2005) Identification of cyanobacterial non-coding RNAs by comparative genome analysis. *Genome Biol.* **6**: R73.

Backert, S. & M. J. Blaser, (2016) The Role of CagA in the Gastric Biology of Helicobacter pylori. *Cancer Res.* **76**: 4028-4031.

Bacolla, A., G. Wang & K. M. Vasquez, (2015) New Perspectives on DNA and RNA Triplexes As Effectors of Biological Activity. *PLoS genetics* **11**: e1005696.

Balaban, N. & R. P. Novick, (1995) Translation of RNAIII, the Staphylococcus aureus agr regulatory RNA molecule, can be activated by a 3'-end deletion. *FEMS Microbiol. Lett.* **133**: 155-161.

Bandyra, K. J., N. Said, V. Pfeiffer, M. W. Gorna, J. Vogel & B. F. Luisi, (2012) The seed region of a small RNA drives the controlled destruction of the target mRNA by the endoribonuclease RNase E. *Mol. Cell* **47**: 943-953.

Bardill, J. P., X. Zhao & B. K. Hammer, (2011) The Vibrio cholerae quorum sensing response is mediated by Hfq-dependent sRNA/mRNA base pairing interactions. *Mol. Microbiol.* **80**: 1381-1394.

Bauerfeind, P., R. Garner, B. E. Dunn & H. L. Mobley, (1997) Synthesis and activity of Helicobacter pylori urease and catalase at low pH. *Gut* **40**: 25-30.

Beier, D. & R. Frank, (2000) Molecular characterization of two-component systems of Helicobacter pylori. *J. Bacteriol.* **182**: 2068-2076.

Beisel, C. L. & G. Storz, (2010) Base pairing small RNAs and their roles in global regulatory networks. *FEMS Microbiol. Rev.* **34**: 866-882.

Beisel, C. L. & G. Storz, (2011) The base-pairing RNA spot 42 participates in a multioutput feedforward loop to help enact catabolite repression in Escherichia coli. *Mol. Cell* **41**: 286-297.

Bejerano-Sagie, M. & K. B. Xavier, (2007) The role of small RNAs in quorum sensing. *Curr. Opin. Microbiol.* **10**: 189-198.

Benoit, S. L. & R. J. Maier, (2011) Mua (HP0868) is a nickel-binding protein that modulates urease activity in Helicobacter pylori. *MBio* **2**: e00039-00011.

Benoit, S. L., E. F. Miller & R. J. Maier, (2013) Helicobacter pylori stores nickel to aid its host colonization. *Infect. Immun.* **81**: 580-584.

Bik, E. M., P. B. Eckburg, S. R. Gill, K. E. Nelson, E. A. Purdom, F. Francois, G. Perez-Perez, M. J. Blaser & D. A. Relman, (2006) Molecular analysis of the bacterial microbiota in the human stomach. *Proc. Natl. Acad. Sci. U. S. A.* **103**: 732-737.

Boisset, S., T. Geissmann, E. Huntzinger, P. Fechter, N. Bendridi, M. Possedko, C. Chevalier, A. C. Helfer, Y. Benito, A. Jacquier, C. Gaspin, F. Vandenesch & P. Romby, (2007) Staphylococcus aureus RNAIII coordinately represses the synthesis of virulence factors and the transcription regulator Rot by an antisense mechanism. *Genes Dev.* **21**: 1353-1366.

Boneca, I. G., C. Ecobichon, C. Chaput, A. Mathieu, S. Guadagnini, M. C. Prevost, F. Colland, A. Labigne & H. de Reuse, (2008) Development of inducible systems to engineer conditional mutants of essential genes of Helicobacter pylori. *Appl. Environ. Microbiol.* **74**: 2095-2102.

Boren, T., P. Falk, K. A. Roth, G. Larson & S. Normark, (1993) Attachment of Helicobacter pylori to human gastric epithelium mediated by blood group antigens. *Science* **262**: 1892-1895.

Brantl, S., (2007) Regulatory mechanisms employed by cis-encoded antisense RNAs. *Curr. Opin. Microbiol.* **10**: 102-109.

Brantl, S. & N. Jahn, (2015) sRNAs in bacterial type I and type III toxin-antitoxin systems. *FEMS Microbiol. Rev.* **39**: 413-427.

Brar, G. A. & J. S. Weissman, (2015) Ribosome profiling reveals the what, when, where and how of protein synthesis. *Nat. Rev. Mol. Cell Biol.* **16**: 651-664.

Broadbent, J. R., R. L. Larsen, V. Deibel & J. L. Steele, (2010) Physiological and transcriptional response of Lactobacillus casei ATCC 334 to acid stress. *J. Bacteriol.* **192**: 2445-2458.

Bury-Mone, S., G. L. Mendz, G. E. Ball, M. Thibonnier, K. Stingl, C. Ecobichon, P. Ave, M. Huerre, A. Labigne, J. M. Thiberge & H. De Reuse, (2008) Roles of alpha and beta carbonic anhydrases of Helicobacter pylori in the urease-dependent response to acidity and in colonization of the murine gastric mucosa. *Infect. Immun.* **76**: 497-509.

Bury-Mone, S., S. Skouloubris, C. Dauga, J. M. Thiberge, D. Dailidiene, D. E. Berg, A. Labigne & H. De Reuse, (2003) Presence of active aliphatic amidases in Helicobacter species able to colonize the stomach. *Infect. Immun.* **71**: 5613-5622.

Bury-Mone, S., S. Skouloubris, A. Labigne & H. De Reuse, (2001) The Helicobacter pylori UreI protein: role in adaptation to acidity and identification of residues essential for its activity and for acid activation. *Mol. Microbiol.* **42**: 1021-1034.

Bury-Mone, S., J. M. Thiberge, M. Contreras, A. Maitournam, A. Labigne & H. De Reuse, (2004) Responsiveness to acidity via metal ion regulators mediates virulence in the gastric pathogen Helicobacter pylori. *Mol. Microbiol.* **53**: 623-638.

Caldelari, I., Y. Chao, P. Romby & J. Vogel, (2013) RNA-mediated regulation in pathogenic bacteria. *Cold Spring Harb. Perspect. Med.* **3**: a010298.

Cancer, I. A. f. R. o., (1994) IARC monographs on the evaluation of carcinogenic risks to humans. *International Agency for Research on Cancer, Lyon, France.* **61**.

Carpenter, B. M., T. K. McDaniel, J. M. Whitmire, H. Gancz, S. Guidotti, S. Censini & D. S. Merrell, (2007) Expanding the Helicobacter pylori genetic toolbox: modification of an endogenous plasmid for use as a transcriptional reporter and complementation vector. *Appl. Environ. Microbiol.* **73**: 7506-7514.

Castanie-Cornet, M. P., T. A. Penfound, D. Smith, J. F. Elliott & J. W. Foster, (1999) Control of acid resistance in Escherichia coli. *J. Bacteriol.* **181**: 3525-3535.

Celli, J. P., B. S. Turner, N. H. Afdhal, R. H. Ewoldt, G. H. McKinley, R. Bansil & S. Erramilli, (2007) Rheology of gastric mucin exhibits a pH-dependent sol-gel transition. *Biomacromolecules* **8**: 1580-1586.

Celli, J. P., B. S. Turner, N. H. Afdhal, S. Keates, I. Ghiran, C. P. Kelly, R. H. Ewoldt, G. H. McKinley, P. So, S. Erramilli & R. Bansil, (2009) Helicobacter pylori moves through mucus by reducing mucin viscoelasticity. *Proc. Natl. Acad. Sci. U. S. A.* **106**: 14321-14326.

Chang, Y. Y., Y. T. Lai, T. Cheng, H. Wang, Y. Yang & H. Sun, (2015) Selective interaction of Hpn-like protein with nickel, zinc and bismuth in vitro and in cells by FRET. *J. Inorg. Biochem.* **142**: 8-14.

Chao, Y., K. Papenfort, R. Reinhardt, C. M. Sharma & J. Vogel, (2012) An atlas of Hfq-bound transcripts reveals 3' UTRs as a genomic reservoir of regulatory small RNAs. *EMBO J.* **31**: 4005-4019.

Chao, Y. & J. Vogel, (2010) The role of Hfq in bacterial pathogens. *Curr. Opin. Microbiol.* **13**: 24-33.

Chao, Y. & J. Vogel, (2016) A 3' UTR-Derived Small RNA Provides the Regulatory Noncoding Arm of the Inner Membrane Stress Response. *Mol. Cell* **61**: 352-363.

Chen, S., A. Zhang, L. B. Blyn & G. Storz, (2004) MicC, a second small-RNA regulator of Omp protein expression in Escherichia coli. *J. Bacteriol.* **186**: 6689-6697.

Chiera, N. M., M. Rowinska-Zyrek, R. Wieczorek, R. Guerrini, D. Witkowska, M. Remelli & H. Kozlowski, (2013) Unexpected impact of the number of glutamine residues on metal complex stability. *Metallomics : integrated biometal science* **5**: 214-221.

Clyne, M., A. Labigne & B. Drumm, (1995) Helicobacter pylori requires an acidic environment to survive in the presence of urea. *Infect. Immun.* **63**: 1669-1673.

Contreras, M., J. M. Thiberge, M. A. Mandrand-Berthelot & A. Labigne, (2003) Characterization of the roles of NikR, a nickel-responsive pleiotropic autoregulator of Helicobacter pylori. *Mol. Microbiol.* **49**: 947-963.

Coornaert, A., A. Lu, P. Mandin, M. Springer, S. Gottesman & M. Guillier, (2010) MicA sRNA links the PhoP regulon to cell envelope stress. *Mol. Microbiol.* **76**: 467-479.

Corcoran, C. P., D. Podkaminski, K. Papenfort, J. H. Urban, J. C. Hinton & J. Vogel, (2012) Superfolder GFP reporters validate diverse new mRNA targets of the classic porin regulator, MicF RNA. *Mol. Microbiol.* **84**: 428-445.

Cussac, V., R. L. Ferrero & A. Labigne, (1992) Expression of Helicobacter pylori urease genes in Escherichia coli grown under nitrogen-limiting conditions. *J. Bacteriol.* **174**: 2466-2473.

Dailidiene, D., G. Dailide, D. Kersulyte & D. E. Berg, (2006) Contraselectable streptomycin susceptibility determinant for genetic manipulation and analysis of Helicobacter pylori. *Appl. Environ. Microbiol.* **72**: 5908-5914.

Danielli, A., G. Amore & V. Scarlato, (2010) Built shallow to maintain homeostasis and persistent infection: insight into the transcriptional regulatory network of the gastric human pathogen Helicobacter pylori. *PLoS Pathog.* **6**: e1000938.

Darling, A. C., B. Mau, F. R. Blattner & N. T. Perna, (2004) Mauve: multiple alignment of conserved genomic sequence with rearrangements. *Genome Res.* **14**: 1394-1403.

De Biase, D., A. Tramonti, F. Bossa & P. Visca, (1999) The response to stationary-phase stress conditions in Escherichia coli: role and regulation of the glutamic acid decarboxylase system. *Mol. Microbiol.* **32**: 1198-1211.

de Reuse, H. & S. Bereswill, (2007) Ten years after the first Helicobacter pylori genome: comparative and functional genomics provide new insights in the variability and adaptability of a persistent pathogen. *FEMS Immunol. Med. Microbiol.* **50**: 165-176.

Deana, A. & J. G. Belasco, (2005) Lost in translation: the influence of ribosomes on bacterial mRNA decay. *Genes Dev.* **19**: 2526-2533.

Debowski, A. W., M. Sehnal, T. Liao, K. A. Stubbs, B. J. Marshall & M. Benghezal, (2015) Expansion of the tetracycline-dependent regulation toolbox for Helicobacter pylori. *Appl. Environ. Microbiol.* **81**: 7969-7980.

Debowski, A. W., P. Verbrugghe, M. Sehnal, B. J. Marshall & M. Benghezal, (2013) Development of a tetracycline-inducible gene expression system for the study of Helicobacter pylori pathogenesis. *Appl. Environ. Microbiol.* **79**: 7351-7359.

Delany, I., R. Ieva, A. Soragni, M. Hilleringmann, R. Rappuoli & V. Scarlato, (2005) In vitro analysis of protein-operator interactions of the NikR and fur metal-responsive regulators of coregulated genes in Helicobacter pylori. *J. Bacteriol.* **187**: 7703-7715.

Delany, I., G. Spohn, R. Rappuoli & V. Scarlato, (2002) Growth phase-dependent regulation of target gene promoters for binding of the essential orphan response regulator HP1043 of Helicobacter pylori. *J. Bacteriol.* **184**: 4800-4810.

Dietz, P., G. Gerlach & D. Beier, (2002) Identification of target genes regulated by the two-component system HP166-HP165 of Helicobacter pylori. *J. Bacteriol.* **184**: 350-362.

Dorer, M. S., S. Talarico & N. R. Salama, (2009) Helicobacter pylori's unconventional role in health and disease. *PLoS Pathog.* **5**: e1000544.

Dugar, G., A. Herbig, K. U. Forstner, N. Heidrich, R. Reinhardt, K. Nieselt & C. M. Sharma, (2013) High-resolution transcriptome maps reveal strain-specific regulatory features of multiple Campylobacter jejuni isolates. *PLoS genetics* **9**: e1003495.

Dugar, G., S. L. Svensson, T. Bischler, S. Waldchen, R. Reinhardt, M. Sauer & C. M. Sharma, (2016) The CsrA-FliW network controls polar localization of the dual-function flagellin mRNA in Campylobacter jejuni. *Nature communications* **7**: 11667.

Duhring, U., I. M. Axmann, W. R. Hess & A. Wilde, (2006) An internal antisense RNA regulates expression of the photosynthesis gene isiA. *Proc. Natl. Acad. Sci. U. S. A.* **103**: 7054-7058.

Dyballa, N. & S. Metzger, (2009) Fast and sensitive colloidal coomassie G-250 staining for proteins in polyacrylamide gels. *Journal of visualized experiments : JoVE*.

Eaton, K. A., F. E. Dewhirst, M. J. Radin, J. G. Fox, B. J. Paster, S. Krakowka & D. R. Morgan, (1993) Helicobacter acinonyx sp. nov., isolated from cheetahs with gastritis. *Int. J. Syst. Bacteriol.* **43**: 99-106.

Eaton, K. A. & S. Krakowka, (1994) Effect of gastric pH on urease-dependent colonization of gnotobiotic piglets by Helicobacter pylori. *Infect. Immun.* **62**: 3604-3607.

Egger, L. A., H. Park & M. Inouye, (1997) Signal transduction via the histidyl-aspartyl phosphorelay. *Genes Cells* **2**: 167-184.

Eppinger, M., C. Baar, B. Linz, G. Raddatz, C. Lanz, H. Keller, G. Morelli, H. Gressmann, M. Achtman & S. C. Schuster, (2006) Who ate whom? Adaptive Helicobacter genomic changes that accompanied a host jump from early humans to large felines. *PLoS genetics* **2**: e120.

Falush, D., T. Wirth, B. Linz, J. K. Pritchard, M. Stephens, M. Kidd, M. J. Blaser, D. Y. Graham, S. Vacher, G. I. Perez-Perez, Y. Yamaoka, F. Megraud, K. Otto, U. Reichard, E. Katzowitsch, X. Wang, M. Achtman & S. Suerbaum, (2003) Traces of human migrations in Helicobacter pylori populations. *Science* **299**: 1582-1585.

Farnbacher, M., T. Jahns, D. Willrodt, R. Daniel, R. Haas, A. Goesmann, S. Kurtz & G. Rieder, (2010) Sequencing, annotation, and comparative genome analysis of the gerbil-adapted Helicobacter pylori strain B8. *BMC Genomics* **11**: 335.

Feng, L., S. T. Rutherford, K. Papenfort, J. D. Bagert, J. C. van Kessel, D. A. Tirrell, N. S. Wingreen & B. L. Bassler, (2015) A qrr noncoding RNA deploys four different regulatory mechanisms to optimize quorum-sensing dynamics. *Cell* **160**: 228-240.

Foster, J. W., (2004) Escherichia coli acid resistance: tales of an amateur acidophile. *Nature reviews. Microbiology* **2**: 898-907.

Fox, J. G., (2002) The non-H pylori helicobacters: their expanding role in gastrointestinal and systemic diseases. *Gut* **50**: 273-283.

Fox, J. G., E. B. Cabot, N. S. Taylor & R. Laraway, (1988) Gastric colonization by Campylobacter pylori subsp. mustelae in ferrets. *Infect. Immun.* **56**: 2994-2996.

Frohlich, K. S., K. Papenfort, A. A. Berger & J. Vogel, (2012) A conserved RpoS-dependent small RNA controls the synthesis of major porin OmpD. *Nucleic Acids Res.* **40**: 3623-3640.

Frohlich, K. S., K. Papenfort, A. Fekete & J. Vogel, (2013) A small RNA activates CFA synthase by isoform-specific mRNA stabilization. *EMBO J.* **32**: 2963-2979.

Frohlich, K. S. & J. Vogel, (2009) Activation of gene expression by small RNA. *Curr. Opin. Microbiol.* **12**: 674-682.

Gan, J., J. E. Tropea, B. P. Austin, D. L. Court, D. S. Waugh & X. Ji, (2006) Structural insight into the mechanism of double-stranded RNA processing by ribonuclease III. *Cell* **124**: 355-366.

Gancz, H., S. Censini & D. S. Merrell, (2006) Iron and pH homeostasis intersect at the level of Fur regulation in the gastric pathogen Helicobacter pylori. *Infect. Immun.* **74**: 602-614.

Ge, R., X. Sun, D. Wang, Q. Zhou & H. Sun, (2011) Histidine-rich protein Hpn from Helicobacter pylori forms amyloid-like fibrils in vitro and inhibits the proliferation of gastric epithelial AGS cells. *Biochim. Biophys. Acta* **1813**: 1422-1427.

Ge, R., R. M. Watt, X. Sun, J. A. Tanner, Q. Y. He, J. D. Huang & H. Sun, (2006a) Expression and characterization of a histidine-rich protein, Hpn: potential for Ni2+ storage in Helicobacter pylori. *Biochem. J.* **393**: 285-293.

Ge, R., Y. Zhang, X. Sun, R. M. Watt, Q. Y. He, J. D. Huang, D. E. Wilcox & H. Sun, (2006b) Thermodynamic and kinetic aspects of metal binding to the histidine-rich protein, Hpn. *J. Am. Chem. Soc.* **128**: 11330-11331.

Geissmann, T. A. & D. Touati, (2004) Hfq, a new chaperoning role: binding to messenger RNA determines access for small RNA regulator. *EMBO J.* **23**: 396-405.

Georg, J. & W. R. Hess, (2011) cis-antisense RNA, another level of gene regulation in bacteria. *Microbiol. Mol. Biol. Rev.* **75**: 286-300.

Giangrossi, M., G. Prosseda, C. N. Tran, A. Brandi, B. Colonna & M. Falconi, (2010) A novel antisense RNA regulates at transcriptional level the virulence gene icsA of Shigella flexneri. *Nucleic Acids Res.* **38**: 3362-3375.

Gilbert, J. V., J. Ramakrishna, F. W. Sunderman, Jr., A. Wright & A. G. Plaut, (1995) Protein Hpn: cloning and characterization of a histidine-rich metal-binding polypeptide in Helicobacter pylori and Helicobacter mustelae. *Infect. Immun.* **63**: 2682-2688.

Gimpel, M., N. Heidrich, U. Mader, H. Krugel & S. Brantl, (2010) A dual-function sRNA from B. subtilis: SR1 acts as a peptide encoding mRNA on the gapA operon. *Mol. Microbiol.* **76**: 990-1009.

Gogol, E. B., V. A. Rhodius, K. Papenfort, J. Vogel & C. A. Gross, (2011) Small RNAs endow a transcriptional activator with essential repressor functions for single-tier control of a global stress regulon. *Proc. Natl. Acad. Sci. U. S. A.* **108**: 12875-12880.

Goodwin, A., D. Kersulyte, G. Sisson, S. J. Veldhuyzen van Zanten, D. E. Berg & P. S. Hoffman, (1998) Metronidazole resistance in Helicobacter pylori is due to null mutations in a gene (rdxA) that encodes an oxygen-insensitive NADPH nitroreductase. *Mol. Microbiol.* **28**: 383-393.

Gopel, Y. & B. Gorke, (2012) Rewiring two-component signal transduction with small RNAs. *Curr. Opin. Microbiol.* **15**: 132-139.

Gottesman, S., (2005) Micros for microbes: non-coding regulatory RNAs in bacteria. *Trends Genet.* **21**: 399-404.

Guillier, M. & S. Gottesman, (2008) The 5' end of two redundant sRNAs is involved in the regulation of multiple targets, including their own regulator. *Nucleic Acids Res.* **36**: 6781-6794.

Guo, M. S., T. B. Updegrove, E. B. Gogol, S. A. Shabalina, C. A. Gross & G. Storz, (2014) MicL, a new sigmaE-dependent sRNA, combats envelope stress by repressing synthesis of Lpp, the major outer membrane lipoprotein. *Genes Dev.* **28**: 1620-1634.

Gurtan, A. M. & P. A. Sharp, (2013) The role of miRNAs in regulating gene expression networks. *J. Mol. Biol.* **425**: 3582-3600.

Gut, H., E. Pennacchietti, R. A. John, F. Bossa, G. Capitani, D. De Biase & M. G. Grutter, (2006) Escherichia coli acid resistance: pH-sensing, activation by chloride and autoinhibition in GadB. *EMBO J.* **25**: 2643-2651.

Hammer, B. K. & B. L. Bassler, (2007) Regulatory small RNAs circumvent the conventional quorum sensing pathway in pandemic Vibrio cholerae. *Proc. Natl. Acad. Sci. U. S. A.* **104**: 11145-11149.

Han, K., B. Tjaden & S. Lory, (2016) GRIL-seq provides a method for identifying direct targets of bacterial small regulatory RNA by in vivo proximity ligation. *Nature microbiology* **2**: 16239.

Hayashi, T., H. Morohashi & M. Hatakeyama, (2013) Bacterial EPIYA effectors--where do they come from? What are they? Where are they going? *Cell. Microbiol.* **15**: 377-385.

Hayes, E. T., J. C. Wilks, P. Sanfilippo, E. Yohannes, D. P. Tate, B. D. Jones, M. D. Radmacher, S. S. BonDurant & J. L. Slonczewski, (2006) Oxygen limitation modulates pH regulation of catabolism and hydrogenases, multidrug transporters, and envelope composition in Escherichia coli K-12. *BMC Microbiol.* **6**: 89.

Helwak, A., G. Kudla, T. Dudnakova & D. Tollervey, (2013) Mapping the human miRNA interactome by CLASH reveals frequent noncanonical binding. *Cell* **153**: 654-665.

Henn, B. M., C. R. Gignoux, M. Jobin, J. M. Granka, J. M. Macpherson, J. M. Kidd, L. Rodriguez-Botigue, S. Ramachandran, L. Hon, A. Brisbin, A. A. Lin, P. A. Underhill, D. Comas, K. K. Kidd, P. J. Norman, P. Parham, C. D. Bustamante, J. L. Mountain & M. W. Feldman, (2011) Hunter-gatherer genomic diversity suggests a southern African origin for modern humans. *Proc. Natl. Acad. Sci. U. S. A.* **108**: 5154-5162.

Herskovits, A. A., E. S. Bochkareva & E. Bibi, (2000) New prospects in studying the bacterial signal recognition particle pathway. *Mol. Microbiol.* **38**: 927-939.

Hobbs, E. C., J. L. Astarita & G. Storz, (2010) Small RNAs and small proteins involved in resistance to cell envelope stress and acid shock in Escherichia coli: analysis of a bar-coded mutant collection. *J. Bacteriol.* **192**: 59-67.

Hoe, C. H., C. A. Raabe, T. S. Rozhdestvensky & T. H. Tang, (2013) Bacterial sRNAs: regulation in stress. *Int. J. Med. Microbiol.* **303**: 217-229.

Holmqvist, E., P. R. Wright, L. Li, T. Bischler, L. Barquist, R. Reinhardt, R. Backofen & J. Vogel, (2016) Global RNA recognition patterns of post-transcriptional regulators Hfq and CsrA revealed by UV crosslinking in vivo. *EMBO J.* **35**: 991-1011.

Hommais, F., E. Krin, J. Y. Coppee, C. Lacroix, E. Yeramian, A. Danchin & P. Bertin, (2004) GadE (YhiE): a novel activator involved in the response to acid environment in Escherichia coli. *Microbiology* **150**: 61-72.

Huntzinger, E., S. Boisset, C. Saveanu, Y. Benito, T. Geissmann, A. Namane, G. Lina, J. Etienne, B. Ehresmann, C. Ehresmann, A. Jacquier, F. Vandenesch & P. Romby, (2005) Staphylococcus aureus RNAIII and the endoribonuclease III coordinately regulate spa gene expression. *EMBO J.* **24**: 824-835.

Ingolia, N. T., S. Ghaemmaghami, J. R. Newman & J. S. Weissman, (2009) Genome-wide analysis in vivo of translation with nucleotide resolution using ribosome profiling. *Science* **324**: 218-223.

Jahn, N. & S. Brantl, (2013) One antitoxin--two functions: SR4 controls toxin mRNA decay and translation. *Nucleic Acids Res.* **41**: 9870-9880.

Jaskiewicz, L. & W. Filipowicz, (2008) Role of Dicer in posttranscriptional RNA silencing. *Curr. Top. Microbiol. Immunol.* **320**: 77-97.

Jin, Y., R. M. Watt, A. Danchin & J. D. Huang, (2009) Small noncoding RNA GcvB is a novel regulator of acid resistance in Escherichia coli. *BMC Genomics* **10**: 165.

Johnson, J. R., C. Clabots & H. Rosen, (2006) Effect of inactivation of the global oxidative stress regulator oxyR on the colonization ability of Escherichia coli O1:K1:H7 in a mouse model of ascending urinary tract infection. *Infect. Immun.* **74**: 461-468.

Josenhans, C., D. Beier, B. Linz, T. F. Meyer & S. Suerbaum, (2007) Pathogenomics of helicobacter. *Int. J. Med. Microbiol.* **297**: 589-600.

Jousselin, A., L. Metzinger & B. Felden, (2009) On the facultative requirement of the bacterial RNA chaperone, Hfq. *Trends Microbiol.* **17**: 399-405.

Jungblut, P. R., D. Bumann, G. Haas, U. Zimny-Arndt, P. Holland, S. Lamer, F. Siejak, A. Aebischer & T. F. Meyer, (2000) Comparative proteome analysis of Helicobacter pylori. *Mol. Microbiol.* **36**: 710-725.

Kaito, C., Y. Saito, G. Nagano, M. Ikuo, Y. Omae, Y. Hanada, X. Han, K. Kuwahara-Arai, T. Hishinuma, T. Baba, T. Ito, K. Hiramatsu & K. Sekimizu, (2011) Transcription and translation products of the cytolysin gene psm-mec on the mobile genetic element SCCmec regulate Staphylococcus aureus virulence. *PLoS Pathog.* **7**: e1001267.

Kansau, I., F. Guillain, J. M. Thiberge & A. Labigne, (1996) Nickel binding and immunological properties of the C-terminal domain of the Helicobacter pylori GroES homologue (HspA). *Mol. Microbiol.* **22**: 1013-1023.

Kawano, M., L. Aravind & G. Storz, (2007) An antisense RNA controls synthesis of an SOS-induced toxin evolved from an antitoxin. *Mol. Microbiol.* **64**: 738-754.

Kazantsev, A. V. & N. R. Pace, (2006) Bacterial RNase P: a new view of an ancient enzyme. *Nature reviews. Microbiology* **4**: 729-740.

Kim, B. H., S. Kim, H. G. Kim, J. Lee, I. S. Lee & Y. K. Park, (2005) The formation of cyclopropane fatty acids in Salmonella enterica serovar Typhimurium. *Microbiology* **151**: 209-218.

Kobayashi, H., T. Suzuki & T. Unemoto, (1986) Streptococcal cytoplasmic pH is regulated by changes in amount and activity of a proton-translocating ATPase. *J. Biol. Chem.* **261**: 627-630.

Kreikemeyer, B., M. D. Boyle, B. A. Buttaro, M. Heinemann & A. Podbielski, (2001) Group A streptococcal growth phase-associated virulence factor regulation by a novel operon (Fas) with homologies to two-component-type regulators requires a small RNA molecule. *Mol. Microbiol.* **39**: 392-406.

Krulwich, T. A., G. Sachs & E. Padan, (2011) Molecular aspects of bacterial pH sensing and homeostasis. *Nature reviews. Microbiology* **9**: 330-343.

Kusters, J. G., A. H. van Vliet & E. J. Kuipers, (2006) Pathogenesis of Helicobacter pylori infection. *Clin. Microbiol. Rev.* **19**: 449-490.

Kwok, T., D. Zabler, S. Urman, M. Rohde, R. Hartig, S. Wessler, R. Misselwitz, J. Berger, N. Sewald, W. Konig & S. Backert, (2007) Helicobacter exploits integrin for type IV secretion and kinase activation. *Nature* **449**: 862-866.

Laalami, S., L. Zig & H. Putzer, (2014) Initiation of mRNA decay in bacteria. *Cell. Mol. Life Sci.* **71**: 1799-1828.

Labigne, A., V. Cussac & P. Courcoux, (1991) Shuttle cloning and nucleotide sequences of Helicobacter pylori genes responsible for urease activity. *J. Bacteriol.* **173**: 1920-1931.

Lalaouna, D., M. C. Carrier, S. Semsey, J. S. Brouard, J. Wang, J. T. Wade & E. Masse, (2015) A 3' external transcribed spacer in a tRNA transcript acts as a sponge for small RNAs to prevent transcriptional noise. *Mol. Cell* **58**: 393-405.

Lalaouna, D., M. Simoneau-Roy, D. Lafontaine & E. Masse, (2013) Regulatory RNAs and target mRNA decay in prokaryotes. *Biochim. Biophys. Acta* **1829**: 742-747.

Lease, R. A., D. Smith, K. McDonough & M. Belfort, (2004) The small noncoding DsrA RNA is an acid resistance regulator in Escherichia coli. *J. Bacteriol.* **186**: 6179-6185.

Lee, A., S. L. Hazell, J. O'Rourke & S. Kouprach, (1988) Isolation of a spiral-shaped bacterium from the cat stomach. *Infect. Immun.* **56**: 2843-2850.

Lee, E. J. & E. A. Groisman, (2010) An antisense RNA that governs the expression kinetics of a multifunctional virulence gene. *Mol. Microbiol.* **76**: 1020-1033.

Lenz, D. H., K. C. Mok, B. N. Lilley, R. V. Kulkarni, N. S. Wingreen & B. L. Bassler, (2004) The small RNA chaperone Hfq and multiple small RNAs control quorum sensing in Vibrio harveyi and Vibrio cholerae. *Cell* **118**: 69-82.

Letunic, I. & P. Bork, (2007) Interactive Tree Of Life (iTOL): an online tool for phylogenetic tree display and annotation. *Bioinformatics* **23**: 127-128.

Letunic, I. & P. Bork, (2016) Interactive tree of life (iTOL) v3: an online tool for the display and annotation of phylogenetic and other trees. *Nucleic Acids Res.* **44**: W242-245.

Li, Y., J. Syed & H. Sugiyama, (2016) RNA-DNA Triplex Formation by Long Noncoding RNAs. *Cell chemical biology* **23**: 1325-1333.

Linz, B., F. Balloux, Y. Moodley, A. Manica, H. Liu, P. Roumagnac, D. Falush, C. Stamer, F. Prugnolle, S. W. van der Merwe, Y. Yamaoka, D. Y. Graham, E. Perez-Trallero, T. Wadstrom, S. Suerbaum & M. Achtman, (2007) An African origin for the intimate association between humans and Helicobacter pylori. *Nature* **445**: 915-918.

Loh, J. T., S. S. Gupta, D. B. Friedman, A. M. Krezel & T. L. Cover, (2010) Analysis of protein expression regulated by the Helicobacter pylori ArsRS two-component signal transduction system. *J. Bacteriol.* **192**: 2034-2043.

Lybecker, M. C. & D. S. Samuels, (2007) Temperature-induced regulation of RpoS by a small RNA in Borrelia burgdorferi. *Mol. Microbiol.* **64**: 1075-1089.

Mahdavi, J., B. Sonden, M. Hurtig, F. O. Olfat, L. Forsberg, N. Roche, J. Angstrom, T. Larsson, S. Teneberg, K. A. Karlsson, S. Altraja, T. Wadstrom, D. Kersulyte, D. E. Berg, A. Dubois, C. Petersson, K. E. Magnusson, T. Norberg, F. Lindh, B. B. Lundskog, A. Arnqvist, L. Hammarstrom & T. Boren, (2002) Helicobacter pylori SabA adhesin in persistent infection and chronic inflammation. *Science* **297**: 573-578.

Majdalani, N., C. Cunning, D. Sledjeski, T. Elliott & S. Gottesman, (1998) DsrA RNA regulates translation of RpoS message by an anti-antisense mechanism, independent of its action as an antisilencer of transcription. *Proc. Natl. Acad. Sci. U. S. A.* **95**: 12462-12467.

Majdalani, N., D. Hernandez & S. Gottesman, (2002) Regulation and mode of action of the second small RNA activator of RpoS translation, RprA. *Mol. Microbiol.* **46**: 813-826.

Mangan, S. & U. Alon, (2003) Structure and function of the feed-forward loop network motif. *Proc. Natl. Acad. Sci. U. S. A.* **100**: 11980-11985.

Mangold, M., M. Siller, B. Roppenser, B. J. Vlaminckx, T. A. Penfound, R. Klein, R. Novak, R. P. Novick & E. Charpentier, (2004) Synthesis of group A streptococcal virulence factors is controlled by a regulatory RNA molecule. *Mol. Microbiol.* **53**: 1515-1527.

Mank, N. N., B. A. Berghoff, Y. N. Hermanns & G. Klug, (2012) Regulation of bacterial photosynthesis genes by the small noncoding RNA PcrZ. *Proc. Natl. Acad. Sci. U. S. A.* **109**: 16306-16311.

Mank, N. N., B. A. Berghoff & G. Klug, (2013) A mixed incoherent feed-forward loop contributes to the regulation of bacterial photosynthesis genes. *RNA Biol.* **10**: 347-352.

Marais, A., G. L. Mendz, S. L. Hazell & F. Megraud, (1999) Metabolism and genetics of Helicobacter pylori: the genome era. *Microbiol. Mol. Biol. Rev.* **63**: 642-674.

Marcus, E. A., A. P. Moshfegh, G. Sachs & D. R. Scott, (2005) The periplasmic alpha-carbonic anhydrase activity of Helicobacter pylori is essential for acid acclimation. *J. Bacteriol.* **187**: 729-738.

Marcus, E. A., G. Sachs, Y. Wen & D. R. Scott, (2016) Phosphorylation-dependent and Phosphorylation-independent Regulation of Helicobacter pylori Acid Acclimation by the ArsRS Two-component System. *Helicobacter* **21**: 69-81.

Marshall, B. J. & J. R. Warren, (1984) Unidentified curved bacilli in the stomach of patients with gastritis and peptic ulceration. *Lancet* **1**: 1311-1315.

Martinez-Antonio, A., S. C. Janga & D. Thieffry, (2008) Functional organisation of Escherichia coli transcriptional regulatory network. *J. Mol. Biol.* **381**: 238-247.
Masse, E., F. E. Escorcia & S. Gottesman, (2003) Coupled degradation of a small regulatory RNA and its mRNA targets in Escherichia coli. *Genes Dev.* **17**: 2374-2383.
Masse, E. & S. Gottesman, (2002) A small RNA regulates the expression of genes involved in iron metabolism in Escherichia coli. *Proc. Natl. Acad. Sci. U. S. A.* **99**: 4620-4625.
Masse, E., H. Salvail, G. Desnoyers & M. Arguin, (2007) Small RNAs controlling iron metabolism. *Curr. Opin. Microbiol.* **10**: 140-145.
Masse, E., C. K. Vanderpool & S. Gottesman, (2005) Effect of RyhB small RNA on global iron use in Escherichia coli. *J. Bacteriol.* **187**: 6962-6971.
Maurer, L. M., E. Yohannes, S. S. Bondurant, M. Radmacher & J. L. Slonczewski, (2005) pH regulates genes for flagellar motility, catabolism, and oxidative stress in Escherichia coli K-12. *J. Bacteriol.* **187**: 304-319.
McClain, M. S., S. S. Duncan, J. A. Gaddy & T. L. Cover, (2013) Control of gene expression in Helicobacter pylori using the Tet repressor. *J. Microbiol. Methods* **95**: 336-341.
McClain, M. S., C. L. Shaffer, D. A. Israel, R. M. Peek, Jr. & T. L. Cover, (2009) Genome sequence analysis of Helicobacter pylori strains associated with gastric ulceration and gastric cancer. *BMC Genomics* **10**: 3.
McGee, D. J., J. Zabaleta, R. J. Viator, T. L. Testerman, A. C. Ochoa & G. L. Mendz, (2004) Purification and characterization of Helicobacter pylori arginase, RocF: unique features among the arginase superfamily. *Eur. J. Biochem.* **271**: 1952-1962.
Melamed, S., A. Peer, R. Faigenbaum-Romm, Y. E. Gatt, N. Reiss, A. Bar, Y. Altuvia, L. Argaman & H. Margalit, (2016) Global Mapping of Small RNA-Target Interactions in Bacteria. *Mol. Cell* **63**: 884-897.
Michaux, C., N. Verneuil, A. Hartke & J. C. Giard, (2014) Physiological roles of small RNA molecules. *Microbiology* **160**: 1007-1019.
Milo, R., S. Shen-Orr, S. Itzkovitz, N. Kashtan, D. Chklovskii & U. Alon, (2002) Network motifs: simple building blocks of complex networks. *Science* **298**: 824-827.
Mizuno, T., M. Y. Chou & M. Inouye, (1984) A unique mechanism regulating gene expression: translational inhibition by a complementary RNA transcript (micRNA). *Proc. Natl. Acad. Sci. U. S. A.* **81**: 1966-1970.
Mobley, H. L., R. M. Garner, G. R. Chippendale, J. V. Gilbert, A. V. Kane & A. G. Plaut, (1999) Role of Hpn and NixA of Helicobacter pylori in susceptibility and resistance to bismuth and other metal ions. *Helicobacter* **4**: 162-169.
Mobley, H. L., M. D. Island & R. P. Hausinger, (1995) Molecular biology of microbial ureases. *Microbiol. Rev.* **59**: 451-480.
Mollenhauer-Rektorschek, M., G. Hanauer, G. Sachs & K. Melchers, (2002) Expression of UreI is required for intragastric transit and colonization of gerbil gastric mucosa by Helicobacter pylori. *Res. Microbiol.* **153**: 659-666.
Moodley, Y. & B. Linz, (2009) Helicobacter pylori Sequences Reflect Past Human Migrations. *Genome dynamics* **6**: 62-74.
Moodley, Y., B. Linz, R. P. Bond, M. Nieuwoudt, H. Soodyall, C. M. Schlebusch, S. Bernhoft, J. Hale, S. Suerbaum, L. Mugisha, S. W. van der Merwe & M. Achtman, (2012) Age of the association between Helicobacter pylori and man. *PLoS Pathog.* **8**: e1002693.
Moore, S. D. & R. T. Sauer, (2007) The tmRNA system for translational surveillance and ribosome rescue. *Annu. Rev. Biochem.* **76**: 101-124.
Morfeldt, E., D. Taylor, A. von Gabain & S. Arvidson, (1995) Activation of alpha-toxin translation in Staphylococcus aureus by the trans-encoded antisense RNA, RNAIII. *EMBO J.* **14**: 4569-4577.

Morita, T., K. Maki & H. Aiba, (2005) RNase E-based ribonucleoprotein complexes: mechanical basis of mRNA destabilization mediated by bacterial noncoding RNAs. *Genes Dev.* **19**: 2176-2186.

Mraheil, M. A., A. Billion, C. Kuenne, J. Pischimarov, B. Kreikemeyer, S. Engelmann, A. Hartke, J. C. Giard, M. Rupnik, S. Vorwerk, M. Beier, J. Retey, T. Hartsch, A. Jacob, F. Cemic, J. Hemberger, T. Chakraborty & T. Hain, (2010) Comparative genome-wide analysis of small RNAs of major Gram-positive pathogens: from identification to application. *Microbial biotechnology* **3**: 658-676.

Mraheil, M. A., A. Billion, W. Mohamed, K. Mukherjee, C. Kuenne, J. Pischimarov, C. Krawitz, J. Retey, T. Hartsch, T. Chakraborty & T. Hain, (2011) The intracellular sRNA transcriptome of Listeria monocytogenes during growth in macrophages. *Nucleic Acids Res.* **39**: 4235-4248.

Muller, C., C. Bahlawane, S. Aubert, C. M. Delay, K. Schauer, I. Michaud-Soret & H. De Reuse, (2011) Hierarchical regulation of the NikR-mediated nickel response in Helicobacter pylori. *Nucleic Acids Res.* **39**: 7564-7575.

Murata-Kamiya, N., (2011) Pathophysiological functions of the CagA oncoprotein during infection by Helicobacter pylori. *Microbes and infection* **13**: 799-807.

Oglesby-Sherrouse, A. G. & E. R. Murphy, (2013) Iron-responsive bacterial small RNAs: variations on a theme. *Metallomics : integrated biometal science* **5**: 276-286.

Opdyke, J. A., J. G. Kang & G. Storz, (2004) GadY, a small-RNA regulator of acid response genes in Escherichia coli. *J. Bacteriol.* **186**: 6698-6705.

Overgaard, M., J. Johansen, J. Moller-Jensen & P. Valentin-Hansen, (2009) Switching off small RNA regulation with trap-mRNA. *Mol. Microbiol.* **73**: 790-800.

Padalon-Brauch, G., R. Hershberg, M. Elgrably-Weiss, K. Baruch, I. Rosenshine, H. Margalit & S. Altuvia, (2008) Small RNAs encoded within genetic islands of Salmonella typhimurium show host-induced expression and role in virulence. *Nucleic Acids Res.* **36**: 1913-1927.

Pain, A., A. Ott, H. Amine, T. Rochat, P. Bouloc & D. Gautheret, (2015) An assessment of bacterial small RNA target prediction programs. *RNA Biol.* **12**: 509-513.

Palframan, S. L., T. Kwok & K. Gabriel, (2012) Vacuolating cytotoxin A (VacA), a key toxin for Helicobacter pylori pathogenesis. *Frontiers in cellular and infection microbiology* **2**: 92.

Panthel, K., P. Dietz, R. Haas & D. Beier, (2003) Two-component systems of Helicobacter pylori contribute to virulence in a mouse infection model. *Infect. Immun.* **71**: 5381-5385.

Papenfort, K., M. Bouvier, F. Mika, C. M. Sharma & J. Vogel, (2010) Evidence for an autonomous 5' target recognition domain in an Hfq-associated small RNA. *Proc. Natl. Acad. Sci. U. S. A.* **107**: 20435-20440.

Papenfort, K., E. Espinosa, J. Casadesus & J. Vogel, (2015) Small RNA-based feedforward loop with AND-gate logic regulates extrachromosomal DNA transfer in Salmonella. *Proc. Natl. Acad. Sci. U. S. A.* **112**: E4772-4781.

Papenfort, K., V. Pfeiffer, F. Mika, S. Lucchini, J. C. Hinton & J. Vogel, (2006) SigmaE-dependent small RNAs of Salmonella respond to membrane stress by accelerating global omp mRNA decay. *Mol. Microbiol.* **62**: 1674-1688.

Papenfort, K. & J. Vogel, (2009) Multiple target regulation by small noncoding RNAs rewires gene expression at the post-transcriptional level. *Res. Microbiol.* **160**: 278-287.

Papenfort, K. & J. Vogel, (2010) Regulatory RNA in bacterial pathogens. *Cell Host Microbe* **8**: 116-127.

Paugh, S. W., D. R. Coss, J. Bao, L. T. Laudermilk, C. R. Grace, A. M. Ferreira, M. B. Waddell, G. Ridout, D. Naeve, M. Leuze, P. F. LoCascio, J. C. Panetta, M. R. Wilkinson, C. H. Pui, C. W. Naeve, E. C. Uberbacher, E. J. Bonten & W. E. Evans, (2016) MicroRNAs Form Triplexes with Double Stranded DNA at Sequence-Specific Binding Sites; a Eukaryotic Mechanism via which microRNAs Could Directly Alter Gene Expression. *PLoS Comput. Biol.* **12**: e1004744.

Pernitzsch, S. R. & C. M. Sharma, (2012) Transcriptome complexity and riboregulation in the human pathogen Helicobacter pylori. *Frontiers in cellular and infection microbiology* **2**: 14.

Pernitzsch, S. R., S. M. Tirier, D. Beier & C. M. Sharma, (2014) A variable homopolymeric G-repeat defines small RNA-mediated posttranscriptional regulation of a chemotaxis receptor in Helicobacter pylori. *Proc. Natl. Acad. Sci. U. S. A.* **111**: E501-510.

Petrak, J., R. Ivanek, O. Toman, R. Cmejla, J. Cmejlova, D. Vyoral, J. Zivny & C. D. Vulpe, (2008) Deja vu in proteomics. A hit parade of repeatedly identified differentially expressed proteins. *Proteomics* **8**: 1744-1749.

Pfeiffer, V., K. Papenfort, S. Lucchini, J. C. Hinton & J. Vogel, (2009) Coding sequence targeting by MicC RNA reveals bacterial mRNA silencing downstream of translational initiation. *Nat. Struct. Mol. Biol.* **16**: 840-846.

Pfeiffer, V., A. Sittka, R. Tomer, K. Tedin, V. Brinkmann & J. Vogel, (2007) A small non-coding RNA of the invasion gene island (SPI-1) represses outer membrane protein synthesis from the Salmonella core genome. *Mol. Microbiol.* **66**: 1174-1191.

Pflock, M., P. Dietz, J. Schar & D. Beier, (2004) Genetic evidence for histidine kinase HP165 being an acid sensor of Helicobacter pylori. *FEMS Microbiol. Lett.* **234**: 51-61.

Pflock, M., N. Finsterer, B. Joseph, H. Mollenkopf, T. F. Meyer & D. Beier, (2006) Characterization of the ArsRS regulon of Helicobacter pylori, involved in acid adaptation. *J. Bacteriol.* **188**: 3449-3462.

Pflock, M., S. Kennard, I. Delany, V. Scarlato & D. Beier, (2005) Acid-induced activation of the urease promoters is mediated directly by the ArsRS two-component system of Helicobacter pylori. *Infect. Immun.* **73**: 6437-6445.

Pichon, C. & B. Felden, (2005) Small RNA genes expressed from Staphylococcus aureus genomic and pathogenicity islands with specific expression among pathogenic strains. *Proc. Natl. Acad. Sci. U. S. A.* **102**: 14249-14254.

Pichon, C. & B. Felden, (2008) Small RNA gene identification and mRNA target predictions in bacteria. *Bioinformatics* **24**: 2807-2813.

Pot, R. G., J. G. Kusters, L. C. Smeets, W. Van Tongeren, C. M. Vandenbroucke-Grauls & A. Bart, (2001) Interspecies transfer of antibiotic resistance between Helicobacter pylori and Helicobacter acinonychis. *Antimicrob. Agents Chemother.* **45**: 2975-2976.

Prevost, K., H. Salvail, G. Desnoyers, J. F. Jacques, E. Phaneuf & E. Masse, (2007) The small RNA RyhB activates the translation of shiA mRNA encoding a permease of shikimate, a compound involved in siderophore synthesis. *Mol. Microbiol.* **64**: 1260-1273.

Pulvermacher, S. C., L. T. Stauffer & G. V. Stauffer, (2009) The small RNA GcvB regulates sstT mRNA expression in Escherichia coli. *J. Bacteriol.* **191**: 238-248.

Raghavan, R., F. R. Kacharia, J. A. Millar, C. D. Sislak & H. Ochman, (2015) Genome rearrangements can make and break small RNA genes. *Genome Biol. Evol.* **7**: 557-566.

Ramani, N., M. Hedeshian & M. Freundlich, (1994) micF antisense RNA has a major role in osmoregulation of OmpF in Escherichia coli. *J. Bacteriol.* **176**: 5005-5010.

Ramirez-Pena, E., J. Trevino, Z. Liu, N. Perez & P. Sumby, (2010) The group A Streptococcus small regulatory RNA FasX enhances streptokinase activity by increasing the stability of the ska mRNA transcript. *Mol. Microbiol.* **78**: 1332-1347.

Redko, Y., S. Aubert, A. Stachowicz, P. Lenormand, A. Namane, F. Darfeuille, M. Thibonnier & H. De Reuse, (2013) A minimal bacterial RNase J-based degradosome is associated with translating ribosomes. *Nucleic Acids Res.* **41**: 288-301.

Redko, Y., E. Galtier, H. Arnion, F. Darfeuille, O. Sismeiro, J. Y. Coppee, C. Medigue, M. Weiman, S. Cruveiller & H. De Reuse, (2016) RNase J depletion leads to massive changes in mRNA abundance in Helicobacter pylori. *RNA Biol.* **13**: 243-253.

Regulski, E. E. & R. R. Breaker, (2008) In-line probing analysis of riboswitches. *Methods Mol. Biol.* **419**: 53-67.

Reuter, J. S. & D. H. Mathews, (2010) RNAstructure: software for RNA secondary structure prediction and analysis. *BMC Bioinformatics* **11**: 129.

Richards, G. R. & C. K. Vanderpool, (2011) Molecular call and response: the physiology of bacterial small RNAs. *Biochim. Biophys. Acta* **1809**: 525-531.

Roberts, S. A. & J. R. Scott, (2007) RivR and the small RNA RivX: the missing links between the CovR regulatory cascade and the Mga regulon. *Mol. Microbiol.* **66**: 1506-1522.

Rolig, A. S., J. Shanks, J. E. Carter & K. M. Ottemann, (2012) Helicobacter pylori requires TlpD-driven chemotaxis to proliferate in the antrum. *Infect. Immun.* **80**: 3713-3720.

Roncarati, D., S. Pelliciari, N. Doniselli, S. Maggi, A. Vannini, L. Valzania, L. Mazzei, B. Zambelli, C. Rivetti & A. Danielli, (2016) Metal-responsive promoter DNA compaction by the ferric uptake regulator. *Nature communications* **7**: 12593.

Rowinska-Zyrek, M., D. Witkowska, S. Bielinska, W. Kamysz & H. Kozlowski, (2011) The -Cys-Cys- motif in Helicobacter pylori's Hpn and HspA proteins is an essential anchoring site for metal ions. *Dalton transactions* **40**: 5604-5610.

Rutherford, S. T., J. C. van Kessel, Y. Shao & B. L. Bassler, (2011) AphA and LuxR/HapR reciprocally control quorum sensing in vibrios. *Genes Dev.* **25**: 397-408.

Sachs, G., D. L. Weeks, K. Melchers & D. R. Scott, (2003) The gastric biology of Helicobacter pylori. *Annu. Rev. Physiol.* **65**: 349-369.

Salama, N. R., M. L. Hartung & A. Muller, (2013) Life in the human stomach: persistence strategies of the bacterial pathogen Helicobacter pylori. *Nature reviews. Microbiology* **11**: 385-399.

Salgado, H., A. Santos-Zavaleta, S. Gama-Castro, M. Peralta-Gil, M. I. Penaloza-Spinola, A. Martinez-Antonio, P. D. Karp & J. Collado-Vides, (2006) The comprehensive updated regulatory network of Escherichia coli K-12. *BMC Bioinformatics* **7**: 5.

Saliba, A. E., C. S. S & J. Vogel, (2017) New RNA-seq approaches for the study of bacterial pathogens. *Curr. Opin. Microbiol.* **35**: 78-87.

Salvail, H., P. Lanthier-Bourbonnais, J. M. Sobota, M. Caza, J. A. Benjamin, M. E. Mendieta, F. Lepine, C. M. Dozois, J. Imlay & E. Masse, (2010) A small RNA promotes siderophore production through transcriptional and metabolic remodeling. *Proc. Natl. Acad. Sci. U. S. A.* **107**: 15223-15228.

Scarlato, V., I. Delany, G. Spohn & D. Beier, (2001) Regulation of transcription in Helicobacter pylori: simple systems or complex circuits? *Int. J. Med. Microbiol.* **291**: 107-117.

Schar, J., A. Sickmann & D. Beier, (2005) Phosphorylation-independent activity of atypical response regulators of Helicobacter pylori. *J. Bacteriol.* **187**: 3100-3109.

Schauer, K., C. Muller, M. Carriere, A. Labigne, C. Cavazza & H. De Reuse, (2010) The Helicobacter pylori GroES cochaperonin HspA functions as a specialized nickel chaperone and sequestration protein through its unique C-terminal extension. *J. Bacteriol.* **192**: 1231-1237.

Schreiber, S., R. Bucker, C. Groll, M. Azevedo-Vethacke, D. Garten, P. Scheid, S. Friedrich, S. Gatermann, C. Josenhans & S. Suerbaum, (2005) Rapid loss of motility of Helicobacter pylori in the gastric lumen in vivo. *Infect. Immun.* **73**: 1584-1589.

Schreiber, S., M. Konradt, C. Groll, P. Scheid, G. Hanauer, H. O. Werling, C. Josenhans & S. Suerbaum, (2004) The spatial orientation of Helicobacter pylori in the gastric mucus. *Proc. Natl. Acad. Sci. U. S. A.* **101**: 5024-5029.

Scott, D. R., E. A. Marcus, D. L. Weeks & G. Sachs, (2002) Mechanisms of acid resistance due to the urease system of Helicobacter pylori. *Gastroenterology* **123**: 187-195.

Scott, D. R., E. A. Marcus, Y. Wen, S. Singh, J. Feng & G. Sachs, (2010) Cytoplasmic histidine kinase (HP0244)-regulated assembly of urease with UreI, a channel for urea and its metabolites, CO2, NH3, and NH4(+), is necessary for acid survival of Helicobacter pylori. *J. Bacteriol.* **192**: 94-103.

Seshadri, S., S. L. Benoit & R. J. Maier, (2007) Roles of His-rich hpn and hpn-like proteins in Helicobacter pylori nickel physiology. *J. Bacteriol.* **189**: 4120-4126.

Shabala, L. & T. Ross, (2008) Cyclopropane fatty acids improve Escherichia coli survival in acidified minimal media by reducing membrane permeability to H+ and enhanced ability to extrude H+. *Res. Microbiol.* **159**: 458-461.

Shames, B., J. G. Fox, F. Dewhirst, L. Yan, Z. Shen & N. S. Taylor, (1995) Identification of widespread Helicobacter hepaticus infection in feces in commercial mouse colonies by culture and PCR assay. *J. Clin. Microbiol.* **33**: 2968-2972.

Sharma, C. M., F. Darfeuille, T. H. Plantinga & J. Vogel, (2007) A small RNA regulates multiple ABC transporter mRNAs by targeting C/A-rich elements inside and upstream of ribosome-binding sites. *Genes Dev.* **21**: 2804-2817.

Sharma, C. M., S. Hoffmann, F. Darfeuille, J. Reignier, S. Findeiss, A. Sittka, S. Chabas, K. Reiche, J. Hackermuller, R. Reinhardt, P. F. Stadler & J. Vogel, (2010) The primary transcriptome of the major human pathogen Helicobacter pylori. *Nature* **464**: 250-255.

Sharma, C. M. & J. Vogel, (2009) Experimental approaches for the discovery and characterization of regulatory small RNA. *Curr. Opin. Microbiol.* **12**: 536-546.

Shen-Orr, S. S., R. Milo, S. Mangan & U. Alon, (2002) Network motifs in the transcriptional regulation network of Escherichia coli. *Nat. Genet.* **31**: 64-68.

Shimoni, Y., G. Friedlander, G. Hetzroni, G. Niv, S. Altuvia, O. Biham & H. Margalit, (2007) Regulation of gene expression by small non-coding RNAs: a quantitative view. *Mol. Syst. Biol.* **3**: 138.

Sittka, A., S. Lucchini, K. Papenfort, C. M. Sharma, K. Rolle, T. T. Binnewies, J. C. Hinton & J. Vogel, (2008) Deep sequencing analysis of small noncoding RNA and mRNA targets of the global post-transcriptional regulator, Hfq. *PLoS genetics* **4**: e1000163.

Sittka, A., V. Pfeiffer, K. Tedin & J. Vogel, (2007) The RNA chaperone Hfq is essential for the virulence of Salmonella typhimurium. *Mol. Microbiol.* **63**: 193-217.

Skouloubris, S., A. Labigne & H. De Reuse, (2001) The AmiE aliphatic amidase and AmiF formamidase of Helicobacter pylori: natural evolution of two enzyme paralogues. *Mol. Microbiol.* **40**: 596-609.

Skouloubris, S., J. M. Thiberge, A. Labigne & H. De Reuse, (1998) The Helicobacter pylori UreI protein is not involved in urease activity but is essential for bacterial survival in vivo. *Infect. Immun.* **66**: 4517-4521.

Slonczewski, J. L., M. Fujisawa, M. Dopson & T. A. Krulwich, (2009) Cytoplasmic pH measurement and homeostasis in bacteria and archaea. *Adv. Microb. Physiol.* **55**: 1-79, 317.

Solnick, J. V. & D. B. Schauer, (2001) Emergence of diverse Helicobacter species in the pathogenesis of gastric and enterohepatic diseases. *Clin. Microbiol. Rev.* **14**: 59-97.

Sonnleitner, E., T. Sorger-Domenigg, M. J. Madej, S. Findeiss, J. Hackermuller, A. Huttenhofer, P. F. Stadler, U. Blasi & I. Moll, (2008) Detection of small RNAs in Pseudomonas aeruginosa by RNomics and structure-based bioinformatic tools. *Microbiology* **154**: 3175-3187.

Stancik, L. M., D. M. Stancik, B. Schmidt, D. M. Barnhart, Y. N. Yoncheva & J. L. Slonczewski, (2002) pH-dependent expression of periplasmic proteins and amino acid catabolism in Escherichia coli. *J. Bacteriol.* **184**: 4246-4258.

Stingl, K. & H. De Reuse, (2005) Staying alive overdosed: how does Helicobacter pylori control urease activity? *Int. J. Med. Microbiol.* **295**: 307-315.

Storz, G., J. Vogel & K. M. Wassarman, (2011) Regulation by small RNAs in bacteria: expanding frontiers. *Mol. Cell* **43**: 880-891.

Stougaard, P., S. Molin & K. Nordstrom, (1981) RNAs involved in copy-number control and incompatibility of plasmid R1. *Proc. Natl. Acad. Sci. U. S. A.* **78**: 6008-6012.

Strugatsky, D., R. McNulty, K. Munson, C. K. Chen, S. M. Soltis, G. Sachs & H. Luecke, (2013) Structure of the proton-gated urea channel from the gastric pathogen Helicobacter pylori. *Nature* **493**: 255-258.

Sullivan, M. J., N. K. Petty & S. A. Beatson, (2011) Easyfig: a genome comparison visualizer. *Bioinformatics* **27**: 1009-1010.

Sundrud, M. S., V. J. Torres, D. Unutmaz & T. L. Cover, (2004) Inhibition of primary human T cell proliferation by Helicobacter pylori vacuolating toxin (VacA) is independent of VacA effects on IL-2 secretion. *Proc. Natl. Acad. Sci. U. S. A.* **101**: 7727-7732.

Svensson, S. L. & C. M. Sharma, (2016) Small RNAs in Bacterial Virulence and Communication. *Microbiology spectrum* **4**.

Sycuro, L. K., Z. Pincus, K. D. Gutierrez, J. Biboy, C. A. Stern, W. Vollmer & N. R. Salama, (2010) Peptidoglycan crosslinking relaxation promotes Helicobacter pylori's helical shape and stomach colonization. *Cell* **141**: 822-833.

Tan, S., J. M. Noto, J. Romero-Gallo, R. M. Peek, Jr. & M. R. Amieva, (2011) Helicobacter pylori perturbs iron trafficking in the epithelium to grow on the cell surface. *PLoS Pathog.* **7**: e1002050.

Terry, K., S. M. Williams, L. Connolly & K. M. Ottemann, (2005) Chemotaxis plays multiple roles during Helicobacter pylori animal infection. *Infect. Immun.* **73**: 803-811.

Thomason, M. K. & G. Storz, (2010) Bacterial antisense RNAs: how many are there, and what are they doing? *Annu. Rev. Genet.* **44**: 167-188.

Tjaden, B., (2008) TargetRNA: a tool for predicting targets of small RNA action in bacteria. *Nucleic Acids Res.* **36**: W109-113.

Tomb, J. F., O. White, A. R. Kerlavage, R. A. Clayton, G. G. Sutton, R. D. Fleischmann, K. A. Ketchum, H. P. Klenk, S. Gill, B. A. Dougherty, K. Nelson, J. Quackenbush, L. Zhou, E. F. Kirkness, S. Peterson, B. Loftus, D. Richardson, R. Dodson, H. G. Khalak, A. Glodek, K. McKenney, L. M. Fitzegerald, N. Lee, M. D. Adams, E. K. Hickey, D. E. Berg, J. D. Gocayne, T. R. Utterback, J. D. Peterson, J. M. Kelley, M. D. Cotton, J. M. Weidman, C. Fujii, C. Bowman, L. Watthey, E. Wallin, W. S. Hayes, M. Borodovsky, P. D. Karp, H. O. Smith, C. M. Fraser & J. C. Venter, (1997) The complete genome sequence of the gastric pathogen Helicobacter pylori. *Nature* **388**: 539-547.

Tramonti, A., M. De Canio & D. De Biase, (2008) GadX/GadW-dependent regulation of the Escherichia coli acid fitness island: transcriptional control at the gadY-gadW divergent promoters and identification of four novel 42 bp GadX/GadW-specific binding sites. *Mol. Microbiol.* **70**: 965-982.

Updegrove, T. B., S. A. Shabalina & G. Storz, (2015) How do base-pairing small RNAs evolve? *FEMS Microbiol. Rev.* **39**: 379-391.

Urban, J. H. & J. Vogel, (2007) Translational control and target recognition by Escherichia coli small RNAs in vivo. *Nucleic Acids Res.* **35**: 1018-1037.

Urbanowski, M. L., L. T. Stauffer & G. V. Stauffer, (2000) The gcvB gene encodes a small untranslated RNA involved in expression of the dipeptide and oligopeptide transport systems in Escherichia coli. *Mol. Microbiol.* **37**: 856-868.

Valentin-Hansen, P., J. Johansen & A. A. Rasmussen, (2007) Small RNAs controlling outer membrane porins. *Curr. Opin. Microbiol.* **10**: 152-155.

van Vliet, A. H., F. D. Ernst & J. G. Kusters, (2004a) NikR-mediated regulation of Helicobacter pylori acid adaptation. *Trends Microbiol.* **12**: 489-494.

van Vliet, A. H., E. J. Kuipers, J. Stoof, S. W. Poppelaars & J. G. Kusters, (2004b) Acid-responsive gene induction of ammonia-producing enzymes in Helicobacter pylori is mediated via a metal-responsive repressor cascade. *Infect. Immun.* **72**: 766-773.

van Vliet, A. H., E. J. Kuipers, B. Waidner, B. J. Davies, N. de Vries, C. W. Penn, C. M. Vandenbroucke-Grauls, M. Kist, S. Bereswill & J. G. Kusters, (2001) Nickel-responsive induction of urease expression in Helicobacter pylori is mediated at the transcriptional level. *Infect. Immun.* **69**: 4891-4897.

van Vliet, A. H., S. W. Poppelaars, B. J. Davies, J. Stoof, S. Bereswill, M. Kist, C. W. Penn, E. J. Kuipers & J. G. Kusters, (2002) NikR mediates nickel-responsive transcriptional induction of urease expression in Helicobacter pylori. *Infect. Immun.* **70**: 2846-2852.

Vannini, A., D. Roncarati & A. Danielli, (2016) The cag-pathogenicity island encoded CncR1 sRNA oppositely modulates Helicobacter pylori motility and adhesion to host cells. *Cell. Mol. Life Sci.* **73**: 3151-3168.

Viegas, S. C., V. Pfeiffer, A. Sittka, I. J. Silva, J. Vogel & C. M. Arraiano, (2007) Characterization of the role of ribonucleases in Salmonella small RNA decay. *Nucleic Acids Res.* **35**: 7651-7664.

Vinella, D., F. Fischer, E. Vorontsov, J. Gallaud, C. Malosse, V. Michel, C. Cavazza, M. Robbe-Saule, P. Richaud, J. Chamot-Rooke, C. Brochier-Armanet & H. De Reuse, (2015) Evolution of Helicobacter: Acquisition by Gastric Species of Two Histidine-Rich Proteins Essential for Colonization. *PLoS Pathog.* **11**: e1005312.

Vogel, J., L. Argaman, E. G. Wagner & S. Altuvia, (2004) The small RNA IstR inhibits synthesis of an SOS-induced toxic peptide. *Curr. Biol.* **14**: 2271-2276.

Vogel, J. & B. F. Luisi, (2011) Hfq and its constellation of RNA. *Nature reviews. Microbiology* **9**: 578-589.

Vogel, J. & E. G. Wagner, (2007) Target identification of small noncoding RNAs in bacteria. *Curr. Opin. Microbiol.* **10**: 262-270.

Wade, J. T. & D. C. Grainger, (2014) Pervasive transcription: illuminating the dark matter of bacterial transcriptomes. *Nature reviews. Microbiology* **12**: 647-653.

Wadler, C. S. & C. K. Vanderpool, (2007) A dual function for a bacterial small RNA: SgrS performs base pairing-dependent regulation and encodes a functional polypeptide. *Proc. Natl. Acad. Sci. U. S. A.* **104**: 20454-20459.

Wagner, E. G., S. Altuvia & P. Romby, (2002) Antisense RNAs in bacteria and their genetic elements. *Adv. Genet.* **46**: 361-398.

Wang, J., W. Rennie, C. Liu, C. S. Carmack, K. Prevost, M. P. Caron, E. Masse, Y. Ding & J. T. Wade, (2015) Identification of bacterial sRNA regulatory targets using ribosome profiling. *Nucleic Acids Res.* **43**: 10308-10320.

Waters, L. S. & G. Storz, (2009) Regulatory RNAs in bacteria. *Cell* **136**: 615-628.

Waters, S. A., S. P. McAteer, G. Kudla, I. Pang, N. P. Deshpande, T. G. Amos, K. W. Leong, M. R. Wilkins, R. Strugnell, D. L. Gally, D. Tollervey & J. J. Tree, (2016) Small RNA interactome of pathogenic E. coli revealed through crosslinking of RNase E. *EMBO J.*

Wattam, A. R., D. Abraham, O. Dalay, T. L. Disz, T. Driscoll, J. L. Gabbard, J. J. Gillespie, R. Gough, D. Hix, R. Kenyon, D. Machi, C. Mao, E. K. Nordberg, R. Olson, R. Overbeek, G. D. Pusch, M. Shukla, J. Schulman, R. L. Stevens, D. E. Sullivan, V. Vonstein, A. Warren, R. Will, M. J. Wilson, H. S. Yoo, C. Zhang, Y. Zhang & B. W. Sobral, (2014) PATRIC, the bacterial bioinformatics database and analysis resource. *Nucleic Acids Res.* **42**: D581-591.

Weeks, D. L., S. Eskandari, D. R. Scott & G. Sachs, (2000) A H+-gated urea channel: the link between Helicobacter pylori urease and gastric colonization. *Science* **287**: 482-485.

Wen, Y., J. Feng & G. Sachs, (2013) Helicobacter pylori 5'ureB-sRNA, a cis-encoded antisense small RNA, negatively regulates ureAB expression by transcription termination. *J. Bacteriol.* **195**: 444-452.

Wen, Y., J. Feng, D. R. Scott, E. A. Marcus & G. Sachs, (2006) Involvement of the HP0165-HP0166 two-component system in expression of some acidic-pH-upregulated genes of Helicobacter pylori. *J. Bacteriol.* **188**: 1750-1761.

Wen, Y., J. Feng, D. R. Scott, E. A. Marcus & G. Sachs, (2009) The pH-responsive regulon of HP0244 (FlgS), the cytoplasmic histidine kinase of Helicobacter pylori. *J. Bacteriol.* **191**: 449-460.

Wen, Y., J. Feng, D. R. Scott, E. A. Marcus & G. Sachs, (2011) A cis-encoded antisense small RNA regulated by the HP0165-HP0166 two-component system controls expression of ureB in Helicobacter pylori. *J. Bacteriol.* **193**: 40-51.

Willhite, D. C., T. L. Cover & S. R. Blanke, (2003) Cellular vacuolation and mitochondrial cytochrome c release are independent outcomes of Helicobacter pylori vacuolating cytotoxin activity that are each dependent on membrane channel formation. *J. Biol. Chem.* **278**: 48204-48209.

Witkowska, D., S. Bielinska, W. Kamysz & H. Kozlowski, (2011) Cu2+ and Ni2+ interactions with N-terminal fragments of Hpn and Hpn-like proteins from Helicobacter pylori: unusual impact of poly-Gln sequence on the complex stability. *J. Inorg. Biochem.* **105**: 208-214.

Witkowska, D., R. Politano, M. Rowinska-Zyrek, R. Guerrini, M. Remelli & H. Kozlowski, (2012) The coordination of NiII and Cu(II) ions to the polyhistidyl motif of Hpn protein: is it as strong as we think? *Chemistry* **18**: 11088-11099.

Wolin, S. L. & P. Walter, (1988) Ribosome pausing and stacking during translation of a eukaryotic mRNA. *EMBO J.* **7**: 3559-3569.

Wright, P. R., A. S. Richter, K. Papenfort, M. Mann, J. Vogel, W. R. Hess, R. Backofen & J. Georg, (2013) Comparative genomics boosts target prediction for bacterial small RNAs. *Proc. Natl. Acad. Sci. U. S. A.* **110**: E3487-3496.

Wroblewski, L. E., R. M. Peek, Jr. & K. T. Wilson, (2010) Helicobacter pylori and gastric cancer: factors that modulate disease risk. *Clin. Microbiol. Rev.* **23**: 713-739.

Xiao, B., W. Li, G. Guo, B. Li, Z. Liu, K. Jia, Y. Guo, X. Mao & Q. Zou, (2009a) Identification of small noncoding RNAs in Helicobacter pylori by a bioinformatics-based approach. *Curr. Microbiol.* **58**: 258-263.

Xiao, B., W. Li, G. Guo, B. S. Li, Z. Liu, B. Tang, X. H. Mao & Q. M. Zou, (2009b) Screening and identification of natural antisense transcripts in Helicobacter pylori by a novel approach based on RNase I protection assay. *Mol. Biol. Rep.* **36**: 1853-1858.

Zeng, Y. B., N. Yang & H. Sun, (2011) Metal-binding properties of an Hpn-like histidine-rich protein. *Chemistry* **17**: 5852-5860.

Zeng, Y. B., D. M. Zhang, H. Li & H. Sun, (2008) Binding of Ni2+ to a histidine- and glutamine-rich protein, Hpn-like. *J. Biol. Inorg. Chem.* **13**: 1121-1131.

Zhou, Q., S. Qi, X. Sun & R. Ge, (2014) The interaction of a histidine-rich protein hpn with the membrane mimics: implications for pathologic roles of Hpn in Helicobacter pylori. *Helicobacter* **19**: 129-135.

Zuker, M., (2003) Mfold web server for nucleic acid folding and hybridization prediction. *Nucleic Acids Res.* **31**: 3406-3415.

7 Appendix

```
sRNA                1      GGCUCCUUGAAUUGAAAUU   19
                           |:|||||| ||||||||||
mRNA (HP1432)       -4     CUGAGGAAAUUAACUUUAA  -22

sRNA                4      UCCUUGAAU-UGAAAUU     19
                           ||||||||| |||||||
mRNA (HP1091)       -6     AGGAACUUAUACUUUAA    -22

sRNA                3      CUCCUUGAAUUGAAAUU     19
                           |||||| ||||:|||||
mRNA (HP0891)       -6     GAGGAA-UUAAUUUUAA    -21

sRNA                2      GCUCCUUGAAUUGAAAUU    19
                           ||||||||| || | |||
mRNA (HP1193)       -5     CGAGGAACUAAAGUAUAA   -22

sRNA                1      GGCUCCUUGAAUUG-AAAUU  19
                           ||||||||:||||  |||||
mRNA (HP0139)       -5     CCGAGGAAUUUAAGGUUUAA -24

sRNA                3      CUCCUUGAA-UUGAAAU     18
                           ||||||||| ||:||||
mRNA (HP0896)       -6     GAGGAACUUUAAUUUUA    -22

sRNA                3      CUCCUU-GAAUUGAAAU     18
                           |||||| :||||:||||
mRNA (HP1268)       -6     GAGGAAAUUUAAUUUUA    -22

sRNA                4      UCCUUGAAUUGA       15
                           ||||||| |:||
mRNA (HP1413)       -6     AGGAACUAAAUU      -20

sRNA                1      GGCUCCUUGA--AUUGAAAUU  19
                           ||   |||||    :||||||
mRNA (HP1086)       -14    CCCCUGAACUAUUCGCUUUAA -35

sRNA                5      CCUUGAAUUGAAA      17
                           ||:|:||||:|||
mRNA (HP0052)       -1     GGGAUUUAAUUUU     -13

sRNA                1      GGCUCCUUGAAUUGAA     16
                           |:|||||||| |||:||
mRNA (HP0695)       -4     CUGAGGAACAUAAUUU    -19
```

```
sRNA                3      CUCCUUGAAUUGAAAUU    19
                           |||||||||:|  ||||
mRNA (HP0953)       -8     GAGGAACUUGAAAUUAA   -24

sRNA                4      UCCUUGAATTGAAAUU    18
                           |||||   ||:|||||
mRNA (HP0243)       -10    AGGAAAAAAAUUUUAA   -22

sRNA                3      CUCCUUGAAUUGAA      16
                           |||||||||||  ||
mRNA (HP0920)       -7     GAGGAACUUAAGUU     -20

sRNA                4      UCCUUGAAUUGAA       16
                           ||||||||||:||
mRNA (HP0926)       -8     AGGAACUUAAUUU      -20

sRNA                3      CUCCUUGAAUUGA       15
                           ||||:|:||||||
mRNA (HP0993)       -8     GAGGGAUUUAACU      -20

sRNA                6      CUUGAA              11
                           ||::||
mRNA (HP0838)       -36    GAGUUU             -41

sRNA                9      GAAUUGAAAU          18
                           :||:||||||
mRNA (HP0263)       +20    UUUGACUUUA         +10

sRNA                3      CUCCUUGAAUUGAAAU    18
                           |||||  |||||||||
mRNA (HP0217)       -6     GAGGA--UUAACUUUA   -19

sRNA                4      UCCUUGAAUUG         14
                           |||||: |||:
mRNA (HP0371)       -11    AGGAAUAUAAU        -21

sRNA                4      UCCUU--GAAUUGAAAU   18
                           |||||  :|||||||||
mRNA (HP0546)       -6     AGGAAAGUUUAACUUUA  -22
```

Supplementary Figure S1. The predicted interaction between ArsZ and its mRNA targets. The single stranded region of ArsZ was used for target prediction. Region between 50 nt upstream (-50) and 20 nt downstream (+20) of

target mRNA translation start site were used for prediction and a p-value threshold of < 0.01. The Shine-Dalgarno sequences are underlined. The details of the targets are listed in Table 1.

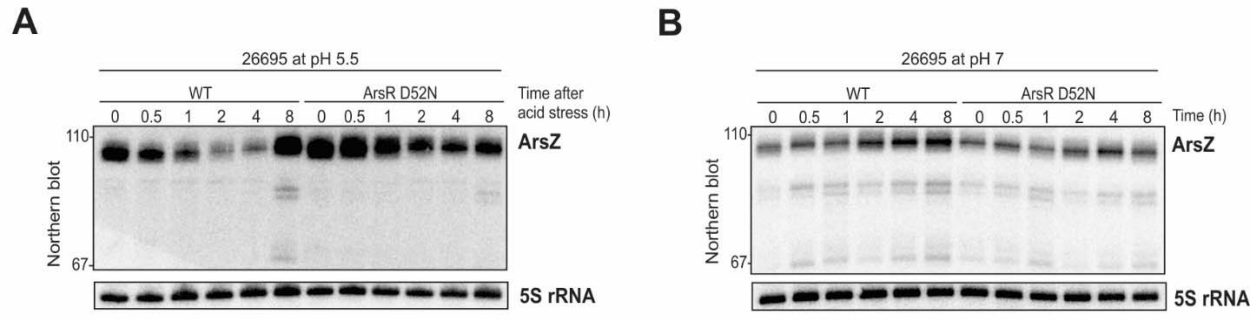

Supplementary Figure S2. ArsZ is regulated in response to low pH. ArsZ expression was compared in an ArsR D52N mutant (unable to be phosphorylated), to the wild-type strain following acid stress at pH 5.5 (A) or maintained pH 7 as control (B). Total RNA was probed for ArsZ on a Northern blot and quantified as fold-change relative to WT (Figure 2.6). Levels of 5S rRNA served as a loading control.

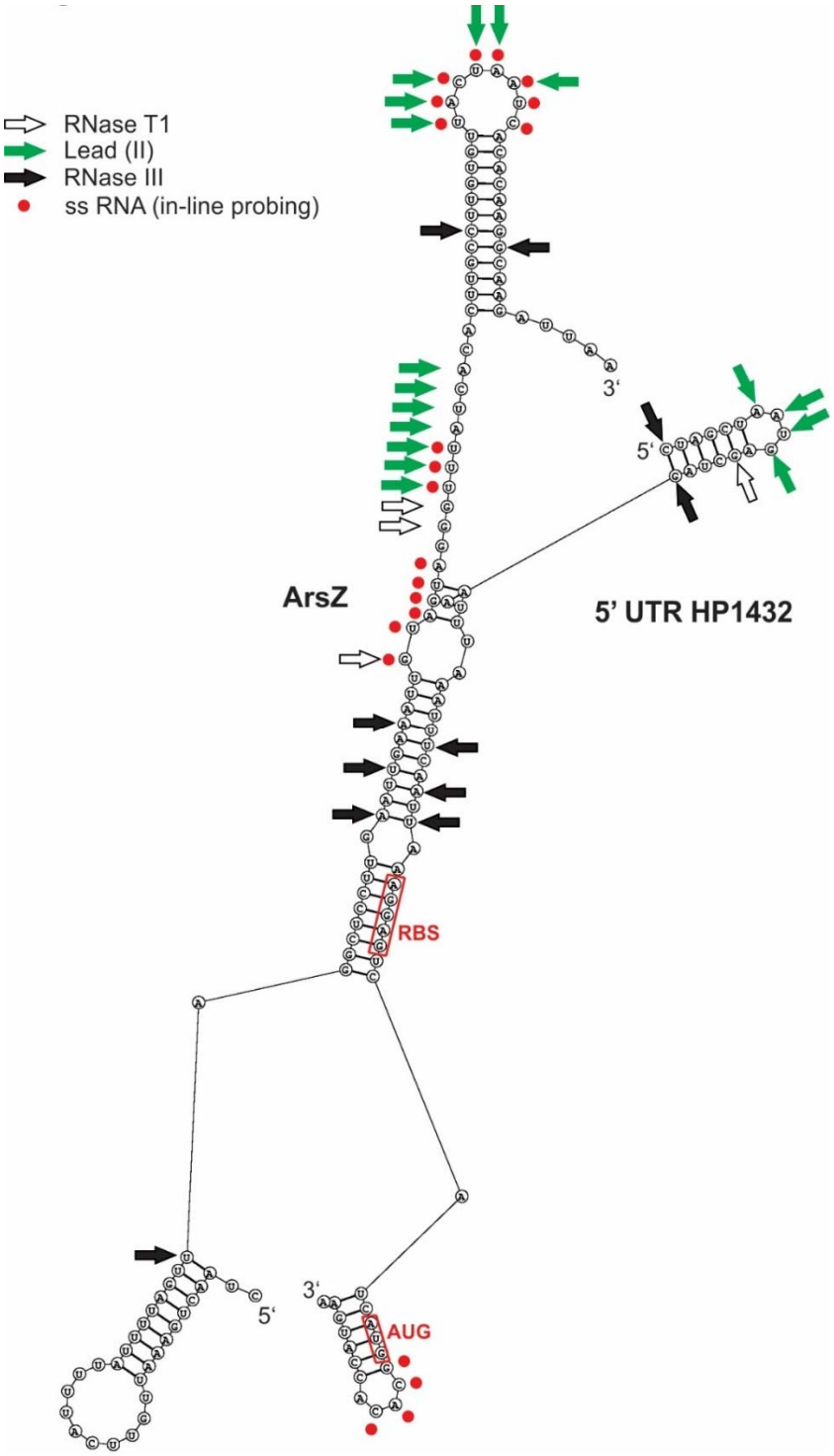

Supplementary Figure S3. **Predicted intermolecular RNA-RNA interaction between ArsZ and 5' UTR of HP1432** including first 5 amino acids using RNAStructure tool (Reuter & Mathews, 2010). The ribosomal binding site (RBS) and start codon are indicated in red boxes. White arrows indicate RNase T1 cleavage sites, green arrows indicate lead (II) cleavage sites, black arrows mark RNase III cleavage sites from structure probing assay (Figure 2.10 B, E). Red circles mark RNA cleavage sites from in-line probing (Figure 2.10 A, D).

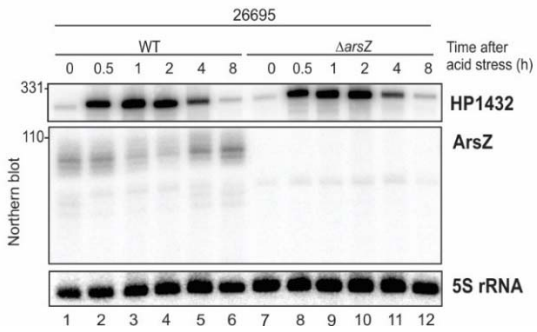

Supplementary Figure S4. ArsZ forms a coherent feed-forward loop. ArsZ expression was compared in an Δ*arsZ* mutant, to the wild-type strain following acid stress at pH 5.5. Total RNA was probed for ArsZ and HP1432 mRNA on a Northern blot and quantified as fold-change relative to WT (Figure 2.16 A). Levels of 5S rRNA served as a loading control.

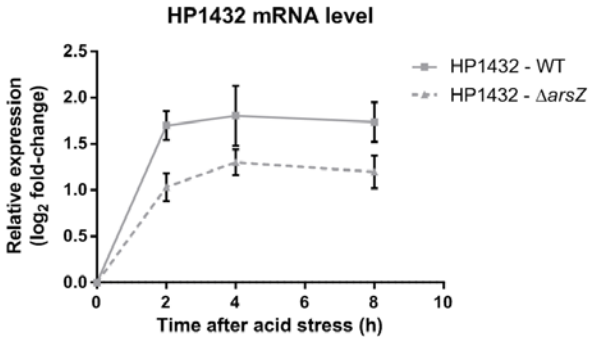

Supplementary Figure S5. Acid stress after acid adaptation. Levels of HP1432 in WT and Δ*arsZ* were measured in total RNA following shift of log-phase bacteria to acidic medium by Northern blotting. All strains were grown to an OD_{600} of 0.4 at pH 5.5. The acid adapted strains were transferred to fresh medium (pH 5.5), and HP1432 mRNA levels from various time points following the shift were quantified on a Northern blot. The fold-change was quantified as $\log_2$ ratio of a specific time point relative to the 0 hour time-point. The data are average of two independent experiments, with error bars representing standard errors

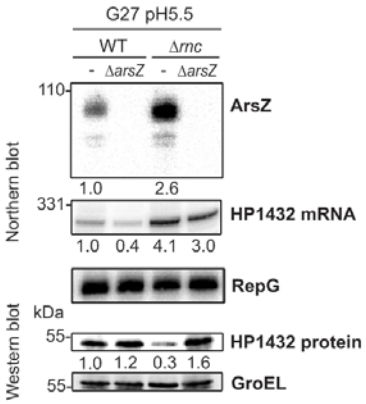

Supplementary Figure S6. The role RNase III in ArsZ-HP1432 interaction *in vivo*. The expression of ArsZ, HP1432, and RepG were quantified on a Northern blot. Levels of 5S rRNA served as a loading control. Anti-poly-Histidine antibody was used to monitor HP1432 protein levels, while GroEL served as a loading control.

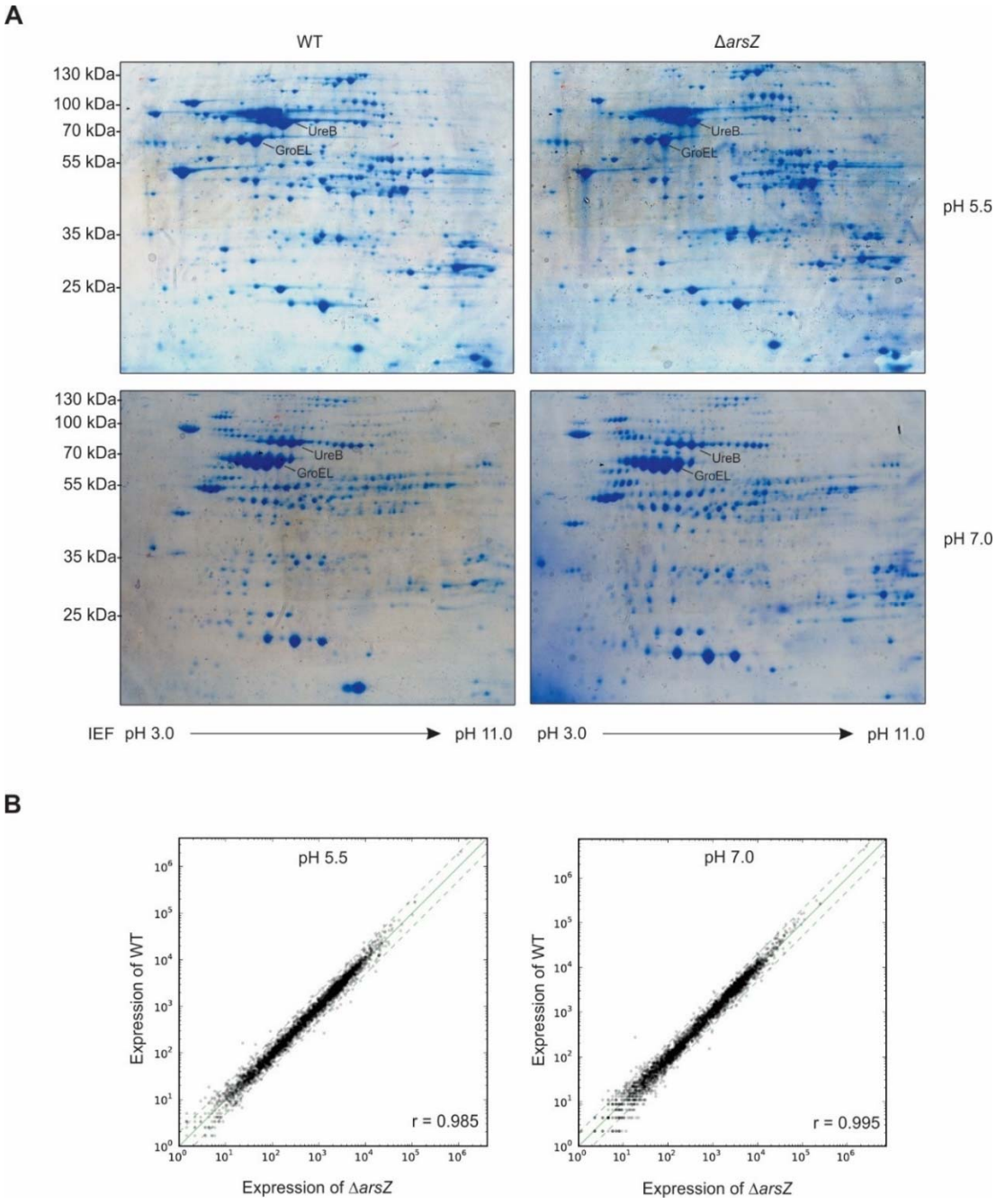

Supplementary Figure S7. Global proteomic and transcriptomic analysis of WT and Δ*arsZ* strains for target identification. WT and Δ*arsZ* strains (26695 background) were grown to an OD_{600} of 0.5-0.7 at pH 5.5 or pH 7. (A) Soluble protein fractions of these samples were resolved on two-dimensional gels. Labelled proteins were identified by comparison of the migration pattern of the gel to previously published work (Jungblut *et al.*, 2000). Since samples were resolved on separate gels, GroEL served as an internal standard. The gels are representative of three independent experiments. No protein spots that were consistently regulated in all three experiments were observed. (B) Total RNA was extracted and subjected to RNA-seq analysis. The correlation coefficient (r) between expression of all genes in WT versus Δ*arsZ* is indicated on the graph.

Supplementary Table S1. The list of bacterial strains used in this study.

Name	Genotype / Description	Strain number	*H. pylori*	Resistance
WT / 26695	Wild-type, kindly provided by D. Scott Merrell.	CSS-0065	26695	-
Δ*arsZ*	*arsZ*::*erm*	CSS-0107	26695	Erm^R
C_{ArsZ}	*arsZ*::*erm, rdxA::arsZ::catGC*	CSS-2168	26695	Erm^R Cm^R
OE-ArsZ	*rdxA::arsZ::catGC*	CSS-2169	26695	Cm^R
ΔHP1432	HP1432::*aphA-3*	CSS-0691	26695	Kan^R
ΔHP1432 Δ*arsZ*	HP1432::*aphA-3*, *arsZ*::*erm*	CSS-3327	26695	Kan^R Erm^R
rpsL	*rpsL* (K43R and K88R), recessive streptomicyn resistance allele.	CSS-0024	26695	Str^R
P_{repG} ArsZ Δ*arsZ*	*rdxA*::P_{repG}-*arsZ::catGC*, *arsZ*::*erm*	CSS-0453	26695	Erm^R Cm^R
P_{repG} RepG-SL1::ArsZ Δ*arsZ*	*rdxA*::P_{repG}-*repG-SL1*::*arsZ::catGC*, *arsZ*::*erm*	CSS-4039	26695	Erm^R Cm^R
WT / G27	Wild-type, kindly provided by D. Scott Merrell.	CSS-0066	G27	-
Δ*arsZ*	*arsZ*::*erm*	CSS-0292	G27	Erm^R
C_{ArsZ}	*arsZ*::*erm, rdxA::arsZ::catGC*	CSS-0816	G27	Erm^R Cm^R
OE-ArsZ	*rdxA::arsZ::catGC*	CSS-0818	G27	Cm^R
P_{ureA} ArsZ	*rdxA*::P_{ureA}-*arsZ::catGC*, *arsZ*::*erm*	CSS-2273	G27	Erm^R Cm^R
P_{tlpB} 1432::*gfp*	HP1432::P_{tlpB}-HP1432*::5'UTR::gfpmut3::genta*	CSS-3335	G27	$Genta^R$
P_{tlpB} 1432::*gfp* Δ*arsZ*	HP1432::P_{tlpB}-HP1432*::5'UTR::gfpmut3::genta, arsZ*::*erm*	CSS-3337	G27	$Genta^R$ Erm^R
P_{tlpB} 1432::*gfp* Δ*arsZ* ArsZ M3	HP1432::P_{tlpB}-HP1432*::5'UTR::gfpmut3::genta, arsZ*::*erm, rdxA::arsZ M3::catGC*	CSS-3339	G27	$Genta^R$ Erm^R Cm^R
P_{tlpB} 1432 M3::*gfp*	HP1432::P_{tlpB}-HP1432*::M3 5'UTR::gfpmut3::genta*	CSS-3341	G27	$Genta^R$
P_{tlpB} 1432 M3::*gfp* Δ*arsZ*	HP1432::P_{tlpB}-HP1432*::M3 5'UTR::gfpmut3::genta, arsZ*::*erm*	CSS-3343	G27	$Genta^R$ Erm^R
P_{tlpB} 1432 M3::*gfp* Δ*arsZ* ArsZ M3	HP1432::P_{tlpB}-HP1432*::M3 5'UTR::gfpmut3::genta, arsZ*::*erm, rdxA::arsZ M3::catGC*	CSS-3345	G27	$Genta^R$ Erm^R Cm^R
P_{HP1432} *ureA*-5'UTR::*gfp*	*rdxA*::P_{HP1432} *ureA-5'UTR::gfpmut3*::*catGC*	CSS-4005	G27	Cm^R
P_{HP1432} *ureA*-5'UTR::*gfp* Δ*arsZ*	*rdxA*::P_{HP1432} *ureA-5'UTR::gfpmut3*::*catGC, arsZ*::*erm*	CSS-4007	G27	Cm^R Erm^R
P_{HP1432} HP1432-5'UTR::*gfp*	*rdxA*::P_{HP1432}-HP1432*::5'UTR::gfpmut3*::*catGC*	CSS-0713	G27	Cm^R
P_{HP1432} HP1432-5'UTR::*gfp* Δ*arsZ*	*rdxA*::P_{HP1432}-HP1432::*5'UTR::gfpmut3*::*catGC, arsZ*::*erm*	CSS-0723	G27	Cm^R Erm^R
WT / G27*	Wild-type, kindly provided by Dagmar Beier.	CSS-0050	G27*	-

Δ*arsS*	*arsS*::*aphA-3, (Dietz et al., 2002)*	CSS-0051	G27*	Kan^R
P_{arsZ} *ureA*-5'UTR::*gfp*	*rdxA*::P_{arsZ} *ureA-5'UTR-gfpmut3*::*catGC*	CSS-4009	G27*	Cm^R
P_{arsZ} *ureA*-5'UTR::*gfp* Δ*arsS*	*rdxA*::P_{arsZ} *ureA-5'UTR-gfpmut3*::*catGC, arsS*::*aphA-3*	CSS-4011	G27*	Kan^R Cm^R
P_{tlpB} *ureA*-5'UTR::*gfp*	*rdxA*::P_{tlpB} *ureA-5'UTR-gfpmut3*::*catGC*	CSS-4013	G27*	Cm^R
P_{tlpB} *ureA*-5'UTR::*gfp* Δ*arsS*	*rdxA*::P_{tlpB} *ureA-5'UTR-gfpmut3*::*catGC, arsS*::*aphA-3*	CSS-4015	G27*	Kan^R Cm^R
P_{ureA} *ureA*-5'UTR::*gfp*	*rdxA*::P_{ureA} *ureA-5'UTR-gfpmut3*::*catGC*	CSS-4001	G27*	Cm^R
P_{ureA} *ureA*-5'UTR::*gfp* Δ*arsS*	*rdxA*::P_{ureA} *ureA-5'UTR-gfpmut3*::*catGC, arsS*::*aphA-3*	CSS-4003	G27*	Kan^R Cm^R
WT / 26695*	Wild-type, kindly provided by Dagmar Beier.	CSS-0038	26695*	-
Δ*arsS*	*arsS*::*aphA-3*, (Beier & Frank, 2000)	CSS-0042	26695*	Kan^R
Δ*flgS*	*flgS* (HP0244)*::aphA-3;* kindly provided by Dagmar Beier.	CSS-0041	26695*	Kan^R
ArsR D52N	*arsR*::*aphA-3*, *cag_PAI*::P_{arsR} *arsRD52N*::*catGC,(Schar et al., 2005)*	CSS-0105	26695*	Kan^R Cm^R
WT/ B8	Wild-type, kindly provided by Rainer Haas.	CSS-0213	B8	-
C_{ArsZ}	*arsZ*::*erm, rdxA::arsZ::catGC*	CSS-4446	B8	Cm^R
WT / India7	Wild-type, kindly provided by Steffen Backert.	CSS-0099	India7	-
WT / P12	Wild-type, kindly provided by Thomas Meyer	CSS-0013	P12	-
WT / Shi470	Wild-type, kindly provided by Steffen Backert.	CSS-0173	Shi470	-
WT / J99	Wild-type, kindly provided by Thomas Meyer	CSS-0011	J99	-
WT / HPAG1	Wild-type, kindly provided by Steffen Backert	CSS-0102	HPAG1	-
WT / *H. acinonychis*	Wild-type, kindly provided by Thomas Meyer	CSS-0018	*H. acinonychis*	-
TOP10	*mcrA* Δ*(mrr-hsdRMS-mcrBC)* Φ80*lacZ* ΔM15 Δ*lacX74 deoR recA1 araD139* Δ*(ara-leu)*7697 *galU galK rpsL endA1 nupG* from Invitrogen	CSS-0296	*E. coli*	-
ArsR::Strep-tag	*arsR::Strep-tag*	CSS-2172	*E. coli*	Amp^R
pHP1432		CSS-2189	*E. coli*	Cm^R
pHP1432, pBAD-ArsZ		CSS-4448	*E. coli*	Amp^R

Supplementary Table S2. The list of plasmids used in this study.

Name	Description	Origin	Reference
pPT3-1	Backbone plasmid for amplification of transcriptional fusion of 5'UTR *ureA* to *gfpmut3* in *rdxA* locus.	p15A/ Amp^R	(Pernitzsch *et al* ., 2014)
pPT7-1	Plasmid for introducing ArsZ under promoter of RepG	p15A/ Amp^R	This study
pPT20-1	Plasmid for complementation of *arsZ* deletion with ArsZ in *H. pylori* 26695 in *rdxA* locus.	p15A/ Amp^R	This study
pPT22-1	Plasmid for introducing translational fusion of HP1432 promoter to *gfpmut3* in *rdxA* locus.	p15A/ Amp^R	This study
pPT28-1	Backbone plasmid carrying 500 up- and downstream flanking region of HP1432 for introduction of promoter exchange and translational fusions in native HP1432 locus.	p15A/ Amp^R	This study
pPT32-1	Plasmid for complementation of *arsZ* deletion with ArsZ in *H. pylori* G27 in *rdxA* locus.	p15A/ Amp^R	This study
pPT33-1	Plasmid for expressing C-terminal Strep-tagged ArsR (HP0166)	p15A/ Amp^R	This study
pPT34-1	Plasmid for complementation of HP1432 deletion with HP1432 in *H. pylori* 26695 in *rdxA* locus. Backbone plasmid for nucleotide exchange in 5'UTR of HP1432.	p15A/ Amp^R	This study
pPT42-1	Plasmid for expressing HP1432 under the control of P_{LtetO} promoter in *E. coli*.	pSC101 Cm^R	This study
pPT65-1	Plasmid for transcriptional fusion of *ureA* promoter to *gfpmut3* in *rdxA* locus.	p15A/ Amp^R	This study
pPT66-1	Plasmid for expressing ArsZ under the promoter of *ureA*.	p15A/ Amp^R	This study
pPT79-1	Plasmid for DNase I footprinting on promoter of HP1432.	p15A/ Amp^R	This study
pPT86-1	Intermediate plasmid carrying translational fusion of HP1432 to *gfpmut3* under the control of *tlpB* promoter in *rdxA* locus. Contains the *catGC* cassette.	p15A/ Amp^R	This study
pPT105-1	Intermediate plasmid carrying translational fusion of HP1432 to *gfpmut3* under the control of *tlpB* promoter in *rdxA* locus. Contains the gentamicin cassette.	p15A/ Amp^R	This study

pPT106-1	Plasmid for overexpression of *arsZ* under P_{BAD} promoter in *E. coli*.	p15A/ Amp^R	This study
pPT108-1	Plasmid for complementation of *arsZ* deletion with nucleotide exchange in ArsZ (ArsZ M3) in *H. pylori* G27 in *rdxA* locus.	p15A/ Amp^R	This study
pPT119-1	Plasmid for DNase I footprinting on promoter of *arsZ*.	p15A/ Amp^R	This study
pPT138-1	Plasmid for complementation of *arsZ* deletion with nucleotide exchange in ArsZ (ArsZ M3) in *H. pylori* 26695 in *rdxA* locus.	p15A/ Amp^R	This study
pPT142-1	Plasmid for introducing translational fusion of HP1432 to *gfpmut3* under the control of *tlpB* promoter in HP1432 locus.	p15A/ Amp^R	This study
pPT147-1	Plasmid for introducing translational fusion of base-pair exchange in 5'UTR of HP1432 (HP1432 M3) to *gfpmut3* under the control of *tlpB* promoter in HP1432 locus.	p15A/ Amp^R	This study
pPT150-1	Plasmid for introducing transcriptional fusion of *arsZ* promoter to *gfpmut3* in *rdxA* locus.	p15A/ Amp^R	This study
pPT151-1	Plasmid for introducing transcriptional fusion of HP1432 promoter to *gfpmut3* in *rdxA* locus.	p15A/ Amp^R	This study
pPT152-1	Plasmid for introducing transcriptional fusion of *tlpB* promoter to *gfpmut3* in *rdxA* locus.	p15A/ Amp^R	This study
pPT153-1	Plasmid for complementation of HP1432 deletion with nucleotide exchange in 5'UTR of HP1432 (HP1432 M3) in *H. pylori* 26695 in *rdxA* locus.	p15A/ Amp^R	This study
pPT156-1	Plasmid for introducing RepG-SL1::ArsZ chimera under the promoter of *repG* in the *rdxA* locus.	p15A/ Amp^R	This study
pBA4-2	Backbone plasmid for introducing HP1432::*gfpmut3* fusion under the control of *tlpB* promoter to gentamicin resistance cassette.	p15A/ Amp^R	(Pernitzsch *et al* ., 2014)
pGD72-3	Backbone plasmid for introducing arsR under the control of PBAD promoter. Contains Strep-tag.		(Dugar *et al.*, 2016)
pSP39-3	Backbone plasmid for introducing ArsZ complementation from *H. pylori* 26695 and G27 in *rdxA* locus.	p15A/ Amp^R	(Pernitzsch *et al* ., 2014)
pSP109-6	Backbone plasmid for introducing translational fusion of HP1432-5'UTR to *gfpmut3* into *rdxA* locus.	p15A/ Amp^R	(Pernitzsch *et al* ., 2014)

pXG-10-sfGFP	Backbone plasmid for introducing HP1432 under the control of P_{LtetO} promoter.	pSC101 Cm^R	(Corcoran *et al*., 2012)

Supplementary Table S3. The list of oligodeoxynucleotides used in this study.

Name	**Sequence (5' → 3')**	**Description**
CSO-0003	GAAAGGAGGGGGAGGT	Northern blot probe for RepG
CSO-0017	GTTTTTTCTAGAGATCAGCCTGCCTTTAGG	Cloning of *arsZ* complementation
CSO-0018	GTTTTTCTCGAGCTTAGCGCTTAATGAAACGC	Cloning of *arsZ* complementation
CSO-0023	CCACCAGCTTATATACCTTAGCA	Verification of HP1432 deletion
CSO-0052	CCTACTACAATTTCAATTCAAGGAGCCTAA	Northern blot probe for ArsZ
CSO-0060	CCAACCAAACCATAAGGAATG	Cloning of *arsZ* under *repG* promoter
CSO-0094	CACCACTTATTCATGCTAAAACAAT	Verification of *arsZ* deletion
CSO-0101	AAACACCCCCATAAGTGCAATTATGGGGATAAATTACTTATTAAATAATTTATAGCTATTGAAAAGA	Cloning of *erm* cassette
CSO-0110	GATTTCATTTTATAATGCAAAATCTAACCAATTA	Cloning of HP1432 promoter to GFP fusion
CSO-0146	GTTTTTATCGATGTATGCTCTTTAAGACCCAGC	Cloning of *arsZ* complementation
CSO-0147	GTTTTTCATATGCTCGAATTCAGATCCACGTT	Cloning of *arsZ* complementation
CSO-0155	ACCGTAGTAATGGTGGTGGT	*In vitro* transcription of HP1432 5'UTR
CSO-0160	AATTATACTAATTTTATAAGGAGGGAAA	Cloning of *erm* cassette
CSO-0161	CTCCTTATAAAATTAGTATAATTTAGGGCTTTATTATAGCAAAAATTATC	Deletion of *arsZ* in *H. pylori* 26695 / G27
CSO-0163	GTTTTTATCGATACTTTAATTGTACATTTATGATAGTTAAGA	Deletion of *arsZ* in *H. pylori* 26695 / G27
CSO-0205	AATTACAACAGTACTGCGATGAGT	Verification of *arsZ* complementation

CSO-0207	AGTTCTGATTTCATGCCCTT	Verification of *arsZ* complementation
CSO-0232	P~CTAACTAAAATTTCTCCTTTTATTTTAGTT	Cloning of *arsZ* under *repG* promoter
CSO-0309	GTTTTTGAATTCTTACTTATTAAATAATTTATAGCTATTGAAAAGA	Verification of *arsZ* deletion
CSO-0313	GTTTTTGGATCCTAGAGATCCGCCATATTGTGT	Cloning of *tlpB*::*gfpmut3* fusion
CSO-0343	TGGTAAGGACTACTAAAATCTTTGG	Deletion of *arsZ* in *H. pylori* G27
CSO-0344	GGATTATGATGCTCAATCAATTG	Deletion of *arsZ* in *H. pylori* G27
CSO-0411	GTTTTTATCGATACTTTAATCATGCGTCTATGATA	Cloning of arsZ promoter-gfpmut3 fusion
CSO-0441	GTTTTTTGCGGCCGCGGGAGTTAACTGCAGGTCTG	*In vitro* transcription of HP1432::*gfp* and *tlpB*::*gfp*
CSO-0443	GTTTTTGCGGCCGCCTCGAATTCAGATCCACGTT	Cloning of *tlpB* GFP fusion
CSO-0470	GTTTTTTCTAGATTTTAAGACAAATAATCAAAAAGCTA	Deletion of HP1432
CSO-0476	P~CTAACTGAAATTGTTCATTTTATTTTAG	Cloning of *arsZ* under *repG* promoter
CSO-0477	P~CTAACTAAAATTTCTCCTTTTATTTTAGTT	Cloning of *arsZ* under *ureA* promoter
CSO-0479	GTTTTTCATATGATACTTTAATTGTACATTTATGATAGTTAAGA	Cloning of *arsZ* complementation
CSO-0480	GTTTTTATCGATATTGCTAACGATTAAGCTGTATT	Cloning of *arsZ* under *repG* promoter
CSO-0581	GTTTTTATCGATTTATTATTTTATCTTTAAGCCTAACTTAA	Cloning of *tlp*::GFP fusion
CSO-0585	GTTTTTTGCTAGCAACAAGCTGAAATTATAGAACACCC	Cloning of *tlp*::GFP fusion
CSO-0594	GTTTTTGCTAGCTGGGGTGAGTTTCATCTCA	Cloning of *ureA* promoter to GFP fusion
CSO-0668	TGAGCTTGTTGCTCTGCTTGT	Northern blot probe for HP1432
CSO-0675	CCTGGTAGCGATATAATAAGGC	Deletion of HP1432

CSO-0676	CTCCTAGTTAGTCACCCGGGTACGT GTGCCATGATGACTCCTT	Deletion of HP1432
CSO-0677	TGTTTTAGTACCTGGAGGGAATACA ATATTGATTGGGGCGTTT	Deletion of HP1432
CSO-0683	GTTTTTTGCTAGCAGTAAAGGAGAA GAACTTTTCACTGGA	Cloning of HP1432 translational GFP fusion
CSO-0687	GTTTTTATCGATATGTTTTAATTCTT TTTGTATAAATAATTC	Cloning of *arsZ* complementation
CSO-0732	GTTTTTGCTAGCGGGCTTTATTATA GCAAAAATTATC	Cloning of *arsZ* promoter-GFP fusion
CSO-0734	ACTTCCTTTTGCGTCATCA	Verification of HP1432 deletion
CSO-0736	GTTTTTATCGATTCTTTCCTTTTTAA TGCAACTTCT	Cloning of HP1432 transcriptional and translational GFP fusion
CSO-0737	GTTTTTGCTAGCTTGTTGCTGTTGTT GTTCATG	Cloning of HP1432 translational GFP fusion
CSO-0738	GTTTTTTGCTAGCACTAGCTAGGAT TTCATTTTATAATGC	Cloning of HP1432 transcriptional GFP fusion
CSO-0790	GTTTTTTCTAGACGTTTAAAACAAG CCTGGT	Cloning of *tlpB*::GFP fusion
CSO-0792	GTTTTTGGATCCTGATTGGGGCGTT TGT	Cloning of *tlpB*::GFP fusion
CSO-0793	GTTTTTCTCGAGAGATCTCGCCAAA GAAATACA	Cloning of *tlpB*::GFP fusion
CSO-1055	GTTTTTCTCGAGGGAGAAACAGTAG AGAGTTGC	Cloning of *arsR*::strep-tag
CSO-1056	AGCGCGTGGAGCCACCCGCAGTT	Cloning of *arsR*::strep-tag
CSO-1057	P-GTATTCTAATTTATAACCAATCCCT	Cloning of *arsR*::strep-tag
CSO-1058	GTTTTTCTCGAGCTAAAACATTAAC AAAGTTAATCGTT	Cloning of *arsR*::strep-tag
CSO-1110	GTTTTTCATATGACGGAGTTAAAAA AGTTAGTTTAAAT	Cloning of HP1432 complementation
CSO-1220	TTAATCTTGCCTTGTGTGATTAGT	*In vitro* transcription of ArsZ

CSO-1252	GTTTTTTTTAATACGACTCACTATAGGCTAGCTAATGAGCTAGAATTTAAA	*In vitro* transcription of HP1432 5'UTR
CSO-1255	GTTTTTGCGGCCGCTTATTTGTATAGTTCATCCATGCC	Cloning of *tlpB* GFP fusion
CSO-1257	P~CTAGCTAATGAGCTAGAATTTAAA	Cloning of *tlpB* GFP fusion
CSO-1266	GTTTTTATCGATCTCGAATTCAGATCCACGTTG	Cloning of *arsZ* under *ureA* promoter
CSO-1298	GTTTTTTCTAGAATGTTTTAATTCTTTTTGTATAAATAATTC	Cloning of *arsZ* under P_{BAD} promoter
CSO-1299	GTTTTTTCTAGATTAAAAGCTAGGAGTAGCCCT	Cloning of HP1432 under P_{LtetO} promoter
CSO-1397	GTTTTTGGATCCTCTTTCCTTTTTAATGCAACTTCT	Cloning of HP1432 for DNase I footprint
CSO-1772	AGCTGAAATTATAGAACACCCTT	Cloning of *tlpB* GFP fusion
CSO-1781	GATGTAATTGTAGCAATGTTTTGATT	Cloning of *arsZ* under *ureA* promoter
CSO-1810	GTTTTTGGATCCGTATGCTCTTTAAGACCCAGC	Cloning of genes for DNase I footprint
CSO-1878	GTTTTTGGATCCTTTATATCCTTTTGTTTTAAAATTTTT	Cloning of *arsZ* for DNase I footprint
CSO-1879	GTTTTTGCGGCCGCATGTTTTAATTCTTTTTGTATAAATAATTC	Cloning of *arsZ* for DNase I footprint
CSO-1880	GTTTTTGCGGCCGCTTGTTGCTGTTGTTGTTCATG	Cloning of HP1432 for DNase I footprint
CSO-2878	TAGAATTTAAATAAGAATTAAAGGAGTCATCATGGCTA	Site-directed mutagenesis of HP1432 5'UTR
CSO-2879	ACTCCTTTAATTCTTATTTAAATTCTAGCTCACTAGCTA	Site-directed mutagenesis of HP1432 5'UTR
CSO-2880	GCTCCTTGAATTCTTATTGTAGTAGGGTTTACCACAC	Site-directed mutagenesis of *arsZ*
CSO-2881	CCCTACTACAATAAGAATTCAAGGAGCCTAACTAAAATAA	Site-directed mutagenesis of *arsZ*
CSO-2901	GTTTTTATCGATAACATCTTTGAATGAAAAAAGCTATA	Cloning of *tlpB*::GFP fusion

CSO-2904	GTTTTTTTTAATACGACTCACTATAGGCTAACTGAAATTGTTCATTTTATTTTAG	*In vitro* transcription of ArsZ M3
CSO-2957	AATTCAAGGAGCCTAACTAAAATAAA	Northern blot probe for ArsZ upstream of base-pair exchange (ArsZ*)
CSO-3316	CAACCTTGATTTCGTTATGTCT	Cloning of 5'UTR of *ureA* GFP fusion
CSO-3317	P~GGGCTTTATTATAGCAAAAATTAT	Cloning of ArsZ promoter to GFP fusion
CSO-3320	GCTCCTTGAATTGAAATTGTAGT	Cloning of *arsZ* under *repG* promoter
HPK1	GTACCCGGGTGACTAACTAGG	Amplification of *aphA-3* cassette
HPK2	TATTCCCTCCAGGTACTAAAACA	Amplification of *aphA-3* cassette
JVO-0485	TCGGAATGGTTAACTGGGTAGTTCCT	Northern blot probe for 5S rRNA
JVO-0900	GGAGAAACAGTAGAGAGTTGC	Cloning of *arsZ* under P_{BAD} promoter
JVO-0901	TTTTTTCTAGATTAAATCAGAACGCAGA	Cloning of *arsZ* under P_{BAD} promoter
JVO-5125	GTTTTTTTTAATACGACTCACTATAGGATCCAACCATTCCTTATGGTT	*In vitro* transcription RepG
JVO-5126	AAAACAACCGCCAAGACA	*In vitro* transcription RepG
JVO-5127	GTTTTTTTTAATACGACTCACTATAGGTGTTTGTTCTTTTGTTTCGTT	*In vitro* transcription *tlpB*::*gfp*
JVO-5183	GGATTATGATGCTCAACCAATTA	Deletion of *arsZ* in *H. pylori* 26695
JVO-5198	TGGTAAGGGCTATCAAAGTCTT	Deletion of *arsZ* in *H. pylori* 26695
pBADfw	ATGCCATAGCATTTTTATCC	Cloning of *arsZ* under P_{BAD} promoter
pZE-A	GTGCCACCTGACGTCTAAGA	Colony PCR on pZE12-derived plasmids
pZE-STOP-XbaI	TAATCTAGAGGCATCAAATAAAACGA	Cloning of HP1432 under P_{LtetO} promoter
pZE-tetO	GTGCTCAGTATCTCTATCACTGA	Cloning of HP1432 under P_{LtetO} promoter

Supplementary Table S4. The sequences of T7 transcripts used for *in vitro* work. Compensatory base-pair exchanges are marked in red while the ribosome binding site and start codon are in bold. The *gfpmut3* gene is marked in green.

Name	**DNA template**	**Oligo-nucleotides**	**Size of T7 transcript (nt)**	**Sequence (5' → 3')**
ArsZ	CSS-0065	CSO-2904 CSO-1220	105	**C**UAACUGAAAUUGUUCAUUUUAUUUU AGUUAGGCUCCUUGAAUUGAAAUUGU AGUAGGGUUUAUCACACUUGCCUUGU GUUACUAAUCACACAAGGCAAGAUUA A
ArsZ M3	pPT138-1	CSO-2904 CSO-1220	105	**C**UAACUGAAAUUGUUCAUUUUAUUUU AGUUAGGCUCCUUGAAUUCUUAUUGU AGUAGGGUUUAUCACACUUGCCUUGU GUUACUAAUCACACAAGGCAAGAUUA A
HP1432 5'UTR	CSS-0065	CSO-1252 CSO-0155	193	**C**UAGCUAAUGAGCUAGAAUUUAAAUU UCAAUUAA**AGGAG**UCAUC**AUG**GCACA CCAUGAACAACAACAGCAACAACAGGC UAACAGCCAACACCACCACCAUCACCA UGC*G*CACCACCACCAUUACUACGG*U*GG CGAACACCAUCACCAUAA*U*GCGCAACA ACACGCCGAACAACAAGCAGAGCAACA AGCUCA
HP1432 M3 5'UTR	pPT153-1	CSO-1252 CSO-0155	193	**C**UAGCUAAUGAGCUAGAAUUUAAAUA AGAAUUAA**AGGAG**UCAUC**AUG**GCACA CCAUGAACAACAACAGCAACAACAGGC UAACAGCCAACACCACCACCAUCACCA UGC*G*CACCACCACCAUUACUACGG*U*GG CGAACACCAUCACCAUAA*U*GCGCAACA ACACGCCGAACAACAAGCAGAGCAACA AGCUCA
HP1432::*gfp*	pPT142-1	CSO-1252 CSO-0441	807	**C**UAGCUAAUGAGCUAGAAUUUAAAUU UCAAUUAA**AGGAG**UCAUC**AUG**GCUAG CAGUAAAGGAGAAGAACUUUUCACUG GAGUUGUCCCAAUUCUUGUUGAAUUA GAUGGUGAUGUUAAUGGGCACAAAUU UUCUGUCAGUGGAGAGGGUGAAGGUG AUGCAACAUACGGAAAACUUACCCUU AAAUUUAUUUGCACUACUGGAAAACU ACCUGUUCCAUGGCCAACACUUGUCAC UACUUUCGGUUAUGGUGUUCAAUGCU UUGCGAGAUACCCAGAUCAUAUGAAA CAGCAUGACUUUUUCAAGAGUGCCAU

				GCCCGAAGGUUAUGUACAGGAAAGAA CUAUAUUUUUCAAAGAUGACGGGAAC UACAAGACACGUGCUGAAGUCAAGUU UGAAGGUGAUACCCUUGUUAAUAGAA UCGAGUUAAAAGGUAUUGAUUUUAAA GAAGAUGGAAACAUUCUUGGACACAA AUUGGAAUACAACUAUAACUCACACA AUGUAUACAUCAUGGCAGACAAACAA AAGAAUGGAAUCAAAGUUAACUUCAA AAUUAGACACAACAUUGAAGAUGGAA GCGUUCAACUAGCAGACCAUUAUCAAC AAAAUACUCCAAUUGGCGAUGGCCCU GUCCUUUUACCAGACAACCAUUACCUG UCCACACAAUCUGCCCUUUCGAAAGAU CCCAACGAAAAGAGAGACCACAUGGUC CUUCUUGAGUUUGUAACAGCUGCUGG GAUUACACAUGGCAUGGAUGAACUAU ACAAAUAAAUGUCCAGACCUGCAGUU AACUCCCGCGGCCGCAAAAAAC
HP1432 M3::*gfp*	pPT147-1	CSO-1252 CSO-0441	807	**C**UAGCUAAUGAGCUAGAAUUUAAAUA AGAAUUAAA**GGAG**UCAUC**AUG**GCUAG CAGUAAAGGAGAAGAACUUUUCACUG GAGUUGUCCCAAUUCUUGUUGAAUUA GAUGGUGAUGUUAAUGGGCACAAAUU UUCUGUCAGUGGAGAGGGUGAAGGUG AUGCAACAUACGGAAAACUUACCCUU AAAUUUAUUUGCACUACUGGAAAACU ACCUGUUCCAUGGCCAACACUUGUCAC UACUUUCGGUUAUGGUGUUCAAUGCU UUGCGAGAUACCCAGAUCAUAUGAAA CAGCAUGACUUUUUCAAGAGUGCCAU GCCCGAAGGUUAUGUACAGGAAAGAA CUAUAUUUUUCAAAGAUGACGGGAAC UACAAGACACGUGCUGAAGUCAAGUU UGAAGGUGAUACCCUUGUUAAUAGAA UCGAGUUAAAAGGUAUUGAUUUUAAA GAAGAUGGAAACAUUCUUGGACACAA AUUGGAAUACAACUAUAACUCACACA AUGUAUACAUCAUGGCAGACAAACAA AAGAAUGGAAUCAAAGUUAACUUCAA AAUUAGACACAACAUUGAAGAUGGAA GCGUUCAACUAGCAGACCAUUAUCAAC AAAAUACUCCAAUUGGCGAUGGCCCU GUCCUUUUACCAGACAACCAUUACCUG UCCACACAAUCUGCCCUUUCGAAAGAU CCCAACGAAAAGAGAGACCACAUGGUC CUUCUUGAGUUUGUAACAGCUGCUGG GAUUACACAUGGCAUGGAUGAACUAU

				ACAAAUAAAUGUCCAGACCUGCAGUU AACUCCCGCGGCCGCAAAAAAC
RepG	CSS-0065	87	JVO-5125 JVO-5126	**A**UCCAACCAUUCCUUAUGGUUUGGUU GGCACCGCUAAGAUUGAAGGGUCACC UCCCCCUCCUUUCCCUUUGUCUUGGCG GUUGUUUU
tlpB::*gfp*	pSP109-6	914	JVO-5127 CSO-0441	**U**GUUUGUUCUUUUGUUUCGUUUUCAA ACAACCGGGUUUUAAUUUUGUUUUGU GCCACUCAUUUUUCGGGGGGGGGGGGG UGCAUUUAGAAGCUAAACUCUAAAAU UAGGGUUUGACUUAAAAAUGAUUUAU **AGGAG**AUAAA**AUG**AUGUUUUCUUCAGC UAGCAGUAAAGGAGAAGAACUUUUCA CUGGAGUUGUCCCAAUUCUUGUUGAA UUAGAUGGUGAUGUUAAUGGGCACAA AUUUUCUGUCAGUGGAGAGGGUGAAG GUGAUGCAACAUACGGAAAACUUACC CUUAAAUUUAUUUGCACUACUGGAAA ACUACCUGUUCCAUGGCCAACACUUGU CACUACUUUCGGUUAUGGUGUUCAAU GCUUUGCGAGAUACCCAGAUCAUAUG AAACAGCAUGACUUUUUCAAGAGUGC CAUGCCCGAAGGUUAUGUACAGGAAA GAACUAUAUUUUUCAAAGAUGACGGG AACUACAAGACACGUGCUGAAGUCAA GUUUGAAGGUGAUACCCUUGUUAAUA GAAUCGAGUUAAAAGGUAUUGAUUUU AAAGAAGAUGGAAACAUUCUUGGACA CAAAUUGGAAUACAACUAUAACUCAC ACAAUGUAUACAUCAUGGCAGACAAA CAAAAGAAUGGAAUCAAAGUUAACUU CAAAAUUAGACACAACAUUGAAGAUG GAAGCGUUCAACUAGCAGACCAUUAU CAACAAAAUACUCCAAUUGGCGAUGG CCCUGUCCUUUUACCAGACAACCAUUA CCUGUCCACACAAUCUGCCCUUUCGAA AGAUCCCAACGAAAAGAGAGACCACA UGGUCCUUCUUGAGUUUGUAACAGCU GCUGGGAUUACACAUGGCAUGGAUGA ACUAUACAAAUAAAUGUCCAGACCUG CAGUUAACUCCCGCGGCCGCAAAAAAC

8 Curriculum vitae

9 Acknowledgement

First and foremost, I would like to express my gratitude to my primary supervisor, Prof. Dr. Cynthia Sharma for giving me the opportunity to work in her group as well as for her continuous support of my PhD journey and related research. She has guided me during my PhD studies through scientific discussions and encouraged me to participate in various international conferences.

Besides my primary supervisor, I would like to thank the rest of my thesis committee: Prof. Dr. Dagmar Beier, and Prof. Dr. Jörg Vogel, not only for their insightful comments and encouragement especially during annual report meetings, but also for the "out-of-the-box" questions which incented me to widen my research from various perspectives. Prof. Dr. Dagmar Beier has also provided me with some *H. pylori* strains which I have used in this research.

I am also very grateful to all those at the GSLS office, especially Dr. Gabriele Blum-Öhler and others who were always so helpful with my concerns and provided me with their assistance throughout my journey here as a PhD student.

The members of the Sharma group have contributed immensely to my personal and professional time here. The team has been a source of friendships as well as good advice and collaboration. It has been an amazing experience working alongside Sandy, Gaurav, Mona, Sarah, Thorsten, Sara, Elisabetta, Belinda, Marcus, and Anika. Going through the thick and thins in this journey would have been much more challenging without all of you.

For this thesis, I would like to thank my reading committee members: Prof. Dr. Cynthia Sharma, Sarah, Mona, Sandy and Sara for their time, effort, translation and helpful comments. My appreciation also goes to Hilde for her technical support.

Last but not least, I would like thank my wife who has been by my side throughout this PhD and my family for their love and care. I am grateful for their understanding and support of my work.

Undertaking this PhD has been a truly life-changing experience for me and it would not have been possible without the support and guidance that I have received, be it directly or indirectly from everyone.

10 Eidesstattliche Erklärung / Affidavit

Affidavit

I hereby confirm that my thesis entitled "Functional characterization of an acid-regulated sRNA in *Helicobacter pylori*" is the result of my own work. I did not receive any help or support from commercial consultants. All sources and / or materials applied are listed and specified in the thesis.

Furthermore, I confirm that this thesis has not yet been submitted as part of another examination process neither in identical nor in similar form.

Würzburg, 18.04.2017

Place, Date Signature

Eidesstattliche Erklärung

Hiermit erkläre ich an Eides statt, die Dissertation "Funtionelle Charakterisierung einer durch Säure regulierten sRNA in *Helicobacter pylori*" eigenständig, d.h. insbesondere selbständig und ohne Hilfe eines kommerziellen Promotionsberaters, angefertigt und keine anderen als die von mir angegebenen Quellen und Hilfsmittel verwendet zu haben.

Ich erkläre außerdem, dass die Dissertation weder in gleicher noch in ähnlicher Form bereits in einem anderen Prüfungsverfahren vorgelegen hat.

Würzburg, 18.04.2017

Ort, Datum Unterschrift